UNIVERSITÉ DE STRASBOURG

EDSC École Doctorale des Sciences Chimiques

ÉCOLE DOCTORALE 222

Laboratoire de Catalyse Chimique
Institut de Science et d'Ingénierie Supramoléculaires

THÈSE de DOCTORAT

présentée par :

Eléna WOLF

Soutenue le 02 Octobre 2015

pour obtenir le grade de : **Docteur de l'Université de Strasbourg**

Discipline/ Spécialité : Chimie organique

Screening and Deconvoluting Complex Mixtures of Catalyst Components in Reaction Development

THÈSE dirigée par :

Prof. EBBESEN Thomas	Directeur de thèse, Université de Strasbourg
Prof. LEHN Jean-Marie	Co-directeur de thèse, Université de Strasbourg

RAPPORTEURS :

Dr TARAN Frédéric	Rapporteur, CEA Saclay
Dr GILLINGHAM Dennis	Rapporteur, Université de Bâle

EXAMINATEUR:

Dr MORAN Joseph	Examinateur, Université de Strasbourg

"We cannot change the cards we are dealt, just how we play the hand" – Randy Pausch

Table of contents

Acknowledgdements

Au terme de ce travail, je tiens particulièrement à remercier un grand nombre de personnes, sans qui, l'accomplissement de cette thèse de doctorat n'aurait été possible. Le soutien sans faille de toutes ces personnes dont la générosité, la bonne humeur et l'intérêt manifesté à l'égard de ma recherche m'ont permis de progresser tant au niveau professionnel que personnel.

Je tiens tout d'abord à remercier mon directeur de thèse, le Professeur Thomas Ebbesen ainsi que mon co-directeur de thèse, le Professeur Jean-Marie Lehn qui m'ont accueillie chaleureusement au sein de l'Institut de Science et d'Ingénierie Supramoléculaires. Ensuite, je tiens tout particulièrement à remercier le Dr Joseph Moran, puisque c'est sous son encadrement et dans son laboratoire que j'ai pu développer ce passionnant projet de recherche. Il s'est toujours montré disponible et m'a accompagnée dans mes choix tout en me prodiguant de précieux conseils tout au long de la thèse.

Je tiens à remercier les rapporteurs de mon jury, le Dr Frédéric Taran, le Dr Dennis Gillingham ainsi que le Dr Aurélien Blanc, membre invité, qui ont accepté de lire et de juger ce travail.

Je remercie également mes collègues de travail au laboratoire. Pour certains, nous avons partagé trois années avec de nombreuses péripéties qui nous ont permis de créer ce lien si particulier. Merci à Florian, qui a été présent tout au début de l'aventure, qui m'a encadrée et enseignée les bonnes pratiques de laboratoire, Malik, qui a toujours été de bons conseils dans les moments de doute, Marian avec qui j'ai passé de merveilleux moments et toutes les discussions de tout et de rien, Ed qui a fait tout son possible pour m'aider dans mes projets mais aussi dans la correction de ce manuscrit…and I don't forget this incredible Lettuce prononciation…and Leandro, do not go to the (careful with the prononciation) 6th floor !!! Je n'oublie pas Ismat, Margot, Guang, Anaelle et Nour qui ont partagé quelques mois avec nous. Aux nouveaux arrivants, Vuk et Sreejith. J'ai été ravie de travailler quelques mois avec vous et j'espère vraiment que vous apprécierez cet environnement exceptionnel de travail autant que moi. Je nous souhaite encore des moments exceptionnels à vivre ensemble et je ne vous souhaite à tous que le meilleur.

Je souhaite également remercier Jean-Louis Schmitt pour quelques conseils en RMN ainsi que pour la location de certains matériels ;). Nathalie, notre secrétaire, qui a fait un travail plus que remarquable.

Je voudrais tout particulièrement remercier mes camarades de promo, Julie, Thierry et Clément, avec qui, autour de repas quelques fois plus que douteux, nous avons partagé nos galères, nos ratés mais aussi d'innombrables fous rires. J'ai eu beaucoup de plaisir à vous côtoyer et je garderai de nombreux souvenirs du temps passé à vos côtés. Je ne vous souhaite que le meilleur mes amis !

A toutes les belles rencontres que j'ai pu faire dans ma vie. J'adresse mes plus vifs remerciements à ma famille, à mes parents, à Cynthia, Alexandre et Caroline. Je remercie également Charlotte, présente depuis le début et bien avant ainsi qu'Anna, qui toutes deux ont joué un rôle essentiel dans ma vie. Je leur dédie ce travail pour leur soutien, leur écoute et leurs perpétuels encouragements.

Et pour finir, je remercie Victorien...

Abreviations

2,6-DMBA	2,6-dimethylbenzoic acid
Å	angström(s)
aa	amino acid
Ac	acetyl
AcOH	acetic acid
acac	acetylacetone
Ala	alanine
Ar	aryl
BBBPY	4,4'-di-*tert*-butyl-2,2'-dipyridil
BAC	boronic acid catalysis
Bn	benzyl
Boc	*tert*-butylcarbonate
Bu_2SnO	dibutyltin oxide
BzOH	benzoic acid
°C	degrés Celsius
cat	catalytic quantity
Cbz	benzylcarbonate
$CHCl_3$	chloroform
CMD	concerted metalation-deprotonation
cod	1,5-cyclooctadiene
DABCO	1,4-diazabicyclo[2.2.2]octane
DCC	N,N' dicyclohexylcarbodiimide
DCE	dichloroethane
DCM	dichloromethane
DEAD	diethyl azodicarboxylate
DIPEA	*N*,*N*-diisopropylethylamine
DMA	dimethylacetamide
4-DMAP	*N*,*N*-dimethyl-4-aminopyridine
DMF	dimethylformamide
DMSO	dimethylsulfoxyde
DNA	deoxyribonucleic acid
DOS	diversity-oriented synthesis
dppf	1,1'-bis(diphenylphosphino)ferrocene
dppp	1,3-bis(diphenylphosphino)propane
ee	enantiomeric excess
EIA	enzyme immunoassay
ELISA	enzyme-linked immunosorbent assay
ELSD	evaporative light scattering detection
equiv	equivalent
ESI	electrospray ionization
Et	ethyl
EtOAc	ethyl acetate
Et_2O	diethylether
EtOH	ethanol
Et_3PO	triethylphosphine oxide
FRET	Förster resonance energy transfer
g	gram(s)
GC-MS	gas chromatography–mass spectrometry
Gly	glycine
h	hour(s)
HDA	hetero Diels-Alder
HFIP	1,1,1,3,3,3-hexafluoro-2-propanol
HPLC	high-pressure liquid chromatography
HR-MS	high resolution mass spectrometry
HTS	high throughput screening
Ile	isoleucine
*i*Pr	*iso*-propyl
*i*PrOH	*iso*-propanol
ISES	*in situ* enzymatic screening

LC-MS	liquid chromatography–mass spectrometry
Leu	leucine
Me	methyl
MeCN	acetonitrile
$MeNO_2$	nitromethane
MeOH	methanol
MesCOOH	2,4,6-trimethylbenzoic acid
min	minute(s)
MS	molecular sieves
MsOH	methanesulfonic acid
$NADH/NAD^+$	nicotinamide adenine dinucleotide reduced/oxidized
*n*Bu	*n*-butyl
NEt_3	triethylamine
$NiCl_2$•dme	nickel(II) chloride ethylene glycol dimethyl ether complex
nM	nanomolaire
NMR	nuclear magnetic resonance
M	molar
mp	melting point
PCC	pyridinium chlorochromate
PCR	polymerase chain reaction
PCy_3	tricyclohexylphosphine
Ph	phenyl
Phe	phenylalanine
PivOH	pivalic acid
PMB	4-methoxybenzyl ether
PPh_3	triphenylphosphine
quant.	Quantitative
rt	room temperature
s	seconde(s)
TBAB	*tetra*-butylammonium bromide
TBDMS	*tert*-butyldimethylsilyl
TBDPS	*tert*-butyldiphenylsilyl
*t*Bu	*tert*-butyl
*t*BuOH	*tert*-butanol
TES	triethylsilyl
TFA	trifluoroacetic acid
TfOH	trifluoromethanesulfonic acid
THF	tetrahydrofuran
TIPS	triisopropylsilyl
TMS	trimethylsilyl
$TMSN_3$	azidotrimethylsilane
Ts	tosyl, *p*-toluenesulfonyl
TS	transition state
TsOH	*p*-toluenesulfonic acid
Val	valine
xantphos	4,5-bis(diphenylphosphino)-9,9-dimethylxanthene

Résumé

Ce travail de thèse se divise en cinq chapitres et décrit une nouvelle approche de type combinatoire pour la découverte de nouveaux systèmes catalytiques dans des réactions d'activation directe d'alcools, d'arylation *ortho*-C-H de composés *N*-(quinolin-8-yl)benzamide, d'alkylation d'indoles en position C3 et dans la réaction asymétrique d'hétéro Diels-Alder.

CHAPITRE 1

Le développement réactionnel est problème multidimensionnel complexe qui, dans un scénario représentatif, implique souvent l'unique convergence de plusieurs paramètres à une réactivité désirée. Le choix incorrect d'un seul paramètre réactionnel tel que le pré-catalyseur, le ligand mais aussi le solvant ou encore l'acide/base peut complètement supprimer la réactivité du système. De ce fait, ce processus requiert souvent de nombreuses expérimentations impliquant le test de toutes les combinaisons en parallèle. L'effort demandé est considérable pour le chimiste et sans garantie de résultat. Pour répondre à la demande toujours croissante de productivité et d'économie de réactions, des approches créatives de criblage ont été développées ces dernières années, chacune présentant leurs forces et leurs faiblesses. Cela dit, le nombre important de reactions nécessaires à l'exploration de juste trois ou quatre paramètres est toujours un challenge pour les chimistes qui n'ont pas accès aux instrumentations spécifiques au criblage à haut debit. Dans cette thèse, nous proposons une nouvelle approche de type combinatoire en deux temps dont l'objectif est de diminuer fortement le nombre d'expérimentations avant d'obtenir un premier résultat. Dans une première phase, il s'agit de cribler un mélange de catalyseurs en one pot et de tester un ou deux paramètres additionnels tels que le solvant, la base, etc. puis dans une deuxième phase, une déconvolution itérative pourra révéler la combinaison de catalyseurs la plus active et/ou sélective (Schéma 1).

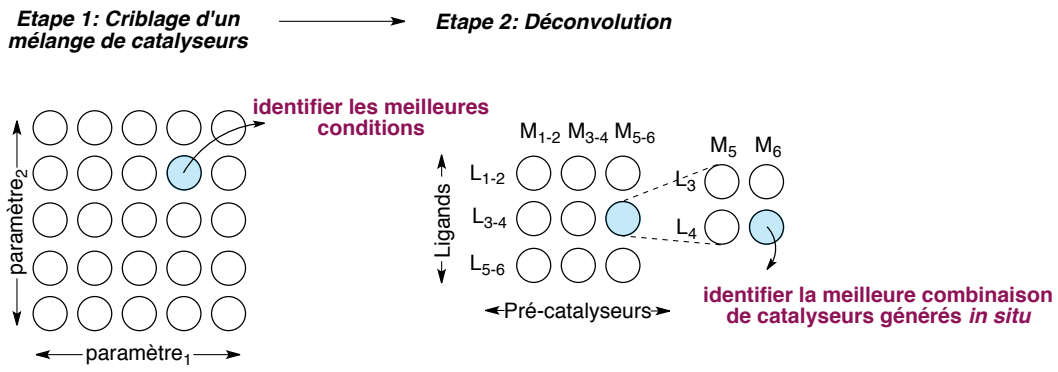

Schéma 1. Nouvelle approche combinatoire générale.

CHAPITRE 2

Le second chapitre de ce manuscrit introduit l'importance de soigneusement optimiser les conditions réactionnelles. Cet exemple d'optimisation traditionnelle a permis de mettre en évidence l'importance de la convergence des paramètres réactionnels qui apporteront réactivité et chimiosélectivité dans des réactions d'activation directe d'alcools. Nous avons montré que le groupement hydroxyle, qui est un nucléofuge peu efficace, peut être activé efficacement par l'hydrate de $B(C_6F_5)_3$ dans la reaction modèle de Friedel-Crafts entre l'alcool **2** et le nucléophile **3** dans le nitrométhane uniquement (Table 1).

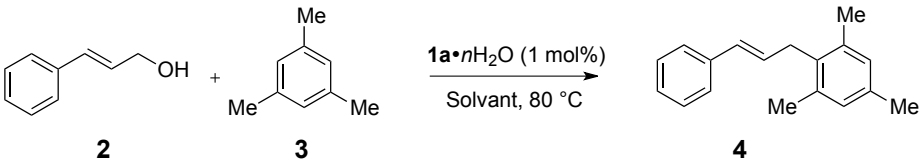

2 **3** **4**

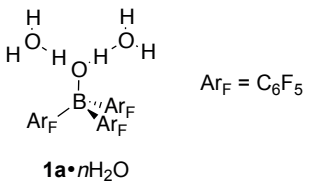

1a•nH$_2$O

Entrée	Solvant	t [h]	Rendement [%]
1-9	DCE, DMF, DMA, DMSO, MeCN, Toluène, EtOAc, THF, Mesitylene	1	<5
10	**$MeNO_2$**	**1**	**86**

Table 1. Influence cruciale du solvant dans une réaction de Friedel-Crafts catalysée par **1a•nH$_2$O**.

De plus, une chimiosélectivité particulière à l'utilisation de $B(C_6F_5)_3 \bullet nH_2O$ dans la réaction de Friedel-Crafts entre l'alcool allylique **5** et le mésitylène **3** pour former le composé **6a** a été observée (Table 2). Habituellement, sous conditions acides, l'alcène exocyclique **6a** peut facilement s'isomériser pour former l'alcène endocyclique **6b**.

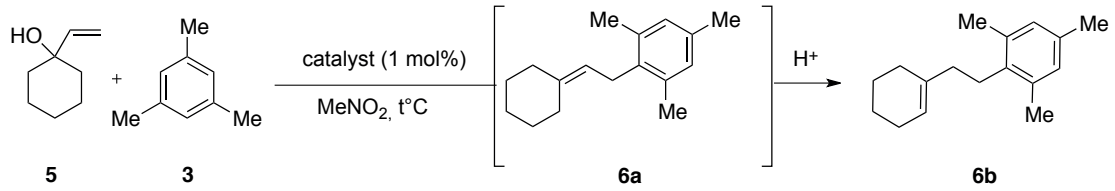

5 **3** **6a** **6b**

Entry	Catalyst	T (°C)	Yield **7a**+**7b** [%]	Ratio **(7a**:**7b)**
1	none	80	<5	n/a
2	TfOH	80	77	1:10
3	HBF_4	80	88	1:9
4	H_2SO_4	80	78	1:5
5	TsOH	80	74	4:1
6	TFA	80	68	>20:1
7	$Ca(NTf)_2/Bu_4NPF_6$	80	74	1:9
8	$Bi(OTf)_3$	80	83	1:12
9	$SC(OTf)_3$	80	83	1:9
10	$BF_3.Et_2O$	80	82	1:10
11	$FeCl_3$	80	82	1:3
12	$AuCl_3$	80	85	6:1
13	$Yb(OTf)_3$	80	62	4:1
14	$B(C_6F_5)(OH)_2$	80	<5	n/a
15	Ph_3B	80	<5	n/a
16	**1a**$\bullet n$$H_2O$	80	92	>20:1
17	**1a**$\bullet n$$H_2O$	22	60	>20:1
18	**1a**$\bullet n$$H_2O$	22	77	>20:1
19	TfOH	22	47	2:1
20	TsOH	22	32	>20:1
21	TFA	22	<5	n/a

Table 2. La chimiosélectivité étudiée par l'utilisation de divers catalyseurs acides dans la réaction de Friedel-Crafts entre l'alcool allylique **5** et le mésitylène **3**.

Ensuite, l'utilisation de $B(C_6F_5)_3 \bullet nH_2O$ dans le nitrométhane s'est révélée être une combinaison très efficace et très douce dans la substitution directe d'alcools allyliques et benzyliques par divers nucléophiles. Une forte compatibilité pour des nucléophiles -*C*, -*N*, -*O*, -*S* ainsi qu'une tolérance envers des groupements qui sont généralement sensibles aux conditions acides ont été démontrées (Schéma 2, équation 1). Après avoir développé des

conditions réactionnelles très douces pour les alcools π-activés, nous avons prolongé l'étude du système catalytique sur les alcools aliphatiques tertiaires, une classe d'alcools très favorable au processus d'élimination en conditions acides. Nous avons pu étendre les conditions réactionnelles développées préalablement à la réaction d'azidation avec TMS-N_3 comme nucléophile (Schéma 2, équation 2).

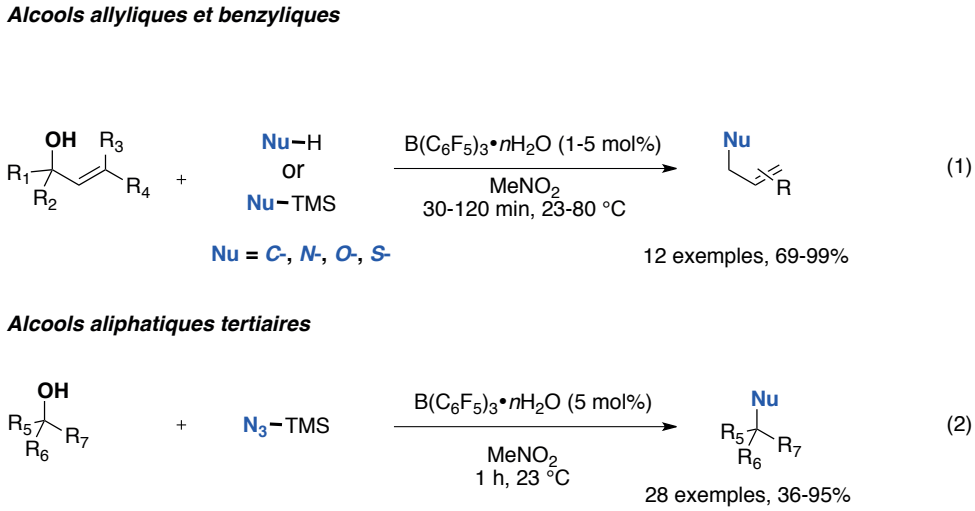

Schéma 2. Utilisation de $B(C_6F_5)_3 \bullet nH_2O$ dans le nitrométhane dans des réactions de substitution nucléophile d'alcools allyliques, benzyliques et aliphatiques tertiaires.

CHAPITRE 3

Le chapitre précédent a démontré l'importance de la convergence de tous les paramètres réactionnels dans la réactivité et la chimiosélectivité des systèmes catalytiques. Dans une volonté de découvrir de nouvelles conditions réactionnelles en un minimum de réactions, ce chapitre présente la première application de l'approche combinatoire avec l'optimisation en parallèle de trois paramètres réactionnels. La stratégie est basée sur la supposition qu'en employant un mélange complexe de catalyseurs générés *in situ* à partir de pré-catalyseurs et de ligands identifiés par la suite par déconvolution, un paramètre additionnel peut être testé pour obtenir une réactivité préliminaire. De cette manière, trois paramètres réactionnels peuvent être testés dans un seul ballon. Ici, nous avons voulu étudier l'effet d'additifs de type ligands bidentates sur l'activité catalytique des acides boroniques ainsi que l'effet du solvant. Utilisés comme pré-catalyseurs, les acides boroniques représentent des candidats idéaux pour

l'approche de type combinatoire puisque ceux ci forment des liaisons covalentes réversibles avec des ligands *O*-bidentates formant ainsi une librairie de nouvelles espèces cycliques qui peuvent être testées en catalyse. Les propriétés électroniques et stériques de ces nouvelles espèces catalytiques peuvent être modulés soit par les substituants que porte le bore, soit par les ligands; les composés générés peuvent être plus ou moins acides et plus ou moins stables dans les conditions réactionnelles (Schéma 3).

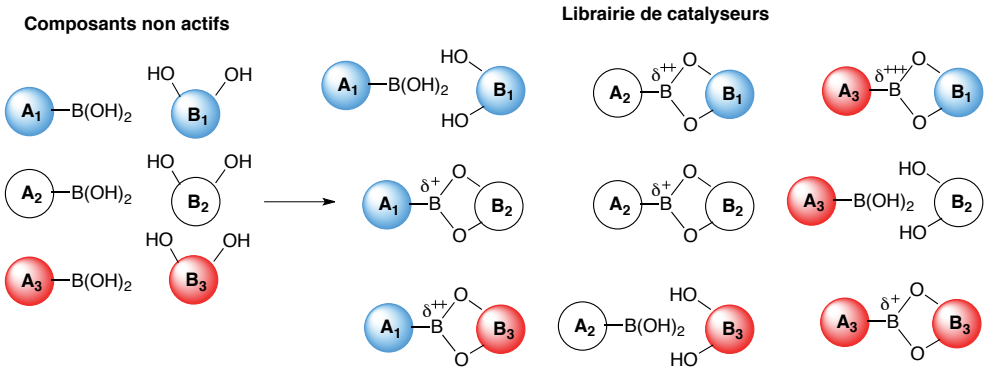

Schéma 3. Génération *in situ* d'une librairie de catalyseurs à partir de composants non actifs.

La réaction de Friedel-Crafts entre l'alcool benzylique **7** et le mésitylène **3** formant le diarylméthane **8**, a été choisie comme modèle puisqu'elle n'est pas catalysée par des acides boroniques ou par les ligands employés dans cette étude. Pour augmenter la diversité structurale du criblage, onze acides boroniques divers et l'acide borique ainsi que douze ligands de type acides carboxyliques, diols ou acides α-hydroxylés, ont été choisis. Quatorze solvants, polaires, protiques, apolaires, aprotiques avec différentes constantes diélectriques, ont été testés (Schéma 4, étape 1). L'étape 1 permet de cribler toutes les combinaisons de catalyseurs et de trouver les conditions optimales de la reaction qui seront conservées par la suite. Sur les quatorze solvants testés, le nitrométhane est celui qui a donné la meilleure conversion. L'objectif de l'étape 2 est de procéder par divisions successives jusqu'à l'identification de la combinaison pré-catalyseur/ligand responsable de l'activité catalytique. A l'issue de la déconvolution, l'acide pentafluorophényleboronique et l'acide oxalique ont été identifiés comme étant la combinaison avec la meilleure activité catalytique (Schéma 4, étape 2).

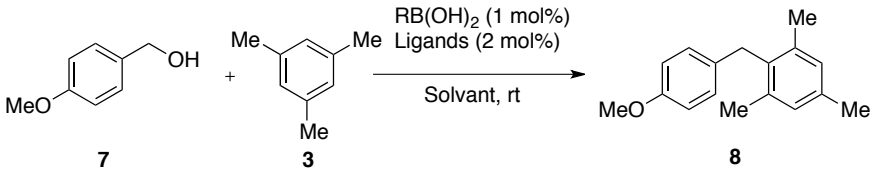

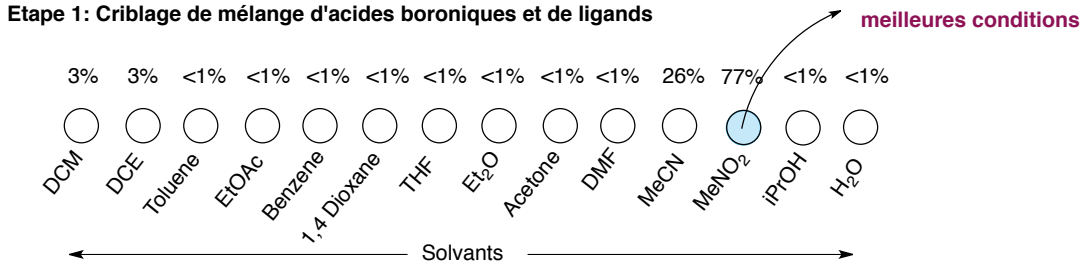

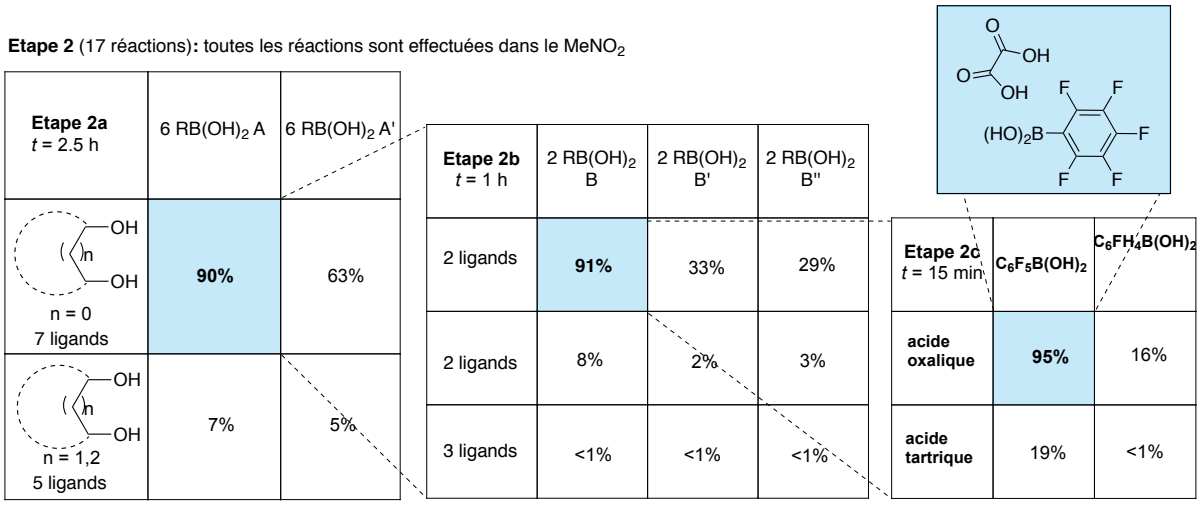

Schéma 4. Identification en deux étapes de conditions réactionnelles très efficaces pour la réaction de Friedel-Crafts.

En accord avec les données issues de la littérature et de données spectrométriques, nous proposons le complexe dioxaborolanedione **9** comme catalyseur actif formé *in situ* par l'acide pentafluorophényleboronique et l'acide oxalique dans un ratio 1:1 (Schéma 5). Des expérience RMN ont été conduites pour étudier la dynamique de l'assemblage entre les deux composants. Quand l'acide pentafluorophényleboronique **9a** et l'acide oxalique **9b** sont combinés dans un ratio 1:1 dans le nitrométhane deutéré, deux ensembles de pics (en plus des pics de l'acide boronique) apparaissent en RMN du fluor montrant que deux nouvelles espèces s'assemblent en quelques secondes. Comme dans le cas de $B(C_6F_5)_3$ qui forme

spontanément des hydrates, ces nouveaux pics pourraient être attribués à l'hydrate **9**•H_2O et au dihydrate dioxaborolanedione **9**•$2H_2O$.

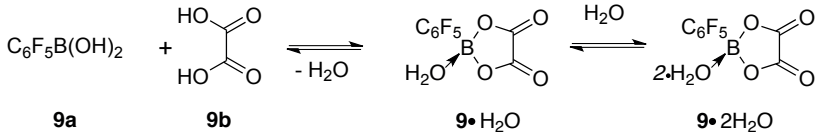

9a **9b** **9**• H_2O **9**• $2H_2O$

Schéma 5. Structures du catalyseur dioxaborolanedione générées *in situ.*

Des expériences de mesures d'acidité par RMN du phosphore ont ensuite été menées par une méthode dérivée de la méthode de Gutmann-Beckett. Le dioxaborolanedione identifié par l'approche combinatoire a montré une acidité plus forte que $B(C_6F_5)_3$•H_2O. De ce fait, il nous a paru intéressant d'étendre la réactivité du système à d'autres alcools allyliques, benzyliques. Une utilisation plus faible de quantité du catalyseur dioxaborolanedione **9** comparée à $C_6F_5B(OH)_2$ (10 à 20 fois moins) mais aussi à $B(C_6F_5)_3$•H_2O (2 à 5 fois moins) sur des substrats similaires, a pu ainsi diminuer le coût de la réaction. De plus, pour la première fois, la substitution d'alcools tertiaires aliphatiques est décrite avec des nucléophiles de type -*C*, -*N* et -*S* avec 5 mol% d'acide pentafluorophényleboronique et 5 mol% d'acide oxalique dans un mélange de solvant nitrométhane/hexafluoroisopropanol (Schéma 6).

Cette nouvelle approche a permis l'identification d'un nouveau catalyseur très efficace dans le nitrométhane dans des réactions de type substitution nucléophile d'alcools. Ce catalyseur a montré une acidité et une réactivité plus forte que $B(C_6F_5)_3$•H_2O tout en gardant des propriétés de stabilité et de compatibilités envers différents groupements réactionnels.

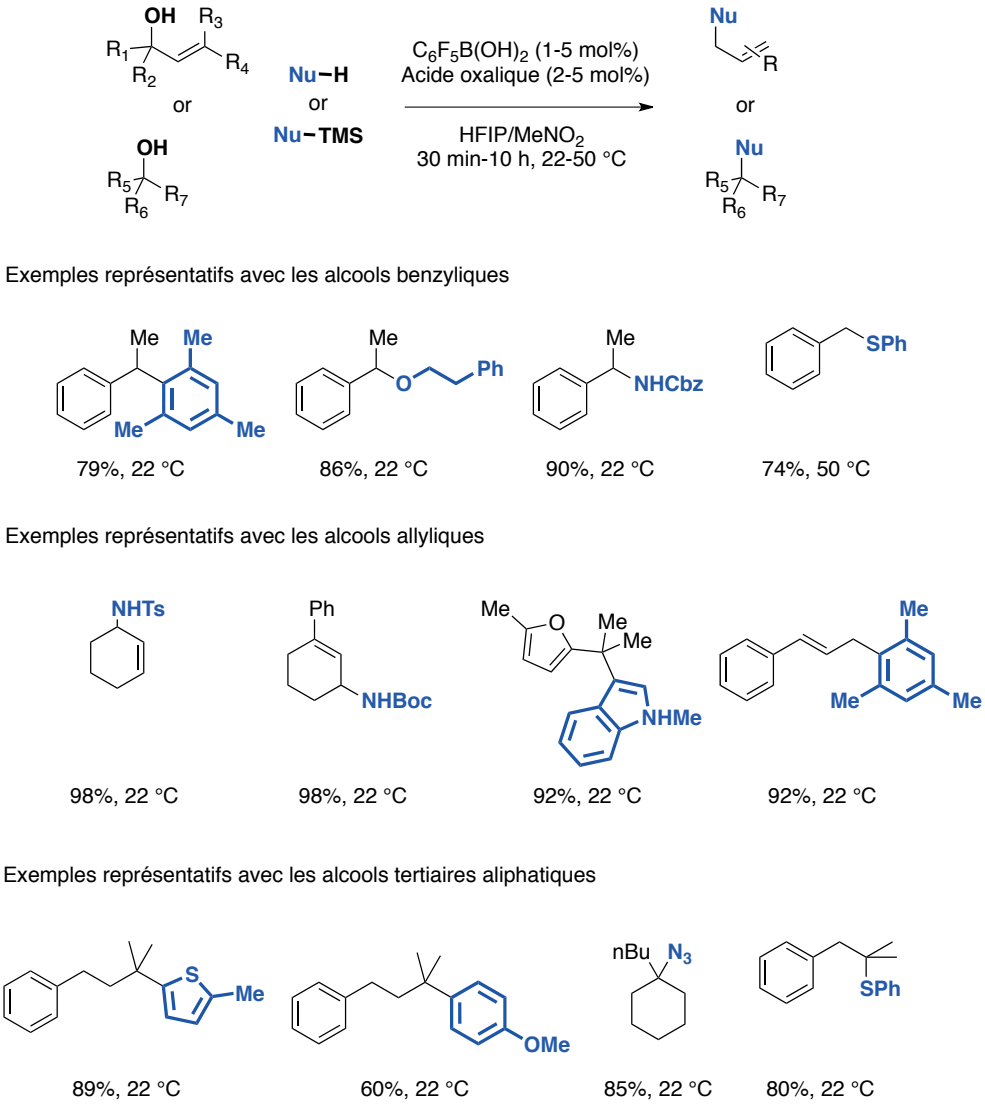

Schéma 6. Le dioxapentafluorophenylborolanedione comme catalyseur efficace dans des substitutions d'alcools π-activés et aliphatiques tertiaires avec une série de nucléophiles.

CHAPITRE 4

Pour évaluer l'applicabilité de la stratégie dans un système plus complexe, nécessitant l'optimisation de plus de trois paramètres réactionnels, nous nous sommes intéressés aux réactions catalysées par des métaux de transition. Dans un premier temps, l'objectif portait sur la découverte de nouvelles conditions réactionnelles dans la monoarylation C-H de composés (quinolin-8-yl)benzamides en l'absence de groupement bloquant dans les positions *ortho* ou *meta*. Dans un deuxième temps, nous avons entrepris cette stratégie pour la découverte de systèmes catalytiques pour l'alkylation sélective C3 d'indoles.

Pour l'arylation sélective, une vue générale rapide de la littérature dans le domaine de l'activation C-H, a permis de sélectionner quatre métaux de transition et neuf ligands labiles. La réaction de couplage entre le composé benzamide **10** et le 4-iodoanisole **11** a été choisie comme réaction cible pour former sélectivement **12**. Avec un mélange de 10 mol% de chaque pré-catalyseur et 5 mol% de chaque ligand dans chaque réaction, trois solvants et trois bases ont été criblés en seulement neuf réactions dans l'étape 1 (Schéma 7). Seule la combinaison Na_2CO_3 dans le 1,4-dioxane a donné le composé souhaité avec une conversion de 10%. Le processus de déconvolution des métaux a révélé que le $Ni(acac)_2$ était responsable de l'activité catalytique. En maintenant Na_2CO_3 comme base et le 1,4-dioxane comme solvant, les neufs ligands ont été arbitrairement divisés en trois groupes et évalués en combinaison avec $Ni(acac)_2$ et $NiCl_2$•dme. Une augmentation significative de la réactivité a été observée dans les réactions contenant PCy_3, MesCOOH et dppf comme ligands (Etape 2b). L'étape suivante a révélé que la combinaison entre $NiCl_2$•dme and MesCOOH a donné la meilleure réactivité dans les conditions expérimentales (Etape 2c). L'optimisation des paramètres continus a permis d'atteindre 75% de conversion pour le produit **12**. Etonnamment, la sélectivité pour le composé monoaryle par rapport au composé bisaryle est excellente (>20:1). Par cette approche, vingt-cinq réactions ont été lancées pour identifier un système catalytique très actif et sélectif vis à vis de la monoarylation de dérivés benzamides au lieu de 324 réactions dans une logique d'optimisation linéaire traditionnelle.

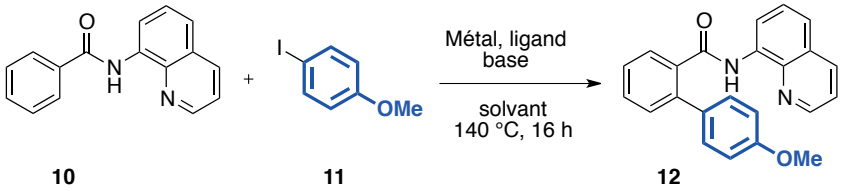

10 **11** **12**

Métaux - $Ni(acac)_2$, $CoCl_2$, $Cu(OAc)_2$, $Fe(acac)_3$. **Ligands** - PCy_3, dppf, dppp, PPh_3, xantphos, MesCOOH, PivOH, 2,6-DMBA, BzOH.

Etape 1: Tous les métaux (10 mol%) et ligands (5 mol%), 3 solvants (2.5 mL) et 3 bases (1.0 mmol).
Etape 2a: Métal individuel (10 mol%) et tous les ligands (5 mol%) avec Na_2CO_3 dans le 1,4-dioxane.

Etape 1	1,4-dioxane	toluene	DMF
NaO^tBu	<5%	<1%	<1%
Na_2CO_3	10%	<5%	<1%
CsF	<1%	<1%	<1%

Etape 2a	Conversion
$Ni(acac)_2$	11%
$CoCl_2$	<1%
$Cu(OAc)_2$	<1%
$Fe(acac)_3$	<1%

Steps 2b-c: All reactions performed in 1,4-dioxane (1 mL) with Na_2CO_3 (5.0 equiv) and 5 mol% of each ligand.

Etape 2b	$Ni(acac)_2$	$NiCl_2$-dme
PCy_3, dppf, MesCOOH	32%	64%
PivOH, dppp, 2,6-DMBA	18%	47%
BzOH, PPh_3, xantphos	21%	48%

Etape 2c	M (10 mol%)/ L (10 mol%)	M (10 mol%)/ L (20 mol%)
$NiCl_2$•dme/PCy_3	33%	40%
$NiCl_2$•dme/dppf	13%	29%
$NiCl_2$•dme/MesCOOH	53%	67%

optimization

$NiCl_2$-dme (15 mol%) / MesCOOH (30 mol%)
1,4-dioxane (0.5 mL)
Na_2CO_3 (5.0 eq)
140 °C, 24 h
75% conversion

Schéma 7. Identification d'un système catalytique très efficace en 25 réactions.

Dans la réaction d'alkylation d'indole avec des métaux de transition, la préférence de réactivité envers la position C3 ou C2 n'a pas été établie au préalable puisque ces deux réactions sont intéressantes et ne sont pas décrites dans la littérature. Ne sachant pas quelle position privilégier, nous avons choisi cinq métaux de réactivités différentes ainsi que neuf ligands. La réaction de couplage entre l'indole **13** et l'iodocyclohexane **14** a été choisie comme réaction modèle pour la formation de **15** ou **16**. Avec un mélange de 10 mol% de chaque métal et 5 mol% de chaque ligand dans chaque réaction, trois solvants et cinq bases ont été criblés en quinze réactions dans l'étape 1 (Schéma 8). Malgré une conversion extrêmement faible, les combinaisons avec AgOAc dans le 1,4-dioxane, le toluène et le *o*-xylène ont donné le dérivé **15**. Le processus de déconvolution des métaux a révélé que seul le $Pd(OAc)_2$ donnait 5% de conversion pour le composé **15**. Avec AgOAc et le *o*-xylène, les neuf ligands ont été arbitrairement divisés en trois groupes et évalués en combinaison avec trois sources de palladium en raison de la faible conversion obtenue. Le meilleur résultat obtenu, est la combinaison entre $Pd(OAc)_2$ avec les ligands xantphos, BBBPY et MesCOOH avec un maximum de 5% de conversion (Etape 2b). L'étape suivante a révélé que la

combinaison entre $Pd(OAc)_2$ et MesCOOH a donné le rendement le plus élevé dans ces conditions expérimentales (Etape 2c). Malheureusement, malgré des efforts significatifs pour tenter d'optimiser les conditions, nous ne sommes pas parvenus à améliorer le rendement de la réaction.

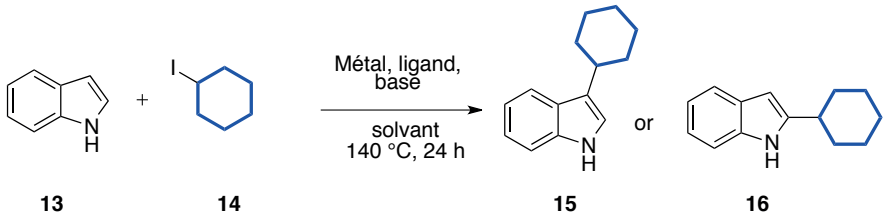

Métaux - $NiCl_2$• dme, $Pd(OAc)_2$, $[Ir(OCH_3)(C_8H_{12})]_2$, $Fe(acac)_3$, $Rh(PPh_3)Cl_2$

Ligands - PCy_3, dppf, dppp, PPh_3, xantphos, MesCOOH, PivOH, 1,10-Phenanthroline, BBBPY.

Etape 1: Tous les métaux (10 mol%) et tous les ligands (5 mol%), 3 solvants and 5 bases.

Etape 2a: Métal individuel (10 mol%) et tous les ligands (5 mol%) criblés avec AgOAc dans l'*o*-xylene.

Etape 1	1,4-dioxane	toluene	*o*-xylène
AgOAc	3%	3%	5%
KOAc	<1%	<1%	<1%
LiO*t*Bu	<1%	<1%	<1%
K_2CO_3	<1%	<1%	<1%
CsF	<1%	<1%	<1%

Etape 2a	**Yield**
$NiCl_2$• dme	<1%
$Pd(OAc)_2$	5%
Ir	<1%
$Fe(acac)_3$	<1%
$Rh(PPh_3)Cl_2$	<1%

Etapes 2b-c: Toutes les réactions se font dans le *o*-xylene avec AgOAc, 10 mol% de métal et 5 mol% de ligand.

Etape 2b	$AllylPdCl_2$	$PdCl_2$	$Pd(OAc)_2$
Xantphos, BBBPY, MesCOOH	2%	<1%	5%
PivOH, dppf, PCy_3	2%	<1%	<1%
1,10-Phen, PPh_3, dppp	<1%	<1%	<1%

Etape 2c	$Pd(OAc)_2$
Xantphos	<1%
BBBPY	<1%
MesCOOH	14%

Schéma 8. Identification d'un système catalytique en 32 combinaisons.

CHAPITRE 5

Le chapitre 5 décrit les perspectives d'utilisation de la méthode combinatoire en catalyse asymétrique. De manière à développer les meilleurs catalyseurs chiraux, il est essentiel de comprendre les règles qui régissent la sélectivité. L'interprétation de l'induction asymétrique repose sur la théorie de l'état de transition formé au cours de la réaction. En considérant deux énantiomères, il est important de souligner que la différence entre les deux états de transitions diastéréoisomériques est extrêmement faible énergétiquement (1-4 kcal/mole). Ces dernières années, la recherche du catalyseur idéal s'est axée sur une approche rationnelle ou sur une approche empirique de type «essais et erreurs». Beaucoup de ligands chiraux ont ainsi révélé une bonne induction asymétrique. Cependant, ces ligands, très efficaces pour une réaction et un substrat donné, ne sont souvent pas généralisables à d'autres substrats ou d'autres réactions. De plus, il est difficile de modifier ponctuellement ces ligands pour optimiser l'induction asymétrique. L'idée est donc d'augmenter les chances d'avoir une bonne énantiosélectivité en générant *in situ* des mélanges de catalyseurs chiraux tout en diminuant le nombre de manipulations à effectuer.

Dans le chapitre 3, nous avons pu voir que l'acide pentafluorophényleboronique et l'acide tartrique formaient également une combinaison active dans la réaction modèle de Friedel-Crafts. Afin de générer la chiralité au sein du catalyseur, l'acide tartrique a donc été choisi pour l'élaboration d'une librairie de ligands chiraux. Nous pouvons donc envisager 1) le développement d'une plateforme de ligands chiraux avec la même structure de base par une approche de type « Synthèse orientée vers la diversité » puis 2) de tester cette série de ligands chiraux en combinaison avec une série d'acides boroniques sur une réaction asymétrique d'hétéro Diels-Alder généralement catalysée par des acides de Lewis. L'acide tartrique est un châssis de départ intéressant dans la mesure où il est facilement modifiable notamment par estérification. Celui-ci peut être diversifié à partir de l'intermédiaire **17** par introduction, sur l'un des groupements hydroxyles libres, d'acides aminés protégés chiraux de types apolaires (Schéma 9). Une deuxième étape d'hydrogénation des groupements benzyl est nécessaire pour l'obtention de six nouveaux ligands chiraux. Cette synthèse permet d'augmenter la diversité structurale en utilisant des composés peu onéreux.

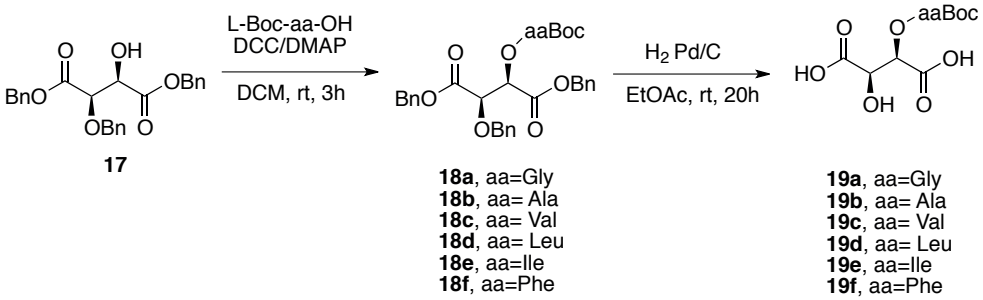

Schéma 9. Synthèse de dérivés d'acide tartrique à partir d'un intermédiaire commun.

La reaction d'hétéro Diels-Alder a été choisie comme modèle pour démontrer le potentiel de cette méthode en catalyse asymétrique. Comme précédemment, les ligands chiraux synthétisés ainsi que les acides boroniques sélectionnés, seront criblés en mélanges en ne variant qu'un seul paramètre par réaction, le solvant. Quatre solvants connus pour induire une bonne réactivité et une bonne énantiosélectivité dans ce type de cyclisation ont été utilisés. Malheureusement, cette première étape n'a pas permis de sélectionner clairement le meilleur solvant puisqu'aucun n'a permis d'obtenir, en même temps, le meilleur rendement et la meilleure énantiosélectivité. Le meilleur compromis en terme de rendement et d'énantiosélectivité a été obtenu avec le dichlorométhane (Schéma 10). L'étape de déconvolution permet d'identifier les combinaisons ligand chiral et acide boronique qui donnent la meilleure énantiosélectivité. Une fois encore, cette seconde étape ne nous a pas permis de choisir une seule catégorie de combinaison gagnante (étape 2a); nous avons donc choisi de tester individuellement les huit combinaisons restantes dans l'étape 2b. La combinaison **19d**/acide *p*-methoxyphénylboronique a induit un excellent excès énantiomérique (96%) avec cependant l'obtention d'un faible rendement pour **(*S*)-22**.

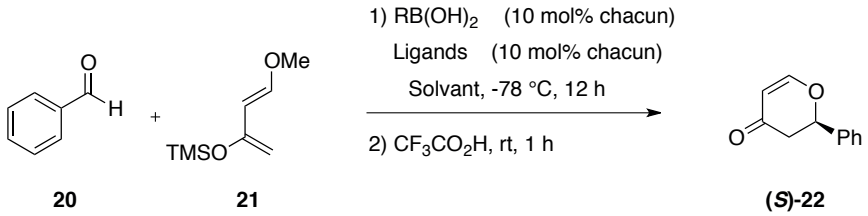

Etape 1: Criblage de mélange d'acides boroniques et de ligands

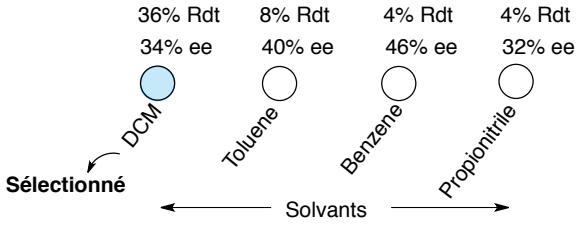

Etape 2 (17 réactions)**:** toutes les réactions sont effectuées dans le DCM

Etape 2a *t* = 12 h	2 acides boroniques B	2 acides boroniques B'	2 acides boroniques B''
19c, 19d	Rdt 10% 2% ee	Rdt 12% 24% ee	Rdt 14% 42% ee
19b, 19e	Rdt 10% 2% ee	Rdt 6% 32% ee	Rdt 38% 40% ee
19a, 19f	Rdt 24% 2% ee	Rdt 13% 12% ee	Rdt 26% 24% ee

Etape 2b *t* = 12 h	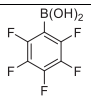	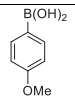
19d	Rdt 50% 54% ee	Rdt 6% 96% ee
19c	Rdt 33% 54% ee	Rdt 9% 38% ee

Etape 2b' *t* = 12 h	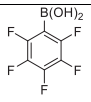	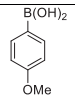
19e	Rdt 53% 72% ee	Rdt 7% 42% ee
19b	Rdt 28% 22% ee	Rdt 18% 34% ee

Schéma 10. Identification d'un catalyseur en deux étapes.

Malheureusement, cette méthode ne nous a pas permis d'identifier un bon catalyseur en un minimum de réactions. Chaque étape a été sujette à débat pour choisir la bonne suite des opérations et a entraîné la nécessité de tester individuellement plusieurs combinaisons. De ce fait, l'approche combinatoire de mélanges complexes de catalyseurs chiraux qui n'ont pas la

même constante d'association peut difficilement se substituer au criblage de combinaisons individuelles.

Le chapitre 6 contient les conclusions générales de ce travail où nous avons développé une méthode de criblage en employant une mixture de catalyseurs tout en testant un ou deux autres paramètres réactionnels supplémentaires en one-pot. Des perspectives d'évolution de ce travail seront également explorées.

La dernière partie est la partie expérimentale, qui présente le détail de chaque expérience, les protocoles de synthèse ainsi que les procédures de caractérisation des produits synthétisés.

CHAPTER 1

General Introduction

1.1 Towards a new paradigm in reaction/catalyst development

1.1.1 The multidimensional problem of catalytic reaction development

Catalytic reaction development is a complex multidimensional problem and involves the convergence of multiple reaction parameters that are often unique to a desired reactivity. In a representative scenario, the incorrect choice of ligand, metal, acid/base, oxidant/reductant or solvent can completely suppress the desired reactivity. Interests in total synthesis[1] or useful chemical transformations[2] have often been the guideline for catalytic reaction development. Highly active catalysts are often designed based on a rational approach that requires knowledge of the relationships between the structural features of catalysts and the substrates. Most of the time, the investigation of such complex systems may need *a priori* understanding of the mechanism in order to efficiently tune parameters and achieve high catalytic activities and yields. The discovery and optimization process therefore requires a number of experiments that grows exponentially with the number of reaction parameters. Screening just three parameters (e.g. metal pre-catalyst, ligand and solvent) and exploring only five possibilities per parameter would require 125 (5^3) reactions. If one concedes that the chances of finding an initial "hit" are governed by probability, performing a large number of experiments should increase the chances of a successful outcome. Using traditional laboratory methods, the time scale for such a process is often measured in months or years and this level of productivity is no longer acceptable for industries that seek shorter and more environmentally friendly processes in the worldwide competition. Methods that rapidly screen multiple parameters in a high throughput manner or that reduce the required number of reactions are thus appealing.

[1] (a) K. C. Nicolaou, S. S. Snyder, *Proc. Natl. Acad. Sci. U.S.A*. **2004**, *101*, 11929–11936; (b) M. S. Taylor, E. N. Jacobsen, *Proc. Natl. Acad. Sci. U.S.A*. **2004**, *101*, 5368–5373.
[2] (a) L. F. Tietze, U. Beifuss, *Angew. Chem. Int. Ed*. **1993**, *32*, 131-163; (b) E. J. Corey, X.-M. Cheng, The Logic of Chemical Synthesis (Wiley-Interscience, New York, 1995); (c) M. Fialkowski, K. J. M. Bishop, V. A. Chubukov, C. J. Campbell, B. A. Grzybowski, *Angew. Chem. Int. Ed*. **2005**, *44*, 7263–7269; (d) K. J. M. Bishop, R. Klajn, B. A. Grzybowski, *Angew. Chem. Int. Ed*. **2006**, *45*, 5348–5354.

1.1.2 From rational strategy to randomly generated systems

1.1.2.1 High-throughput screening technology

During the past decades, high-throughput screening (HTS) approaches have been applied to increase the pace of development of new catalysts and/or reactions. With the development of miniaturization technology that uses standard 96 well microplates (Scheme 1.1), it is now possible to rapidly uncover novel reactivity by searching through a multitude of conditions.[3] To enable the simultaneous variation of reaction parameters, multidimensional approaches were developed where a large number of parameters can be optimized in the laboratory. Often thousands of conditions can be screened within a day, making the discovery process a lot more accessible. Randomly generated reaction conditions can be tested without resorting to rational approaches based on mechanistic preconceptions, thus enabling unexpected discoveries. Moreover, the parallel development of automated HTS technology benefits from the increased consistency and reproducibility of robotics compared to human hands. Furthermore, high-throughput screening techniques must rely on convenient and robust analytical tools. Very often, those techniques rely on standard analytical methods such as GC-MS or LC-MS, but creative alternative high-throughput detection methods have also been developed. Groundbreaking approaches will be discussed in section 1.2.2.2 and 1.2.2.3.

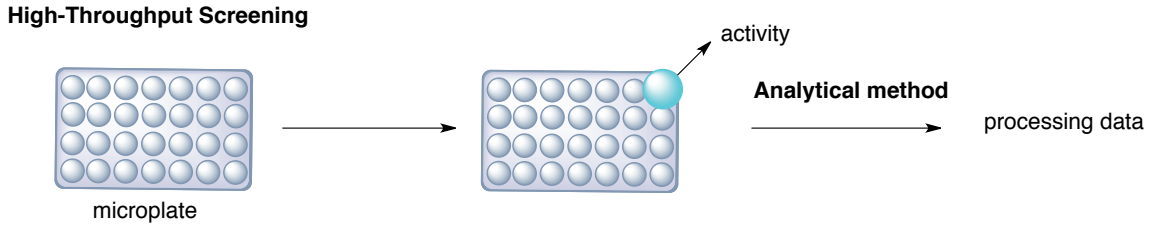

Scheme 1.1. HTS with standard microplates and analytical tools.

[3] For reviews on HTS technique, see: (a) M. T. Reetz, *Angew. Chem. Int. Ed.* **2001**, *40*, 312–329; (b) M. T. Reetz, *Angew. Chem. Int. Ed.* **2002**, *41*, 1335–1338; (b) J. G. de Vries, A. H. M. de Vries, *Eur. J. Org. Chem*. **2003**, 799–811.

1.1.2.2 Combinatorial chemistry

Another general strategy to facilitate the process of reaction/catalyst discovery relies on combinatorial chemistry to generate complex mixtures *in situ* from simple building blocks (Scheme 1.2). Here in a single process, a large mixture of compounds can be generated and screened against a specific target. The approach of mixing and synthesizing innumerable compounds is a strategy that has been adopted by Nature for billions of years.

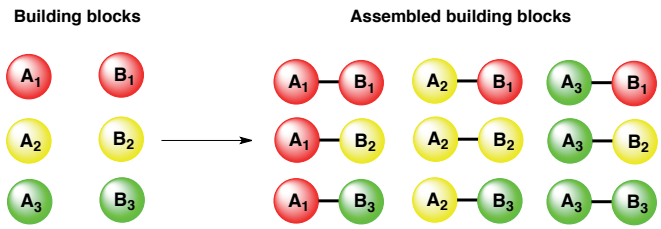

Scheme 1.2. *In situ* assembled compounds from simpler components in combinatorial chemistry.

A related concept that implicates reversible reactions is Dynamic Combinatorial Chemistry.[4] The resulting combinatorial library is a complex mixture of molecules that is defined by its distribution under thermodynamic control, though not all combinations are necessarily formed under a given set of conditions. Combinatorial approaches employing complex mixtures have long been applied in medicinal chemistry for the discovery of new drug scaffolds by screening mixtures against receptors or enzymes.[5] However, the use of complex mixtures is much less commonly employed in catalytic reaction development.

An overview of screening approaches for catalyst development and reaction development showcasing the use of high-throughput screening technology and combinatorial chemistry will be given.

[4] P. T. Corbett, J. Leclaire, L. Vial, K. R. West, J.-L. Wietor, J. K. M. Sanders, S. Otto, *Chem. Rev.* **2006**, *106*, 3652–3711.
[5] (a) N. K. Terrett, M. Gardner, D. W. Gordon, R. J. Kobylecki, J. Steele, *Tetrahedron* **1995**, *51*, 8135–8173; (b) R. W. Armstrong, A. P. Combs, P. A. Tempest, S. D. Brown, T. A. Keating, *Acc. Chem. Res.* **1996**, *29*, 123–131.

1.2 Representative applications in catalyst development

Due to the enormous complexities related to catalysis, success in catalyst development for a given target reaction is arguably just as often the result of serendipity as it is the result of knowledge-based chemical intuition. Given these realities, several impressive examples of catalytic reaction development have been enabled by combinatorial methodologies and HTS approaches over the last twenty years.[6] In seminal work by Menger in 1995, more than 100 catalysts were generated by the immobilization of eight carboxylic acids on a polyallyl amine backbone in the presence of a variety of metals. Each polymer was then screened individually for activity as phosphatase mimics for the hydrolysis of bis(*p*-nitrophenyl) phosphate **1** (Scheme 1.3).[7] A specific polymer composed of 15% imidazole, 10% phenol, 7.5% octyl in the presence of 5% Fe^{3+} (all percentages refer to the percentage of amine groups that were functionalized) led to the best rate acceleration (>3 x 10^4).

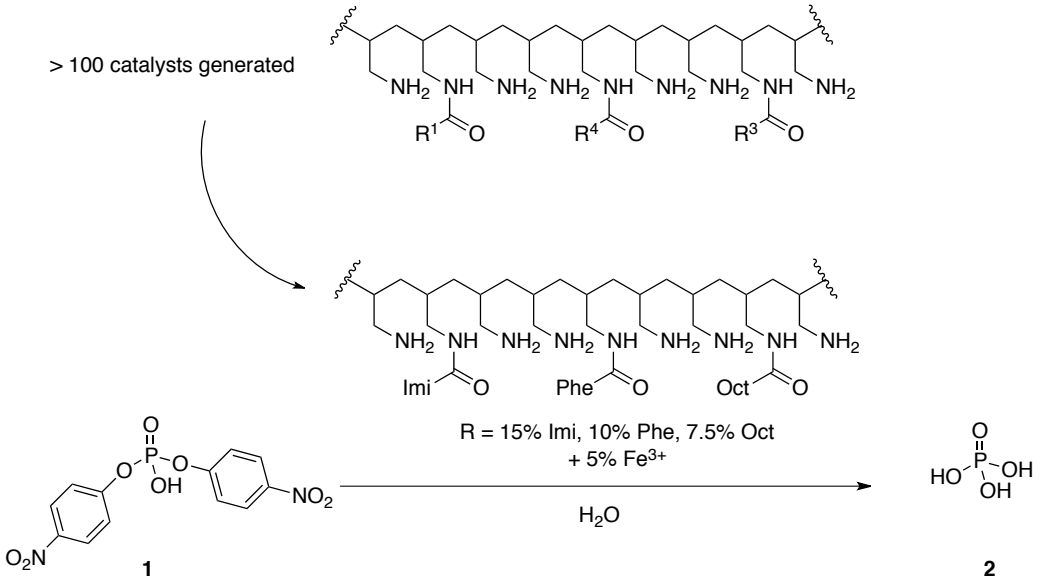

Scheme 1.3. Combinatorial methodology for the discovery of catalysts derived from eight functionalized carboxylic acids immobilized on polyallyl amine.

[6] (a) C. Gennari, U. Piarulli, *Chem. Rev.* **2003**, *103*, 3071–3100; (b) C. Jaekel, R. Paciello, *Chem. Rev.* **2006***, 106*, 2912–2942; (c) K. D. Collins, T. Gensch, F. Glorius, *Nat. Chem*. **2014**, *6*, 859–871.
[7] F. M. Menger, A. V. Eliseev, V. A. Migulin, *J. Org. Chem.* **1995**, *60*, 6666–6667.

In 1996, Burgess reported the first high-throughput catalyst screening that explores metal, ligand and solvent as a multidimensional problem (Scheme 1.4).[8] To exploit this concept, diastereoselective control of intramolecular metallocarbene C-H insertion from compound **3** to **(*R*)-4** or **(*S*)-5** was chosen as a probe. By screening each ligand with multiple metal sources in four different solvents, 96 different catalyst systems were generated in a microtitre plate. The presence of a chiral menthyl ester group allowed for the diastereoisomeric products to be separated using an analytical HPLC equipped with a silica column.[9] Via HPLC analysis, the yield and stereoselectivity could be determined in less than a week. Previously reported conditions for this transformation used Rh[10] or Cu[11] sources to achieve the transformation. Though the authors showed that the best diastereomeric ratios were obtained using the combination of a Cu pre-catalyst with ligand **6b** (61% yield, dr 3.9:1), comparable diastereoselectivities (dr 3.5:1) and higher yields (75%) were furnished via the novel combination of a silver pre-catalyst with ligand **6b**.

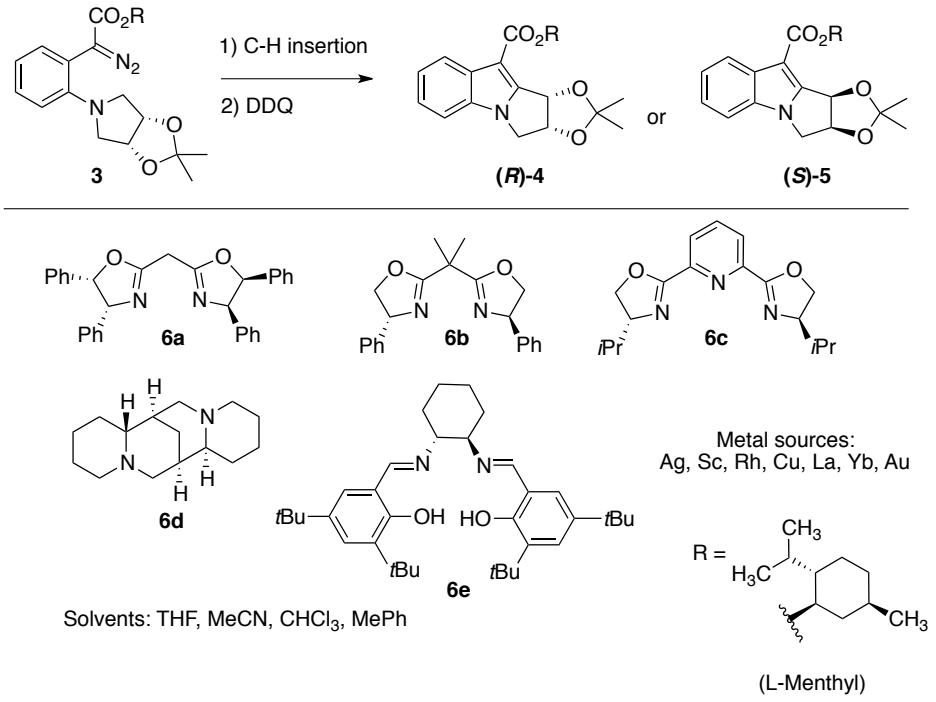

Scheme 1.4. First high-throughput catalyst screening exploring the interdependence of three parameters for high yield and stereoselectivity.

[8] K. Burgess, H. J. Lim, A. M. Porte, G. A. Sulikowski, *Angew. Chem. Int. Ed.* **1996**, *35*, 220–222.
[9] H.-J. Lim, G. A. Sulikowski, *J. Org. Chem.* **1995**, *60*, 2326–2327.
[10] M. P. Doyle, *Chem. Rev.* **1986**, *86*, 919–939.
[11] H.-J. Lim, G. A. Sulikowski, *J. Org. Chem.* **1995**, *60*, 2326–2327.

Later, Jacobsen highlighted the use of solid supported peptide based ligands for HTS in asymmetric olefin epoxidation.[12] In a first step, sixteen different chiral ligand scaffolds with twelve diverse end caps (16 x 12 = 192 ligand structures) were immobilized on a polystyrene support prior to pre-catalyst insertion. A set of thirty metals was added individually to the 192 ligands, potentially forming 5760 combinations. In a second step, all the generated complexes were screened on styrene derivative **7** in a single vessel to highlight a compatible oxidant/solvent system, revealing H_2O_2 and a 1:1 mixture DCM/*t*-BuOH as the lead conditions to give epoxide **8**. In a third step, screening thirty metals against the entire library pool identified a lead catalyst. $FeCl_2$ was shown to be the best pre-catalyst followed by a deconvolution process where two end caps gave promising results. Subsequent parallel libraries were used to determine ligand features important for high catalytic activity and to identify enantioselective catalyst structures such as **9** (Scheme 1.5).

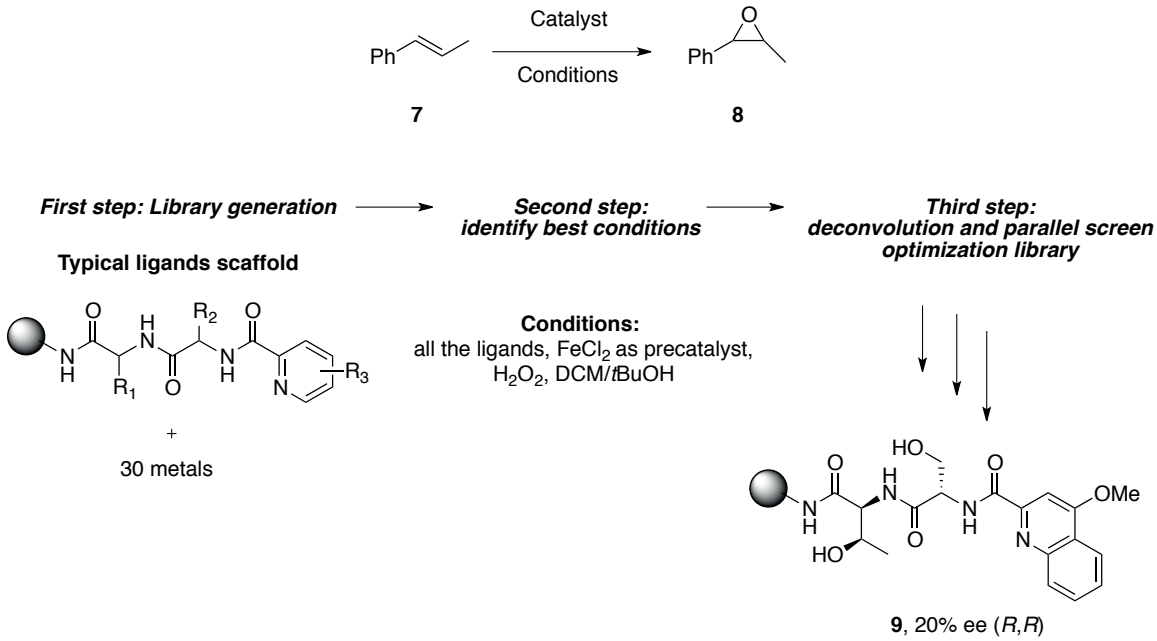

Scheme 1.5. Three-step combinatorial screen for the identification of new catalysts for asymmetric epoxidation.

Ding described the high-throughput screening of chiral diol–titanium–diol complexes for hetero Diels-Alder (HDA) reactions (Scheme 1.6).[13] The 2:1 self-assembly of BINOL derivatives with Ti was investigated with a library of 103 catalysts. Homocombination **13a**/Ti/**13a** revealed an enantiomeric excess of over 75% for compounds **12,** whereas

[12] M. B. Francis, E. N. Jacobsen, *Angew. Chem. Int. Ed.* **1999**, *38*, 937–941.
[13] J. Long, J. Hu, X. Shen, B. Ji, K. Ding, *J. Am. Chem. Soc*. **2002**, *124*, 10–11.

heterocombination **13a**/Ti/**13b** gave compounds **12** in over 95% ee. Soon after, Reetz reported the asymmetric hydrogenation of acetamidoacrylate catalyzed by *in situ* generated rhodium complexes assembled from two monodentate phosphine ligands. In many cases, a significant improvement of the stereoselective induction was observed when heterocombinations were screened.[14] Subsequently, Ding applied this concept to evaluate heterocombinations of chiral ligands with achiral ligands.[15] In general, enhanced stereoselectivity is observed with ligand heterocombinations, indicating that beneficial cooperative interactions give rise to more active or selective catalyst systems than the simple homocombinations.

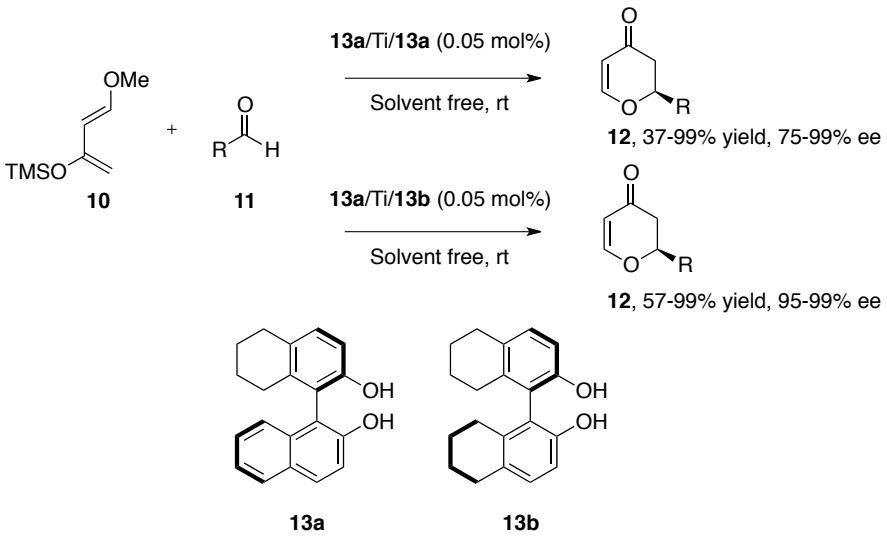

Scheme 1.6. Comparison of Ti catalysts derived from homocombinations and heterocombinations of chiral ligands in a HDA reaction.

Breit and coworkers achieved a breakthrough in the field of combinatorial catalysis by demonstrating a deconvolution approach to identify the most active and enantioselective catalyst for asymmetric hydrogenation from a complex mixture of catalysts.[16] A dynamic combinatorial library of bidentate phosphine ligands were generated through a H-bonding[17] self-assembly process between monodentate phosphine ligands L^{AD} and L^{DA}, providing 120 potential different combinations when combined with a rhodium pre-catalyst. Iterative deconvolution was performed in three steps; 1) the entire pool of ligands was divided into

[14] M. T. Reetz, T. Sell, A. Meiswinkel, G. Mehler, *Angew. Chem. Int. Ed.* **2003**, *42*, 790–793.
[15] K. Ding, *Chem. Commun.* **2008**, 909–921.
[16] J. Wieland, B. Breit, *Nat. Chem*. **2010**, *2*, 832–837.
[17] B. Breit, W. Seiche, *J. Am. Chem. Soc.* **2001**, *125*, 6608–6609.

four small groups, each containing six L^{AD} ligands and four to six L^{DA} ligands. Each subgroup was screened against the desired reaction (Scheme 1.7). In the second step, the subgroup that led to the best conversion and best enantiomeric excess was divided into smaller subsets and was evaluated again. Finally, the last step required testing the four remaining combinations to identify the best catalyst(s). Overall, this procedure needed only seventeen reactions to uncover the most efficient catalyst. In contrast, a traditional approach would have required 120 reactions.

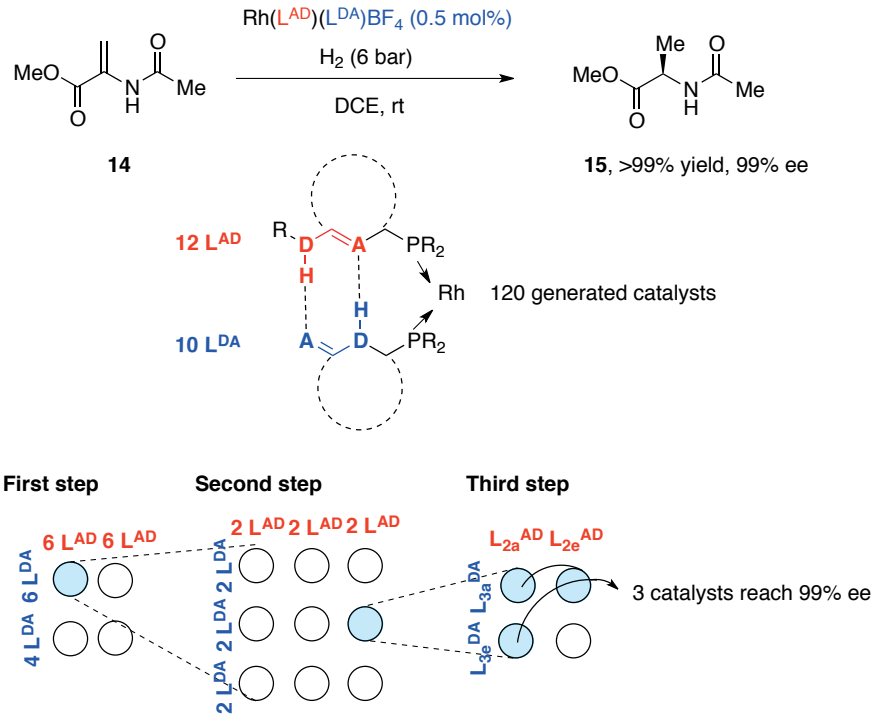

Scheme 1.7. Combinatorial approach and iterative deconvolution of 120 *in situ* generated catalysts for the identification of the most selective catalyst in 17 reactions.

1.3 Applications to reaction discovery

Porco and co-workers used a multi-well plate strategy to unearth new chemical scaffolds in drug discovery processes.[18] In order to maximize the chemical space explored, they assayed the reactivity of alkynylbenzaldehyde **16** with eighteen nucleophilic, electrophilic or cycloaddition partners in the presence of eleven metal catalysts (Scheme 1.8). Each combination of coupling partner and metal was screened in a separate reaction vessel. An initial reaction screen was performed on an analytical scale (5 μmol), and all reactions

[18] A. B. Beeler, S. Su, C. A. Singleton, J. A. Porco Jr, *J. Am. Chem. Soc.* **2007**, *129*, 1413–1419.

were analyzed using LC/MS/ELSD.[19] In this paradigm, conversions to a major compound of more than 20% based on ELSD area were studied and scaled up on traditional scale followed by full characterization of newly formed compounds. An important number of transformations were observed, typically involving Au and Ag pre-catalysts as shown in scheme 1.8. This approach uses a simple reaction set up coupled to simple analysis as the key advantage but only limited truly novel reactivity is discovered.

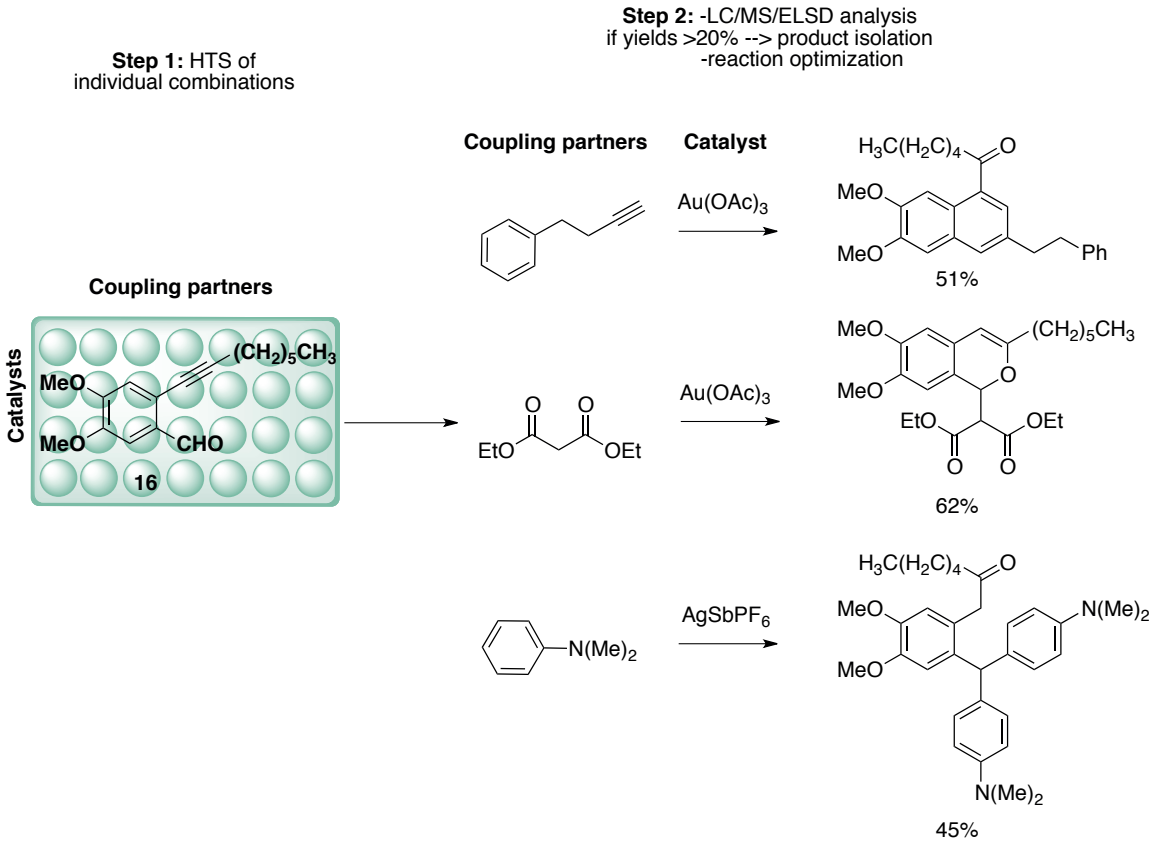

Scheme 1.8. Multi-well strategy to discover new chemical scaffolds.

In closely related work, MacMillan reported a HTS approach exploiting automated robotics coupled to GC-MS analysis.[20] In a first step, the process evaluated reactivity between a pool of substrates (e.g. alkynes, alkenes, nitriles, ketones, alcohols, etc.) exposed to a photoredox catalyst system and visible light in 96 well plates (Scheme 1.9). More than one thousand reactions can be screened in one day by only one experimentalist using the setup. One hit discovered during this screening process was the reaction between tertiary

[19] L. Fang, J. Pan, B. Yan, *Biotechnol. Bioeng*. **2001**, *71*, 162–171.
[20] A. McNally, C. K. Prier, D. W. C. MacMillan, *Science* **2011**, *334*, 1114–1117.

amine **17** and cyano-compound **18** leading to α-aminocyanobenzene **19** in 11% yield. After a routine optimization varying different Ir salts, bases and solvents, the authors disclosed an impressive substrate scope with reactions that proceed at room temperature within several hours. This coupled HTS/analysis process has the advantage of being able to screen thousands of reactions per day with minimal efforts but requires specific instrumentations and serial analysis.

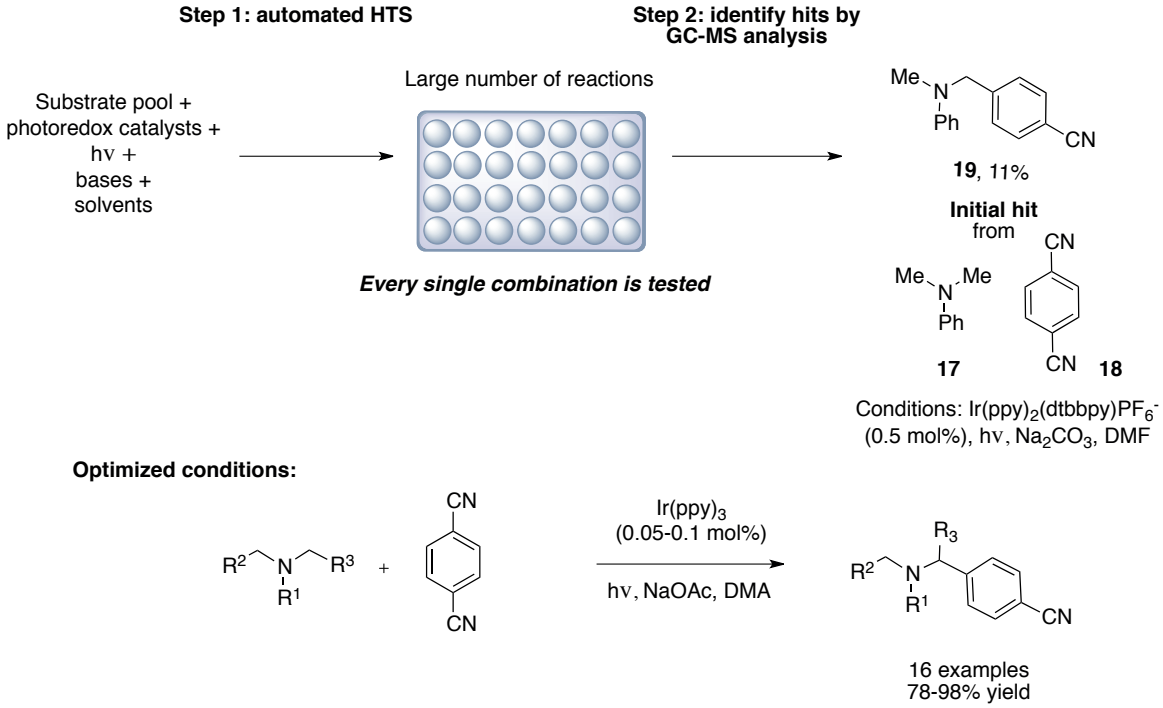

Scheme 1.9. HTS approach with automated robotics coupled to GC-MS analysis.

Hartwig investigated a novel approach to uncover novel reactivity by subjecting a complex mixture of diverse substrates to one pre-catalyst and one ligand at a time in a high throughput fashion. Seventeen different substrates were screened and potential coupling reactions were assayed by GC-MS.[21] The HTS showed several new signals in mass spectrometry, in particular an unknown compound that had a mass of 312 g/mol. The complexity of the analysis required an approach that could identify the two coupling partners responsible for the product formation. Towards that objective, a deconvolution strategy was used whereby the substrates were divided into smaller subsets (Scheme 1.10). When the expected mass was identified, the subsets were selected and were divided again into smaller subsets until the combination gave the right mass. The hydroarylation reaction between

[21] D. W. Robbins, J. F. Hartwig, *Science* **2011**, *333*, 1423–1427.

alkyne **20** and boronic acid **21** led to triaryl alkene **22**, the compound with a mass of 312 g/mol. After optimization of the reaction conditions, good reactivity and selectivity for the (*Z*)-olefin was found with a nickel-catalyzed system. Here, multiple reactions are screened in one vessel and analyzed as mixtures by the chemist making this process extremely difficult and time consuming.

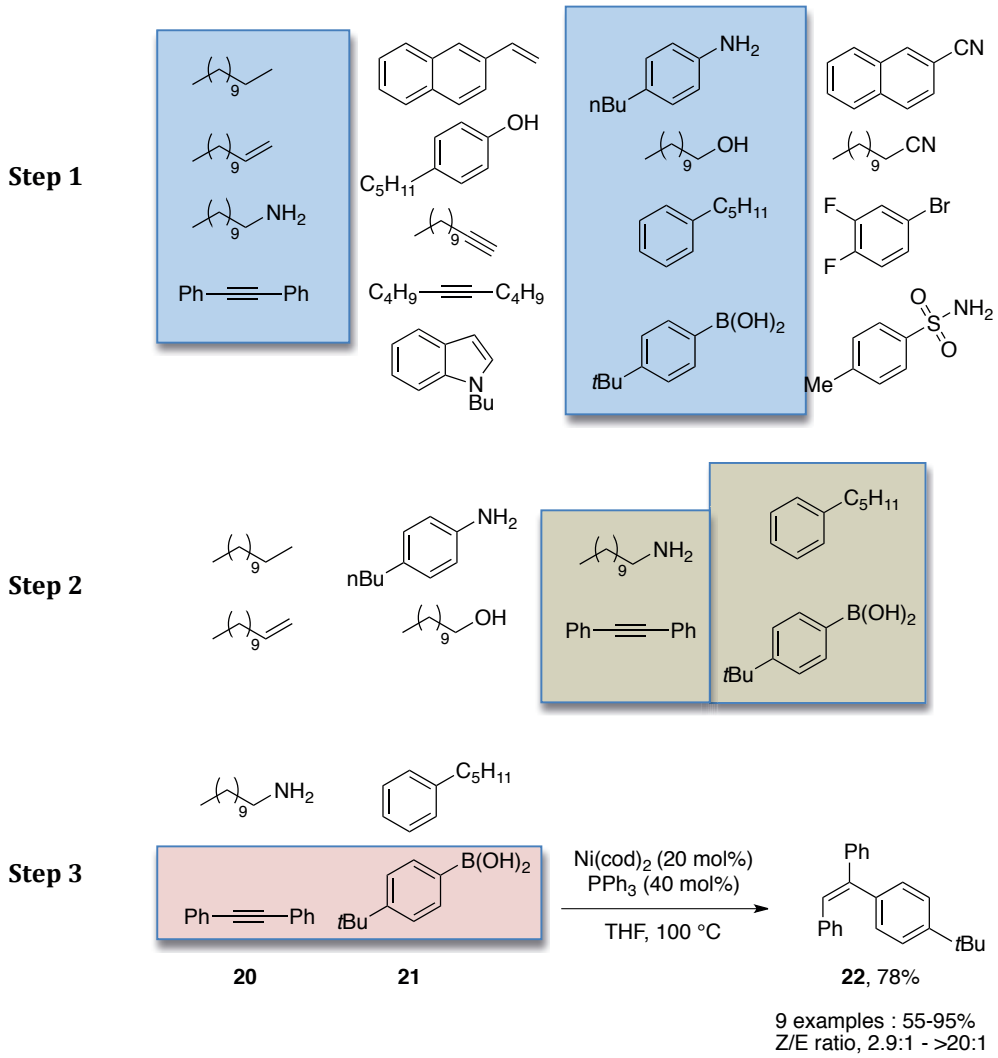

Scheme 1.10. HTS coupled to GC-MS analysis and deconvolution strategy to identify the coupling result.

In summary, multidimensional screens have been used to discover new catalysts or reactions in a variety of contexts and applications. However, they typically require access to specialized high throughput analytical equipment in order to serve as an expedient way to explore the intersection of at least three or four reaction parameters. Discovery strategies

based upon multisubstrate or multicatalyst screens produce complex mixtures that make subsequent analysis difficult. The previous examples described rapid catalyst or reaction discoveries, yet the identification of the substrates or catalysts responsible for the reactivity was non-trivial and required significant analytical efforts. Alternative creative screening approaches that address this dual screening/analytical challenge would be appealing.

1.4 Alternative screening approaches

1.4.1 Molecular tags

To respond to the analytical challenges associated with HTS approaches, specific tools have been developed over the last twenty years to streamline the reaction discovery process. Taran and co-workers have used enzymes to quantify the detection of target molecules. By employing a competitive enzyme immunoassay (EIA) based on the specific binding of antibodies,[22] yields and also enantiomeric excess of a desired compound can be measured by choosing an antibody that binds equally to the two enantiomers of the product or with an enantiospecific antibody, respectively. A three-step HTS procedure was carried out in search for chiral catalysts for the transfer hydrogenation of benzoyl formic acid **23** to mandelic acid **24** (Scheme 1.11).[23] First, every combination of 22 chiral diamine ligands with four metal pre-catalysts (two Ru sources, one Rh and one Ir) was tested. In a second step, the crude reaction mixtures were transferred to two 96-well microplates that contained a specific antibody in each well. For the yield determination, an enzyme conjugate that binds to the antibody is added and is responsible for the absorbance detected. Then, by a binding competition process, the product **24** that has a strong affinity with the antibody replaces the enzyme conjugate on the antibody whereas **23** cannot displace it. Decreasing absorbance results in an increasing concentration of product **24**. For the stereoselectivity determination, **(*S*)-24** that has a strong affinity with the antibody can replace the enzyme whereas **(*R*)-24**, which has lower affinity with the antibody, cannot. Again, a decreasing absorbance is correlated to an increasing concentration of **(*S*)-24** in solution. The lead combination Ru/ligand **25** gave quantitative yield with 81% ee for **(*S*)-24**. The analytical results were later

[22] F. Taran, P. Y. Renard, C. Créminon, A. Valleix, Y. Frobert, P. Pradelles, J. Grassi, C. Mioskowski, *Tetrahedron Lett.* **1999**, *40*, 1891–1894.
[23] F. Taran, C. Gauchet, B. Mohar, S. Meunier, A. Valleix, P. Y. Renard, C. Creminon, Jacques Grassi, A. Wagner, C. Mioskowski, *Angew. Chem. Int. Ed.* **2002**, *41*, 124–127.

independently confirmed to give 98% yield and 79% ee, validating the assay. In this way, hundreds of reactions can be screened in parallel and analyzed very quickly.

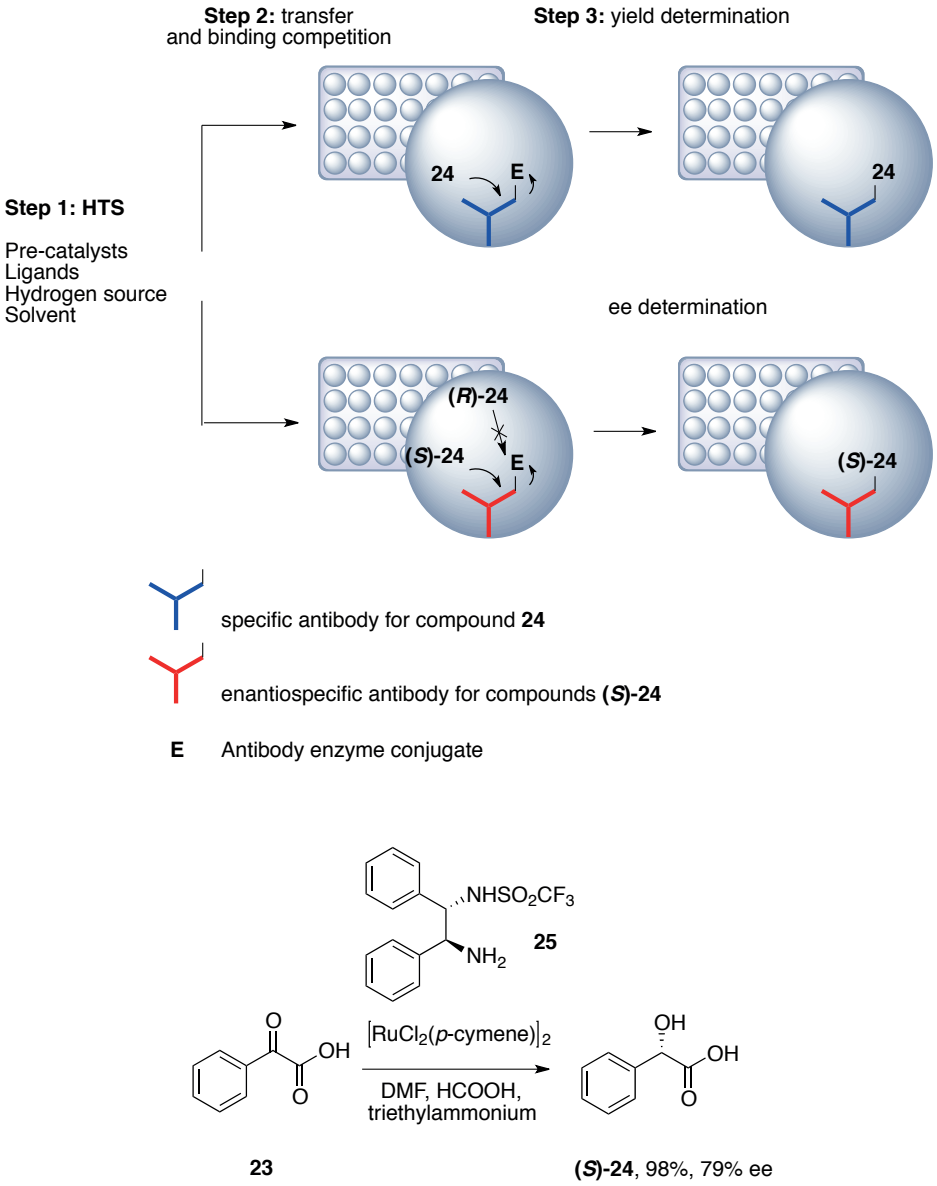

Scheme 1.11. HTS employing a competitive enzyme immunoassay to measure yield and enantiomeric excess in the asymmetric reduction of benzoyl formic acid **23** to **(*S*)-24**.

In 2005, a related immunoassay was developed for the optimization of classical cross coupling reactions.[24] ELISA immunoassays[25,26] require the binding of two different epitopes,

[24] P. Vicennati, N. Bensel, A. Wagner, C. Créminon, F. Taran, *Angew. Chem. Int. Ed*, **2005**, 44, 6863–6866.

representing the parts of an antigen that can be recognized by an antibody; one epitope that binds to a non-fluorescent antibody that is fixed on a solid support and a second epitope that binds a fluorescent antibody. If a covalent bond is formed between two reaction partners, immobilization of the tagged material on the solid support followed by binding with a signaling enzyme allow the reaction products to be detected and quantified by absorption measurements. Taran and coworkers applied this methodology to the optimization of Pd-catalyzed Sonogashira cross couplings in well plates (Scheme 1.12). The successful conditions were reproduced without decreased yields under typical laboratory conditions and in the absence of the tags.

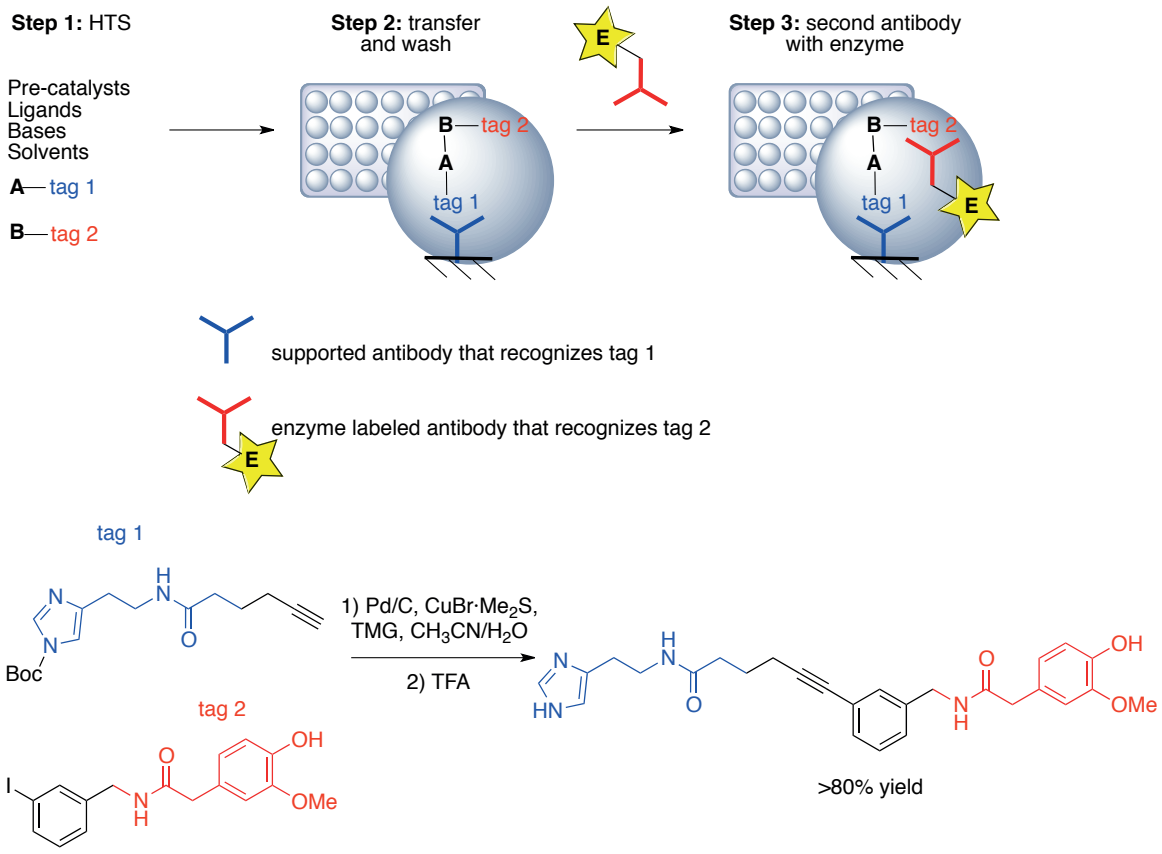

Scheme 1.12. HTS employing an ELISA immunoassay to identify a Sonogashira cross coupling.

After demonstrating the proof of concept for their methodology, Taran and coworkers applied the same approach to the discovery of new intermolecular catalytic reactions. In a

[25] E. Engvall, P. Perlma, *Immunochemistry* **1971**, *8*, 871–874.
[26] B. K. Van Weemen, *FEBS Lett.* **1971**, *15*, 232–236.

first group of reactants, twenty-one molecules, each bearing different functional groups, were all labeled with a certain tag. In a second group of reactants, sixteen compounds, each bearing different functional groups, were labeled with a second tag. In a HTS process, all possible combinations of reactions between the molecules of each group were tested in the presence of different catalysts, triethylamine as a base and DMA as a solvent.[27] In total, twenty-two hits over 5% yield were generated, thirteen of which were known transformations. The remaining nine novel reactions were scaled up and re-investigated under typical laboratory conditions in the absence of tags. Of these nine hits, seven gave a complex mixture of products and two gave well-defined products. Upon optimization, these two represented new copper-catalyzed routes to isoureas and 2-iminothiazolidines (Scheme 1.13). In this screening approach, parallel reaction analysis is of major interest and has demonstrated broad applicability but specialized biochemical skills and extensive pre-screen work are required.

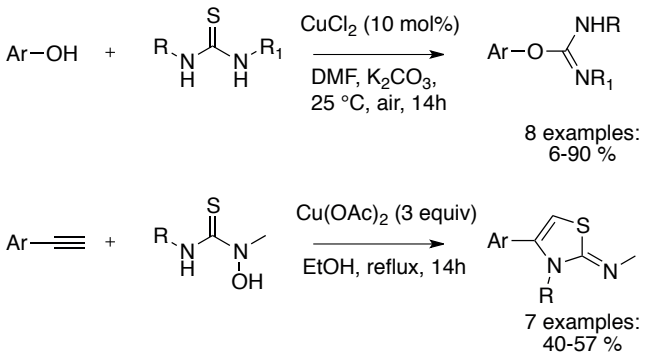

Scheme 1.13. HTS employing an ELISA immunoassay to identify two novel transformations.

In 2004, Liu developed a reaction discovery approach based on DNA templated screening.[28,29] In this method, substrates to be screened are divided into two groups. In the first group, molecules are covalently bound to DNA strands with one coding and one complementary region. In a second group, molecules are covalently interacting with a complementary strand via a disulfide bond and a biotin-tagged linker (Scheme 1.14). In a first step, the two groups are mixed together and Watson-Crick pairing of the single DNA strands permits their recognition and hybridization. In a second step, the newfound induced intramolecularity between the previously intermolecular reactive functional groups may

[27] J. Quinton, S. Kolodych, M. Chaumonet, V. Bevilacqua, M.-C. Nevers, H. Volland, S. Gabillet, P. Thuéry, C. Créminon, F. Taran, *Angew. Chem. Int. Ed.* **2012**, *51*, 6144–6148.
[28] Z. J. Gartner, D. R. Liu, *J. Am. Chem. Soc.* **2001**, *123*, 6961–6963.
[29] M. W. Kanan, M. M. Rozenman, K. Sakurai, T. M. Snyder, D. R. Liu, *Nature* **2004**, *431*, 545–549.

promote a reaction under a chosen set of reaction conditions. If no new covalent bond was formed between the strands during the second step, disulfide bond cleavage effectively removes the biotin tag from the DNA strand, In a third step, the remaining covalently bound strands (ie. the reactions that worked) are selected using streptavidin-biotin affinity labeling. After isolation, PCR amplification and DNA microarray analysis of the coded DNA strands leads to the identification of the successful transformation. By studying 168 substrate pairs using Na_2PdCl_4 as the catalyst, the screening revealed an unexpected hydrative coupling reaction between an alkene and an alkyne to give an enone. In this methodology, the reactions can be run on very small scale due to PCR amplification and all can be run in one vessel, but inherent incompatibilities with DNA give poor general applicability.

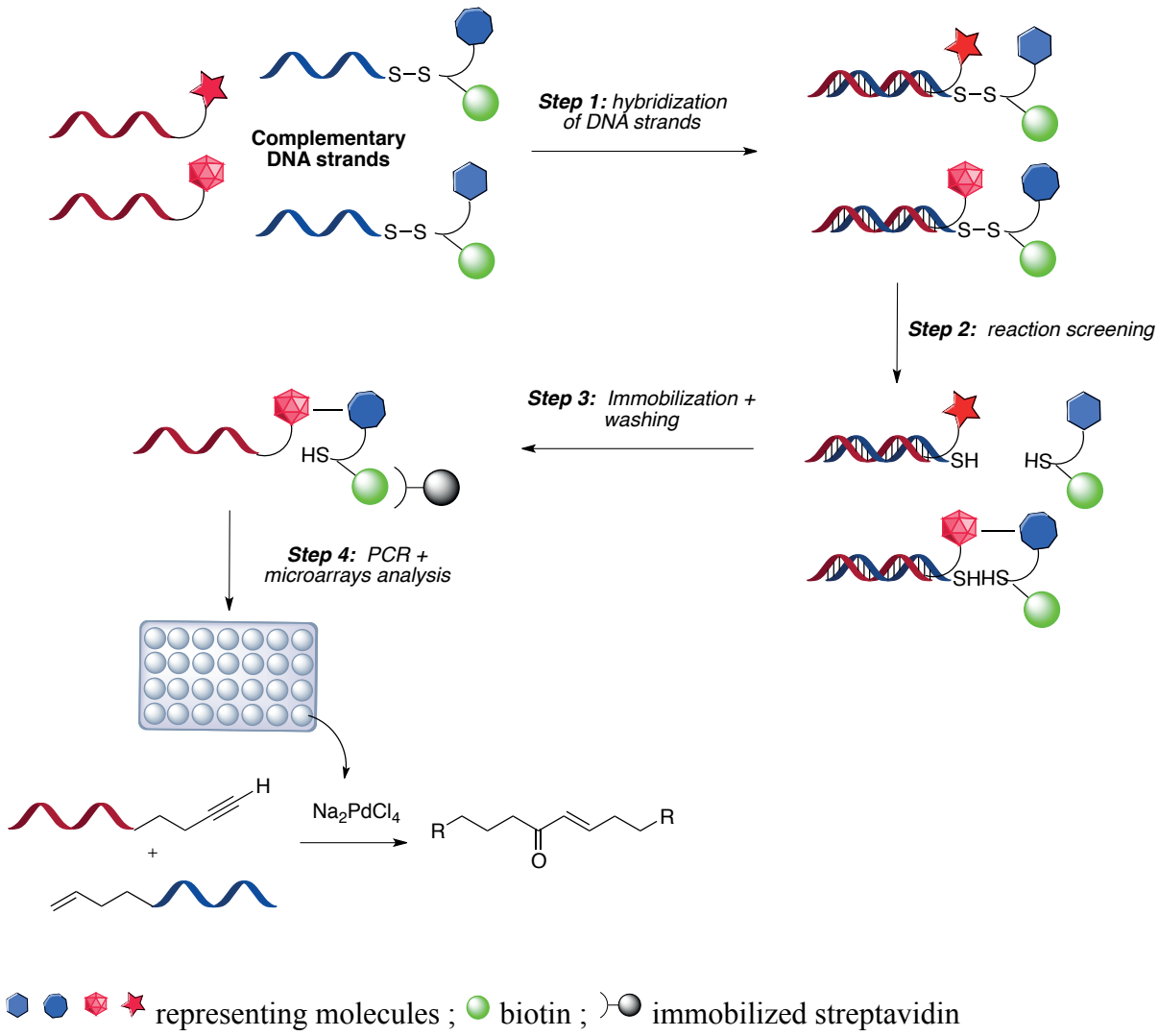

Scheme 1.14. DNA-templated reaction discovery of Pd-catalyzed enone formation from an alkene and an alkyne.

Crabtree and coworkers described a catalyst discovery tool based on colorimetry and fluorescence that does not require enzymes or antibodies. Reactive dyes bearing alkene or imine functional groups were selected such that a color change occurs upon catalytic hydrosilylation (Scheme 1.15), [30] providing a quantitative visual tool to monitor reaction progress. Reaction rates can be estimated by noting the initial time (t_i) corresponding to the first sign of bleaching (approximately 40% conversion) and the final time (t_f) corresponding to a total change of color (>95% conversion). Of all the catalysts screened, $(Rh(cod)(PPh_3)_2)PF_6$ was the best in both transformations (entry 6). Obviously, such screening methods are restricted to specific reaction classes.

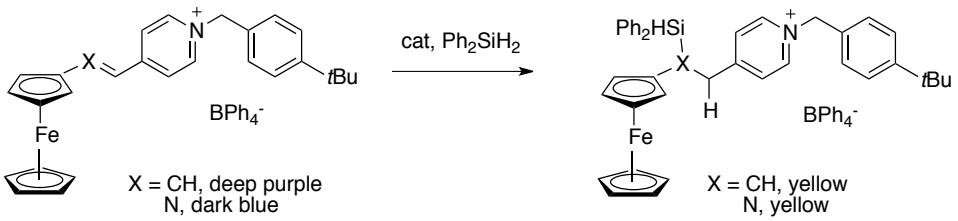

Entry	Catalyst	dye (X=CH) t_i/t_f-t_i	dye (X=N) t_i/t_f-t_i
1-5	Ni salts, Zr salt, Rh salts	-	-
6	$(Rh(cod)(PPh_3)_2)PF_6$	5/32 min	2/9 min
7	$(Rh(nbd)(PPh_3)_2)PF_6$	4/56 min	15/90 min
8	$RhCl(PPh_3)_3$	3/117 min	3/177 min
9	$(Ir(cod)(PPh_3)BF_4$	5/>45 min	5/>45 min
10	$RuCl_2(PPh_3)_2$	10/>45 min	10/>45 min
11	$(Pd(Ar_2PC_6H_4CH_2)OAc)_2$	1/114 min	1/114 min

Scheme 1.15. Reactive dyes bearing alkenes or imines that change color upon hydrosilylation.

In 2001, Hartwig described a FRET (Förster resonance energy transfer)-based method for the discovery of reaction conditions for cyanoacetate arylation.[31] In general, FRET occurs when the fluorescence emission band of a donor overlaps with the excitation band of an acceptor while the two are within a distance of 80 Å.[32] Their model reaction system is

[30] A. C. Cooper, L. H. McAlexander, D.-H. Lee, M. T. Torres, R. H. Crabtree. *J. Am. Chem. Soc*. **1998**, *120*, 9971–9972.
[31] S. R. Stauffer, N. A. Beare, J. P. Stambuli, J. F. Hartwig, *J. Am. Chem. Soc*. **2001**, 123, 4641–4642.
[32] (a) P. G. Wu, L. Brand, *Anal. Biochem.* **1994**, *218*, 1–13; (b) L. Stryer, R. P. Haugland, *Proc. Natl. Acad. Sci. U.S.A.* **1967**, *58*, 719–726.

composed of the cyanoester derivative **26** bearing a strongly fluorescent dansyl fluorophore and an azodye quencher **27** bearing an arylbromide moiety (Scheme 1.16). If the coupling between **26** and **27** occurs, the accompanying decrease in fluorescence allows the reaction yield to be estimated. Using a 96-well microplate, the screening of 113 ligands and multiple bases led to the identification of a very efficient catalytic system via Pd-catalysis. Fluorescent detection approaches inevitably need special tags that make undirected screens difficult to set up.

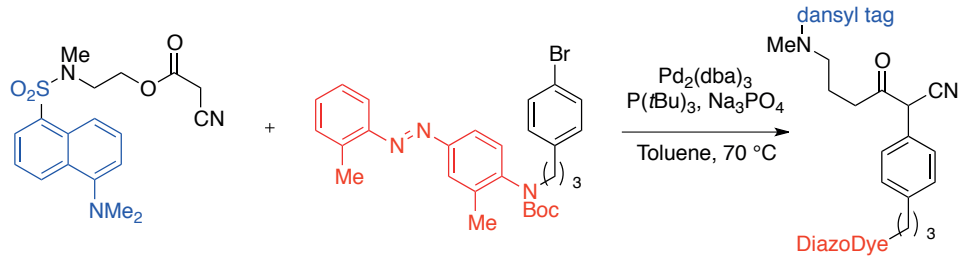

26 **27** **28**

Strong fluorophore **Fluorescence quencher** **Weak fluorophore (FRET)**

Scheme 1.16. Combined HTS and FRET strategy to identify efficient conditions for cyanoacetate arylation.

1.4.2 Tag free approaches

A tag free approach to HTS reaction optimization is appealing since it avoids laborious preparation of labeled starting materials. Berkowitz and coworkers reported an approach known as *In Situ* Enzymatic Screening (ISES), in which a well-established enzymatic reaction is coupled with a target reaction. The reaction network therefore produces a specific byproduct in addition to the desired synthetic product. The byproduct should diffuse into the aqueous phase where it can be transformed by the enzymatic process. The application of this methodology was described for an intramolecular allylic amination reaction (Scheme 1.17).[33] The ethanol byproduct diffuses to the aqueous phase, where it undergoes subsequent enzymatic oxidation to form NADH as a byproduct, which possesses an absorption maximum at 340 nm. The linear relationship between the release of NADH and its absorbance allows the yield of the desired compound to be estimated. Reactivity was

[33] D. B. Berkowitz, M. Bose, S. Choi, *Angew. Chem. Int. Ed.* **2002**, *41*, 1603–1607.

observed when several metal pre-catalysts were screened in one pot. In order to identify which metal was responsible for the catalysis, metals were removed one at a time until Ni was shown to be of great importance. To further optimize the conditions, $Ni(cod)_2$ was kept as the optimal pre-catalyst and multiple ligands were screened by using the same enzymatic process. The best system was determined to be the combination of Ni and the bidentate phosphine ligand dppb. This screening approach is highly limited to substrates that release alcohol as a byproduct during their reaction pathway.

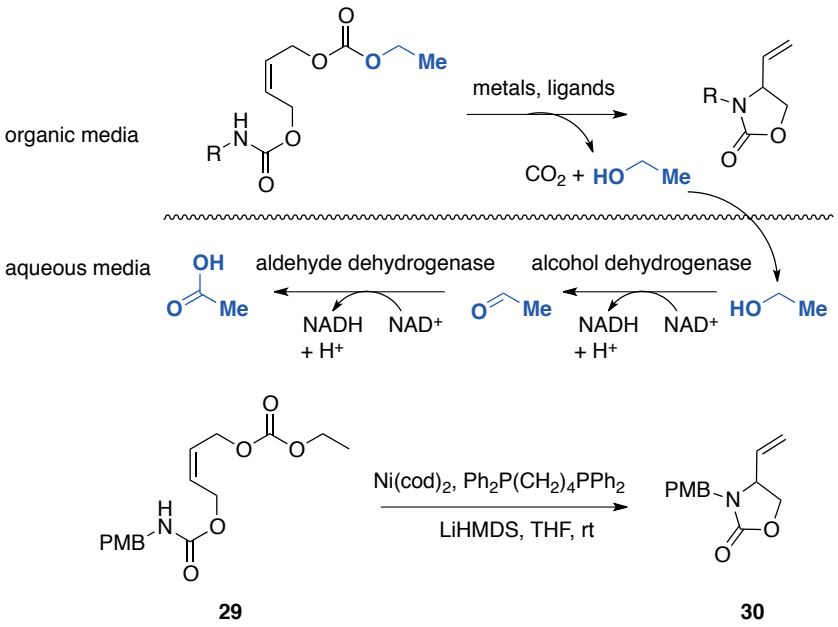

Scheme 1.17. Coupling of ethanol formation with enzymatic NADH release for the detection of an intramolecular allylic amination.

ESI-MS is an analytic technique, especially suited to the detection of ionic species and can thus be envisaged to examine reaction intermediates. Seminal reports by Chen described the detection of reaction intermediates bound to cationic catalysts in ethylene polymerization.[34] As polymerization progresses, the growing polymer binds to the metal and the selection of the best catalyst is made by detection of the longest chain. In this study, the screening of different catalysts as mixtures is possible due to different m/z values observed for each cationic intermediate.

From these observations, Pfaltz aimed to develop a method to measure induced enantioselectivites of different chiral catalysts for the kinetic resolution of the mass-labelled

[34] P. Chen, *Angew. Chem. Int. Ed.* **2003**, *42*, 2832–2847.

allylic esters displayed in red and blue in scheme 1.18.[35] Those two compounds are called pseudoenantiomers because they are differentiated by their absolute configuration and also by a slightly different aryl substituent so as to be suitable for the mass detection technique. An equimolar amount of the allylic esters are subjected to substoichiometric amounts of Pd complex with an achiral ligand or a chiral ligand. The measurement of the relative ratios of the cationic intermediates formed allows to determine the selectivity of the catalysts. The achiral complex provided signals of equal intensity and the chiral complex showed a 9:91 ratio towards allylic ester in blue. In this study, multiple metal–ligand systems have been screened simultaneously (up to 10 different catalysts) in respect to mass differentiation allowing fast catalyst screening and reaction discovery. Even if this method provides direct measurement of the catalyst activity, the requirement of the formation of ionic intermediates is a major drawback and limits the applicability to general reaction discovery.

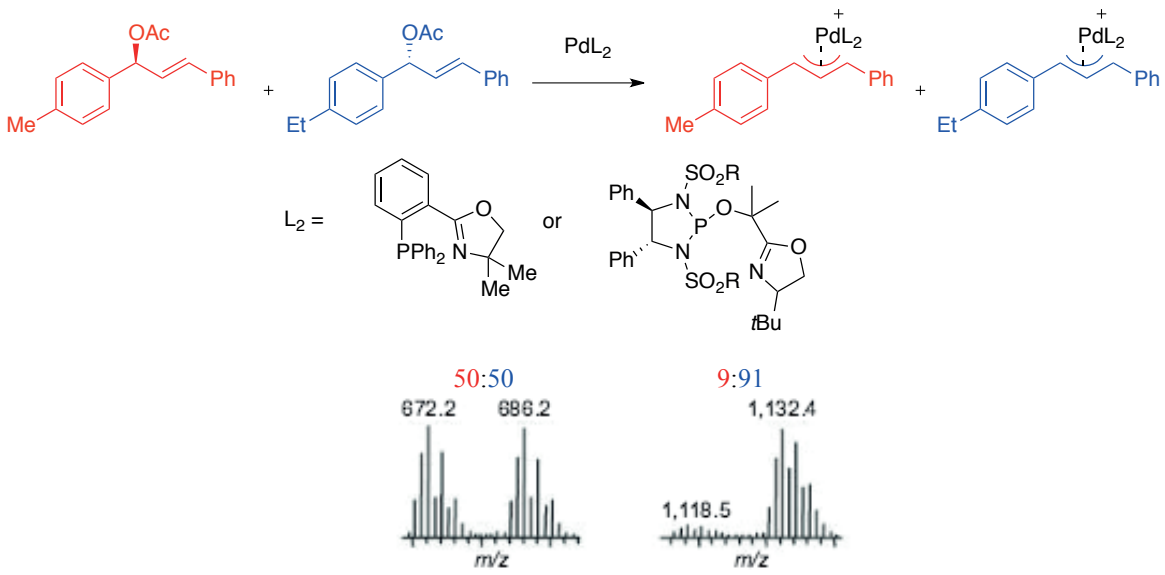

Scheme 1.18. ESI-MS detection of cationic intermediates to determine induced enantioselectivity in dynamic resolution of allylic esters.

1.5 Critical summary

All the methods that have been described in Chapter 1.4 and 1.5 led to the discovery of novel reactivity or novel reaction conditions. With HTS strategies, large numbers of reactions could be screened in parallel and analyzed in an efficient manner. In parallel, unique restrictions apply to each screening method. The need of specialized skills or specific

[35] C. Markert, A. Pfaltz, *Angew. Chem. Int. Ed.* **2004**, *43*, 2498–2500.

instrumental overhead is encountered quite often and thus not readily appliable to common chemical laboratories. While the multi-well strategies can be carried out with commercial materials, a suitable tandem separation/analysis instrument is required to analyze the outcome of each reaction and often those materials are expensive and thus not accessible to everyone. In the immunoassays screening approach, many reactions can be discovered but specific knowledge and extensive pre-work are required. In the fluorescence assays, products are carefully chosen such that their formation or degradation is spectroscopically quantifiable but extensive pre-work needs to be done to install the fluorophores and poor applicability is shown. Positive aspects in the DNA-template method lie on the small scale on which the reactions can be run in HTS; the use of PCR can allow the screens to be run on femtomole amounts. In contrast, severe limitations in substrate scope, applicability, compatibility with usual reaction conditions (organic solvents) are inherent to the method tools. The DNA-templated method requires substrates or solvents that do not interact with DNA. While the fast quantifying ability of ISES methology is appealing, limitation to substrates that release alcohol as a byproduct is a major inconvenience for reaction discovery via this method.

1.6 Aim of the thesis

Linear optimization approaches have thus far been the traditional way of improving reaction yield or selectivity. Likewise, mechanistic intuition and serendipity have long been the traditional ways of discovering new reactions and catalysts. Unfortunately, the enormous complexity of chemistry and the many variables associated with a given reaction make this approach tedious and highly time consuming. Even with an excellent rational mechanistic hypothesis, success in reaction or catalyst development usually remains directly proportional to the number of experiments that are attempted.

To overcome these problems, many creative screening approaches have been developed for catalytic reaction discovery or optimization with the goal of making a large number of experiments easier to interpret and manage and ultimately to increase the rate of discovery. While the purposes of the many methods surveyed in this chapter vary widely, a general trend is that the bottleneck tends to be analysis rather than the ability to set up many experiments. Analytical methods that are extremely rapid and easy to interpret tend to have limited generality and applicability or require laborious synthesis of labeled starting materials. On the other hand, methods that are highly general (e.g. GC-MS) tend to be slower, more expensive and more difficult to interpret. The large number of reactions necessary to

explore the intersection of 3 or 4 reaction parameters still deters chemists who do not have access to expensive and specialized HTS facilities. Complementary approaches that can reduce the number of reactions required to obtain a lead result for a specific transformation are therefore appealing. Thus, we aim to develop new approaches to catalyst development and catalytic reaction discovery that still provide a large dose of serendipity without requiring such a large number of experiments. Strategies based on screening complex mixtures of catalysts might offer an alternative to traditional discovery approaches and a complementary method to HTS.

From this perspective, in Chapter 2 we will see a traditional example of catalytic methods development that serves to highlight those reaction parameters that are of the highest priority to explore during a screening process. More generally, the importance of solvent effects and acid/base additives in catalytic reactions are demonstrated. Specifically, the combination of nitromethane and $B(C_6F_5)_3 \bullet H_2O$ were found to exhibit exceptional reactivity and chemoselectivity in direct alcohol substitution.

In Chapter 3, we will demonstrate a proof of principle for a simple combinatorial method that can drastically reduce the number of experiments required to find a lead result by screening complex mixtures of *in situ* generated catalysts. Screening mixtures of *in situ* generated boron catalysts against one or two additional reaction parameters led to the rapid discovery of new catalytic systems for direct alcohol substitution.

In Chapter 4, to evaluate the screening approach in more mechanistically complex and diverse catalytic systems, we investigated two different types of transition metal-catalyzed C-H activation.

In Chapter 5, we set out to explore the limitations of the combinatorial strategy as it relates to the development of catalytic asymmetric reactions by employing mixtures of chiral ligands and boron pre-catalysts in a model hetero Diels-Alder reaction.

Finally, Chapter 6 will summarize the conclusion of the thesis, provide some examples of how the combinatorial method developed in this thesis has been applied by others in the laboratory in different contexts, and lay out the perspectives for future applications and directions for the concepts developed herein.

CHAPTER 2

Neutral Lewis Acids – Effective and Chemoselective Catalysts for Direct Alcohol Substitution[36]

[36] Portions of this chapter have been published: (a) M. Hellal, F. C. Falk, E. Wolf, M. Dryzhakov, J. Moran, "Breaking the Dichotomy of Reactivity vs Chemoselectivity in Catalytic S_N1 Reactions of Alcohols", *Org. Biomol. Chem.* **2014***, 12,* 5990–5994; (b) M. Dryzhakov,‡ M. Hellal,‡ E. Wolf, F. C. Falk. J. Moran, "Nitro-Assisted Brønsted Acid Catalysis: Application to a Challenging Catalytic Azidation", *J. Am. Chem. Soc.* **2015**, 10.1021/jacs.5b06055.

2.1 Introduction

2.1.1 Overview of alcohol activation

The nucleophilic substitution of alcohols is an important class of transformations that allows access to a wide variety of compounds. Due to the poor leaving group ability of the hydroxide anion, a two-step protocol for the nucleophilic substitution of alcohols is commonplace. Alcohols are often converted to the corresponding acetate, tosylate or halide intermediates with higher electrofuge abilities prior to nucleophilic substitution. One-step procedures employing stoichiometric amounts of activating reagents, such as the Mitsunobu reaction, have been widely developed.[37] Unfortunately, these approaches are often highly wasteful as they are non-ideal in terms of atom economy, step economy or both. The direct catalytic nucleophilic substitution of alcohols is therefore an important goal in modern chemistry and appears among the major green chemistry research areas.[38] In 2005, the ACS Green Chemistry Roundtable identified catalytic direct alcohol activation as a top challenge because it is an ideal transformation that produces water as the only byproduct (Scheme 2.1).

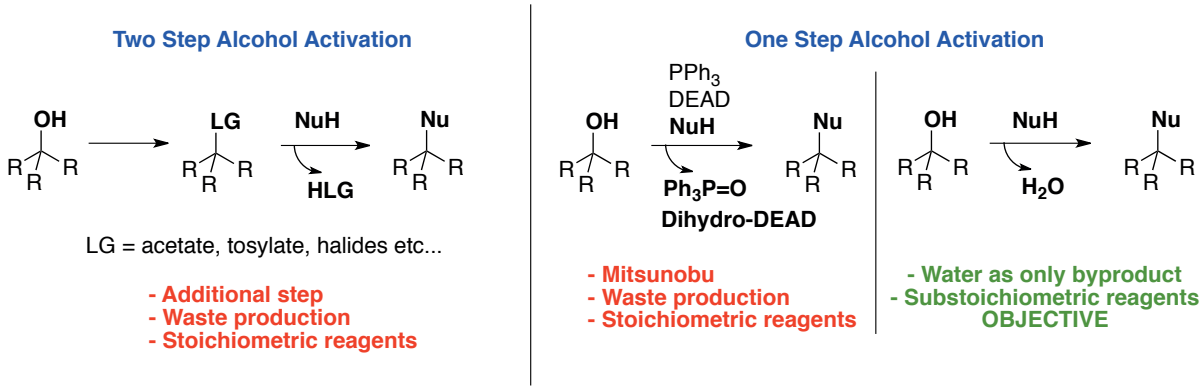

Scheme 2.1. Two- and one-step alcohol activation with ACS Green Chemistry objectives.

`

[37] (a) O. Mitsunobu, *Synthesis* **1981**, 1–28; (b) D. L. Hughes, R. A. Reamer, J. J. Bergan, J. J. Grabowski, *J. Am. Chem. Soc.* **1988**, *110*, 6487–6491; (c) M. Varasi, K. A. M. Walker, M. L. Maddox, *J. Org. Chem.* **1987**, *52*, 4235–4238.

[38] D. J. C. Constable, P. J. Dunn, J. D. Hayler, G. R. Humphrey, J. L. J. Leazer, R. J. Linderman, K. Lorenz, J. Manley, B. A. Pearlman, A. Wells, *Green Chem.* **2007**, *9*, 411–420.

2.1.2 Carbocationic intermediates and S_N1 pathways

Direct nucleophilic substitution of benzylic, propargylic, and allylic alcohols, collectively referred to as π-activated alcohols, and tertiary aliphatic alcohols may be achieved via Brønsted or Lewis acid-catalyzed S_N1 pathways. These catalysts facilitate the ionization of the C–O bond by electrophilic activation of the hydroxyl group (Scheme 2.2).

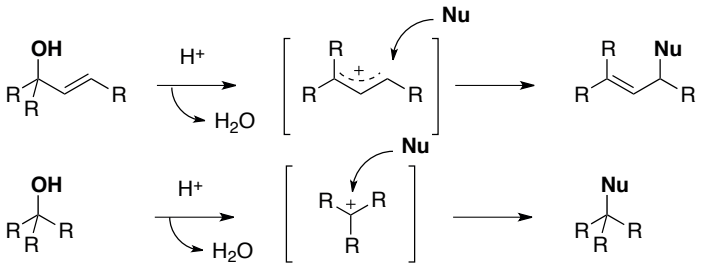

Scheme 2.2. Carbocation intermediates from alcohols and subsequent nucleophilic substitution.

The involvement of an S_N1-type pathway is highly dependent on the stability and reactivity of the cationic species generated and on the properties of the nucleophile. In such a manner, one can predict that some alcohols would be more reactive than others considering the carbocation electronics and sterics. Thus, in general, π-activated alcohols that benefit by definition from mesomeric effects can lead to stabilized carbocations and subsequent reaction with different nucleophiles.[39,40] Presumably, tertiary aliphatic carbocations where the positive charge is next to three alkyl groups with positive inductive effects, can form moderately stable carbocation intermediates.[41] Interestingly, reactivity follows the trend of the alcohol propensity to generate carbocations but variances from the nucleophile have been highlightened in using different metal catalysts.[42] General trends have been reported recently by the group of Samec, where generally higher conversions were observed for *S*-, *C*- and *N*-nucleophiles in the presence of Lewis acids and for *O*-centered nucleophiles in the presence

[39] H. Mayr, B. Kempf, A. R. Ofial, *Acc. Chem. Res,* **2003**, *36*, 66–77.
[40] H. Mayr, A. R. Ofial, *in Carbocation Chemistry* (Eds : G.A. Olah, G. K. S. Prakash); Wiley, Hoboken, (N.J.), **2004**, ch. 13, p. 331.
[41] (a) G. A. Olah, A. M. White, *J. Am. Chem. Soc.* **1969**, *91*, 5801–5810; (b) G. A. Olah, *Angew. Chem. Int. Ed.* **1995**, *34*, 1393–1405.
[42] S. Biswas, J. S. M. Samec, *Chem. Asian. J.* **2013**, *8*, 974–981.

of metals. Results showed that the nucleophilic substitution efficiency was more dependent on the nucleophile than on the electrophile.

The past ten years have seen an explosion of publications concerning Brønsted and Lewis acid catalyzed dehydrative substitution of π-activated alcohols[43] but several key challenges remain. Notably, dehydrative substitution of tertiary aliphatic alcohols is typically limited to processes where the 'catalyst' is present in stoichiometric quantities. Herein we provide a brief overview of the relevant literature.

2.1.3 General overview on acid catalyzed π-activated alcohol activation

2.1.3.1 Substitution via Brønsted acid catalysis

Hydroxyl activation is well known to occur under Brønsted acid catalysis. The last stage of the synthesis of tolderodine, for the treatment of urinary incontinence, has been performed using a Friedel-Crafts type transformation.[44] Initially, De Casto described a preliminary procedure with alcohol **31** and *p*-cresol **32** using Fe (III) chloride hexahydrate that did not lead to the formation of compound **33**. The tertiary amine coordinates to the metal center and inhibits the catalyst. However, in the presence of superstoichiometric quantities of strong Brønsted acids such as aqueous perchloric acid, the amine is fully protonated and leaves the benzylic alcohol available for *p*-cresol substitution (Scheme 2.3).

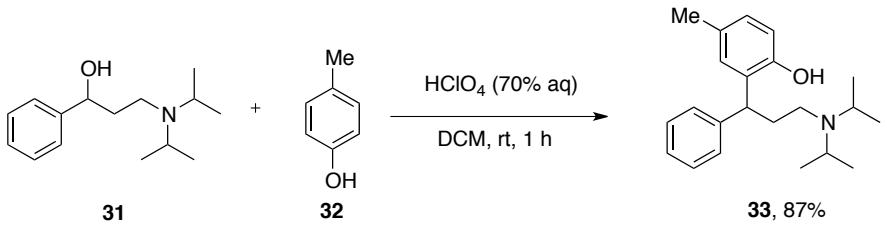

Scheme 2.3. Synthesis of *rac*-tolderodine involving a Friedel-Crafts reaction of a phenyl propane aminoalcohol with *p*-cresol.

[43] For reviews on direct activation of alcohols in cationic reactions, see: a) M. Bandini, M. Tragni, *Org. Biomol. Chem.* **2009**, *7*, 1501–1507; b) P. G. Cozzi, F. Benfatti, *Angew. Chem. Int. Ed.* **2010**, *49*, 264–267; d) E. Emer, R. Sinisi, M. G. Capdevila, D. Petruzziello, F. De Vincentiis, P. G. Cozzi, *Eur. J. Org. Chem.* **2011**, 647-666; e) B. Sundararaju, M. Achard, C. Bruneau, *Chem. Soc. Rev.* **2012**, *41*, 4467–4483.

[44] K. A. De Castro, H. Rhee, *Synthesis* **2008**, 1841–1844.

Sanz described an efficient direct nucleophilic substitution of propargylic alcohol **34** with diketone nucleophile **35** and diketoester **36**.[45] Substoichimetric amounts of *p*-toluenesulfonic acid led to the propargylated dicarbonyls **37** and **38,** respectively (Scheme 2.4). The procedure is suitable for several secondary and tertiary propargylic alcohols. Unfortunately, *p*-toluenesulfonic acid, even in catalytic amounts, is not compatible with common acid-sensitive protecting groups such as OTIPS.[46]

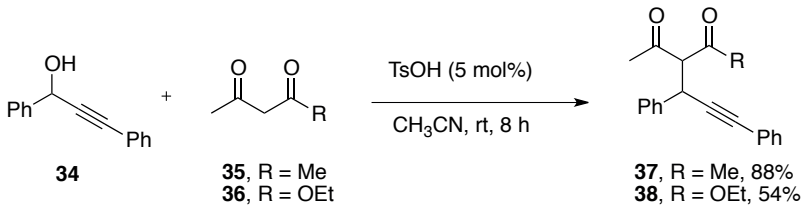

Scheme 2.4. Reaction between propargylic alcohols and diketone/diketoester in the presence of TsOH.

In 2008, Shimizu tested common Brønsted acids as catalysts for the allylic amination of trans-1,3-diphenyl-2-propen-1-ol **39** with primary protected amines in water. [47] TFA, MsOH, TsOH, and TfOH failed to afford the desired compound. Calix[4]resorcinarene sulfonic acid **44**, a water-soluble catalyst, gave excellent yields with *p*-toluenesulfonamide **40** and benzylcarbamate **41** as nucleophiles (Scheme 2.5). Probably because of low solubility of the starting materials in water, the hydrophobic environment of the cavity helps to bring the reagents together.

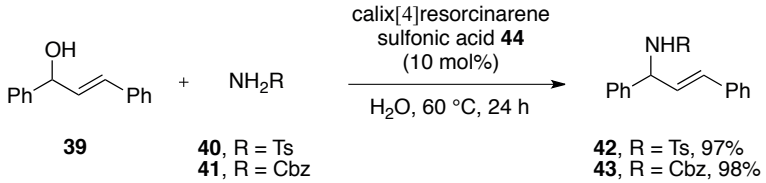

Scheme 2.5. Allylic amination in the presence of water-soluble calix[4]resorcinarene **44**.

Kaneda developed a remarkably efficient solid Brønsted acid catalyst with the use of H-montmorillonite, prepared via a mixture of Na^+-montmorillonite and aqueous HCl (1.1 wt

[45] R. Sanz, D. Miguel, A. Martínez, J. M. Ávarez-Gutiérrez, F. Rodríguez, *Org. Lett*. **2007**, *9*, 727–730.
[46] J. S. Panek, C. E. Masse*, J. Org. Chem.* **1997**, *62*, 8290–8291.
[47] S. Shirakawa, S. Shimizu, *Synlett* **2008**, 1539–1542.

%). This heterogeneous catalyst showed outstanding reactivity towards π-activated alcohols as well as secondary aliphatic alcohol **45** and diketone **46** (Scheme 2.6).[48,49]

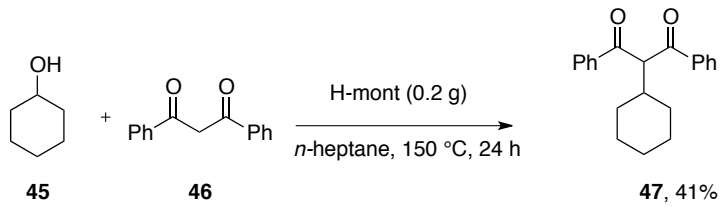

Scheme 2.6. Reaction between secondary aliphatic alcohol **45** and diketone **46** via heterogenous montmorillonite catalysis.

2.1.3.2 Substitution via Lewis acid catalysis

Lewis acid-mediated alcohol activation proceeds by coordination of the hydroxyl group to the Lewis acid followed by carbocation formation. However, given the tendency of Lewis acids to form acidic hydrates or of cationic Lewis acids to hydrolyze to strong Brønsted acids in the presence of water or hydroxyl groups, Brønsted acid catalysis is generally difficult to rule out as a competing pathway. In 1986, Uemura reported the first Lewis acid-mediated Friedel-Crafts reaction from benzylic alcohol **48** and toluene via proposed chlorinated intermediate **49** (Scheme 2.7).[50] Although stoichiometric $TeCl_4$ was typically employed throughout the study, only 0.1 equivalents of $TeCl_4$ were required to afford diarylalcane **50** with excellent yields.

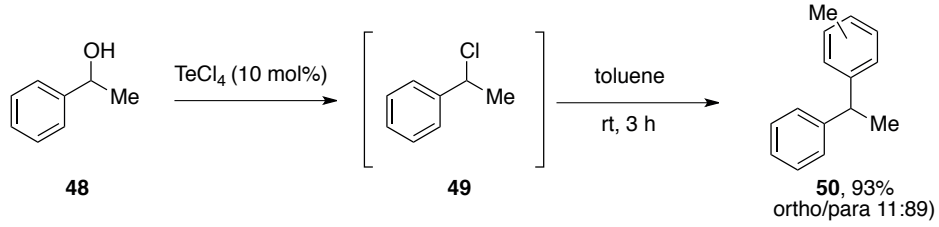

Scheme 2.7. First Lewis acid mediated Friedel-Crafts reaction directly from alcohols.

[48] (a) K. Motokura, N. Fujita, K. Mori, T. Mizugaki, K. Ebitani, K. Kaneda, *Angew. Chem. Int. Ed.* **2006**, *45*, 2605–2609.
[49] K. Motokura, N. Nagagiri, T. Mizugaki, K. Ebitani, K. Kaneda, *J. Org. Chem.* **2006**, *72*, 6006–6015.
[50] T. Yamauchi, K. Hattori, S. Mizutaki, K. Tamaki, S. Uemura, *Bull. Chem. Soc. Jpn*. **1986**, *59*, 3617–3620.

Later on, Friedel-Crafts reactions of benzylic alcohols were performed by Fukuzawa with the use of $Sc(OTf)_3$.[51] Alkylations to afford the desired 1,1-diarylalkanes with various electron poor aromatic rings such as benzene, xylenes, or mesitylene were obtained in up to 73% yield (Scheme 2.8).

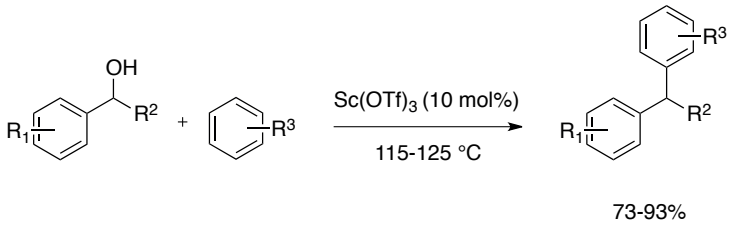

Scheme 2.8. Scandium catalyzed Friedel-Crafts reaction from alcohol.

With stoichiometric quantities of $BF_3 \bullet Et_2O$, Poli could react diphenylmethanol **51** with ethyl acetoacetate **36** in DCM giving corresponding product **52** in excellent yield (Scheme 2.9).[52] Unfortunately, when these conditions were employed in transformations of alcohols carrying a TBDMS group, even at 0 °C in substoichiometric quantities, $BF_3 \bullet Et_2O$ cleaved the protecting group.[53] This phenomenon can presumably be explained by cationic Lewis acid hydrolysis to strong Brønsted acids due to the generation of water during the course of the reaction.

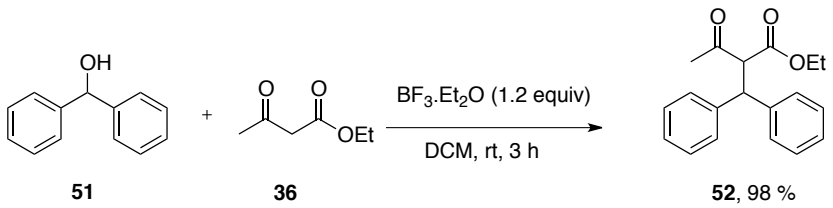

Scheme 2.9. Reaction of diphenylmethanol and diketoester **36** in the presence of stoichiometric $BF_3 \bullet Et_2O$.

Baba performed direct allylic and benzylic alcohol substitution with malonate derivatives using $InCl_3$ (Scheme 2.10). Under those conditions, the use of toluene as a solvent, did not lead to secondary Friedel-Crafts reaction and gave diketone compounds in moderate to excellent yields.[54] Although protic acids or fluoride sources are commonly used for the

[51] (a) T. Tsuchimoto, K. Tobita, T. Hiyama, S.-I. Fukuzawa, *Synlett* **1996**, 557–559; (b) T. Tsuchimoto, K. Tobita, T. Hiyama, S.-I. Fukuzawa, *J. Org. Chem*. **1997**, *62*, 6997–7005.
[52] F. Bisaro, G. Prestat, M. Vitale, G. Poli, *Synlett* **2002**, 1823–1826.
[53] T. K. M. Shing, Q. Jiang, T. C. W. Mark, *J. Org. Chem.* **1998**, *63*, 2056–2057.
[54] M. Yasuda, T. Somyo, A. Baba, *Angew. Chem. Int. Ed.* **2006**, *45*, 793–796.

removal of silyl protecting groups, $InCl_3$ has been introduced to mediate desilylation reactions particularly for TBDMS group.[55]

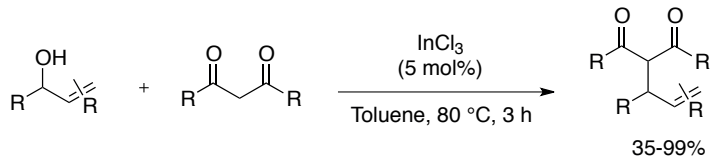

Scheme 2.10. Reaction of allylic or benzylic alcohols with diketones in the presence of $InCl_3$.

Rueping disclosed an efficient $Bi(OTf)_3$-catalyzed reaction between 1-phenylethanol **48** and diketone **35** to give **53** with 91% yield.[56] The developed method is interesting because toluene or xylene, considered as weak nucleophiles, were also suitable for this transformation (Scheme 2.11). Whereas high reactivity is observed, the strongly cationic $Bi(OTf)_3$ shows no chemoselectivity in the presence of several silyl groups.[57]

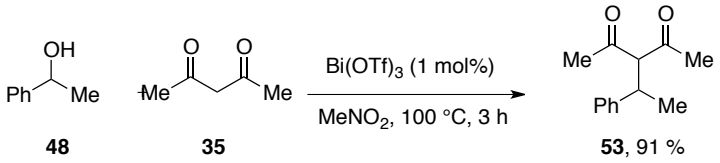

Scheme 2.11. Reaction of a benzylic alcohol with diketones in the presence of $Bi(OTf)_3$.

In 2010, Niggemann reported a calcium catalyzed Friedel-Crafts reaction with good substrate and nucleophile scope.[58] Interestingly, the intermediate **56a** generated during the arylation of allylic alcohol **54** isomerized under the reaction conditions to form the endocyclic alkene product **56b** (Scheme 2.12). This rearrangement causes complete conversion to the isomerized product due to the release of harsh Brønsted acid byproducts into the reaction mixture.

[55] J. S. Yadav, B. V. S. Reddy, C. Madan, *New J. Chem*. **2000**, *24*, 853–854.
[56] M. Rueping, B. J. Nachtsheim, A. Kuenkel, *Org. Lett.* **2007**, *9*, 825–828.
[57] H. Firouzabadi, I. Mohammadpoor-Baltork, S. Kolagar, *Synth. Commun.* **2001**, *31*, 905–909.
[58] M. Niggemann, M. J. Meel, *Angew. Chem. Int. Ed.* **2010**, *49*, 3684–3687.

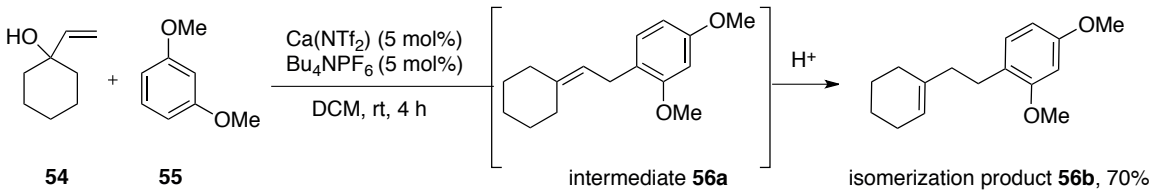

Scheme 2.12. Reaction of secondary allylic alcohol **54** via calcium mediated Friedel-Crafts reaction with unavoidable acid-isomerization.

2.1.3.3 Boronic Acid Catalysis (BAC)

Boronic acids are organoboron compounds that have one carbon-based substituent and two hydroxyl groups. With an sp^2 hybridized boron atom and six valence electrons, they have a vacant p-orbital that possesses Lewis acidic character. The two hydroxyl functions can be considered as potential hydrogen donors and makes them weak Brønsted acids (Scheme 2.13).

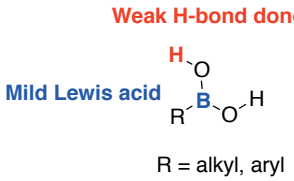

Scheme 2.13. Acidic characteristics of boronic acids

In the past ten years, boronic acids have emerged as attractive organocatalysts for mild catalytic reactions, including direct esterification or amidation,[59] epoxide opening,[60] Biginelli reactions[61] Diels–Alder reactions,[62] dipolar cycloadditions,[63] aldol condensations,[64] and ene reactions.[65] In all of these examples, reversible covalent bond formation between the boronic acid catalyst and the substrate is invoked to explain the observed catalysis (Scheme 2.14, equation 1). Moreover, a diverse library of inexpensive substituted aryl boronic acids is commercially available, primarily due to their use as coupling partners in the Suzuki–

[59] K. Ishihara, S. Ohara and H. Yamamoto, *J. Org. Chem*. **1996**, *61*, 4196–4197.
[60] X-D Hu, C-A Fan, F-M Zhang and Y-Q Tu, *Angew. Chem. Int. Ed*. **2004**, *43*, 1702–1705.
[61] A. Debache, B. Boumoud, M. Amimour, A. Belfaitah, S. Rhouati, B. Carboni, *Tetrahedron Lett*. **2006**, *47*, 5697–5699.
[62] H. Zheng and D. G. Hall, *Tetrahedron Lett.* **2010**, *51*, 3561–3564.
[63] H. Zheng, R. McDonald and D. G. Hall, *Chem. Eur. J*. **2010**, *16*, 5454–5460.
[64] K. Arnold, A. S. Batsanov, B. Davies, C. Grosjean, T. Schuetz, A. Whiting, K. Zawatzky, *Chem. Commun*. **2008**, 3879–3881.
[65] M. Li, T. Yang, D. J. Dixon, *Chem. Commun*. **2010**, *46*, 2191–2193.

Miyaura reaction.[66] They are generally air and moisture stable, highly soluble in most organic solvents and relatively non-toxic.[67] Boronic acids have also been claimed to enable direct alcohol activation by assisting ionization of alcohols to carbocations via the formation of reversible covalent bonds (Scheme 2.14, equation 2). Applications of boronic acid catalysis in dehydrative alcohol substitution will be outlined in detail below.

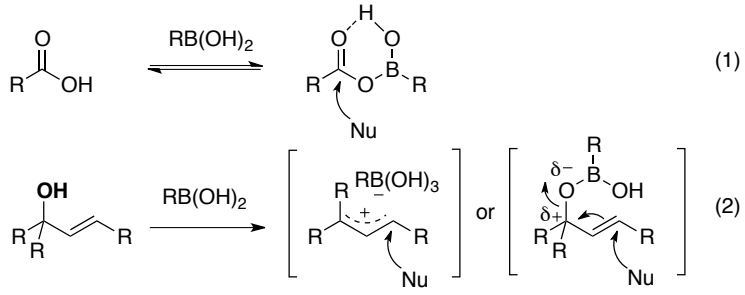

Scheme 2.14. Two activation modes with boronic acids.

McCubbin reported the Friedel-Crafts reaction of diverse allylic alcohols with a variety of electron-rich arenes by using 10 mol% of pentafluorophenylboronic acid as catalyst at room temperature. The presence of activated 4Å molecular sieves was essential in that reaction. The mechanism of the reaction is presumed to proceed through an S_N1' pathway via an allylic carbocation (Scheme 2.15).[68] The same approach was extended towards benzylic alcohol [69] and propargylic alcohols, [70] by employing higher reaction temperatures. Unfortunately, the scope was limited to electron-rich arene nucleophiles.

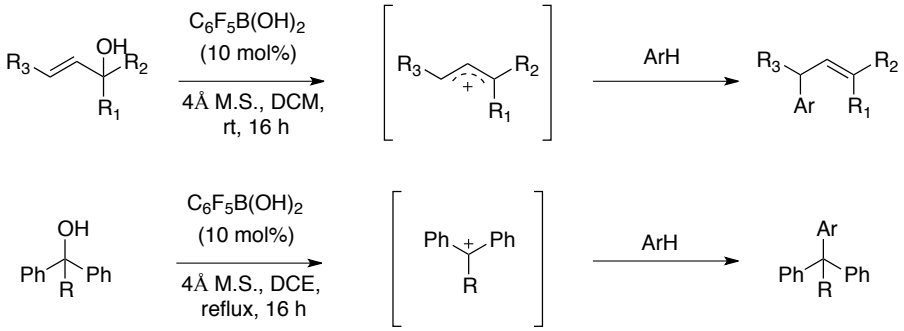

Scheme 2.15. Friedel-Crafts reactions of allylic and benzylic alcohols under pentafluorophenylboronic acid catalysis via S_N1-type pathway.

[66] S. D. Walker, T. E. Barder, J. R. Martinelli, S. L. Buchwald, *Angew. Chem. Int. Ed.* **2004**, *43*, 1871.
[67] D. G. Hall, *Boronic Acids—Preparation and Applications in Organic Synthesis and Medicine*; Wiley-VCH: Weinheim, ***2005***.
[68] J. A. McCubbin, H. Hosseini, O. V. Krokhin, *J. Org. Chem.* **2010**, *75*, 959–962
[69] J. A. McCubbin, O. V. Krokhin, *Tetrahedron Lett.* **2010**, *51*, 2447–2449.
[70] J. A. McCubbin, C. Nassar, O. V. Krokhin, *Synthesis* **2011**, *2011*, 3152–3160.

Hall and coworkers showed that allylic alcohols could rearrange to the more stable isomer in the absence of nucleophile by way of a 1,3-transposition catalyzed by tetrafluorophenylboronic acid. In this way, better E/Z selectivities were obtained than by metal-catalyzed methods, prompting them to explore the Meyer–Schuster rearrangement of propargylic alcohols under the same conditions. Again, E/Z selectivities superior to 20:1 were obtained with a wide range of substrates (Scheme 2.16).[71]

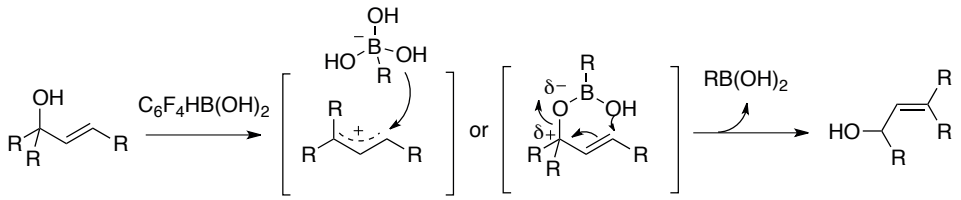

Scheme 2.16. Boronic acid catalyzed 1,3-transpositions.

In 2012, Hall described the carbo- and hetero-cyclization of allylic alcohols. By using 10 or 20 mol% of tetrafluorophenylboronic acid, most substrates provided cyclic products at room temperature in nitromethane as a solvent (Scheme 2.17, equation 1).[72] Furthermore, extension with 10 mol% of 2,3-difluoro-4-methylpyridinium boronic acid in the dehydrative cyclization of bis-benzylic alcohol **57** bearing a TIPS-protected phenol led to complete conversion of **58** at 50 °C, with the silyl ether remaining intact (Scheme 2.17, equation 2). Different reactivity was observed when tetrafluorophenylboronic acid catalyst was subjected to benzylic and allylic alcohol **59** as compared to allylic alcohol **60** (Scheme 2.18). Despite potentially forming the same product, **59** led to compound **61** after 25 hours of reaction time, whereas no conversion was observed starting from compound **60**.

[71] H. Zheng, M. Lejkowski, D. G. Hall, *Chem. Sci*. **2011**, *2*, 1305–1310.
[72] H. Zheng, S. Ghanhari, S. Nakamura, D. G. Hall, *Angew. Chem. Int. Ed.* **2012**, *51*, 6187–6190.

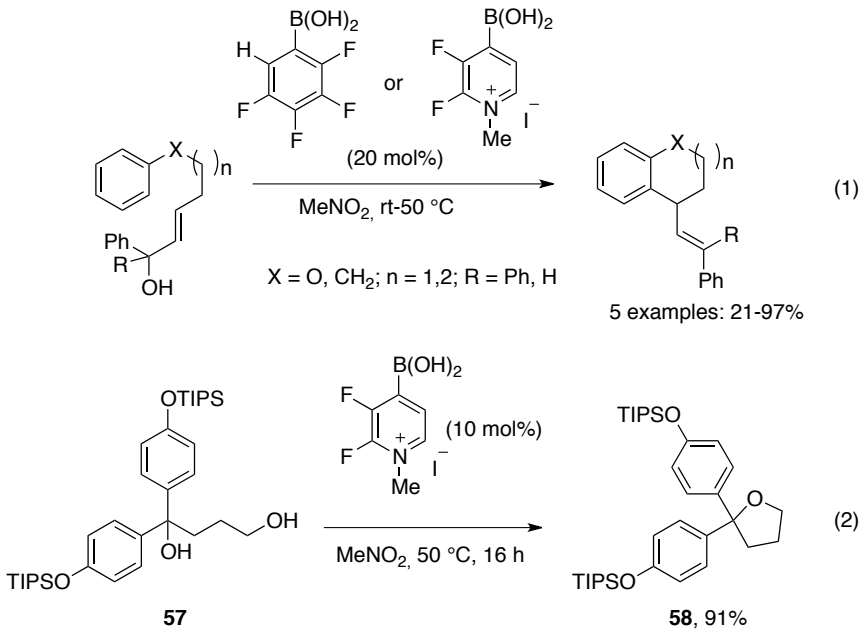

Scheme 2.17. Carbo- and hetero-cyclizations via mild boronic acid catalysis.

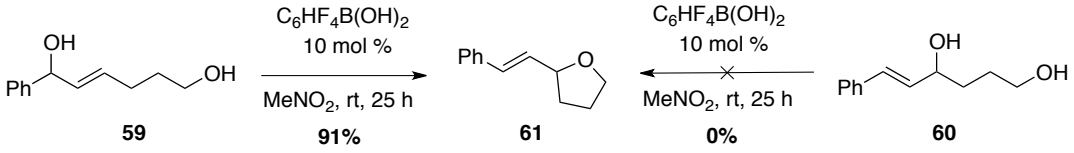

Scheme 2.18. Differential reactivity of benzylic and allylic alcohol **59** and allylic alcohol **60**.

Very recently, McCubbin reported that the same tetrafluorophenylboronic acid was an active catalyst for direct intermolecular Friedel–Crafts alkylations to form prenyl motifs (Scheme 2.19, left).[73] A 4:1 mixture of hexafluoroisopropanol (HFIP) and $MeNO_2$ was indispensable to afford good yields at room temperature. Several examples showed increased reactivity of the catalyst 2,3,4,5-tetrafluorophenylboronic acid compared to pentafluorophenylboronic acid, which was ascribed to a secondary interaction between the *ortho*-hydrogen substituent of the catalyst and the substrate (Scheme 2.19, right).

[73] C. L. Ricardo, X. Mo, J. A. McCubbin, D. G. Hall, *Chem. Eur. J.* **2015**, *21*, 4218–4223.

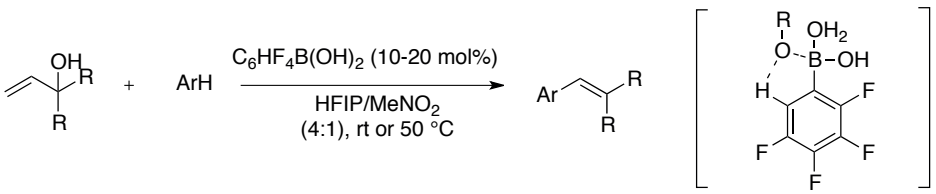

Scheme 2.19. Direct Friedel–Crafts alkylations of prenyl alcohols with arenes (left). Possible stabilizing role of *ortho*-H in catalyst $C_6HF_4B(OH)_2$ (right).

Some of the limitations of electron-poor boronic acid catalysts include limited alcohol scope for intermolecular reactions, extended reaction time and high catalyst loadings (10-20 mol%). Despite those drawbacks, the emergence of boronic acid catalysis opens access to milder conditions in alcohol activation when compared to reported methods using cationic Lewis acids and harsh Brønsted acids. In this context, a catalyst for alcohol substitution that combines high reactivity and functional group tolerance has yet to be developed. Alternative catalyst design strategies are likely required to break the dichotomy between high reactivity and high chemoselectivity.

2.2 $B(C_6F_5)_3$ in nitromethane, a winning combination

2.2.1 Hydration states of $B(C_6F_5)_3$

Our laboratory became interested in exploiting strong *neutral* Lewis acid hydrates that might generate a network of intermolecular hydrogen bonds with a hydrogen bond accepting substrate while avoiding the hydrolytic generation of stronger Brønsted acids that are responsible for poor chemoselectivity. One simple example of such a system is the commercially available tris(pentafluorophenyl)borane **62**, a compound that rapidly forms a dynamic mixture of hydrates (**62**•$n$$H_2O$). Evaporation of a $CDCl_3$ solution of $B(C_6F_5)_3$ and multiple equivalents of water gave crystals (Scheme 2.20).[74] X-ray crystallography revealed that one molecule of water is bound directly to the boron centre, whilst the remaining two water molecules are dispersed via hydrogen bonding. The first hydration is strongly favored and $B(C_6F_5)_3$ is rapidly and irreversibly hydrated upon exposure to moisture and air. Thus,

[74] (a) A. A. Danopoulos, J. R. Galsworthy, M. L. H. Green, S. Cafferkey, L. H. Doerrer, M. B. Hursthouse, *Chem. Commun.* **1998**, 2529–2530; (b) T. Beringhelli, D. Maggioni, G. D'Alfonso, *Organometallics* **2001**, *20*, 4927–4938.

hydrates of $B(C_6F_5)_3$ are the major species in solution if an anhydrous environment is not rigorously maintained.

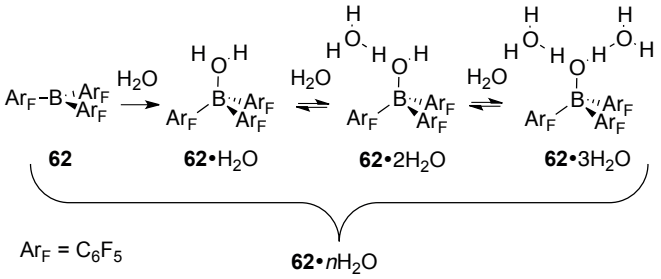

Scheme 2.20. Dynamic equilibrium between hydrated forms of $B(C_6F_5)_3$.

2.2.2 Solvent dependence

Solvent has been shown to have considerable effects on the rate of many reactions by modifying the dielectric constant, donicity or H-bond donating ability of the reaction medium as well as exhibiting specific solvent effects.[75] To find the best solvent for the model dehydrative reaction between cinnamyl alcohol **63** and mesitylene **64,** we started with 1 mol% of **62•***n*H_2O (Table 2.1) and tested non-polar and polar solvents having different dielectric constants. We detected a huge solvent dependence in $MeNO_2$ (entry 7), while more typical Friedel-Crafts solvents such as DCE or toluene (entries 1 and 6) were not efficient in that transformation.

[75] C. Reichardt, *Solvents and Solvent Effects in Organic Chemistry*, 3rd updated and enlarged ed.; Wiley-VCH: Weinheim, **2003**; (b) C. Laurence, P. Nicolet, M. T. Dalati, J.-L. M. Abboud, R. Notario, *J. Phys. Chem.* **1994**, *98*, 5807–5816; (c) Y. Y. Borovikov, V. A. Topchii, *Theor. Exp. Chem*. **1976**, *11*, 89–92.

Table 2.1. Solvent dependence on a model Friedel-Crafts reaction. [a,b]

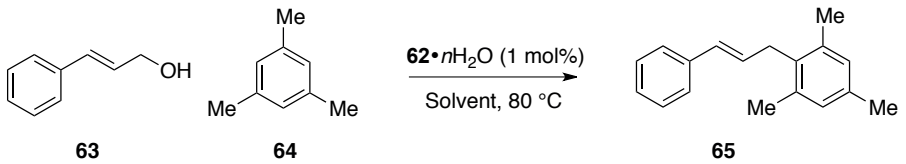

63 **64** **65**

Entry	Solvent	*t* [h]	Yield [%]
1	DCE	1	<5
2	DMF	1	<5
3	DMA	1	<5
4	DMSO	1	<5
5	MeCN	1	<5
6	Toluene	1	<5
7	**$MeNO_2$**	**1**	**86**
8	EtOAc	1	<5
9	THF	1	<5
10	Mesitylene	1	<5

Conditions: [a] 1.0 equiv **63** (0.2 M in $MeNO_2$), 3.0 equiv **64**, 80 °C. [b] Yields of isolated product purified by column chromatography on silica gel.

2.2.3 Comparing $B(C_6F_5)_3$ with other boron catalysts

Catalyst **62•***n*H_2O was found to be more efficient than analogous boron-containing Lewis acids such as boranes, borinic acids, boronic acids and boric acid in 1 h of reaction time (Table 2.2, entries 1,4,5,6,7). Modest conversions were found with pentafluorophenylboronic acid and tetrafluorophenylboronic acid, which had previously been reported as catalysts for dehydrative substitution of alcohols (entries 2 and 3).[67-73] Surprisingly, when the catalyst loading was decreased to 1 mol%, the yield of compound **65** increased when **62•***n*H_2O was the catalyst (entry 9). At that loading, boronic acid catalysts produced trace amounts of **65** (entry 10). BF_3•THF, a Lewis acid of comparable strength, was not as effective as **62•***n*H_2O (entry 11). In the absence of catalyst, only small traces of compound **65** were detected (entry 8).

Table 2.2. Survey of boron-based catalysts for the Friedel-Crafts reaction between cinnamyl alcohol and mesitylene. [a,b]

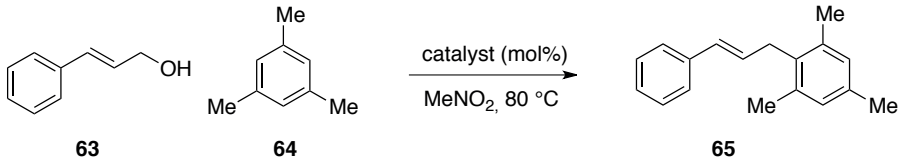

63 **64** **65**

Entry	Catalyst	Cat. loading [mol%]	*t* [h]	Yield[b] [%]
1	**62**•*n*H_2O	10	1	65
2	$C_6F_5B(OH)_2$	10	1	22
3	$C_6HF_4B(OH)_2$	10	1	13
4	Ph_3B	10	1	31
5	Ph_2BOH	10	1	17
6	$PhB(OH)_2$	10	1	<5
7	$B(OH)_3$	10	1	12
8	none	n/a	1	<5
9	**62**•*n*H_2O	1	1	86
10	$C_6F_5B(OH)_2$ or $C_6HF_4B(OH)_2$	1	1	<5
11	BF_3•THF	1	1	68

Conditions: [a] 1.0 equiv **63** (0.2 M in $MeNO_2$), 3.0 equiv **64**, 80 °C. [b] Yields of isolated product purified by column chromatography on silica gel.

2.2.4 Chemoselectivity

To evaluate the chemoselectivity of **62**•*n*H_2O compared to other Brønsted or Lewis acid catalysts, we examined the reaction between allylic alcohol **54** and mesitylene **64**. The initially formed exocyclic alkene product is known to rearrange to the more stable endocyclic isomer in the presence of strong Brønsted acids.[58] We conducted the reaction with a variety of common Brønsted and Lewis acid catalysts described in the alcohol activation literature. Reactions were studied at 80 °C and at room temperature to best independently evaluate chemoselectivity and reactivity (Table 2.3). At 80 °C, all acids tested were able to activate alcohol **54** and lead to compound **66a** except for pentafluorophenylboronic acid and triphenylborane (entries 14 and 15). TfOH, HBF_4, H_2SO_4, $Ca(NTf)_2/Bu_4NPF_6$, $Bi(OTf)_3$, $Sc(OTf)_3$, BF_3•Et_2O and $FeCl_3$ (entries 2, 3, 4, 6, 8, 9, 10, 11) were all accompanied by complete rearrangement towards **66b** while TsOH, $AuCl_3$ and $Yb(OTf)_3$ (entries 5, 12, 13) led to partial isomerization. **62**•*n*H_2O was the only catalyst showing complete selectivity at 80 °C towards **66a** (92%, >20:1) while also conserving its reactivity at room temperature, yielding compound **66a** in 77% yield after leaving the reaction for an additional 3 h (entry 18). In contrast, other strong Brønsted acids were either less effective at room temperature or gave

poor chemoselectivity (entry 19, 20) whereas weaker Brønsted acids such as TFA did not lead to any of the desired compound (entry 21).

Table 2.3. Survey of boron-based catalysts for the Friedel-Crafts reaction between allylic alcohol **54** and mesitylene.[a,b]

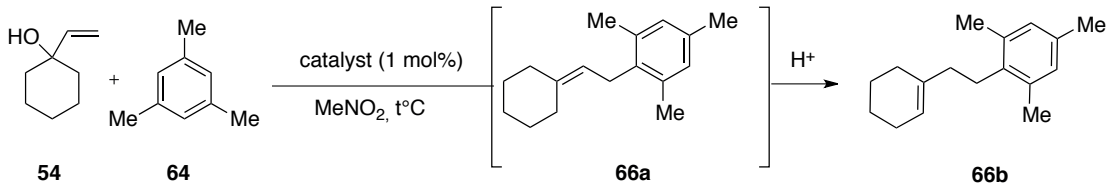

54 **64** **66a** **66b**

Entry	Catalyst	T (°C)	Yield **66a**+**66b** [%]	Ratio **(66a**:**66b)**
1	none	80	<5	n/a
2	TfOH	80	77	1:10
3	HBF_4	80	88	1:9
4	H_2SO_4	80	78	1:5
5	TsOH	80	74	4:1
6	TFA	80	68	>20:1
7	$Ca(NTf)_2/Bu_4NPF_6$	80	74	1:9
8	$Bi(OTf)_3$	80	83	1:12
9	$Sc(OTf)_3$	80	83	1:9
10	$BF_3.Et_2O$	80	82	1:10
11	$FeCl_3$	80	82	1:3
12	$AuCl_3$	80	85	6:1
13	$Yb(OTf)_3$	80	62	4:1
14	$C_6F_5B(OH)_2$	80	<5	n/a
15	Ph_3B	80	<5	n/a
16	**62**•$n$$H_2O$	80	92	>20:1
17	**62**•$n$$H_2O$	22	60	>20:1
18[c]	**62**•$n$$H_2O$	22	77	>20:1
19	TfOH	22	47	2:1
20	TsOH	22	32	>20:1
21	TFA	22	<5	n/a

Conditions: [a] 1.0 equiv **54** (0.2 M in $MeNO_2$), 3.0 equiv **64**, 1 h. [b] Isolated yield after silica gel chromatography. [c] Reaction time of 4 h.

With **62**•$n$$H_2O$ identified as a superior chemoselective catalyst, we aimed to test selectivity towards common protecting groups that were not stable under previously described conditions (see introduction of the chapter). TIPS-protected benzylic alcohol **67a** reacted with thiophenol in 92% yield after 1 h with no detectable cleavage of the silyl ether at 80 °C. To further explore the limitations on chemoselectivity, TES-protected phenol product **68b** ($\approx 10^3$ times more labile) was isolated intact in 69% yield with 5% of the free phenolic thioether. Benzylic alcohol **67c** converts to **68c** in 81% yield without cleavage of the PMB-protecting group by carrying out the reaction at room temperature for 4 h. The PMB group

was not stable at 80 °C under these conditions. We then screened a diverse array of representative nucleophiles against common π-activated alcohols. Thioacetic acid reacted with diphenylmethanol **51** to give thioesters **68d**. Etherification of secondary benzylic alcohol **48** is accomplished with 2-phenylethanol to give ether **68e**. Allylation of alcohol **39** with allyltrimethylsilane occurs in high yield to give **68f**. Friedel-Crafts reaction of (*E*)-3-methyl-5-(2,6,6-trimethylcyclohex-1-en-1-yl)pent-2-en-1-ol **67-d** with mesitylene occured at 80 °C to give arene **68g**. Alkylated heterocycles **68h** and **68i** can be accessed from tertiary benzylic alcohols by reaction with *N*-methylindole and 2-methylfuran, respectively. **67e** was suitable to nucleophilic substitution with alkyl thiol nucleophiles affording **68j** with 90% yield. Nucleophiles including *t*-butyl carbamate and benzylcarbamate reacted with allylic and propargylic alcohols **39** and **34**, resulting in *N*-protected amine **68k** and **68l** without cleavage of the protecting groups under the reaction conditions (Table 2.4).

Table 2.4. Representative nucleophile and alcohol scope.[a,b]

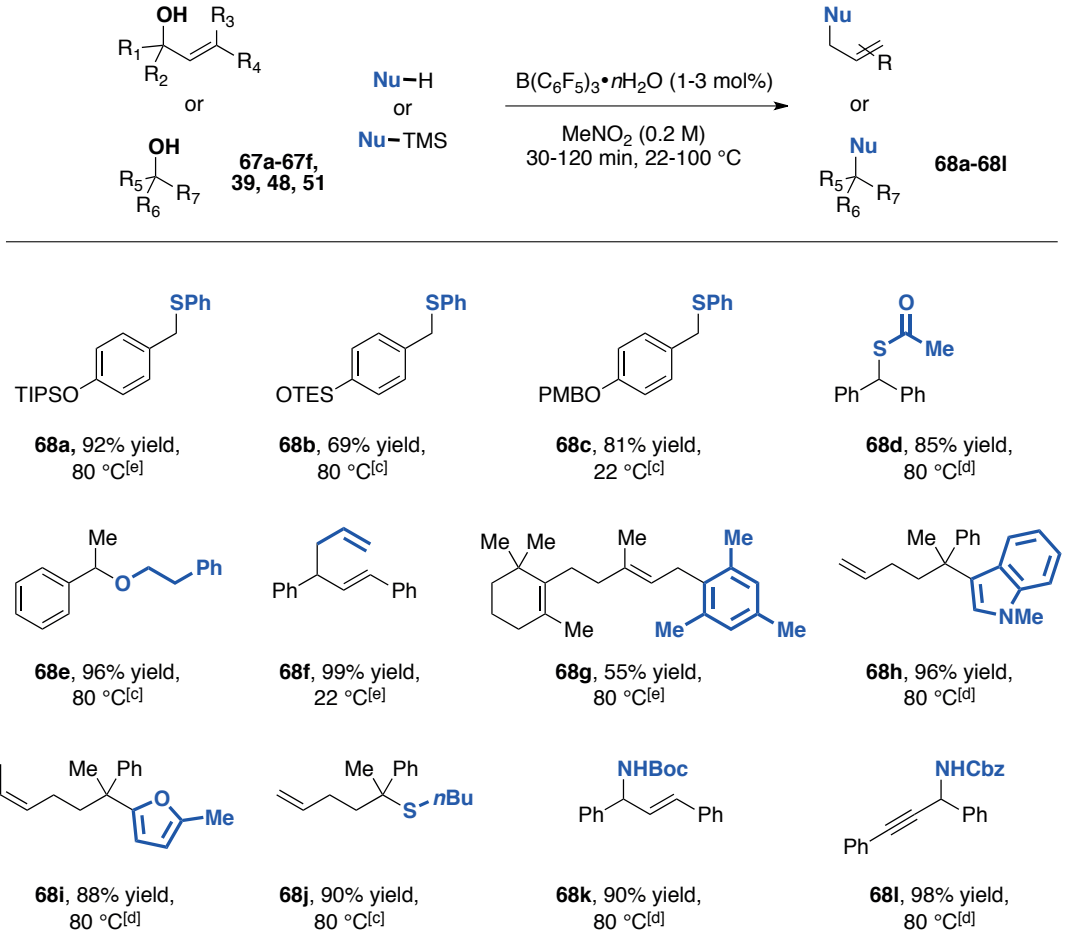

Conditions: [a] 1 equiv alcohol (0.2 M in $MeNO_2$), 1.1 – 3.0 equiv nucleophile; [b] Yields of isolated product purified by column chromatography on silica gel; [c] 1 mol% $B(C_6F_5)_3 \bullet nH_2O$; [d] 2 mol% $B(C_6F_5)_3 \bullet nH_2O$; [e] 3 mol% $B(C_6F_5)_3 \bullet nH_2O$.

To compare the efficiency of boronic acid catalysts and **62**•nH$_2$O, we conducted the cyclodehydration reactions reported by Hall (Scheme 2.21). Whereas, even with 10 mol% of $C_6F_5B(OH)_2$, reactivity was not observed,[72] **62**•nH$_2$O converted **60** to **61** in 82% yield at 1 mol% catalyst loading under otherwise identical conditions. Secondary propargylic alcohol **69** was cyclized to 2-alkynyl tetrahydrofuran **70** in 87% yield without an additional pre-activation step[76] while tertiary aliphatic alcohol **71** formed the tetrahydrofuran **72** in 79% yield after 4 h. Even primary aliphatic alcohols, which are typically only activated by strong acids, exhibited interesting activity presumably operating by an S_N2-type mechanism. Hydroxytosylamide **73** cyclized to pyrrolidine **74** in almost quantitative yield, a reaction previously accomplished only by stoichiometric pre-activation.[77]

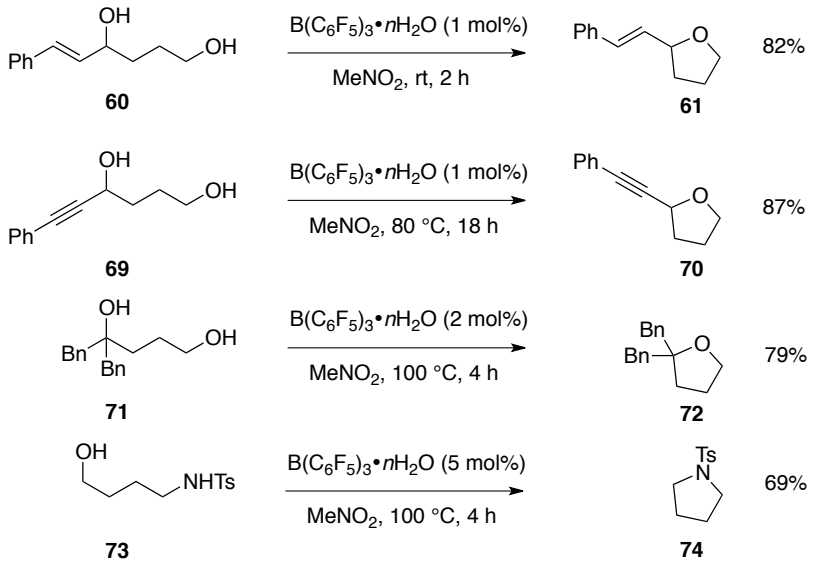

Scheme 2.21. Representative intramolecular reactions.

2.2.5 Conclusion

To conclude, we report that the hydrates of $B(C_6F_5)_3$ possess an optimal balance between reactivity and chemoselectivity compared to the common catalysts described in the literature for direct alcohol activation. At the same time, we have highlighted the strong match between $B(C_6F_5)_3$ and nitromethane solvent that seems to be an excellent combination to afford high reactivity and chemoselectivity. Moreover, we showed this catalyst reaction system to be

[76] D. S. B. Daniels, A. L. Thompson, E. A. Anderson, *Angew. Chem. Int. Ed.* **2011**, *50*, 11506–11510.
[77] H. Aikawa, S. Tago, K. Umetsu, N. Haginiwa, N. Asao, *Tetrahedron* **2009**, *65*, 1774–1784.

tolerant of a wide range of *C*-, *N*-, *O*- and *S*-nucleophiles and acid-sensitive functional groups without the requirement of precautions to exclude moisture before running the experiments. In addition, **62**•nH$_2$O enabled catalytic S$_N$1- and S$_N$2-type cyclodehydrations of primary aliphatic alcohols usually catalyzed by stoichiometric quantities of acids. This work constitutes a practical, chemoselective and step-economic method for an important class of transformation.

2.3 Tertiary aliphatic alcohol activation

In the previous section, we showed that a diverse set of π-activated alcohols and nucleophiles react under B(C$_6$F$_5$)$_3$•nH$_2$O catalysis in nitromethane. However, unlike π-activated alcohols, direct tertiary aliphatic alcohol activation methods are much less developed and few examples exist where catalytic nucleophilic substitution can be achieved using substoichiometric catalyst loadings. Therefore, we elected to explore this method for the activation of tertiary aliphatic alcohols, a less reactive class of alcohols that also are prone to competitive elimination under acidic conditions.

2.3.1 State of the art

In general, concentrated solutions of strong acids are required to enable direct dehydrative substitution of tertiary aliphatic alcohols. Acid-catalyzed dehydrative thioetherification of *t*-amylalcohol **75** has been reported using concentrated sulfuric acid as a solvent and thiophenol as the nucleophile (Scheme 2.22).[78] After fifteen minutes of reaction time, compound **76** was isolated with 69% yield.

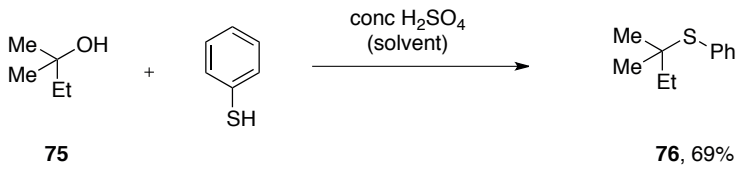

Scheme 2.22. Thioetherification with *t*-amylalcohol in the presence of concentrated sulfuric acid as a solvent.

[78] V. N. Ipatieff, H. Pines, B. S. Friedman, *J. Am. Chem. Soc*. **1938**, *60*, 2731–2734.

The first reaction that described tertiary aliphatic alcohol activation in a Friedel-Crafts type reaction was reported in 1942 by Kharasch.[79] The method was using 800 mol% of oleum which is a solution of sulfur trioxide in sulfuric acid, forming bis-alkylated compound from *t*BuOH and 1,4-dimethoxybenzene with good yield (Scheme 2.23).

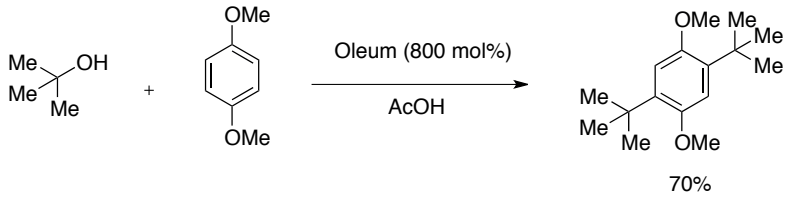

Scheme 2.23. Friedel-Crafts reaction with *t*BuOH in the presence of fuming sulfuric acid.

The first azidation of tertiary aliphatic alcohols was reported by Hiroaki in 1977.[80] Several adamantyl azide derivatives were synthesized by treatment with 57% H_2SO_4 in $CHCl_3$ requiring sodium azide, a poisonous and explosive reactant that seriously limits the preparative applicability of this approach. After that, Andisik described the use of stoichiometric $TiCl_4$ with either cis- or trans-4-*tert*-butyl-1-methylcyclohexanol and hydrazoic acid giving a 50:50 mixture of cis- and trans-1-azido-4-*tert*-butyl-1-methylcyclohexane consistent with a carbocation intermediate being formed during the reaction (Scheme 2.24).[81a] A few years later, Zwierzak described a milder methodology of azidation with $TMSN_3$ presumably via initial silyl transfer to the alcohol prior to N_3 substitution (Scheme 2.25).[81b] Unfortunately, the scope and yields for this method were extremely limited, with only three substrates described. Furthermore, stoichiometric $BF_3 \bullet Et_2O$ was required.

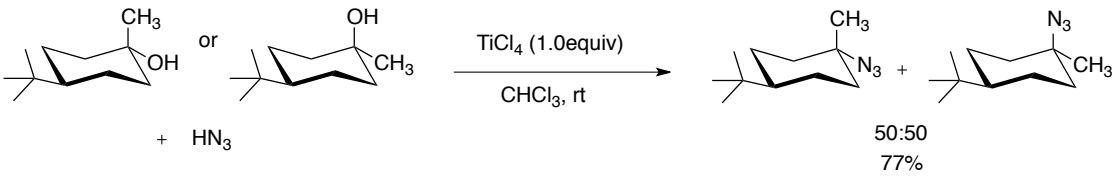

Scheme 2.24. Azidation of cyclohexanol derivatives leading to a 50:50 mixture of isomers with stoichiometric $TiCl_4$.

[79] P. F. Oesper, C. P. Smyth, M. S. Kharasch, *J Am. Chem. Soc*. **1942**, *54*, 937–940.
[80] T. Sasaki, S. Eguchi, T. Katada, O. Hiroaki, *J. Org. Chem*. **1977**, *42*, 3741–3743.
[81] (a) A. Hassner, R. Fibiger, D. Andisik, *J. Org. Chem*. **1984**, *49*, 4237–4244; (b) A. Koziara, A. Zwierzak, *Tetrahedron Lett*. **1987**, *28*, 6513–6516.

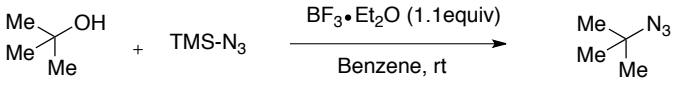

Scheme 2.25. Azidation of *t*BuOH with stoichiometric BF_3•Et_2O.

In surprising contrast to the advances with π-activated alcohols, little progress has been made since these early reports. The use of superstoichiometric amounts of harsh mineral acids[79] or stoichiometric cationic Lewis acids[81] is still a requirement to afford direct nucleophilic substitution of aliphatic alcohols. Methods requiring pre-activation of the alcohols as tosylates, trifluoroacetates or halide derivatives are still widely used. Direct catalytic tertiary aliphatic alcohol activation therefore represents an important goal for sustainable organic synthesis as it would avoid these intermediates altogether.

2.3.2 Azidation with $B(C_6F_5)_3$ in nitromethane

We became interested in the azidation of tertiary aliphatic alcohols with $TMSN_3$, a useful transformation for introducing nitrogen-based functional groups, including those from Huisgen-type cycloadditions[82] and the Staudinger ligation.[83] Moreover the azido motif is present in several pharmaceuticals, the most well known example being azidothymidine (AZT), an antiretroviral drug, used in HIV treatment.

2.3.2.1 Solvent effect

Initial attempts at exploring reactivity in a variety of common polar and non-polar aprotic solvents with 5 mol% of $B(C_6F_5)_3$•nH_2O either did not result in any reaction or rapidly produced silyl ether **78** from alcohol **77a** but gave no azide **79a** after extended reaction times (Table 2.5). Small amounts (<10%) of **79** were detected in DCM and DCE after 1 h. Again, the use of nitromethane as solvent led to rapid formation of silyl ether **78** in less than five minutes followed by complete conversion to give azide **79a** in less than 1 h at room temperature in 80% isolated yield.

[82] E. Lallana, R. Riguera, E. Fernandez-Megia, *Angew. Chem. Int. Ed.* **2011**, *50*, 8794–8804.
[83] C. I. Schilling, N. Jung, M. Biskup, U. Schepers, S. Brase, *Chem. Soc. Rev*. **2011**, *40*, 4840–4871.

Table 2.5. Azidation of alcohol **77a** in different solvents.[a,b]

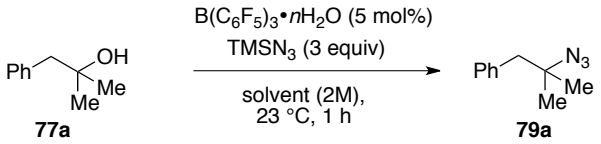

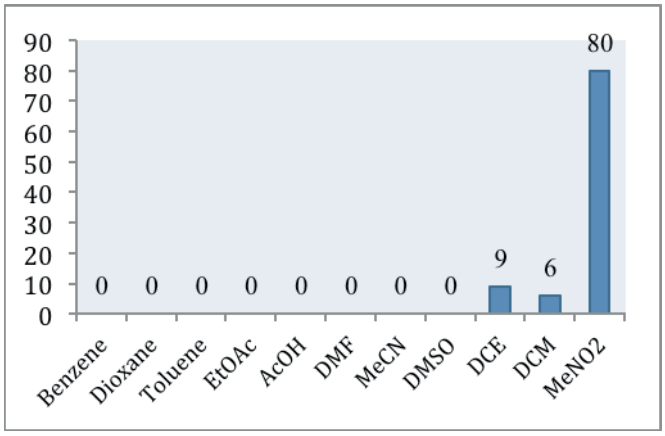

Conditions: [a] 1 equiv **77a** (2 M in $MeNO_2$), 3.0 equiv $TMSN_3$; [b] Yield of isolated product purified by column chromatography on silica gel.

2.3.2.2 The catalytic effect of nitro compounds

Azidation was also efficient when substoichiometric amounts of nitro-containing additives were employed in 'unreactive' solvents. 50 mol% *p*-nitroanisole loading was enough to co-catalyze the reaction between alcohol **77a** and $TMSN_3$ in benzene, affording **79a** with 65% isolated yield after 24 h (Scheme **2.26**).

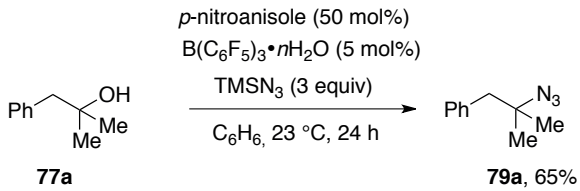

Scheme 2.26. Azidation of **77a** with substoichiometric amounts of *p*-nitroanisole.

Investigation by others in the laboratory of other nitro-based solvents showed that electronic effects had an impact on the reaction rate (Scheme 2.27).[84] Clearly electron-rich nitrocompounds, such as *p*-nitroanisole has a much larger promoting effect than electron-poor analogues such as *p*-trifluoromethylnitrobenzene. These results strongly support that nitro compounds have a strong effect on the reaction rate and are probably acting as co-catalysts in the azidation reaction.

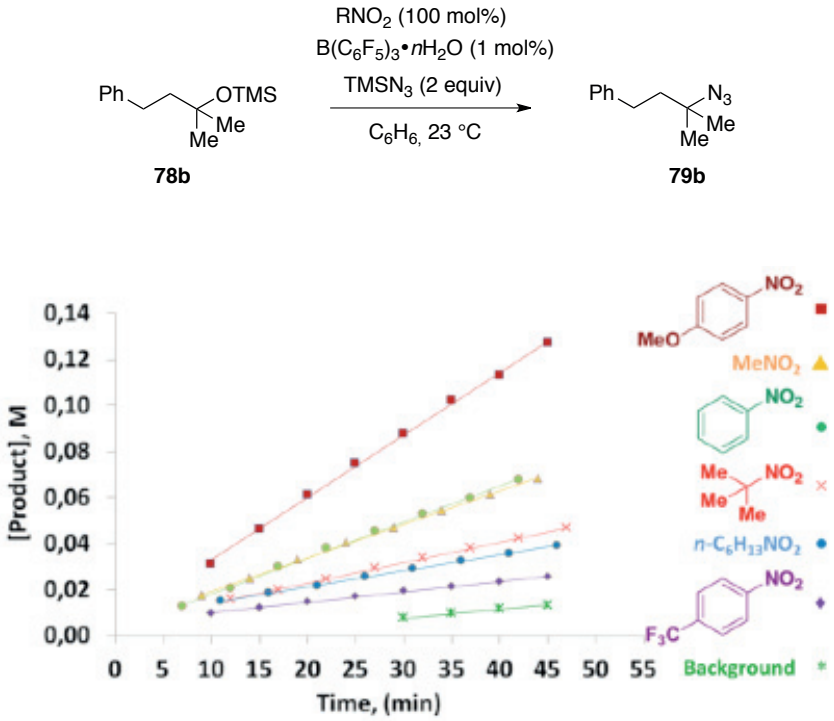

Scheme 2.27. Influence of nitro compounds on the reaction rates.

2.3.2.3 $B(C_6F_5)_3 \bullet nH_2O$, a superior Brønsted acid

The substoichiometric catalytic dehydroazidation methods of Rueping for allylic alcohols with silver salts[85] and Sawama for secondary benzylic silyl ethers with $FeCl_3$,[86] were ineffective for tertiary aliphatic alcohols (Table 2.6, entries 2 and 3). Although all catalysts gave promising conversions, except for sulfuric acid (entry 4), $B(C_6F_5)_3 \bullet nH_2O$ was clearly

[84] Kinetic studies were accomplished by Marian Dryzhakov.
[85] M. Rueping, C. Vila, U. Uria, *Org. Lett.* **2012**, *14*, 768–771.
[86] Y. Sawama, S. Nagata, Y. Yabe, K. Morita, Y. Monguchi, H. Sajiki, *Chem. Eur. J.* **2012**, *18*, 16608–16611.

superior presumably because its highly chemoselective nature minimizes silyl ether cleavage compared to harsh Brønsted acids or hydrolysis-prone cationic Lewis acids.

Table 2.6. Survey of common catalysts in dehydrative reactions.[a,b]

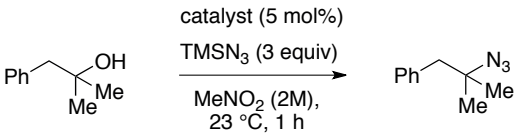

77a **79a**

Entry	Catalyst	Yield [%]
1	$B(C_6F_5)_3 \bullet nH_2O$	80
2	AgOTf	46
3	$FeCl_3$	58
4	H_2SO_4	<5
5	$Sc(OTf)_3$	66
6	TfOH	65
7	$Ca(NTf)_2/Bu_4NPF_6$	66
8	$Bi(OTf)_3$	72

Conditions: [a] 1.0 equiv **77a** (0.2 M in $MeNO_2$), 3.0 equiv $TMSN_3$, 23 °C; [b] Yields of isolated product purified by column chromatography on silica gel.

2.3.2.4 Kinetic concentration dependence studies and aggregate formation

The finding that nitro compounds act as co-catalysts in the azidation of tertiary aliphatic alcohols was highly surprising. In this context, we became intrigued by Pocker's hydrochlorination of olefins carried out in nitromethane leading to second order concentration dependence in HCl.[87] From these results, we postulated that H-bond accepting additives might accelerate Brønsted acid catalyzed reactions. Kinetic and spectroscopic investigations by others in the laboratory[88] suggest that $B(C_6F_5)_3 \bullet nH_2O$ was not acting as an isolated catalyst. The reaction in benzene in the presence of catalytic nitromethane has a second-order (1.96±0.04) rate dependence on the concentration of nitro compound, an approximately second-order (1.8±0.1) rate dependence on the concentration of acid, an approximately first-order (0.83±0.02) rate dependence on the concentration of silyl ether **78a** and a zero-order (-0.025±0.002) rate dependence on the concentration of $TMSN_3$. These results suggest that the catalytically competent Brønsted acid is a H-bonded aggregate nitro

[87] Y. Pocker, K. D. Stevens, *J. Am. Chem. Soc.* **1969**, *91*, 4205–4210.
[88] Spectroscopic and kinetic studies were accomplished by Marian Dryzhakov and Dr Malik Hellal.

compound (Scheme 2.28). Cooperative interactions between H-bond donating groups is well known to increase reactivity but was a surprising outcome of this research.

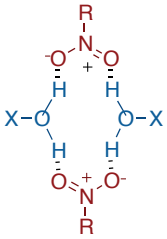

Scheme 2.28. Aggregate formation leading to a superior catalyst.

2.3.2.5 General scope in azidation reaction

By employing $B(C_6F_5)_3 \bullet nH_2O$ in nitromethane, a wide variety of tertiary aliphatic alcohols underwent rapid dehydroazidation with moderate to excellent yields (Table 2.7). Starting with the α,α-dimethylbenzenepropanol **77b**, azidation was complete in 1 h with 5 mol% of catalyst loading (87% yield). Halide substituents on the *para*-position of the aromatic ring did not affect the reaction rate giving compounds **79c** and **79d** with 90% and 85% yield respectively. Silyl ethers survived under these conditions affording **79e** and **79f** with negligible deprotection. Electron rich arenes carrying a *p*-methoxy group furnished the corresponding azide **79g** in 86% yield. Nitro-containing substrate **77h** reacts even in the absence of nitro additive affording compound **79h** with 44% yield. Bulkier substituents such as ethyl groups on the tertiary aliphatic center led to good conversion of **79i** in 64% yield, whereas *iso*-propyl groups gave only moderate yield by favoring elimination (**79j**). Alcohols bearing pendant indoles undergo azidation without intramolecular carbocation capture (**79k**, **79l**). Linear alkyl alcohols underwent azido-substitution giving good yields for **79m**-**79p**. Homoallylic alcohol **77q** was suitable for smooth substitution to give **79q** despite the possibility of a hydride shift to generate a benzylic and allylic carbocation. No bis-azidation or carbocation rearrangements were observed in alcohols bearing primary, secondary and tertiary alkenes (**79r**-**79v**). Steroids, despite the low solubility in nitromethane, are suitable to azidation under those conditions (**79w**). Cyclic alcohols derivatives are also compatible (**79x**-**79aa**). Finally, azidation of tertiary aliphatic alcohols in the presence of primary or secondary aliphatic alcohols proceeded with high yields and complete selectivity at the tertiary position even when competing cyclization is possible (**79bb, 79cc**). Moreover, of those twenty-eight compounds, twenty-one were new compounds.

Table 2.7. Substrate scope.[a,b]

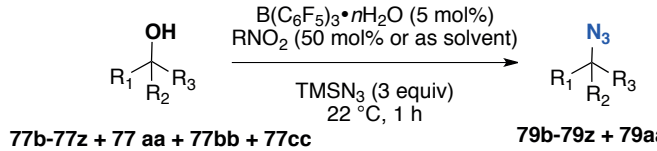

77b-77z + 77 aa + 77bb + 77cc → **79b-79z + 79aa + 79bb + 79cc**

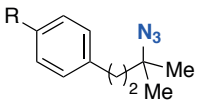

87%, 65%[c,d] (R = H, **79b**)
90% (R = Br, **79c**)
85% (R = Cl, **79d**)
89% (R = OTIPS, **79e**)
69% (R = OTES, **79f**)
86% (R = OMe, **79g**)
44%[d] (R = NO_2, **79h**)

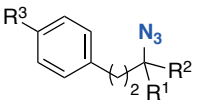

64% (R^1 = R^2 = Et, R^3 = Br, **79i**)
36% (R^1 = *i*Pr, R^2 = Me, R^3 = H, **79j**)

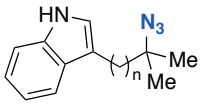

81%, 92%[c] (n = 1, **79k**)
52% (n = 3, **79l**)

79% (R = Bn, **79m**)
95%[e], 93%[c,d] (R = Me, **79n**)
85% (R = C_8H_{17}, **79o**)

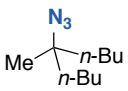

75%, 70%[c,d] (**79p**)

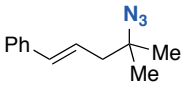

46%[g] (**79q**)

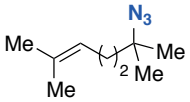

70%[e] (**79r**)

73%[e] (**79s**)

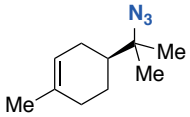

58% (**79t**)

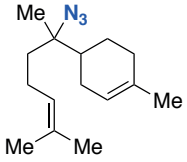

53% (**79u**)

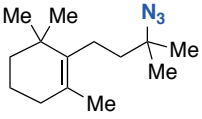

74%, 42%[c,d] (**79v**)

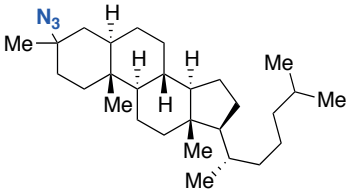

58% (**79w**)

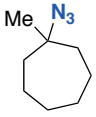

77%, 31%[c,d] (**79x**)

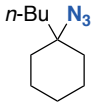

87%, 81%[c,d] (**79y**)

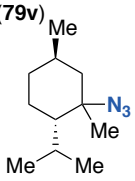

45% (**79z**)

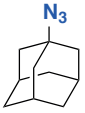

92% (**79aa**)

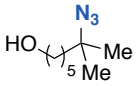

64%[h] (**79bb**)

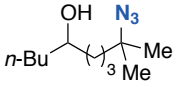

70% (**79cc**)

Conditions: [a] Alcohol (2M in $MeNO_2$), $TMSN_3$, 5−60 min; [b] Isolated yields after silica gel chromatography; [c] 50 mol % *p*-nitroanisole, C_6H_6, 24 h; [d] 1 mol % $B(C_6F_5)_3$•*n*H_2O; [e] Yield estimated by ^1H NMR using 1.0 equiv of anisole as internal standard; [f] Neat, 1 h; [g] Reaction carried out at 0 °C; [h] Reaction carried out at 90 °C.

2.3.3 Conclusion

In summary, nitromethane dramatically accelerates the acid catalyzed azidation of tertiary aliphatic alcohols and enables substoichiometric catalysis of the reaction for the first time. Electron-rich nitro compounds are co-catalysts for the reaction. Kinetic and spectroscopic experiments support a mechanism in which hydrogen-bond aggregates of nitro compounds and Brønsted acids are the catalytically competent species. The deliberate formation of aggregates of nitro compounds and Brønsted acids might represent a new general approach to accelerate Brønsted acid catalysis.

2.4. Chapter 2 conclusion

In conclusion, we have described the very efficient combination of $B(C_6F_5)_3 \bullet nH_2O$ and nitromethane towards direct catalytic intermolecular nucleophilic substitution of allylic, benzylic and tertiary aliphatic alcohols. Additionally we have described dehydrative cyclizations of primary aliphatic alcohols.

More generally, we have identified the principal reaction parameters required for high reactivity. Solvent, acid, nucleophile, alcohol and temperature all need to be carefully optimized for the reaction to occur. Despite the expected simplicity of Brønsted acid catalysis, the role of the components were found to be much more complex and the magnitude and mechanistic role of the nitromethane solvent could not have been predicted prior to the experimental result. These observations highlight the multidimensional and unpredictable nature of catalysis, and prompted us to develop catalyst-screening approaches that maximize the chances of observing cooperative effects.

CHAPTER 3

Discovery of a highly active *in situ* generated dioxaborolanedione catalyst by screening mixtures [89]

[89] Portions of this chapter have been published: E. Wolf, E. Richmond, J. Moran, "Identifying Lead Hits in Catalyst Discovery by Screening and Deconvoluting Complex Mixtures of Catalyst Components", *Chem. Sci.* **2015***, 6,* 2501–2505.

3.1 Introduction

3.1.1 *In situ* generation of catalyst libraries as mixtures and deconvolution strategies

As previously discussed, a specific combination of reaction parameters is often crucial to observe a desired catalytic reaction and extensive experimentation is often required to find the best catalytic system. The optimization process usually requires number of reactions that grows exponentially as the number of reaction parameters increases. In response to this fundamental problem, approaches that can reduce the number of reactions required to obtain a lead result for a specific transformation and that do not require high throughput instrumentation are appealing. Towards this goal, we have devised an approach for the identification of lead results in catalyst discovery based on the assumption that pre-catalysts and ligands can be screened as mixtures, forming a complex library of catalysts *in situ*, and later deconvoluted. By employing a complex mixture of all pre-catalysts and ligands in every reaction, one or two additional reaction parameters (e.g. solvent, acid/base, etc.) are screened to identify a promising result (Scheme 3.1, Step 1). In this way, three or four reaction parameters can be surveyed at once in a single small block of reactions, effectively 'front-loading' the problem of catalyst discovery. The pre-catalysts and ligands that contribute most to catalysis are identified by iterative deconvolution in the same manner as described by Breit (Scheme 3.1, Step 2).[90] It is expected that the rate of the desired reaction will increase during the deconvolution process, as the equilibrium population of the most active catalyst should be higher. However, if decreasing yields are observed during deconvolution, this may signal the presence of cooperative effects between more than two components or between two compounds in the same category (e.g. cooperative effects between two pre-catalysts or two ligands). Typical catalyst screening strategies are not designed to uncover such scenarios and it is at present unclear how common such scenarios might be. Following the identification of the essential catalyst components, traditional reaction optimization can be carried out by varying the continuous parameters such as the number of equivalents or loadings of the various catalyst components.

[90] J. Wieland, B. Breit, *Nat. Chem*. **2010**, *2*, 832–837. See also the general introduction on page 35.

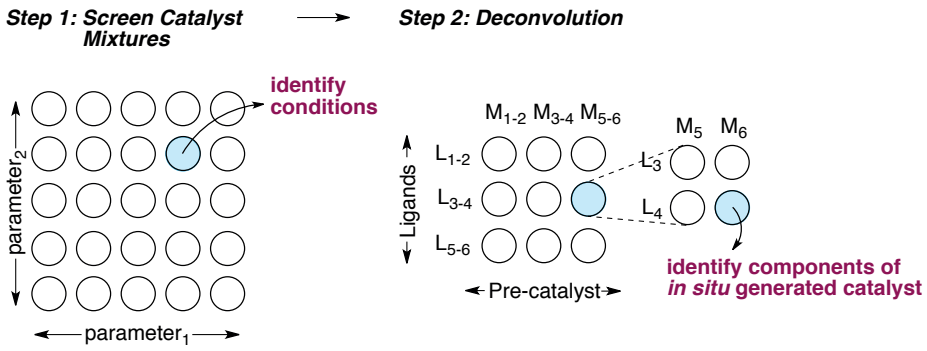

Scheme 3.1. Step 1 and Step 2 of the combinatorial approach.

3.1.2 Boronic acids as ideal candidates for screening mixtures

3.1.2.1 Complexes of boronic acid derivatives with bidentate ligands

Mixing boronic acid derivatives **80** and bidentate *O*-ligands can lead to the reversible dehydrative formation of the corresponding 1:1 complex **81** (Scheme 3.2). These complexes are often found in a neutral and trigonal planar form, but can also exist in an anionic tetrahedral form (**82**) above a critical pH value for a particular species.[91] This unique feature permits the reversible recognition of various motifs such as diols where a rapid, reversible equilibrium continues to gain interest in the recognition of carbohydrates.[92]

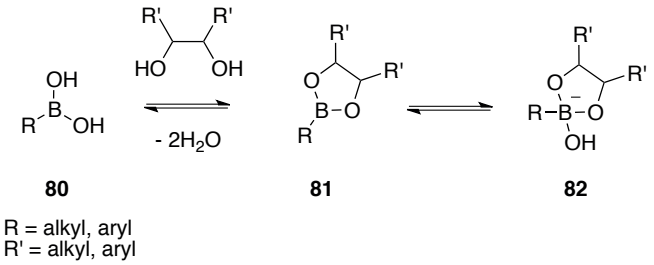

Scheme 3.2. Boronic acids and *O*-bidentate ligands form boronic and boronate esters in solution.

Several reports have tried to measure the dynamics of boronic acid complexation reactions with a variety of ligands and boronic acids. The equilibrium constants of diverse

[91] D. G. Hall, *Boronic Acids–Preparation and Applications in Organic Synthesis Medicine and Materials*, ed. Wiley-VCH, Weinheim, 2nd edn, **2011.**
[92] S. Lim, J. O. Escobedo, M. Lowry, R. M. Strongin, *Chem. Commun.* **2011**, *47*, 8295–8297.

ligands, including diols, α-hydroxyacids and dicarboxylic acids have been determined.[93] The equilibrium constants of the complexes are affected by both components and generally increase as ligand and boronic acid derivatives become more acidic (Table 3.1). For example, oxalic acid and phenylboronic acid, both displaying low p*K*a values in their category, also possess the largest equilibrium constant in their category. Conversely, catechol and boric acid, each displaying the highest p*K*a values, led to the complex that showed the lowest equilibrium constant.

Table 3.1. Equilibrium constants of different 1:1 complexes of boron acids and ligands. Data are taken from reference L. Babcock, R. Pizer, *Inorg. Chem*. **1980**, *19*, 56-61.

Ligand	p*Ka* (ligand)	*m*-$NO_2PhB(OH)_2$, p*Ka* = 6.96	$PhB(OH)_2$ p*Ka* = 8.72	$B(OH)_3$ p*Ka* = 8.98
oxalic acid	1.04		3.2	
malonic acid	2.59		2.6×10^{-2}	
salicylic acid	2.83	1.1	6.8×10^{-2}	1.1×10^{-2}
tartaric acid	2.89			1.8×10^{-2}
mandelic acid	3.22	1.9×10^{-1}	1.5×10^{-2}	
catechol	9.27		4.7×10^{-5}	1.1×10^{-5}

3.1.2.2 Boron complexes in catalysis

Many reports describe catalytic applications of boronic acids and their specific assembling properties with a variety of ligands. In asymmetric catalysis, the most famous is probably the Corey-Bakshi-Shibata (CBS) catalyst **85** for ketone reduction exemplified with acetophenone **83** giving (*R*)-1-phenylethanol **84** with quantitative yield and 97% ee (Scheme 3.3, equation 1).[94] The class of catalysts forms under reflux condensation of a proline-derived amino alcohol with various boronic acids. Yamamoto described the Chiral (Acyloxy)Borane (CAB) catalyst **89** in asymmetric Diels-Alder reaction between dienophile **86** and cyclopentadiene (Scheme 3.3, equation 2).[95] The catalyst is generated upon mixing tartaric acid derivatives with BH_3•THF for several minutes. In 2006, Yamamoto reported the use of *in situ* generated boronic ester catalyst **91** in amide condensations reactions (Scheme 3.3, equation 3).[96] Azeotropic removal of water was required to achieve dehydrative condensation of boric acid with tetrachlorocatechol by displacing the equilibrium to the cyclic boron

[93] L. Babcock, R. Pizer, *Inorg. Chem*. **1980**, *19*, 56–61.
[94] E. J. Corey, R. K. Bakshi, S. Shibata, *J. Am. Chem. Soc.* **1987**, *109*, 5551–5553.
[95] K, Furuta, S. Shimizu, Y. Miwa, H. Yamamoto, *J. Org. Chem*. **1989**, *54*, 1481–1483.
[96] T. Maki, K. Ishihara, H. Yamamoto, *Org. Lett*. **2006**, *8*, 1431–1434.

species. Boronic ester **91** showed remarkable rate acceleration (93% after 1 h) compared to a previously developed amidation catalyst, 3,5-trifluoromethylboronic acid, which furnished only 8% yield of the amide **90** under the same conditions. Maruoka and co-workers described a dual catalyst that possesses a Brønsted acidic carboxylate that interacts with a Lewis acidic boron atom, a class of catalysts referred to as Lewis acid-Assisted Brønsted acid (Scheme 3.3, equation 4).[97,98] The intramolecular hydrogen bond to an acceptor species can increase the Lewis acidity of the boron atom in catalyst **95**, enhancing the reactivity of the complex in a trans-aziridination reaction.

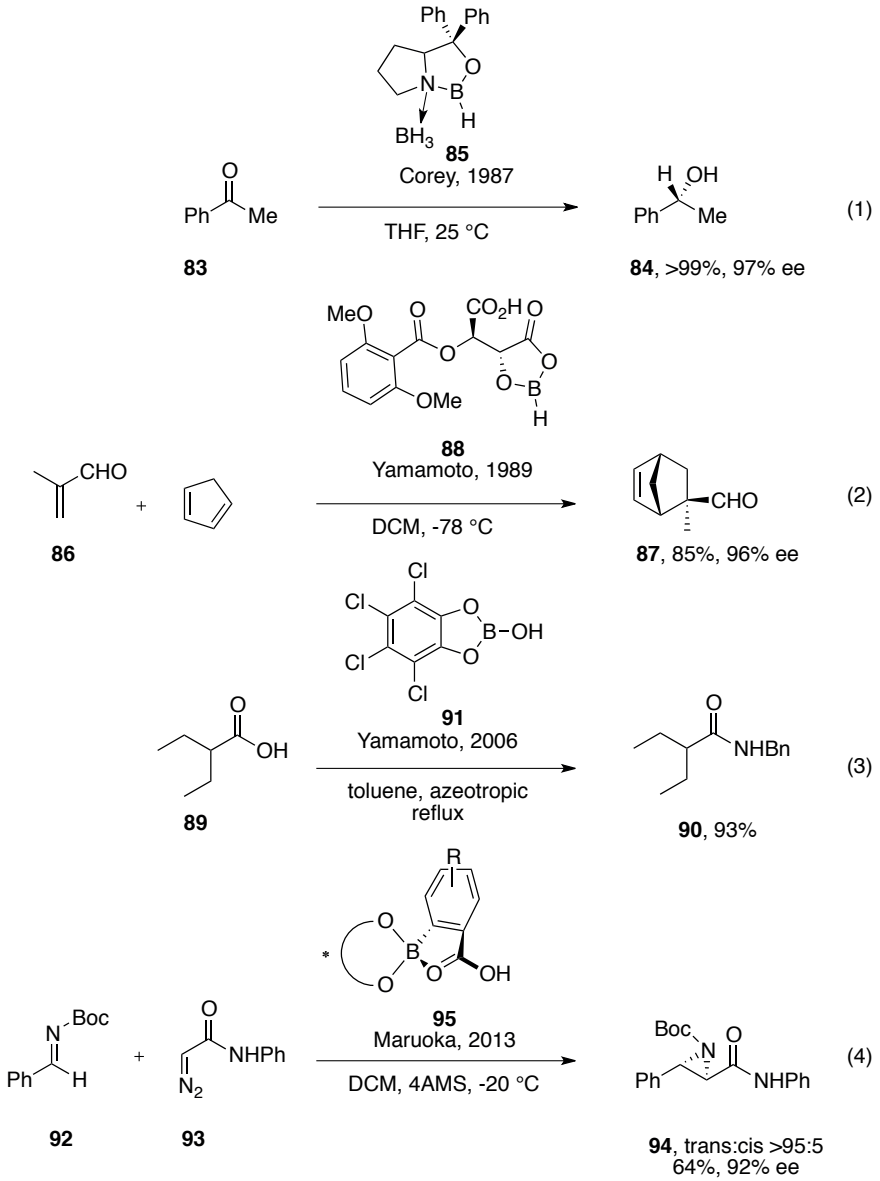

Scheme 3.3. Boron catalysts described in the literature.

[97] T. Hashimoto, A. O. Galvez, K. Maruoka, *J. Am. Chem. Soc.* **2013**, *135*, 17667–17670.
[98] For review on dual acid catalysis, see: Y. Yamamoto, K. Futatsugi, *Angew. Chem. Int. Ed.* **2005**, *44*, 1924–1942.

Most boron catalysts described are generated through dehydrative reactions, previously prepared in a separate synthetic step or by *in situ* synthesis typically requiring reflux or dehydrating agents to offset unfavorable thermodynamics.

3.2 Application of the combinatorial strategy

3.2.1 Choice of the library components

Boron catalysts generated *in situ* from boronic acids and bidentate *O*-ligands are ideal candidates to screen by our proposed combinatorial approach against a specific transformation. Their electronic and steric properties can be modulated by exchange of B-O covalent bonds, yet the optimal intersection of catalyst assembly and catalyst activity remains unclear. Some catalysts might form only to a small extent in equilibrium but be excellent catalysts while others might form readily but be poor catalysts under the reaction conditions. The complex mixture can be thought of as a dynamic combinatorial library[99] composed of *in situ*-generated cyclic boron species (Scheme 3.4). Here, the objective was to test our proposed combinatorial method to identify a catalytically active combination of bidentate *O*-ligand and boron pre-catalysts by screening a complex mixture of these components. To increase the discovery potential of active systems, the generated library should therefore be as diverse as possible.

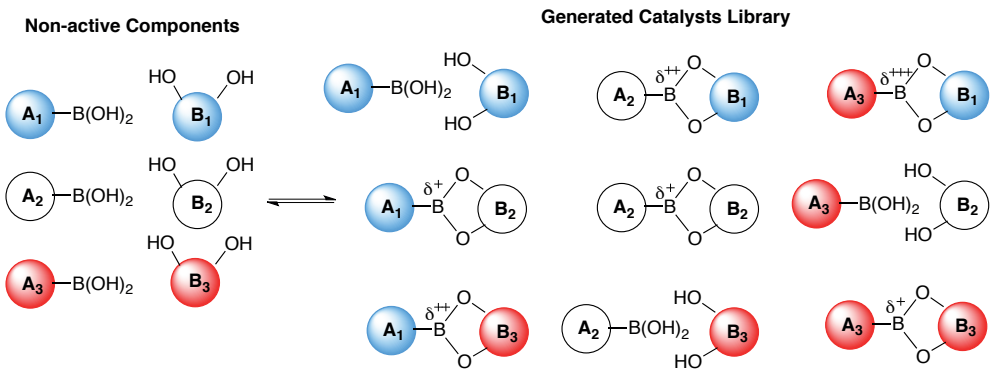

Scheme 3.4. Dynamic combinatorial library of boron catalysts displaying different equilibrium constants and catalytic activities.

[99] P. Dydio, P.-A. R. Breuil, J. N. H. Reek, *Isr. J. Chem.* **2013**, *53*, 61–74.

3.2.2 Library of boronic acids

To achieve structural and electronic diversity among the potential catalysts, twelve diverse boronic acids were chosen, including strongly electron-deficient boron species carrying multiple halogen atoms as well as those carrying electron-donating functional groups. Boric acid was also chosen (Scheme 3.5).

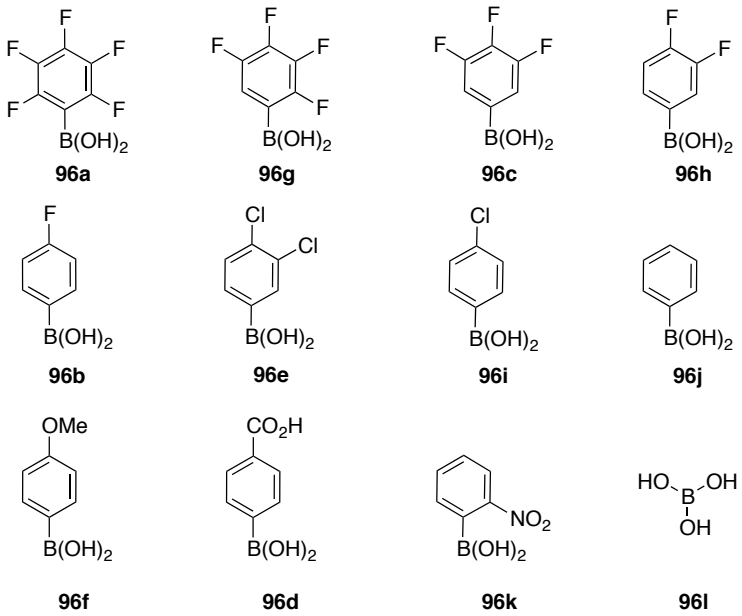

Scheme 3.5. Boronic acid library.

3.2.3 *O*-ligands

Twelve bidentate or polydentate *O*-ligands were chosen with the goal of maximizing their structural diversity, including diols, catechols, hydroxyacids and diacids capable of forming 5-membered boronic esters (**97a-97g**) and capable of forming 6- or 7-membered boronic esters (**97h-97l**) (Scheme 3.6).

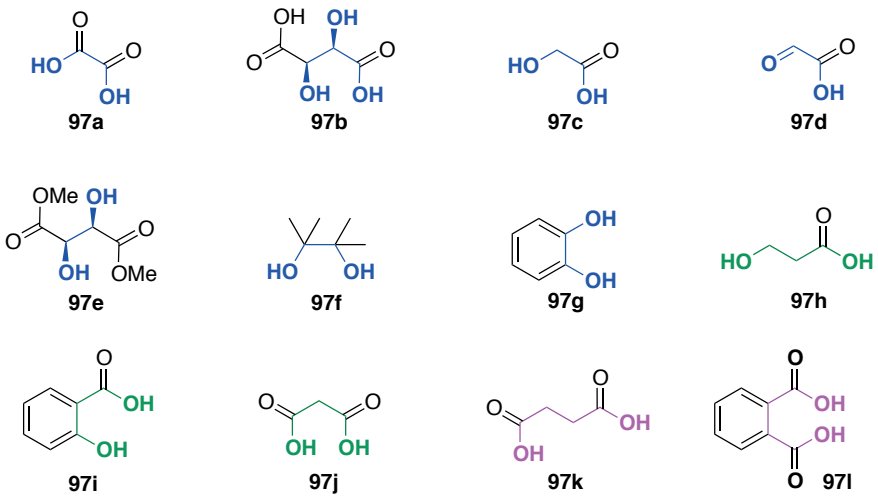

Scheme 3.6. Diverse *O*-ligands library. In blue, ligands forming a 5-membered ring with boronic acids; in green, ligands forming a 6-membered ring with the boronic acids; in pink, ligands forming a 7-membered ring with boronic acids.

3.2.4 The dehydrative Friedel-Crafts reaction as a model reaction

The dehydrative Friedel-Crafts reaction was chosen as a probe since it is known to be triggered by relatively strong Lewis or Brønsted acids. The specific transformation between *p*-methoxybenzyl alcohol **98** and mesitylene **64** to give diarylmethane **99** is not enabled by boronic acids or carboxylic acids alone at room temperature (Scheme 3.7).

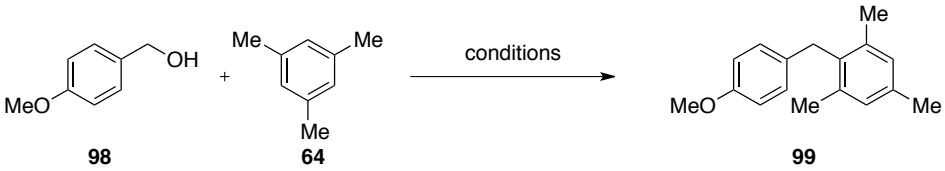

Scheme 3.7. Model reaction.

3.2.4.1 Step 1: Screen Catalyst Mixtures

The first step of the combinatorial approach will identify the best conditions for the reaction to occur. In this particular Friedel-Crafts reaction, apart from the catalysts themselves, the solvent is likely a critical parameter. A mixture of all twelve boron pre-catalysts (1 mol% each) and all twelve *O*-ligands (2 mol%) were screened against fourteen

different solvents, including but not limited to those that are typically employed in Friedel-Crafts reactions in the literature (Scheme 3.8). The screening resulted in 77% yield of compound **99** in $MeNO_2$, 26% in MeCN, 3% in DCM and DCE and less than 1% in the ten other solvents tested. Though the identities of the most active components were not yet known, this lead result was identified in just 14 reactions but covering 2068 possible combinations of boronic acid, ligand and solvent (12 x 12 x 14).

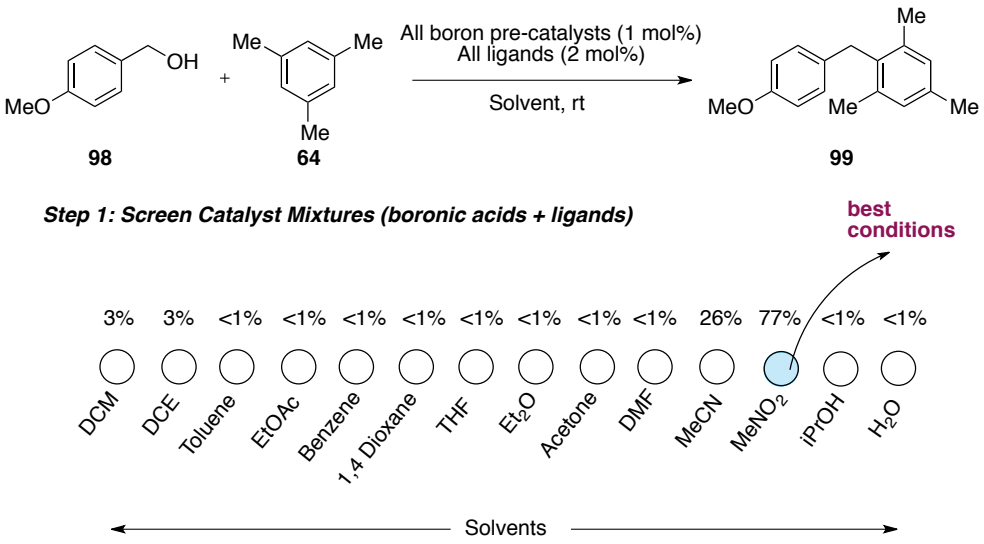

Scheme 3.8. Step 1: Screening mixtures against 14 different solvents.

3.2.4.2 Step 2: Deconvolution of mixtures to find the best catalyst

In Step 2a of the screening process, boron pre-catalysts were randomly divided into two groups each containing six boronic acids (Scheme 3.9). Ligands were divided into two groups, those that form a 5-membered ring with the boronic acid and those that form a 6- or a 7-membered ring with the boronic acid. The four possible combinations of groups were screened with 1 mol% of each boronic acid and 2 mol% of each *O*-ligand present in the reaction at the same time. The best result was found to come from the mixture of boronic acids **96a-96f** and from the mixture of *O*-ligands **97a-97g**, which went to completion after 2.5 h at room temperature.

In Step 2b of the iterative deconvolution process, the winning boronic acids were broken up into three arbitrary groups, **96a-96b**, **96c-96d** and **96e-96f**. Likewise, the winning *O*-ligands were divided into three groups, **97a-97b**, **97c-97d** and **97e-97g**. Of the resulting

nine reactions, the most potent combination was found to be **96a-96b** with **97a-97b**, which went to completion after just 1 h. Indeed, the time for reaction completion decreases with each optimization step, as the optimal catalyst is present in higher concentration.

In Step 2c, the remaining four combinations were tested individually. Impressively, mixing just 1 mol% of **96a** with 2 mol% of **97a** led to 95% yield of **99** after just 15 min at room temperature. Using the iterative deconvolution strategy, only 17 manipulations were required to identify the best combination.

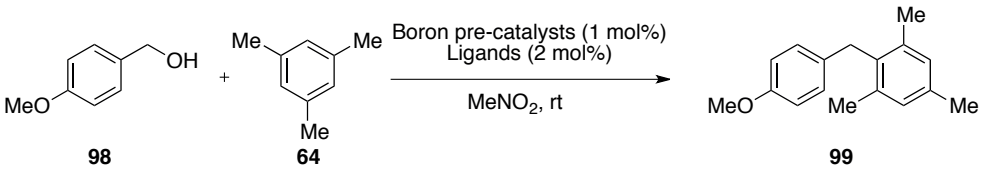

Step 2 (17 reactions)**:** All reactions performed in $MeNO_2$

Step 2a t = 2.5 h	$RB(OH)_2$ **96a-96f**	$RB(OH)_2$ **96g-96l**
n = 0 **97a-97g**	**90% yield**	63%
n = 1-2 **97h-97l**	7%	5%

Step 2b t = 1 h	**96a**, **96b**	**96c**, **96d**	**96e**, **96f**
97a **97b**	**91%**	33%	29%
97c **97d**	8%	2%	3%
97e **97f** **97g**	<1%	<1%	<1%

Step 2c t = 15 min	**96a**	**96a**
97a	**95%**	16%
97b	19%	<1%

Conditions: [a] 1.0 equiv **98**, 3.0 equiv **64**; [b] Yield determined by ^1H NMR in $CDCl_3$ with DMSO (1 equiv) as internal standard.

Scheme 3.7. Combinatorial identification of *in situ*-generated boron catalysts for the dehydrative Friedel-Crafts reaction.[a,b]

Using this two-step method, only 31 reactions were required to screen and deconvolute 2016 possible *in situ* generated catalysts in fourteen different solvents, with eventual success foreshadowed by the initial hit in step 1.

3.3 Linear optimization

3.3.1 Linear optimization of the ligand

To compare the results from the combinatorial screen with what might be found by a traditional screening approach, we tested all ligands in combination with the most active boronic acid **96a** revealed by the combinatorial approach. Linear optimization showed that only specific *O*-ligands displayed significant catalytic activity in the presence of **96a**, including hydroxyacids **97b-97d**, salicylic acid **97i**, malonic acid **97j**, the most reactive ligand being oxalic acid **97a**. This general trend follows the stability constants described by Pfizer. Increased reactivity was observed in the Friedel-Crafts reaction with the most acidic ligand partners. To make sure that the catalytic activity comes from the combination of boronic acid and ligand, control experiments were run with 10 mol% of ligand and boronic acid individually. Neither component is able to catalyze the reaction on its own except for oxalic acid **97a**. However, this reactivity was much slower than the combination of **96a** and **97a** (10 mol% of **97a**, 4 h, 18%). We observed a strong ligand dependence on the rate of catalysis.

Table 3.2. Linear optimization to find the best ligand for the Friedel-Crafts reaction.[a,b]

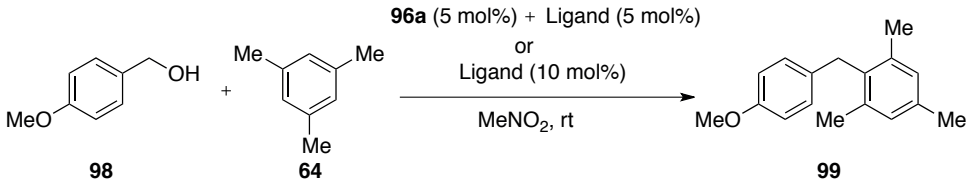

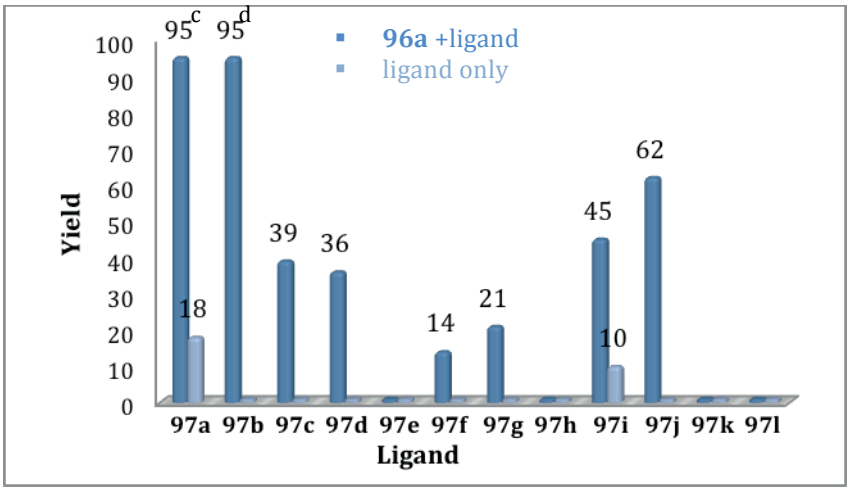

Conditions: [a] 1.0 equiv **98**, 3.0 equiv **64**, 4 h; [b] Yield determined by ^{1}H NMR in $CDCl_3$ with DMSO (1 equiv) as internal standard; [c] Yield determined after 5 minutes; [d] Yield determined after 90 minutes.

3.3.2 Linear optimization of the boronic acid

We also undertook a linear optimization of boronic acids, keeping oxalic acid **97a** as the ligand (Table 3.3). All boron compounds surveyed showed some catalytic activity in the presence of **97a** with electron-poor boronic acids being the most active compounds. Reducing the strength or number of the electron withdrawing substituents on the boronic acid generally led to reduced reactivity. Boronic acids with electron donating groups on the phenyl ring such as **96f** and boric acid **96l** showed the lowest reactivity but still led to a complete reaction within four hours. 4-Carboxyphenylboronic acid **96d** was the only boronic acid that gave no conversion to the desired compound, probably due to its low solubility in nitromethane. As previously, control experiments were run with 10 mol% of boronic acid in the absence of ligand and displayed no catalytic activity after 4 h of reaction time.

Table 3.3. Linear optimization to determine the best boronic acid for the Friedel-Crafts reaction.[a,b]

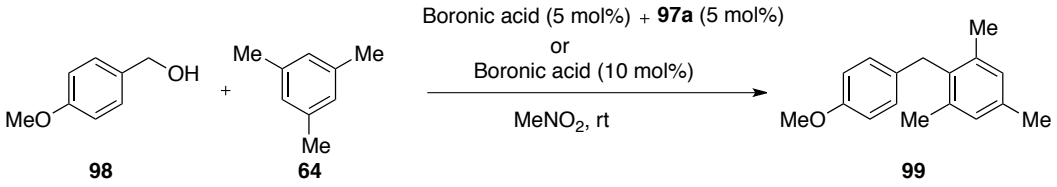

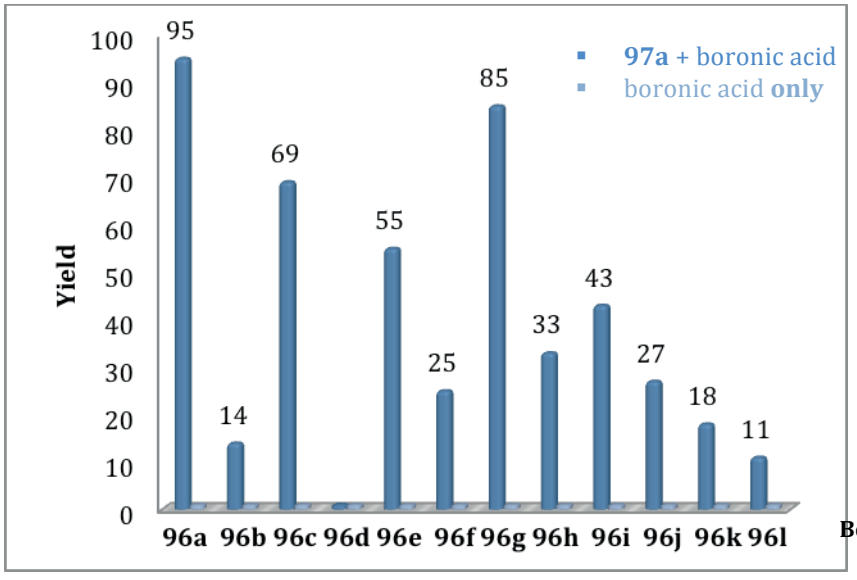

Conditions: [a] 1.0 equiv **98**, 3.0 equiv **64**, 5 minutes; [b] Yield determined by ^{1}H NMR in $CDCl_3$ with DMSO (1 equiv) as internal standard.

3.4 *In situ* formation of dioxaborolanedione

3.4.1 (1:1) complex

Dioxaborolanediones were first synthesized in 1971 by Paetzold and coworkers by oxalic acid with dichloroboranes under an inert atmosphere.[100] Dioxaborolanediones were later reported as electrolytes in lithium batteries, where they were prepared by refluxing boronic acids and oxalic acids with a Dean-Stark apparatus.[101] Pizer described the 1:1 assembly between oxalic acid **97a** and several other boronic acids with different rate and stability constants.[102] However, in all of these cases, very poor characterization was carried out and little was known about the nature of the equilibrium or hydration states of electron-poor dioxaborolanediones. Furthermore, dioxaborolanediones or mixtures of boronic acids with oxalic acid have not previously been described in catalysis. Given the impressive observed catalytic activity resulting from the combination of boronic acid **96a** with oxalic acid **97a**, we wished to investigate the nature of the species that are formed in solution upon mixing these components. ESI-TOF mass spectrometric experiments in our hands detected the presence of catalyst **100** coordinated to a molecule of water, presumably coordinated to the boron atom (Molecular ion mass: 282.98 in negative mode). The free dioxaborolanedione was not detected. In line with this observation and our previous experience with the hydrates of $B(C_6F_5)_3$, we expected the initial 1:1 assembly of **96a** and **97a** to form dioxaborolanedione hydrate **100** and bishydrate **100** (Scheme 3.10). However, further spectroscopic experiments were required to evaluate the equilibrium between the various forms and to gain insight into whether the catalyst might operate as a Lewis acid or Brønsted acid.

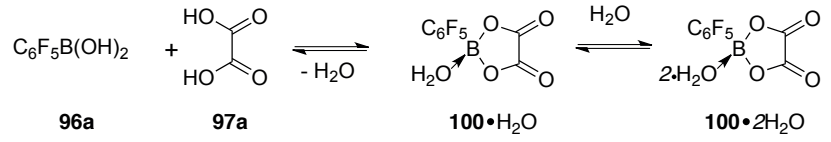

96a **97a** **100•H_2O** **100•2H_2O**

Scheme 3.10. Proposed structures of *in situ* generated boron catalyst.

[100] (a) P. I. Paetzold, W. Sheibitz, E. Scholl, Z. Naturforsch., B: *Chem. Sci.* **1971**, *26*, 646–649; (b) P. Paetzold, S. Neyses, L. Geret, *Z. Anorg. Allg. Chem.* **1995**, *621*, 732–736.
[101] L. F. Li, H. S. Lee, H. Li, X. Q. Yang, X. J. Huang, *Electrochem. Commun.* **2009**, *11*, 2296–2299.
[102] (a) S. Friedman and R. Pizer, *J. Am. Chem. Soc.* **1975**, *97*, 6059–6062; (b) L. Babcock, R. Pizer, *Inorg. Chem.* **1980**, *19*, 56–61; (c) R. Pizer, P. J. Ricatto, *Inorg. Chem.* **1994**, *33*, 2402–2406.

3.4.2 Monitoring catalyst assembly in ^{19}F NMR

3.4.2.1 Different oxalic acid ratios

Spectroscopic experiments were conducted to study the dynamics of the covalent assembly of **96a** with **97a**. When **96a** and **97a** are combined in a 1:1 ratio in CD_3NO_2, two new sets of peaks appear in the ^{19}F NMR and are at equilibrium before the first spectrum can be recorded. Diagnostic peaks in the *ortho*-F region are assigned to dioxaborolanedione hydrate **100**•H_2O (-137.0 ppm) and its dihydrate **100**•*2*H_2O (-136.3 ppm) based on the following experiments (Figure 3.1). Addition of excess equivalents of **97a** causes the peaks assigned to **100**•H_2O and the peaks assigned to **100**•*2*H_2O to grow at the expense of the resonances corresponding to **96a**.

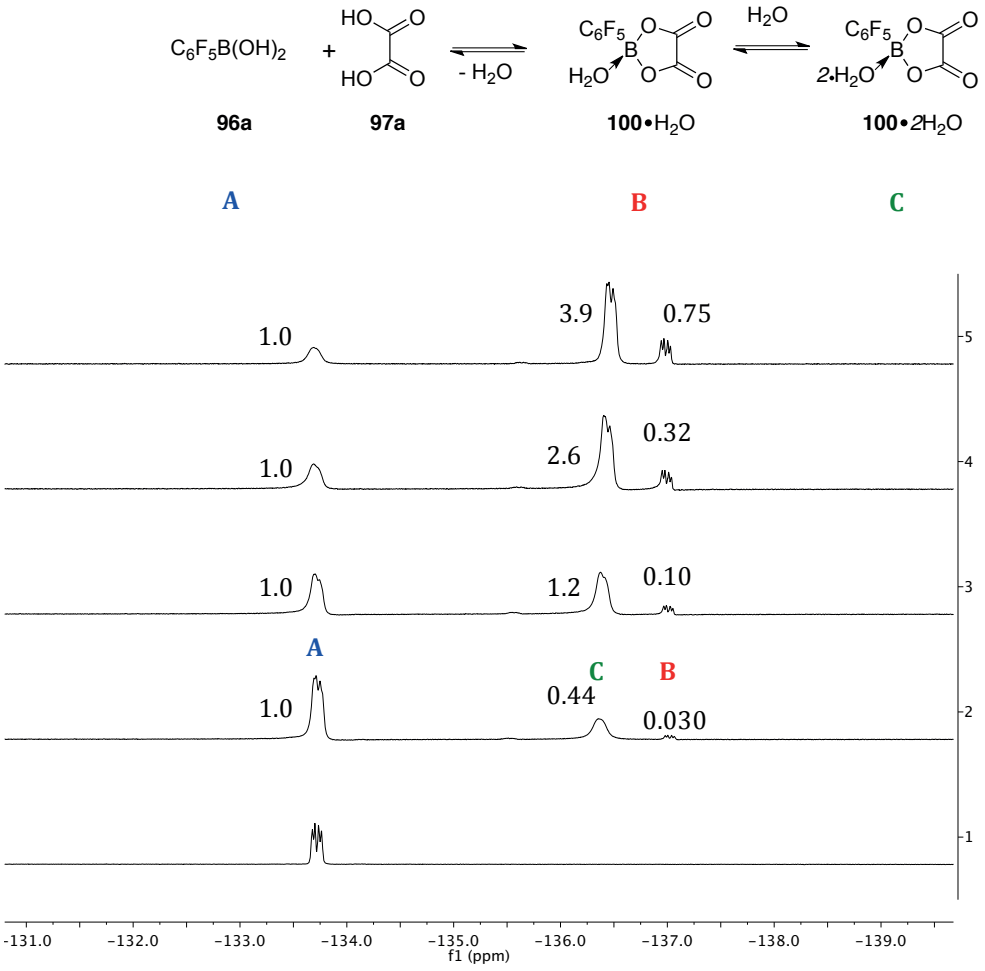

Figure 3.1. *Ortho*-F region of ^{19}F NMR spectra of a mixture of **96a** and **97a** in CD_3NO_2 in different ratios (1) no oxalic acid **97a**; (2) 1 equiv **97a**; (3) 2 equiv **97a**; (4) 3 equiv **97a**; (5) 4 equiv **97a**.

Different ratios of oxalic acid were tested in parallel on the Friedel-Crafts reaction and showed that when oxalic acid is in excess relative to pentafluorophenylboronic acid, better yields within the same amount of time are observed. With 2 equivalents of **97a** relative to **96a**, 95% yield could be observed after 15 minutes of reaction time (Table 3.4). In accordance with the NMR experiments in section 6.2.1, a plausible explanation for this observation lies on the presumable equilibrium displacement towards the cyclic catalyst **100** when oxalic acid is added in excess, resulting in an increased amount of active catalyst in solution.

Table 3.4. Evaluation of different ratios of boronic acid **96a** to oxalic acid **97a** on the Friedel-Crafts reaction.[a,b]

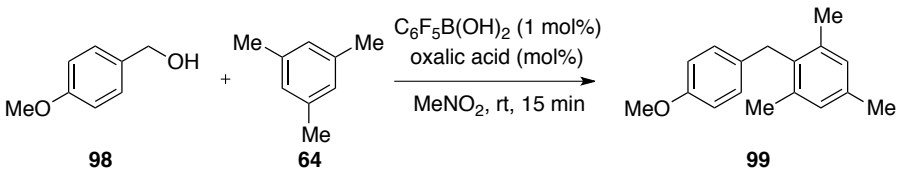

98 **64** **99**

Entry	Ratio **96a**/ **97a**	Yield [%]
1	1:4	96
2	1:3	95
3	1:2	95
4	1:1	65

Conditions: [a] Alcohol **98**, nucleophile **64**, 15 min; [b] Yield determined by ^{1}H NMR in $CDCl_3$ with DMSO (1 equiv) as internal standard.

3.4.2.2 Addition of water

Two equivalents of water are released during the course of the catalyst assembly and during the Friedel-Crafts reaction water is released as a stoichiometric byproduct. We therefore aimed to study the effect of water on the catalyst assembly. Counterintuitively, addition of an excess of water (1-24 equiv) does not favor hydrolysis back to **96a** but instead causes **100**•*2*H_2O to grow at the expense of **100**•H_2O and **96a** (Figure 3.2, experiment 4). A slight gradual upfield shift of the resonances corresponding to **96a** and **100**•*2*H_2O is observed as the water concentration is increased over this range, likely due to bulk solvent effects. Hydration of dioxaborolanedione **100** is apparently thermodynamically preferred to hydrolysis and is a driving force for covalent assembly, giving the acid its water-tolerant properties.

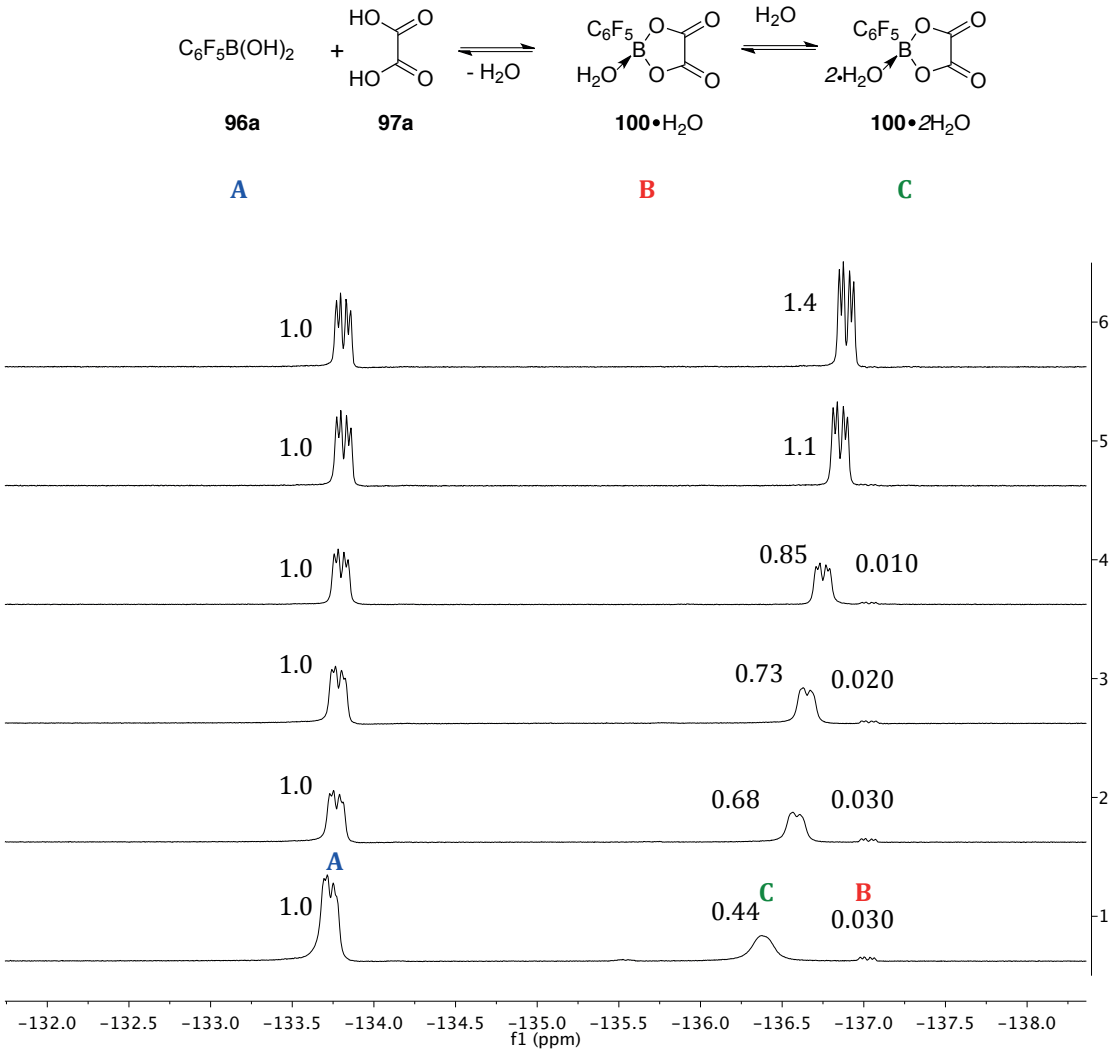

Figure 3.2. *Ortho*-F region of ^{19}F NMR spectra of a mixture of **96a** and **97a** in CD_3NO_2 with additional water (1) no H_2O; (2) 4 equiv H_2O; (3) 8 equiv H_2O; (4) 12 equiv H_2O; (5) 24 equiv H_2O; (6) 36 equiv H_2O.

3.4.3 Monitoring catalyst assembly in ^{11}B NMR

Although ^{11}B NMR is not that sensitive, it generally allows distinguishing between trigonal planar and tetrahedral boron geometries.[103] The boron resonance from its trigonal form as a boronic acid usually results in the range of 30 ppm with dramatic upfield shift when converted to the corresponding tetrahedral form as a boronate (10-0 ppm). Boron NMR

[103] W. G. Henderson, M. J. How, G. R. Kennedy, E. F. Mooney, *Carbohydrate Res*. **1973**, *28*, 1–12.

experiments with different ratios of oxalic acid and water were thus conducted (Figure 3.3). When boronic acid **96a** was dissolved in CD_3NO_2 without any additive, only one peak was observed at 31.5 ppm, in the range usually observed for boronic acid components.[104] The addition of one equivalent of oxalic acid **97a** caused the appearance of one additional peak at 9.5 ppm. In light of the ^{19}F NMR data indicating the presence of at least three species, we suspect that the observed new single peak arises from overlap of the signals corresponding to the monohydrate form and also the dihydrate form of **100**.

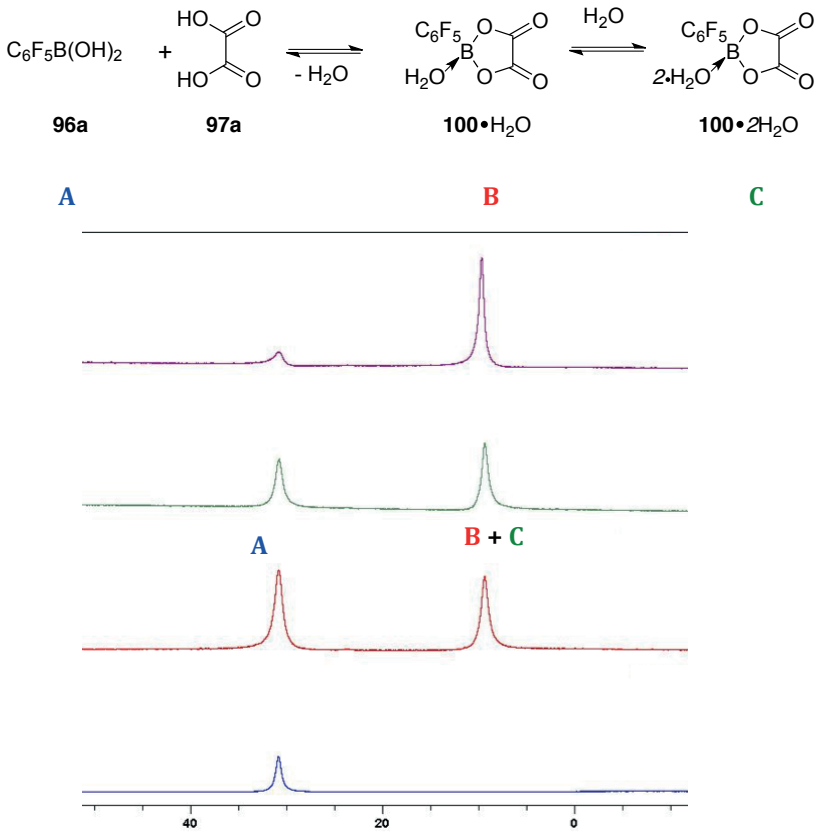

Figure 3.3. ^{11}B NMR spectra of a mixture of **96a** and **97a** in CD_3NO_2 (1) no oxalic acid 97a; (2) 1 equiv oxalic acid **97a**; (3) 2 equiv oxalic acid **97a**; (4) 2 equiv oxalic acid **97a** and 24 equiv H_2O.

[104] C. Adamo, C. Amatore, I. Ciofini, A. Jutand, H. Lakmini, *J. Am. Chem. Soc.* **2006**, *128*, 6829–6836.

3.4.4 Catalyst assembly in other solvents

The combinatorial screening approach has revealed the excellent synergy between nitromethane and catalyst **100** for the Friedel-Crafts reaction between alcohol **98** and mesitylene. However, we also observed 26% of the desired product **99** in MeCN and traces of compound **99** in DCM and DCE (3% in each). The marked difference in reactivity between the solvents might arise for a number of reasons, including slower catalyst assembly in certain solvents or solvent effects on the reaction itself. To evaluate these competing hypotheses, ^{19}F NMR experiments were designed to monitor catalyst formation in CD_3CN and CD_2Cl_2. The results show that catalyst assembly occurs in CD_3CN with approximately the same rate of formation for **100** than in CD_3NO_2, but dihydration of **100** is slightly less favored (Figure 3.4, experiments 1 and 2). In contrast, the same experiments in CD_2Cl_2 were conducted and showed that within the same timescale, catalyst **100** did not form (Figure 3.4, experiments 3 and 4). Thus solvent plays a critical role both in catalyst assembly and on the reaction itself. Presumably, nitromethane has a positive effect on the rate of the catalyst formation and also provides a favorable solvent effect in the reaction itself.

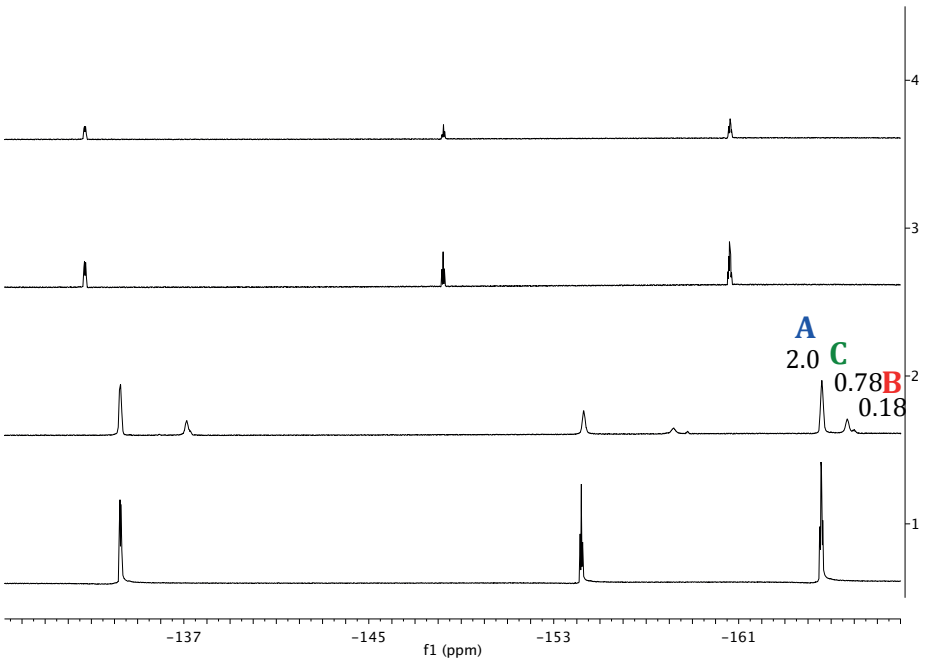

Figure 3.4. ^{19}F NMR spectra of a mixture of **96a** and **97a** (1) no **97a** in CD_3CN; (2) 2 equiv **97a** in CD_3CN (3) no **97a** in CD_2Cl_2; (4) 2 equiv **97a** in CD_2Cl_2.

3.5 Kinetics of the Friedel-Crafts reaction

In an attempt to differentiate the catalytic activity of monohydrate **100** and dihydrate **100**, we investigated the kinetics of the Friedel-Crafts reaction (Figure 3.5). As water is released during the course of the reaction, we wanted to study the influence of the equilibrium displacement towards the dihydrate form on the reaction rate. The general trend offers a logarithmic curve, starting very fast until achieving a plateau after 30 minutes of reaction time. This study, in parallel with Figure 3.2, shows that even when the dihydrate form is the only catalyst present, the Friedel-Crafts reaction still proceeds, meaning that probably both hydrated catalyst forms are active in the dehydrative reaction. Taken together, the spectroscopic and kinetic observations seem to favor Brønsted acid catalysis over Lewis acid catalysis, though the latter cannot be rigorously excluded.

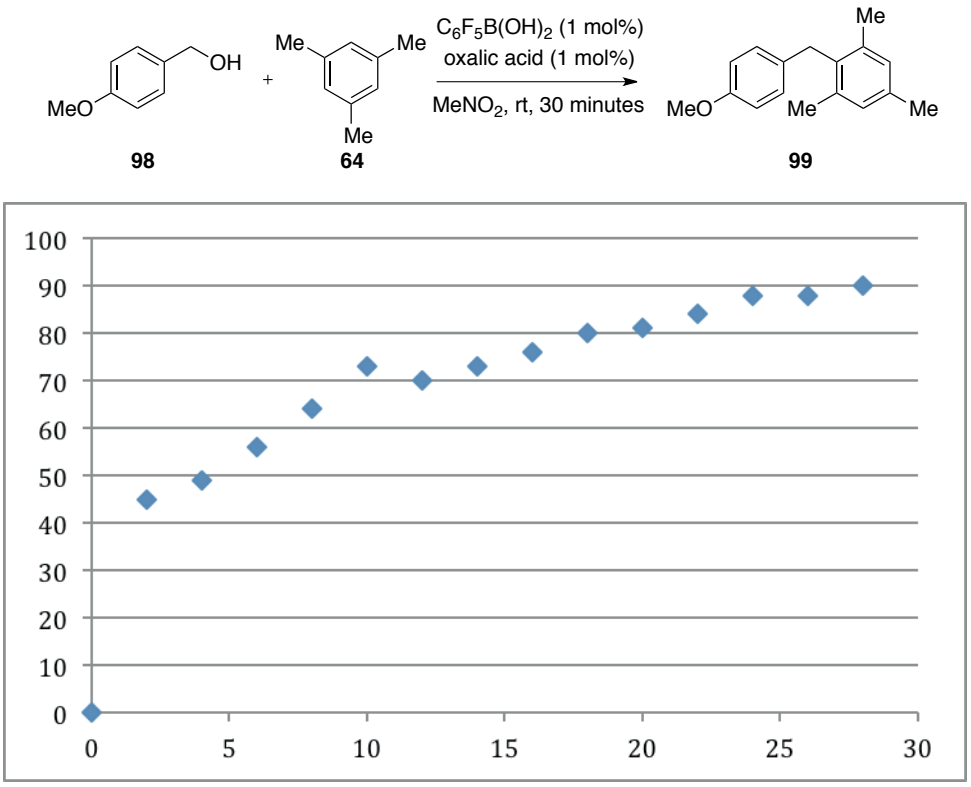

Figure 3.5. Monitoring the conversion of compound **98** to **99**.

3.6 Quantifying acidity

To evaluate the acidity of dioxaborolanedione hydrate **100** compared to other acids, a variant of the Gutmann-Beckett method was used. The classical Gutmann-Beckett approach[105] measures chemical shifts in ^{31}P NMR between a solution of free Et_3PO in the ^{31}P NMR compared to a solution containing a mixture of Et_3PO and a coordinated Lewis acid (LA) of interest in a non coordinating solvent (Scheme 3.11). The greater the strength of the Lewis acid, the more the peak will be shifted downfield. Though the Gutmann-Beckett method is typically used to measure Lewis acidity, we proposed that the same method can in principle be applied to measure Brønsted acidity, since Et_3PO is a well known hydrogen bond acceptor. With such a scale, meaningful quantitative comparisons between Brønsted and Lewis acid catalysts could then be established.

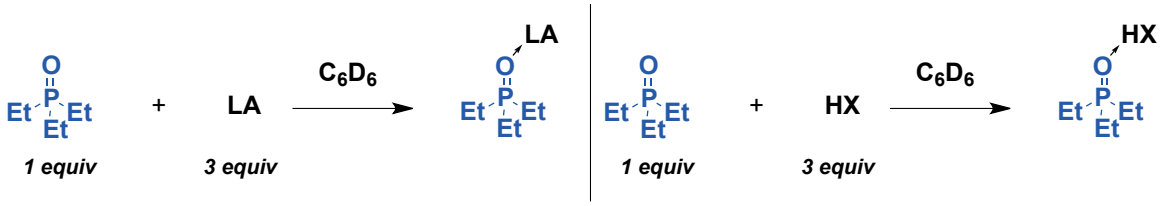

Scheme 3.11. Classic Gutmann-Beckett method for evaluation of Lewis acidities (left) and our variant for Brønsted acidities (right).

As a reference point, preparation of mixtures of Et_3PO and $B(C_6F_5)_3 \bullet nH_2O$ (1:3) resulted in a signal at 75.6 ppm (Figure 3.6, Experiment 7), a value that is surprisingly similar to several reported values for dry $B(C_6F_5)_3$ carefully handled in a glove box.[106] Applying the same procedure to oxalic acid **97a** or to boronic acid **96a** led to the complete disappearance of the signal at 47.0 ppm of free triethylphosphine and resulted in the appearance of signals at 53.8 and 64.1 ppm, respectively (Experiment 2 and 3). A 3:3:1 mixture of **96a**, **97a** and Et_3PO revealed a single peak at 79.9 ppm (Experiment 4). Therefore, catalyst **100** resulted in a Gutmann-Beckett acidity that is 115% that of $B(C_6F_5)_3 \bullet nH_2O$.[107] We also evaluated the 3:3:1

[105] a) M. A. Beckett, G. C. Strickland, J. R. Holland, K. Sukumar Varma, *Polymer* **1996**, *37*, 4629–4631; b) V. Gutmann, *Coord. Chem. Rev*. **1976**, *18*, 225–255.
[106] a) M. Mewald R. Fröhlich, M. Oestreich, *Chem. Eur. J*. **2011**, *17*, 9406–9414; b) Z. Lu, Z. Cheng, Z. Chen, L. Weng, Z. H. Li, H. Wang, *Angew. Chem. Int. Ed.* **2011**, *50*, 12227–12231.
[107] Gutmann-Beckett acidities are commonly expressed as a percentage relative to a common standard (eg. $B(C_6F_5)_3$). For example, see: L. Greb, C.-G. Daniel, K. Bergander, J. Paradies, *Angew. Chem. Int. Ed.* **2013**, *52*, 5876–5879.

mixture of boric acid, **97a** and Et_3PO and observed a decreased acidity (Experiment 6) compared to **100** explaining the weaker conversion to Friedel-Crafts product **99** with this catalyst combination. Measurement of the acidity of TsOH by this method resulted in a chemical shift of 72.1 ppm (Experiment 8), which represents a weaker value than the one observed for catalyst **100**. Comparable acidity of catalyst **100** with HCl (37%) was observed with this method (Experiment 9), showing that catalyst **100** could have p*K*a values comparable to strong acids.

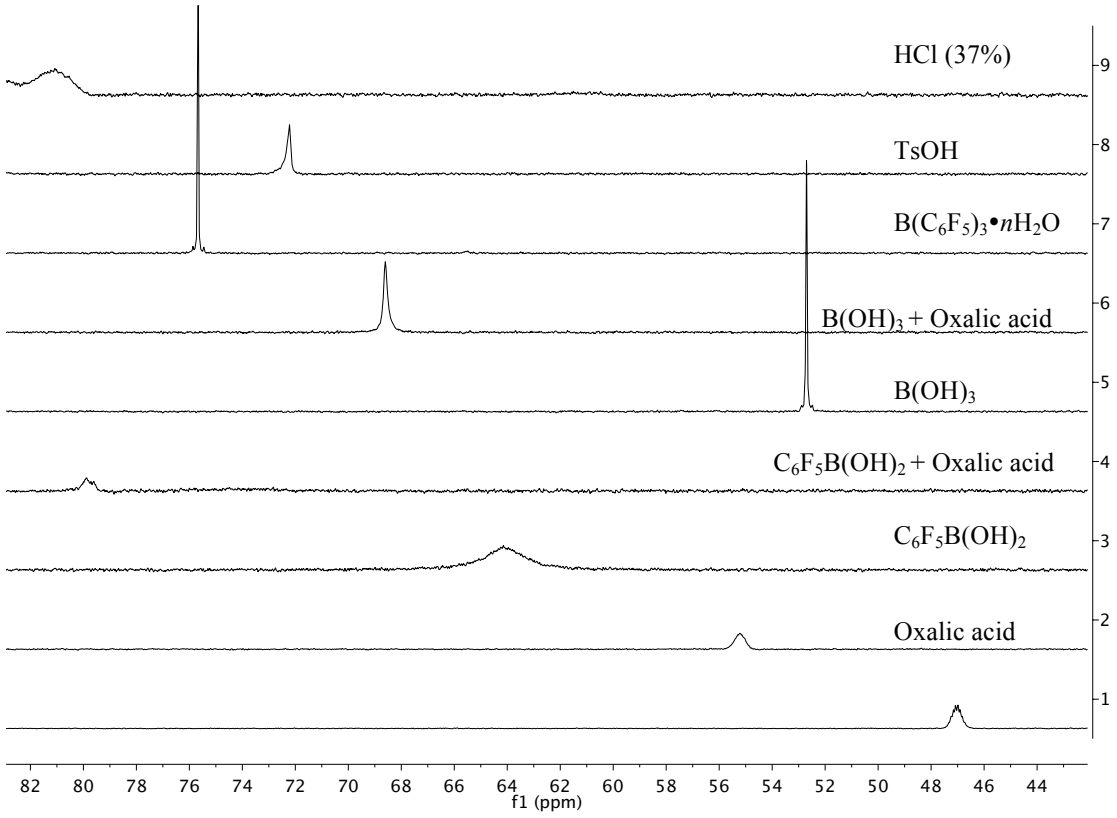

Figure 3.6. ^{31}P NMR showing Gutmann-Beckett experiments containing 1 equiv Et_3PO in C_6D_6 in the presence of (1) nothing; (2) 3 equiv oxalic acid **97a**; (3) 3 equiv pentafluorophenylboronic acid **96a**; (4) 3 equiv pentafluorophenylboronic acid **96a** and 3 equiv oxalic acid **97a**; (5) 3 equiv boric acid; (6) 3 equiv boric acid and 3 equiv oxalic acid **97a**; (7) 3 equiv $B(C_6F_5)_3•nH_2O$; (8) 3 equiv TsOH (9) 3 equiv aq. HCl (37%).

3.7 Substrate and Nucleophile scope

3.7.1 Chemoselectivity

To evaluate the chemoselectivity of **100•***n*H_2O, we submitted the reaction between substrate **54** and mesitylene **64** to afford compound **66a** selectively, a transformation that is incompatible with the presence of trace amounts of Brønsted acids (Scheme 3.12). We previously demonstrated in Chapter 2 that in a survey of various catalysts including monoprotic Brønsted acids, hydrolyzable Lewis acids and non-hydrolyzable Lewis acids, only the strong non-hydrolyzable Lewis acid $B(C_6F_5)_3$ could rapidly furnish **66a** at 22 °C and at 80 °C without accompanying Brønsted acid catalyzed olefin isomerization to **66b** at both temperatures.[36] Under identical conditions and reaction times, catalytic reactions employing 1 mol% each of $C_6F_5B(OH)_2$ **96a** and oxalic acid **97a** led to formation of **66a** without detection of **66b** at 22 °C or at 80 °C. These results indicate that the hydrates of **100** possess an attenuated kinetic Brønsted acidity with respect to alkenes.

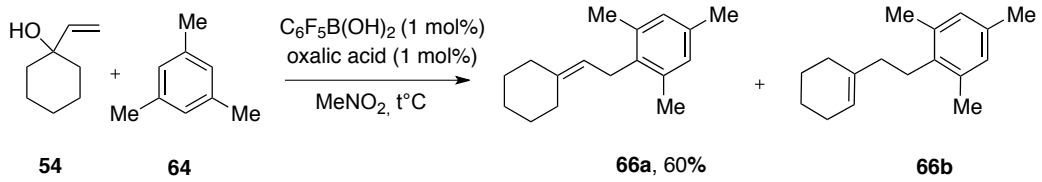

54 **64** **66a**, 60% **66b**

Scheme 3.12. Chemoselective Friedel-Crafts reaction with catalyst **100•***n*H_2O between exocyclic allylic alcohol **54** and mesitylene.

3.7.2 Allylic and benzylic alcohols

We subjected different alcohols to the same reaction conditions to evaluate the compatibility of substrates and nucleophiles (Scheme 3.13). Within less than 30 minutes at room temperature, alcohols that are dually substituted by both allylic and benzylic groups gave excellent yields in the presence of different *C*-, *N*-, *S*- and *O*- nucleophiles with 1 mol% of **96a** and 1 or 2 mol% of **97a**. Tertiary alcohol **101** gave Friedel-Crafts compound **103** with 99% and Boc-protected amine compound **104** with 98% yield with 1 mol% of **96a** and 2 mol% of **97a**. The reaction between secondary alcohol **39** and 1,3-cyclohexanedione gave 96% of desired compound **105**, whereas reaction with indole afforded **106** with nearly

quantitative yield. Amination with *tert*-butylcarbamate or azidation with TMS-N_3 went to completion in less than 15 minutes, leading to compounds **107** and **108** with 95 and 96% yield respectively. Using thiophenol as nucleophile on alcohol **39** led to thioether **109** with 95% yield. Intramolecular reactivity of *O*-nucleophile was observed with alcohol **102** giving cyclized chromene **110** with 90% yield.

Scheme 3.13. Allylic benzylic alcohol and nucleophile scope.[a,b]

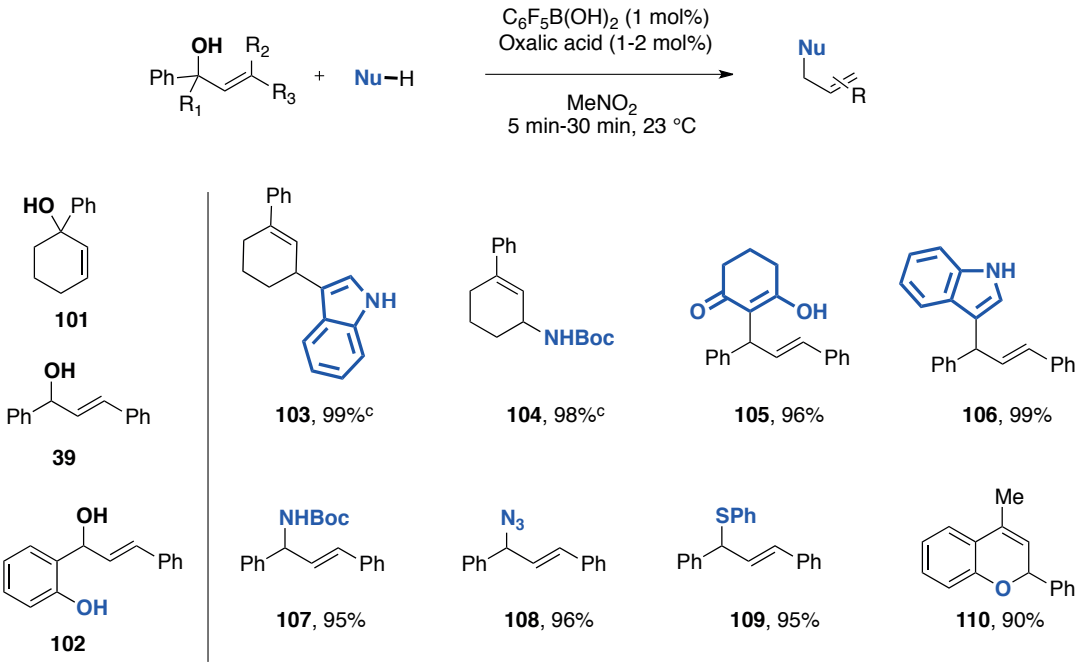

Conditions: [a] Alcohol, nucleophile, 1 mol% $C_6F_5B(OH)_2$ and 1 mol% oxalic acid in $MeNO_2$, 5-30 min; [b] Isolated yields after silica gel chromatography; [c] 1 mol% $C_6F_5B(OH)_2$ and 2 mol% oxalic acid.

3.7.3 Allylic alcohols

We further investigated allylic alcohols with *C*-, *N*- and *O*- nucleophiles (Scheme 3.14). Cyclodehydration of **60**, a reaction that reportedly does not proceed with 10 mol% of boronic acid catalyst alone, occurs rapidly at room temperature in the presence of 1 mol% each of **96a** and **97a**.[72] The Friedel-Crafts reaction between tertiary allylic alcohol **112** and *N*-methylindole afforded compound **114** with 92% yield. In the case of secondary allylic alcohol **111**, a challenging substrate to activate, a mixture of hexafluoroisopropanol (HFIP) and nitromethane (4:1) as solvents was necessary to afford *N*-tosyl protected amine compound

115 at room temperature with 98% yield. HFIP has excellent H-bond donor abilities and a high dielectric constant of 80.1[108] and thus probably facilitates the ionization process during alcohol activation.[109] Having the optimized reaction conditions in hand, mesitylene was reacted with cinnamyl alcohol **63** and underwent arylation giving **65** within 30 minutes in excellent yield.

Scheme 3.14. Allylic alcohol and nucleophile scope.[a,b]

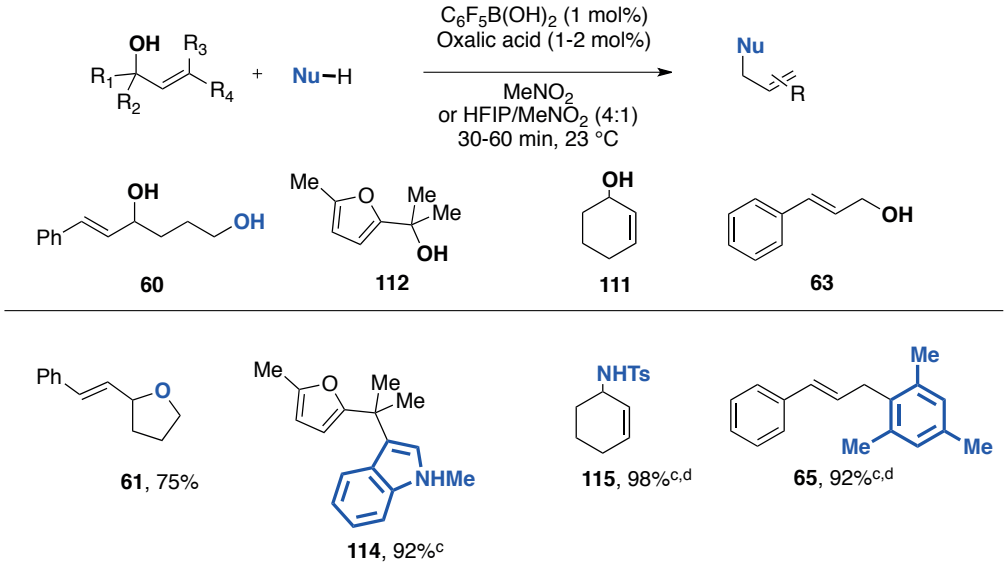

Conditions: [a] Alcohol, nucleophile, 1 mol% $C_6F_5B(OH)_2$ and 1 mol% oxalic acid in $MeNO_2$, 30-60 min; [b] Isolated yields after silica gel chromatography; [c] 1 mol% $C_6F_5B(OH)_2$ and 2 mol% oxalic acid; [d] HFIP/$MeNO_2$ (4 :1) used as a solvent mixture.

3.7.4 Benzylic alcohols

Maintaining the HFIP/nitromethane mixture as an excellent solvent combination, secondary alcohol **51** reacted with thioacetic acid as nucleophile leading to product **68d** with 73% yield after 1 h at room temperature (Scheme 3.15). We further explored representative tertiary benzylic alcohol **76e** with 2-methylfuran, which rapidly afforded **116** in 92% yield. We submitted secondary alcohol **48** to a series of representative nucleophiles for C-C, C-N, C-S and C-O bond formation. With 1 mol% of **96a** and 2 mol% of **97a**, Friedel-Crafts compounds **117**, **118** and **119** were obtained with excellent yields. Benzyl carbamate,

[108] D.-P. Hong, M. Hoshino, R. Kuboi, Y. Goto, *J. Am. Chem. Soc*. **1999**, *121*, 8427–8433.
[109] P. Trillo, A. Baeza, C. Najera, *J. Org. Chem.* **2012**, *77*, 7344–7354.

thiophenol and 2-phenylethanol all performed nucleophilic substitution under the reaction conditions with 86-92% yield. The challenging reaction between primary benzylic alcohol **115** and thiophenol required heating to 50 °C for 10 hours to give thioether **122** with a yield of 74%. The TIPS protecting group on alcohol **67a** survived under nitromethane solvent conditions affording **68a** with 91% yield.

Scheme 3.15. Benzylic alcohol and nucleophile scope.[a,b]

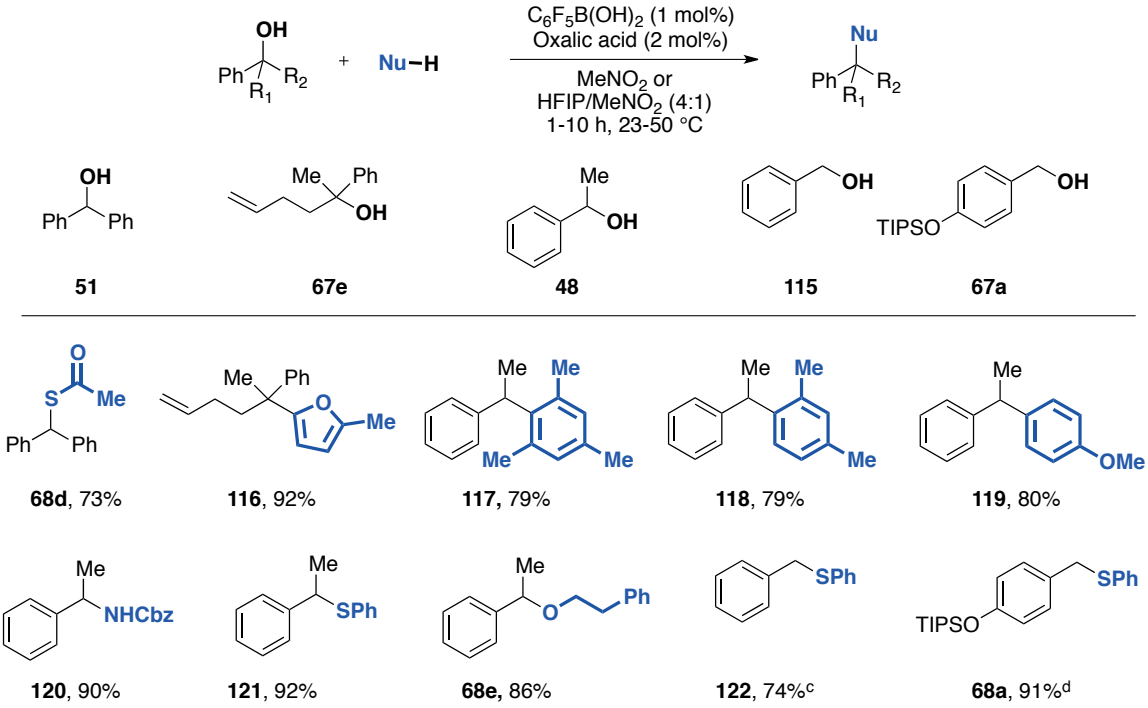

Conditions: [a] Alcohol (HFIP/$MeNO_2$ 4 :1), nucleophile, 1 mol% $C_6F_5B(OH)_2$ and 2 mol% oxalic acid, 1 h; [b] Isolated yields after silica gel chromatography; [c] reaction heated at 50 °C during 10 h; [d] $MeNO_2$ used as a solvent.

3.7.5 Tertiary aliphatic alcohols

To evaluate the potential of the system, we sought to test different tertiary aliphatic alcohols with a variety of nucleophiles under our optimized conditions (Scheme 3.16). In our literature survey in Chapter 2, we demonstrated that tertiary aliphatic alcohols are generally more reluctant to undergo substitution compared to π-activated alcohols and typically require concentrated mineral acids as solvent or co-solvent. With the goal of developing substoichiometric catalytic nucleophilic substitution of tertiary aliphatic alcohols, we conducted with alcohol **77b**, a series of Friedel-Crafts reaction with 5 mol% of **96a** and 5

mol% of **97a** in a mixture HFIP/nitromethane. With 2-methylthiophene, product **123** was formed with 89% yield after 1 h at room temperature. Anisole and 1,3-dimethoxybenzene were reacted with alcohol **77b** to give **124** and **125** with 60 and 40% yield, respectively, with the competing elimination process being favored when weak nucleophiles are employed. Thioetherification was observed with elimination-prone alcohol **77b**, leading to compound **126** with excellent yield. Cyclic alcohol **77y** provided complete conversion to **79y** after 1 hour with TMS-N_3 as nucleophile. Finally, compound **77a** was reacted with thiophenol to give tertiary aliphatic thioether **127** with 80% yield.

Scheme 3.16. Tertiary aliphatic alcohols and nucleophile scope.[a,b]

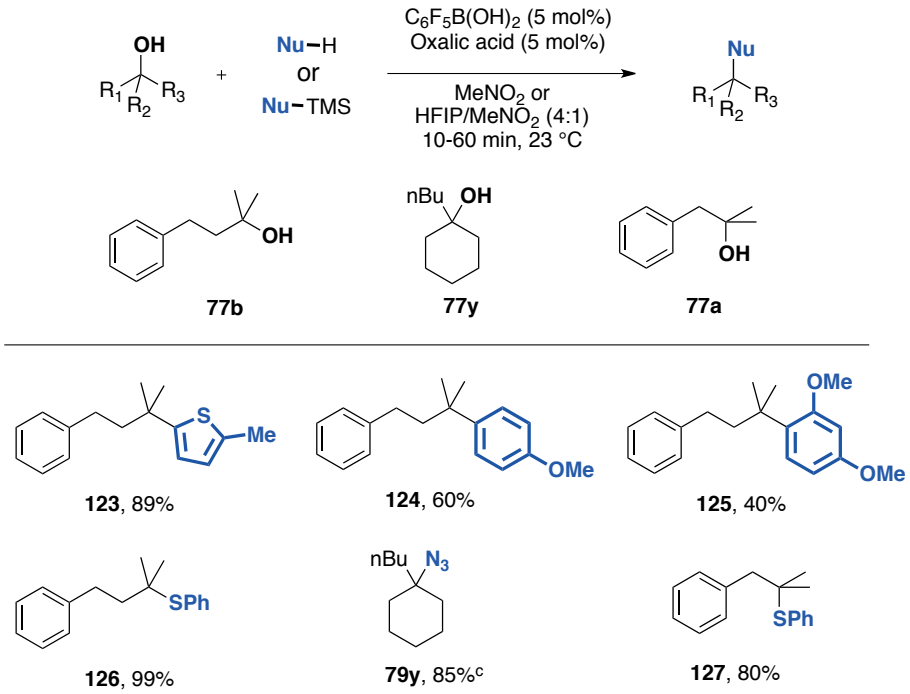

Conditions: [a] Alcohol (HFIP/$MeNO_2$ 4 :1), nucleophile 5 mol% $C_6F_5B(OH)_2$ and 5 mol% oxalic acid,10-60 min; [b] Isolated yields after silica gel chromatography; [c] $MeNO_2$ used as a solvent.

3.8 Comparison with existing methods

In Chapter 1, we saw that the conditions reported by Hall and MacCubbin for the synthesis of Friedel-Crafts compound **118** required 20 mol% of tetrafluorophenylboronic acid in HFIP/$MeNO_2$ (Scheme 3.17).[73] However, in our hands, 20 mol% of tetrafluorophenylboronic acid did not result in any catalysis. Hall reported that 10 mol% of tetrafluorophenylboronic acid did not deliver any compound **61** in $MeNO_2$.[72] With 1 mol% of $B(C_6F_5)_3$•H_2O in

nitromethane, we observed good reactivity with challenging substrates and nucleophiles, leading to compounds **68d** and **68e** with excellent yields upon heating (Chapter 2).[36] With the catalytic system **96a** + **97a** in our hands, we obtained a 20-fold reduction in catalyst loading compared to the reports of Hall and McCubbin to obtain **118** with 79% yield and we observed compound **61** with 75% yield. Moreover, while the previous method with $B(C_6F_5)_3 \bullet H_2O$ required heating to 80 °C to give corresponding products, the newly developed catalyst system rapidly furnishes compounds **68d** and **68e** in good yields at room temperature under identical catalyst loadings.

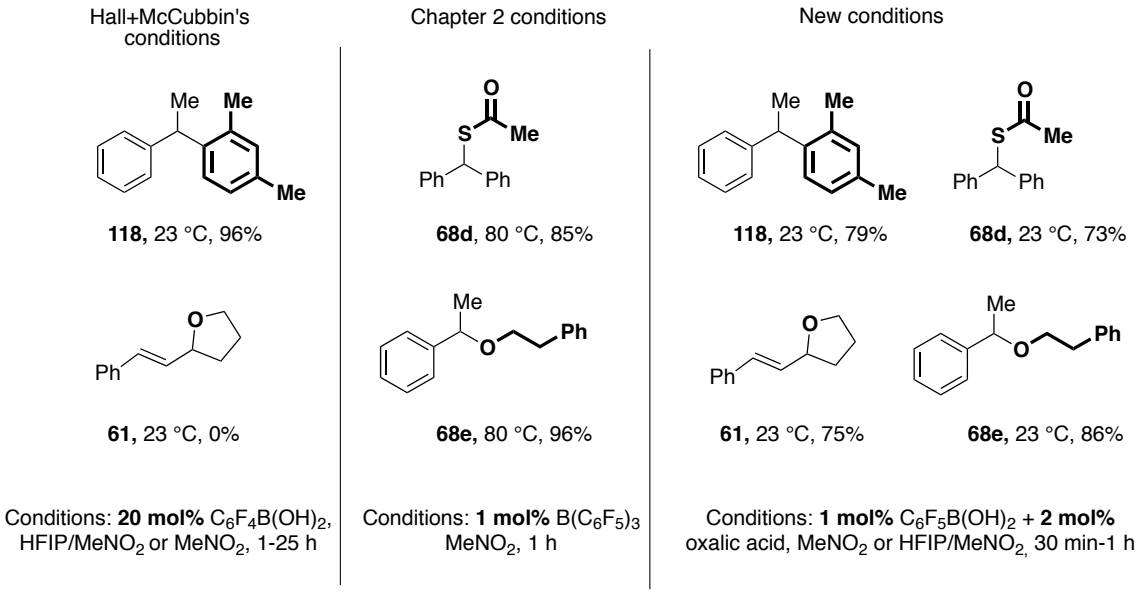

Scheme 3.17. 20-fold reduction in catalyst loading compared to reported conditions and lower reaction temperatures compared to Chapter 2 conditions.

3.9 Chapter 3 conclusion

A two-step combinatorial method for discovering lead hits from mixtures of *in situ*-generated catalysts was developed. The method was evaluated in a dehydrative Friedel-Crafts reaction against a library of boron catalysts assembled from boronic acids and *O*-bidentate ligands. An initial step required 14 reactions to identify the best solvent and a further 17 reactions to identify the optimal combination of catalyst components. Spectrometric, spectroscopic and kinetic investigations showed that the catalyst forms rapidly, exists in a mixture of hydrated states and seems to be a very strong Brønsted acid. The identified dioxaborolanedione had not previously found application in catalysis and is generated rapidly

from two mild commercial components – a property that is attractive when it is unsafe or inconvenient to directly handle highly reactive compounds. Though this initial attempt at catalyst discovery using the screening method was a success, it is necessary to test it in much more mechanistically complex catalytic systems to better assess its usefulness.

CHAPTER 4

Application of the combinatorial approach towards transition metal-catalyzed C-H activation and indole alkylation [90]

[90] Portions of this chapter have been published: E. Wolf, E. Richmond, J. Moran, "Identifying Lead Hits in Catalyst Discovery by Screening and Deconvoluting Complex Mixtures of Catalyst Components", *Chem. Sci.* **2015***, 6,* 2501–2505.

4.1 Introduction

4.1.1 Four-dimensional screening for transition metal catalyzed reactions

In Chapter 3, we demonstrated the effectiveness of a three-dimensional screen for the evaluation of mixtures of pre-catalysts and ligands against one other reaction parameter in a model Friedel-Crafts reaction. To assay the catalyst discovery strategy in a system that is more mechanistically complex and that requires the exploration of a larger number of reaction parameters, we chose to pursue transition metal catalyzed reactions. *In situ* generated transition metal catalysts are involved in countless reactions in the literature, however the desired reactivity is often highly dependent, an often unpredictably so, on a variety of reaction parameters. It is not uncommon that the harmonious interaction of at least four reaction parameters (e.g. solvent, base additive, metal pre-catalyst and ligand) is a prerequisite for catalysis.

During the past decades, transition metal catalysis has been extensively explored in organic synthesis for various demands in the chemical, pharmaceutical or petroleum industries. In this research area, transition-metal-catalyzed C–C bond formation has attracted significant attention. Traditional cross-couplings such as the Sonogashira, Suzuki or Heck reactions, are widely applied as powerful synthetic tools in preparative organic chemistry.[110] In contrast to those common cross-coupling reactions, C–H activation can offer sustainable methods to construct diverse organic molecules starting from simple compounds. Direct functionalization of inert C–H bonds (435 kJ/mol for sp^3-hybridized bond, 472 kJ/mol for sp^2-hybridized bond) has emerged as a powerful method in organic synthesis.[111]

[110] For selected reviews on C-C bond formation via traditional cross-coupling reactions, see: (a) C. C. C. J. Seechurn, M. O. Kitching, T. J. Colacot, V. Snieckus, *Angew. Chem. Int. Ed.* **2012**, *51*, 5062–5085; (b) H. Li, C. C. C. J. Seechurn T. J. Colacot, *ACS Catal.* **2012**, *2*, 1147–1164; (c) *Chem. Soc. Rev.* **2011**, *40*, 4877–5208, Special Issue 10 "Cross coupling reactions in organic synthesis"; (d) B. M. Rosen, K. W. Quasdorf, D. A. Wilson, N. Zhang, A.-M. Resmerita, N. K. Garg, V. Percec, *Chem. Rev.* **2011**, *111*, 1346–1416; (e) G. Cahiez and A. Moyeux, *Chem. Rev.* **2010**, *110*, 1435–1462.

[111] For selected reviews on C-H functionalization, see: (a) J. A. Labinger, J. E. Bercaw, *Nature* **2002**, *417*, 507-514; (b) H. M. Davis, R. Beckwith, *Chem. Rev*. **2003**, *103*, 2861–2903; (c) N. Kuhl, M. N. Hopkinson, J. Wencel-Delord, F. Glorius, *Angew. Chem. Int. Ed.* **2012**, *51*, 10236–10254; (d) J. Yamaguchi, A. D. Yamaguchi, K. Itami, *Angew. Chem. Int. Ed*. **2012**, *51*, 8960–9009; (e) K. M. Engle, T.-S. Mei, M. Wasa, J.-Q. Yu, *Acc. Chem. Res*. **2012**, *45*, 788–802 (f) P. Thansandote, M. Lautens, *Chem. Eur. J*. **2009**, *15*, 5874–5883, and references cited therein.

4.1.2 C-H activation in C-C bond forming reactions

Due to the ubiquitous nature of C−H bonds in organic molecules, their activation is challenging and requires catalytic systems that are sufficiently reactive to cleave the C-H bond and yet are selective for a particular C-H bond. In the past decades, various late transition metals (Pd,[112] Rh,[113] Ru,[114] etc.) have been shown to be efficient cleavage promoters in catalytic direct C-C bond formations involving C-H bond activation. The mechanism of the C-H bond activation step relies on factors such as the metal, the ligands, and the nature of the C-H bond (e.g., sp^3-hybridized bond vs sp^2-hybridized bond). As the focus of this thesis is to discover new reaction conditions, only a few selected examples of C–H activation are discussed, in particular those that offered large insight into the mechanisms of catalysis.

In the late 1960s, pioneering work in C-H activation by Shilov described the conversion of methane, water and stoichiometric potassium tetrachloroplatinate into methanol, methyl chloride and other byproducts using catalytic potassium hexachloroplatinate (Scheme 4.1, equation 1).[115] The first direct observation of oxidative addition with Ir complexes into C-H bonds of simple alkanes was reported by Bergman in 1982 (Scheme 4.1, equation 2).[116]

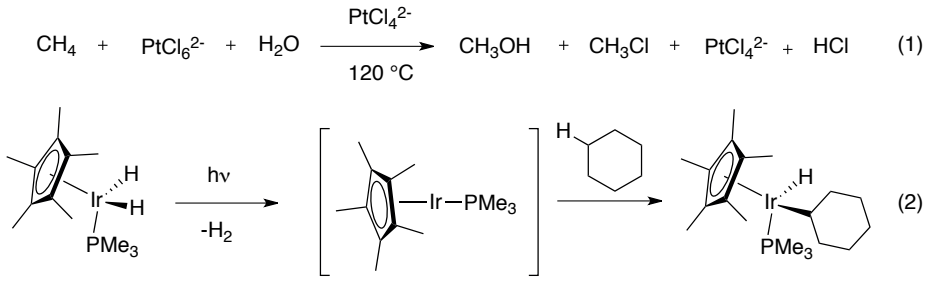

Scheme 4.1. First examples of C-H activation.

[112] For review on Pd-catalyzed C-H activation, see: X. Chen, K. M. Engle, D.-H. Wang, J.-Q. Yu, *Angew. Chem. Int. Ed.* **2009**, *48*, 5094–5115.
[113] For review on Rh-catalyzed C-H activation, see: H. U. Vora, A. P. Silvestri, C. J. Engelin, J.-Q. Yu, *Angew. Chem. Int. Ed*. **2014**, *53*, 2683–2686.
[114] For review on Ru-catalyzed C-H activation, see: S. D. Sarkar, W. Liu, S. I. Kozhushkov, L. Ackermann, *Adv. Synth. Catal*. **2014**, *356*, 1461–1479.
[115] A. E. Shilov, G. B. Shulpin, *Russ. Chem. Rev.* **1987***, 56*, 442–464.
[116] A. H. Janowicz, R. G. Bergman, *J. Am. Chem. Soc.* **1982**, *104*, 352–354.

In 1993, Chatani and coworkers described a Ru complex capable of catalytic *ortho*-C-H bond activation of aromatic ketones followed by olefin insertion (Scheme 4.2).[117] Coordination of the carbonyl group to the metal is likely involved in the mechanism, thus facilitating the formation of a cyclometallated intermediate upon C-H insertion. The insertion of the olefin into the metal-H bond followed by reductive elimination leads to the appropriate ketones. This work is a seminal example of the use of directing groups to facilitate C-H activation and is commonly referred to as "directed C-H activation".

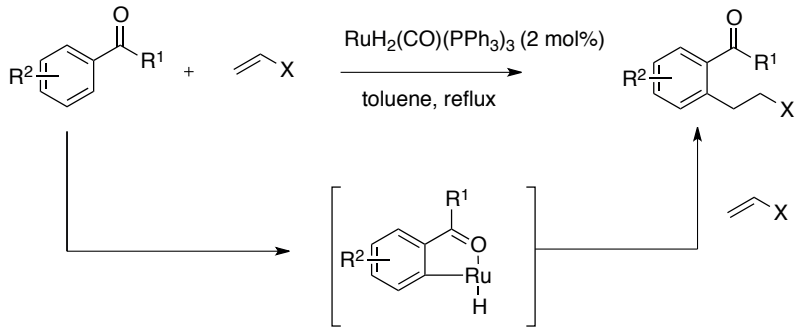

Scheme 4.2. Ru-catalyzed C-H activation with aromatic ketones and olefins.

In 2006, Itami published a Rh-catalyzed C-H arylation between thiophene **128** and iodocompound **129** (Scheme 4.3).[118] The authors suspected a mechanism involving a Rh(I)/Rh(III) cycle with oxidative addition of aryl iodide **129** to Rh(I), generation of cationic Rh species followed by electrophilic aromatic substitution (SEAr) of thiophene **128** at the metal and reductive elimination to form **130** with regeneration of the active catalyst. Strongly π-accepting ligands facilitated electrophilic metalation by providing an electron-deficient rhodium center.

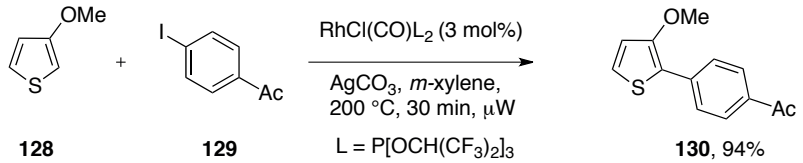

Scheme 4.3. Rh-catalyzed C-H activation with thiophene **128** and iodocompound **129**.

[117] S. Murai, F. Kakiuchi, S. Sekine, Y. Tanaka, A Kamatani, M. Sonoda, N. Chatani, *Nature* **1993**, *366*, 529–531.
[118] (a) S. Yanagisawa, T. Sudo, R. Noyori, K. Itami, *J. Am. Chem. Soc*. **2006**, *128*, 11748–11749; (b) S. Yanagisawa, T. Sudo, R. Noyori, K. Itami, *Tetrahedron* **2008**, *64*, 6073–6081.

The same year, Fagnou and coworkers demonstrated direct arylation of unactivated arenes by a combination of $Pd(OAc)_2$ and pivalic acid co-catalysts (Scheme 4.4).[119] Mechanistic investigations showed that pivalate is involved in C-H bond cleavage by a mechanism that is now referred to as the concerted metallation-deprotonation (CMD) pathway. In a CMD pathway, the Pd-C bond formation step and C-H bond cleavage of the arene happen simultaneously to afford a Pd(II) diaryl species. This is then followed by reductive elimination of the corresponding biaryl product to regenerate the active catalyst.

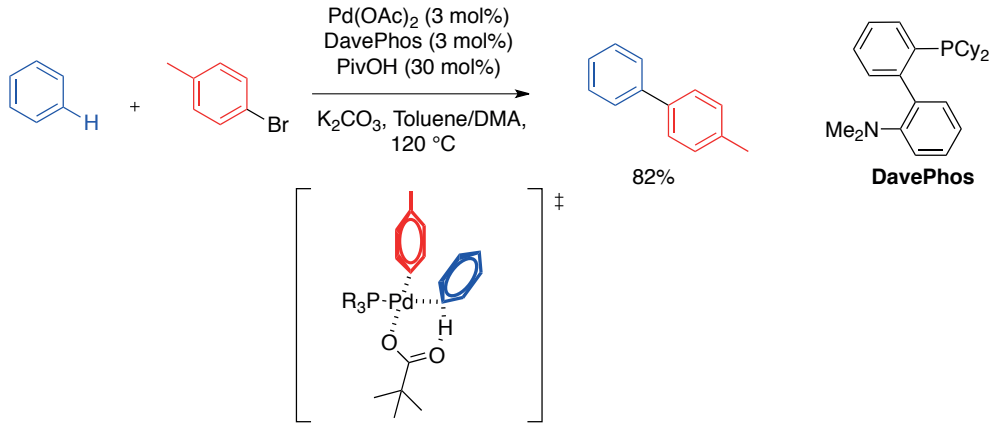

Scheme 4.4. Pd and pivalic acid cocatalysts involved in a CMD pathway for the direct C-H arylation of unactivated arene.

Even though the field of catalytic C-H activation has experienced an explosion of interest in the past decade – far more than can be covered in this brief introduction, the ubiquitous nature of the C-H bond means that plenty of transformations are still to be discovered and that major challenges in regio- and chemoselectivity still persist. Finally, there is also the desire to discover C-H activation catalysts that are based on cheaper, more abundant metals.

4.2 Discovery of a Ni-catalyzed selective C-H arylation

4.2.1 Directed C-H activation: The 8-aminoquinoline directing group

As we saw previously, regioselectivity is a major challenge in C-H activation when more than one C-H group can be activated. The use of a directing group has been recognized

[119] (a) M. Lafrance, C. N. Rowley, T. K. Woo, K. Fagnou, *J. Am. Chem. Soc.* **2006**, *128*, 8754–8756; (b) M. Lafrance, K. Fagnou, *J. Am. Chem. Soc.* **2006**, *128*, 16496–16497.

as a good way to achieve regioselectivity by forcing the catalyst to come into proximity with the targeted C-H bond. Numerous examples of monodentate *N*-chelating groups such as pyridine,[120] 1,2,3-triazole,[121] amides,[122] or guanidine,[123] have been used in site-selective C-H arylations. Elegant examples using bidentate chelation assistance are also reported to be efficient in those transformations.[124] Since the seminal report of Daugulis,[125] the 8-aminoquinoline motif, that can be removed under basic conditions,[126] has been used for the purpose of C-H activation reactions in combination with Pd, Ru, Cu, Ni, Co and Fe catalyst systems.[127] In particular, 8-aminoquinoline directed *o*-arylation of *ortho*-methoxybenzamide **131** with benzyl bromide **132** was described by Daugulis and coworkers under Pd catalysis (Scheme 4.5, equation 1).[128] Compound **133** was obtained with 61% yield. When no blocking group was present at the *ortho*- or *meta*-positions, bis-benzylated compound **135** was obtained (Scheme 4.5, equation 2).

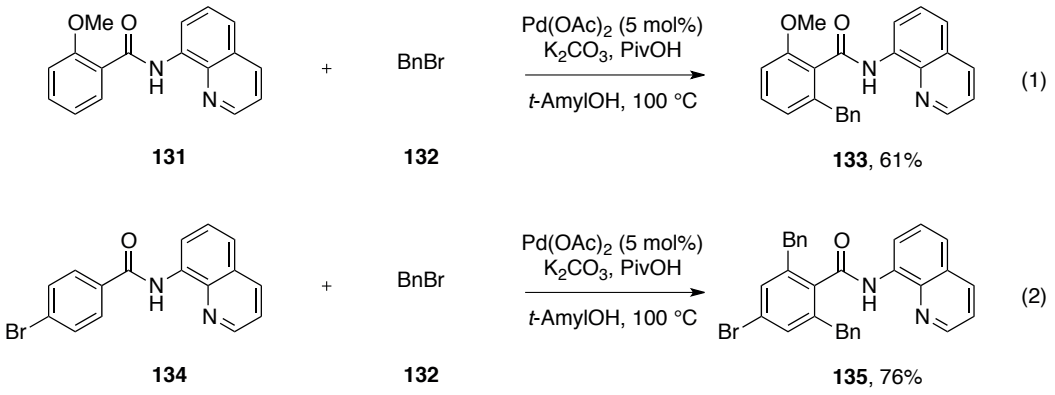

Scheme 4.5. Scope and limitations with 8-aminoquinoline-assisted Pd-catalyzed alkylation.

By employing a $[RuCl_2(p\text{-cymene})]_2/PPh_3$ catalyst system and aryl bromides as coupling partners, Chatani and co-workers reported the efficient transformation of compound

[120] (a) S. R. Neufeldt, M. S. Sanford, *Adv. Synth. Catal.* **2012**, *354*, 3517−3522; (b) J.-H. Chu, C.-C. Wu, D.-H. Chang, Y.-M. Lee, M.-J. Wu, *Organometallics* **2013**, *32*, 272−282.
[121] S. Shi, W. Liu, P. He, C. Kuang, *Org. Biomol. Chem*. **2014**, *12*, 3576−3580.
[122] (a) D.-D. Li, T.-T. Yuan, G.-W. Wang, *J. Org. Chem.* **2012**, *77*, 3341−3347; (b) F. Yang, F. Song, W. Li, J. Lan, J. You, *RSC Adv.* **2013**, *3*, 9649−9652; (c) C. Wan, J. Zhao, M. Xu, J. Huang, *J. Org. Chem.* **2014**, *79*, 4751−4756.
[123] J. Shao, W. Chen, M. A. Giulianotti, R. A. Houghten, Y. Yu, *Org. Lett*. **2012**, *14*, 5452−5455.
[124] For review on bidentate chelation assistance for directed C-H activation, see: G. Rouquet, N. Chatani, *Angew. Chem. Int. Ed*. **2013**, *52*, 11726−11743.
[125] V. G. Zaitsev, D. Shabashov, O. Daugulis, *J. Am. Chem. Soc.* **2005**, *127*, 13154−13155.
[126] T. Truong, K. Klimovica, O. Daugulis, *J. Am. Chem. Soc.* **2013**, *135*, 9342−9345.
[127] M. Corbet, F. De Campo, *Angew. Chem. Int. Ed.* **2013**, *52*, 9896−9898.
[128] E. T. Nadres, G. I. F. Santos, D. Shabashov, O. Daugulis, *J. Org. Chem*. **2013**, *78*, 9689−9714.

136 to arylated compound **138 (**Scheme 4.6).[129] As in the Pd-catalyzed reports, a blocking group at the *ortho*- or *meta*- position of the benzamide is required to avoid undesired bisarylated compounds.

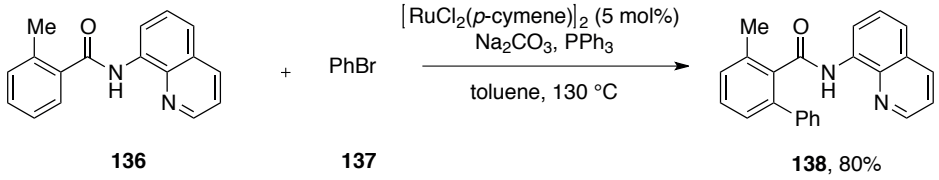

136 **137** **138**, 80%

Scheme 4.6. 8-Aminoquinoline-assisted Ru-catalyzed C-H arylation.

Nickel complexes also display high catalytic activities in *ortho*-directed activation of benzamides. Chatani reported the use of $Ni(OTf)_2/PPh_3$ and Na_2CO_3 to efficiently alkylate C−H bonds with unactivated alkyl halides (Scheme 4.7, equation 1).[130] Conversely, sp^3 C-H arylation was observed when $Ni(OTf)_2$ and $MesCO_2H$ were employed as the catalyst system (Scheme 4.7, equation 2).[131]

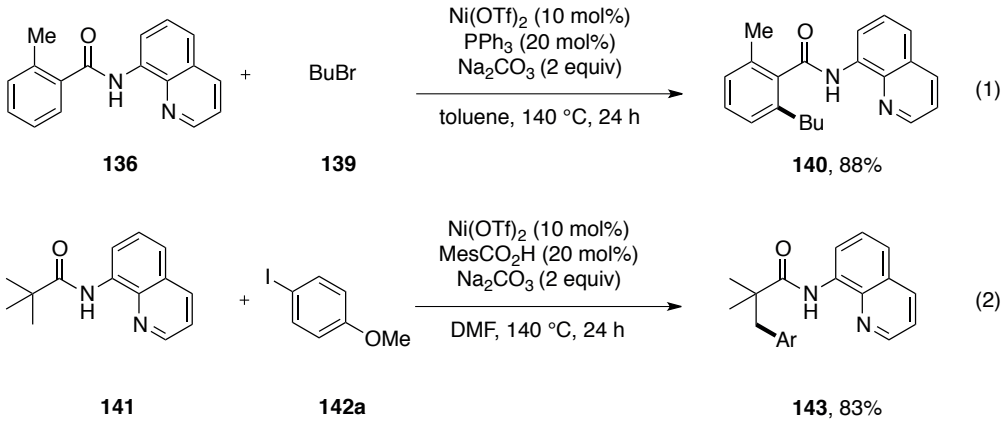

136 **139** **140**, 88%

141 **142a** **143**, 83%

Scheme 4.7. Examples of 8-aminoquinoline-directed Ni-catalyzed C-H activation.

In 2014, Daugulis and co-workers reported a catalytic system based on Co and Mn as an oxidative cocatalyst to couple alkene **145** to the benzamide **144** (Scheme 4.8).[132] The reaction proceeds efficiently at room temperature to give cyclic compound **146** with 90% yield.

---

[129] Y. Aihara, N. Chatani, *Chem. Sci*. **2013**, *4*, 664–670.
[130] Y. Aihara, N. Chatani, *J. Am. Chem. Soc.* **2013**, *135*, 5308–5311.
[131] Y. Aihara, N. Chatani, *J. Am. Chem. Soc*. **2014**, *136*, 898–901.
[132] L. Grigorjeva, O. Daugulis, *Org. Lett*. **2014**, *16*, 4684−4687.

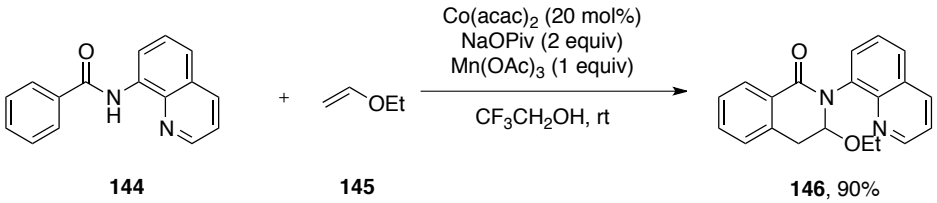

Scheme 4.8. Example of 8-aminoquinoline-directed Co-catalyzed C-H activation of sp^2 C−H bonds with alkene.

An Fe-catalyzed directed ortho-allylation was described for the first time by Nakamura to give corresponding allylbenzene **148** from benzamide **144** and allylether **147** (Scheme 4.9).[133] With excellent yield and high selectivity, no isomerization of the double bond to styrene derivatives was observed.

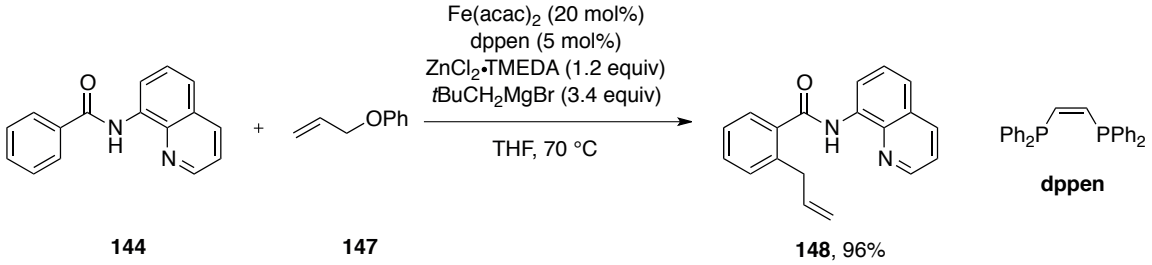

Scheme 4.9. Example of 8-aminoquinoline-directed Fe-catalyzed C-H activation of sp^2 C−H bonds with allylether **147**.

Direct bisaryl coupling by double C-H bond cleavage of two arenes has been reported with Cu salts.[134] The transformation between benzamide **144** and heteroarene **149** required two equivalents of $Cu(OAc)_2$ to afford compound **150** with 83% yield (Scheme 4.10).

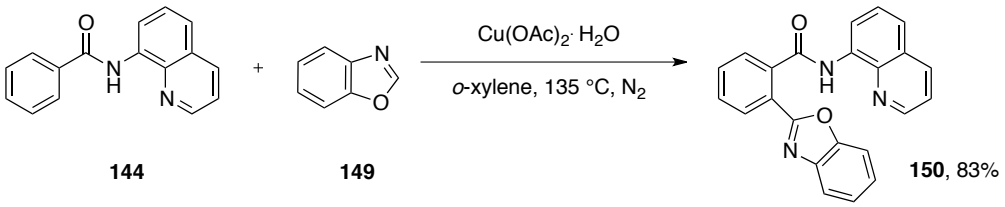

Scheme 4.10. Example of 8-aminoquinoline-directed Cu-mediated C-H/C-H coupling between benzamide **144** and benzoxazole.

[133] S. Asako, L. Ilies, E. Nakamura, *J. Am. Chem. Soc*. **2013**, *135*, 17755−17757.
[134] M. Nishino, K. Hirano, T. Satoh, M. Miura, *Angew. Chem. Int. Ed.* **2013**, *52*, 4457−4461.

4.2.2 Choice of the model reaction

At the outset of this project, a clear gap in the literature was the ability to perform 8-aminoquinoline-directed catalytic *ortho*-arylation with metals other than Pd and Ru. Another general challenge in the area is the ability to perform such reactions in a mono-selective fashion in the absence of blocking groups at the *ortho*- or *meta*- positions. In this context, we sought to apply our screening method to the discovery of selective C-H monoarylation of benzamide derivatives catalyzed by base metals in the absence of blocking groups at the *ortho*- or *meta*- positions (Scheme 4.11). We aimed to find conditions combining high reactivity, selectivity, and air or moisture compatibility with inexpensive components.

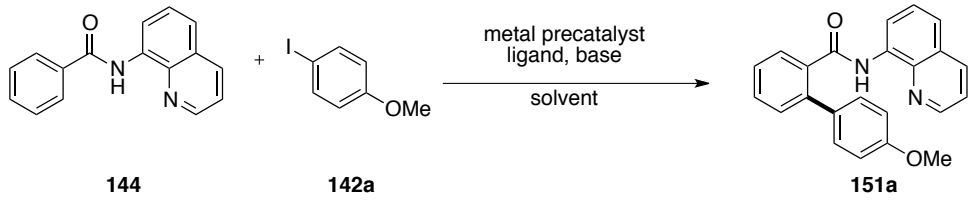

144 **142a** **151a**

Scheme 4.11. *O*-arylation of benzamide **144** with 4-iodoanisole **142a** as a model reaction.

4.2.3 Choice of the components

After surveying the literature for typical pre-catalysts and ligands employed in C-H activation reactions, $Ni(acac)_2$,[135] $Fe(acac)_3$,[136] $CoCl_2$[137] and $Cu(OAc)_2$[138] were selected as potent viable pre-catalysts for such a transformation. Similarly, the nine ligands - PCy_3, dppf, dppp, PPh_3, xantphos, MesCOOH, PivOH, 2,6-DMBA, BzOH - are all inexpensive, commercially available and representative of the typical ligand classes employed in C-H activation reactions. Those components represent the parameters to be screened as complex mixtures in our combinatorial approach.

[135] For selected example of Ni-catalyzed Csp^3-H arylation, see: Y. Aihara, N. Chatani, *J. Am. Chem. Soc*. **2014**, *136*, 898–901.
[136] For review on Fe-catalyzed C-H activation, see: C.-L. Sun, B.-J. Li, Z.-J. Shi, *Chem. Rev.* **2011**, *111*, 1293–1314.
[137] For selected example of Co-catalyzed C-H activation, see: B. J. Fallon, E. Derat, M. Amatore, C. Aubert, F. Chemla, F. Ferreira, A. Perez-Luna, M. Petit, *J. Am. Chem. Soc.* **2015**, *137*, 2448–2451.
[138] For selected example of Cu-catalyzed C-H activation, see: G. C. Reddy, P. Balasubramanyam, N. Salvanna, B. Das, *Eur. J. Org. Chem*. **2012**, 471–474.

For the additional parameters to be screened individually, we selected NaO*t*Bu, Na_2CO_3, CsF as three representative classes of bases and toluene, 1,4-dioxane and DMF as three high boiling point solvents.

4.2.4 Combinatorial screen

4.2.4.1 Step 1

After multigram-scale preparation of benzamide starting material **114** from 8-aminoquinoline and benzoylchloride according to a literature procedure,[139] the first step aimed to establish the crucial fundamental reaction parameters (e.g. solvent, base). In this initial stage, the model reaction of benzamide **144** and 4-iodoanisole **142a** was evaluated in three solvents and three bases with all pre-catalysts and ligands present in all nine reactions. To minimize the likelihood of one ligand sequestering all of a given metal, the pre-catalysts were used in excess compared to the ligand. Each reaction vessel contained 10 mol% of each metal salt and 5 mol% of each ligand (Scheme 4.12). The temperature was chosen as 140 °C to be a typical temperature used in related C-H activation reactions. The reactions were monitored by TLC analysis and conversions were established by ^{1}H NMR of the crude reaction mixtures.

Even if limited conversion was observed (10%), the combination of Na_2CO_3 in 1,4-dioxane at 140 °C was the most efficient to give the desired *o*-arylation product **151a**. Notably, all other conditions did not lead to reasonable conversions (Scheme 4.12, step 1). Due to the modest conversions observed in these initial reactions, we decided at this point to identify the active metal pre-catalyst prior to the deconvolution process to have the possibility to test other salts of the active metal. $Ni(acac)_2$ was identified as the active pre-catalyst, while $Fe(acac)_3$, $CoCl_2$ and $Cu(OAc)_2$ did not exhibit catalytic activity (Scheme 4.12, step 2a).

[139] F.-R. Gou, X.-C. Wang, P.-F. Huo, H.-P. Bi, Z.-H. Guan, Y.-M. Liang, *Org. Lett.* **2009**, *11*, 5726–5729.

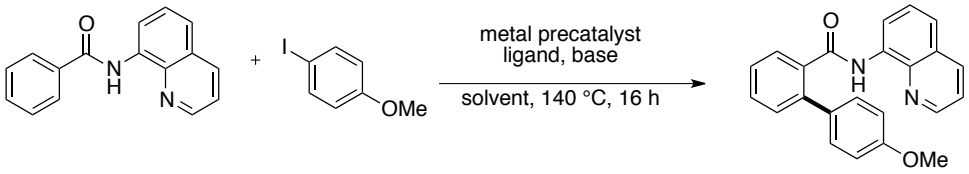

144 **142a** **151a**

Metal Precatalysts - $Ni(acac)_2$, $CoCl_2$, $Cu(OAc)_2$, $Fe(acac)_3$. **Ligands** - PCy_3, dppf, dppp, PPh_3, xantphos, MesCOOH, PivOH, 2,6-DMBA, BzOH.

Step 1: All Metal (10 mol%) and Ligand (5 mol%) components, 3 solvents (2.5 mL) and 3 bases (1.0 mmol) screened.
Step 2a: Individual metal salt (10 mol%) and *all* ligand components (5 mol%) screened with Na_2CO_3 in 1,4-dioxane.

Step 1	1,4-dioxane	toluene	DMF
NaO^{t}Bu	<5%	<1%	<1%
Na_2CO_3	10%	<5%	<1%
CsF	<1%	<1%	<1%

Step 2a	**Conversion**
$Ni(acac)_2$	11%
$CoCl_2$	<1%
$Cu(OAc)_2$	<1%
$Fe(acac)_3$	<1%

Scheme 4.12. First step to establish the lead conditions.

4.2.4.2 Step 2

For the deconvolution stage, maintaining Na_2CO_3 as base and 1,4-dioxane as solvent, the nine ligands were arbitrarily divided into groups of three and evaluated in combination with two Ni sources, $Ni(acac)_2$ and $NiCl_2$•dme. As can be seen (Scheme 4.13, step 2b), a significant enhancement of reaction efficiency was observed in the two reactions employing PCy_3, MesCOOH and dppf as ligands relative to the other conversions with the same base metal salt. We selected those three ligands and $NiCl_2$•dme that gave the best yield for compound **151a** under these conditions. Finally screening the remaining individual combinations (Scheme 4.13, step 2c) established $NiCl_2$•dme and MesCOOH as the most efficient combination of catalyst and ligand. Tuning the ligand/metal ratio gave 67% conversion to monoarylated compound **151a**. In this system, careful choice of the base, solvent, metal pre-catalyst and the presence of MesCOOH were essential to secure high yields of the desired product.

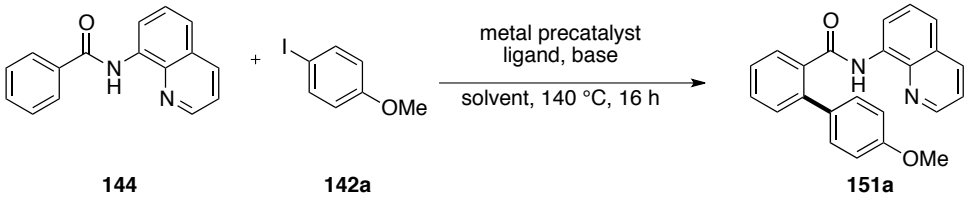

Metal Precatalysts - $Ni(acac)_2$, $CoCl_2$, $Cu(OAc)_2$, $Fe(acac)_3$. **Ligands** - PCy_3, dppf, dppp, PPh_3, xantphos, MesCOOH, PivOH, 2,6-DMBA, BzOH.

Steps 2b-c: All reactions performed in 1,4-dioxane (1 mL) with Na_2CO_3 (5.0 equiv) and 5 mol% of each ligand.

Step 2b	$Ni(acac)_2$	$NiCl_2$·dme
PCy_3, dppf, MesCOOH	32%	64%
PivOH, dppp, 2,6-DMBA	18%	47%
BzOH, PPh_3, xantphos	21%	48%

Step 2c	M (10 mol%)/ L (10 mol%)	M (10 mol%)/ L (20 mol%)
$NiCl_2$·dme/PCy_3	33%	40%
$NiCl_2$·dme/dppf	13%	29%
$NiCl_2$·dme/MesCOOH	53%	67%

Scheme 4.13. Step 2: Deconvolution to identify the optimal combination of pre-catalysts and ligand.

4.2.5 Further optimization and substrate scope

Further optimization of the continuous variables led to better conversion (Scheme 4.14). Increased loadings of Ni pre-catalyst (15 mol%) and MesCOOH (30 mol%) were required to reach 75% conversion and gave 65% isolated yield of the desired compound **151a**. To our delight, the selectivity for the monoarylated compound over the bisarylated compound was excellent (>20:1).

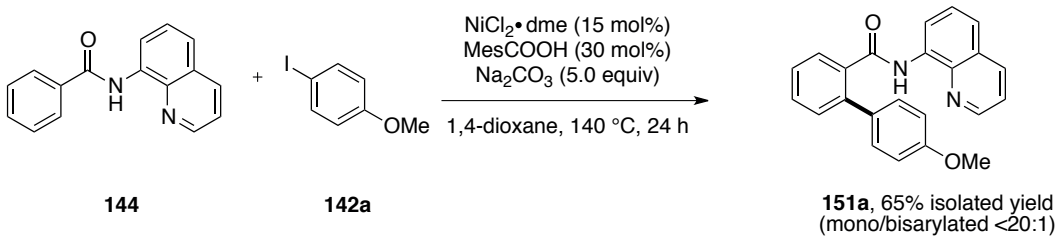

Scheme 4.14. Optimized conditions.

Whilst completing the deconvolution of this reaction system, Chatani and coworkers disclosed a closely related Ni-catalyzed *ortho*-arylation system.[140] Their system proceeds under $Ni(OTf)_2$-catalyzed ligand-free conditions in toluene at 160 °C but again employs only *ortho*- or *meta*-substituted benzamides. By testing these conditions on our model substrate, a

[140] A. Yokota, Y. Aihara, N. Chatani, *J. Org. Chem.* **2014**, *79*, 11922–11932.

loss of selectivity was observed. Indeed, reaction of **144** with **142a** under Chatani's conditions gave complete conversion to a 3:1 mixture of mono- and bisarylation products (Scheme 4.15). Interestingly, in contrast to the positive ligand effect observed in our screen, Chatani and co-workers found most ligands decreased reactivity under their conditions. This result speaks to the importance of casting a wide net during the screening process in order to avoid optimizing within a local minimum.

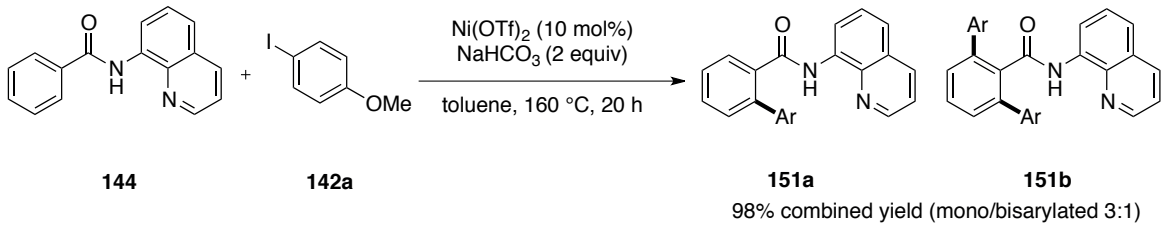

Scheme 4.15. Reaction between **144** and **142a** under Chatani's reported conditions.

We next applied our optimized reaction conditions to other aryliodide compounds (Scheme 4.16). Iodobenzene **142c** led to compound **151c** with 75% conversion with excellent selectivity for monoarylation. Iodocompounds with functional groups in the *meta*-position such as methyl- or methoxy-groups afforded compound **151d** and **151e** with 65 and 59% conversion respectively while keeping the selectivity above 20:1 for monoarylation. Electron-withdrawing groups on the phenyl ring such as chloride, led to a slight loss of selectivity of monoarylation over bisarylation (15:1). Stronger electron-withdrawing substituents on iodocompounds including ester or trifluoromethyl groups led to a slight decreased selectivity for the corresponding monoarylated product **151g** and a complete loss of selectivity in the case of product **151h**. Unfortunately, a highly electron-poor aryliodide was not suitable for coupling under our conditions (**151i**). Attempts to couple arylbromides were unsuccessful under those conditions. Electron-poor benzamides led to reasonable selectivity. For example, compound **154** was obtained in 74% conversion with a 10:1 ratio of monoarylation to bisarylation.

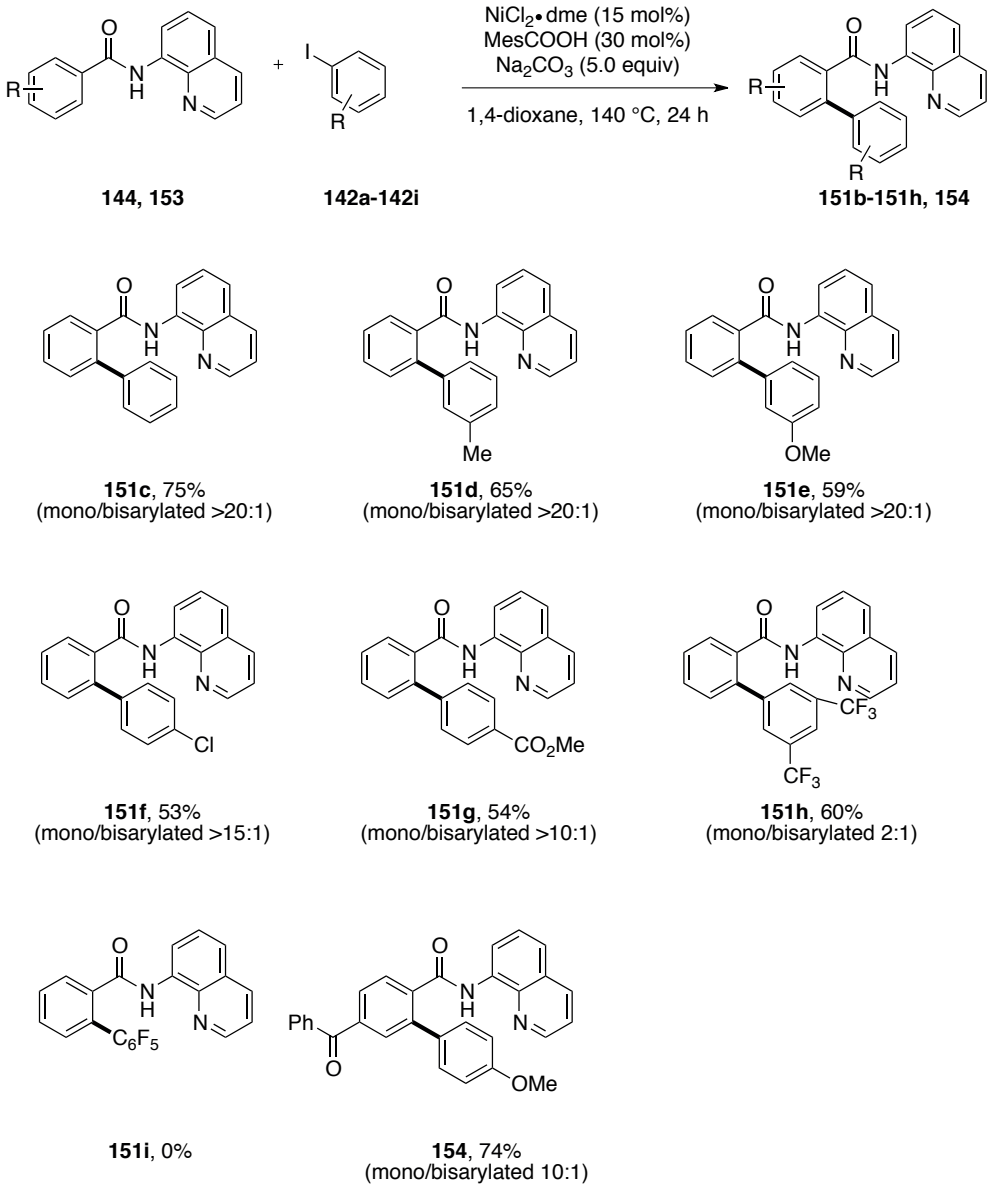

Scheme 4.16. Substrate scope.

4.3 Discovery of catalytic indole alkylation with secondary alkyl halides

4.3.1 Context in indole Csp^3 cross coupling

Indole is an important structural unit that is ubiquitous in biochemical, biological and medicinal structures and functions.[141] The efficient functionalization of indole derivatives has

[141] (a) R. J. Sundberg, *The Chemistry of Indoles*; Academic Press: New York, **1970**; (b) R. H. Thomson, *The Chemistry of Natural Products*; Blackie and Son: Glasgow, **1985**; (c) P. N. Craig, *Comprehensive Medicinal Chemistry*, Vol. 8, (Ed.: C. J. Drayton), Pergamon, New York, **1991**; (d) M. Negwer, *Organic Drugs and Their Synonyms: An International Survey*, 7th edn., Akademie Verlag, Berlin, **1994**.

therefore attracted much attention, especially in regard to C−H bond activation. In this context, direct C2- or C3-arylations of indoles have been sucessfully achieved with diverse transition metals such as Pd, Cu, Rh, Fe or Ni.[142]

In contrast to the numerous examples of direct arylation of indoles to give arylindoles, the direct alkylation of indoles to give alkylindoles is much less reported in the transition metal catalysis literature. Although reports of catalytic methods such as alkenylation, conjugated addition or Friedel-Crafts reactions for C3-indoles[143] and alkylation through lithiation process for C2-indoles exist,[144] attempts to access a direct C-H alkylation are still limited. In 2011, Bach and co-workers reported the first Csp^3 Pd-catalyzed cross-coupling of indoles, involving a norbornene-mediated migration of the palladium species from the C3- to C2-position via C−H bond activation of indole (Scheme 4.17).[145] Indole **155** and primary bromo-compound **156** led to C2-alkylated compound **157** with 67% conversion but only 9% yield.

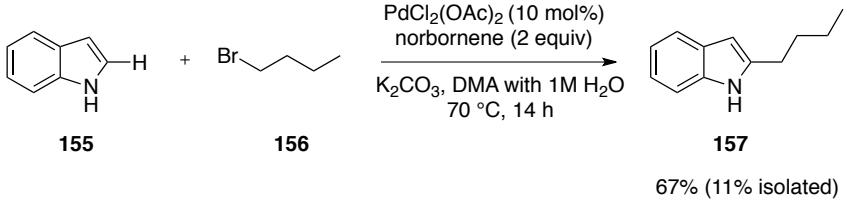

Scheme 4.17. C2-indole alkylation with primary alkyl halides via norbornene mediated Pd C-H activation.

Although secondary alkyl halides have been widely explored with typical nucleophilic partners in cross coupling reactions,[146] very few examples of direct C-H activation of heterocycles and coupling with secondary aliphatic halides have been reported. In 2012, Hu and co-workers published a Cu-catalyzed direct alkylation of benzoxazole derivatives with secondary alkyl halides.[147] Compound **149** and iodocyclopentane **158** gave compound **159** with 80% yield (Scheme 4.18, equation 1). Later on, with the same reagents, Zhou described a

[142] For review on indole arylation, see: L. Joucla, L. Djakovitch, *Adv. Synth. Catal.* **2009**, *351*, 673–714.
[143] M. Bandini, A. Melloni, A. Umani-Ronchi, *Angew. Chem. Int. Ed*. **2004**, *43*, 550–556; M. Bandini, A. Eichholzer, *Angew. Chem. Int. Ed*. **2009**, *48*, 9608–9644.
[144] A.R. Katritsky, K. Akutagawa, *Tetrahedron Lett.* **1985**, *26*, 5935–5938.
[145] (a) L. Jiao, T. Bach, *J. Am. Chem. Soc*. **2011**, *133*, 12990-12993; (b) L. Jiao, E. Herdtweck, T. Bach, *J. Am. Chem. Soc.* **2012**, *134*, 14563–14572.
[146] For review on secondary alkyl halide cross couplings, see: A. Rudolph, M. Lautens, *Angew. Chem. Int. Ed*. **2009**, *48*, 2656–2670.
[147] P. Ren, I. Salihu, R. Scopelliti, X. Hu, *Org. Lett.* **2012**, *14*, 1748–1751.

Pd-catalyzed cross coupling, where benzoxazole **149** reacted with iodocyclohexane **160** to afford compound **161** with 70% yield (Scheme 4.18, equation 2).[148] Both mechanisms are suspected to go through radical pathways.

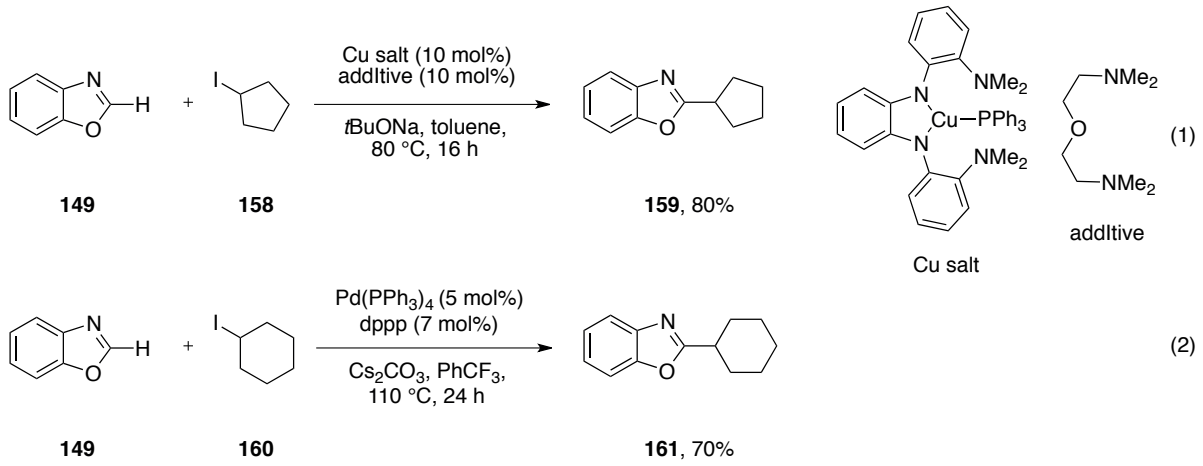

Scheme 4.18. Cu and Pd catalyzed C-H activation with benzoxazole and secondary aliphatic iodides.

As no reports mention the cross coupling of free indoles with unactivated secondary halides, challenging substrates that prone β-hydride elimination, exploiting the aforementioned four-dimensional screening strategy would be a good opportunity to find new and interesting reactivity.

4.3.2 Choice of the model reaction

The same strategy was applied to the discovery of new catalytic systems in indole alkylation. The coupling reaction between **155** and iodocyclohexane **160** was chosen to be the model reaction for indole alkylation (Scheme 4.19). As no C2- or C3-indole alkylation has been previously reported with secondary aliphatic halides, no established reactivity was preferred.

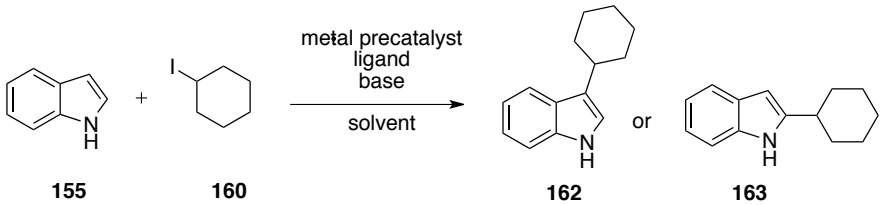

Scheme 4.19. Alkylation of indole with iodocyclohexane as a model reaction.

[148] X. Wu, J. Wei Ting See, K. Xu, H. Hirao, J. Roger, J.-C. Hierso, J. (S.) Zhou, *Angew. Chem. Int. Ed.* **2014**, *53*, 13573–13577.

4.3.3 Choice of the components

Based on the literature described in section 4.3.1 and selected examples in direct indole arylation, we chose a variety of five metals - $NiCl_2$•dme,[149] $Pd(OAc)_2$,[150] $[Ir(OMe)(cod)]_2$,[151] $Fe(acac)_3$,[152] $Rh(PPh_3)Cl_2$[153] - bearing different inherent reactivities with different oxidation states and nine ligands - PCy_3, dppf, dppp, PPh_3, xantphos, MesCOOH, PivOH, 1,10-Phenanthroline, BBBPY - that are typical representative coordinating agents in transition metal-catalyzed reactions.

With the mixture of metals and ligands in every reaction, five bases - AgOAc, KOAc, LiO*t*Bu, K_2CO_3 and CsF - and three solvents - 1,4 dioxane, toluene and *o*-xylene - were surveyed as additional parameters.

4.3.4 Combinatorial screen

4.3.4.1 Step 1

With a mixture of all the metals and ligands in each vessel, five bases and three solvents were screened in fifteen reactions (Scheme 4.20, step 1). To minimize the chance of complete sequestration of a particular metal by the ligands, 5 mol% of each ligand were added to the reaction mixture, representing half the loading compared to the metals. The reactions were monitored by TLC analysis and the yields were measured by GC-MS analysis with dodecane as internal standard that was calibrated against an authentic sample of the product. Despite an extremely low conversion, the combination of AgOAc in *o*-xylene gave only C3-alkylated indole **162** with a yield of 5%. The same conditions in 1,4-dioxane or toluene both gave 3% yield. Pursuing the combination of AgOAc and *o*-xylene, we wanted to clarify the active pre-catalyst in this system before running the deconvolution process. We therefore performed Step 2a to individually test each pre-catalyst. No reaction was observed with Ni, Ir,

---

[149] For selected example of Ni-catalyzed Csp^3-H arylation, see: Y. Aihara, N. Chatani, *J. Am. Chem. Soc*. **2014**, *136*, 898–901.
[150] For selected example of Pd-catalyzed direct C2 indole arylation, see: X. Wang, B. S. Lane, D. Sames, *J. Am. Chem. Soc*. **2005**, *127*, 4996–4997.
[151] For selected example of Rh-catalyzed direct C2 indole arylation, see: S. Pan, N. Ryu, T. Shibata, *J. Am. Chem. Soc*. **2012**, *134*, 17474–17477.
[152] For review on Fe-catalyzed C-H activation, see: C.-L. Sun, B.-J. Li, Z.-J. Shi, *Chem. Rev.* **2011**, *111*, 1293–1314.
[153] For selected example of Rh-catalyzed direct C2 indole arylation, see: N. Lebrasseur, I. Larrosa, *J. Am. Chem. Soc*. **2008**, *130*, 2926–2927.

Fe or Rh. Only Pd gave compound **162** with a yield of 5%. The use of the specific combination between $Pd(OAc)_2$ and AgOAc has been highlighted in Larossa's C-H arylation with Ag acting as a halide abstractor to regenerate catalytically active Pd species *in situ*.[154]

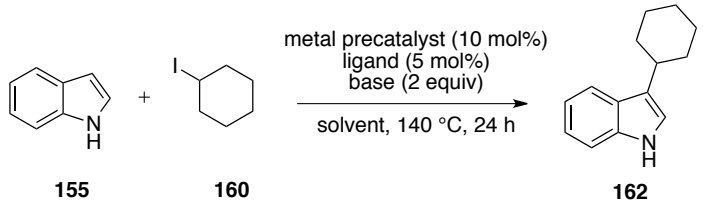

Metals - $NiCl_2$•dme, $Pd(OAc)_2$, $[Ir(OMe)(cod)]_2$, $Fe(acac)_3$, $Rh(PPh_3)Cl_2$ **Ligands** - PCy_3, dppf, dppp, PPh_3, xantphos, MesCOOH, PivOH, 1,10-Phenanthroline, BBBPY .

Step 1: All the metals (10 mol%) and all the ligands (5 mol%), 3 solvents and 5 bases.
Step 2a: Individual metal (10 mol%) and all the ligands (5 mol%) screened with AgOAc in *o*-xylene.

Step 1	1,4-dioxane	toluene	*o*-xylene
AgOAc	3%	3%	5%
KOAc	<1%	<1%	<1%
LiO*t*Bu	<1%	<1%	<1%
K_2CO_3	<1%	<1%	<1%
CsF	<1%	<1%	<1%

Step 2a	**Conversion**
$NiCl_2$• dme	<1%
$Pd(OAc)_2$	5%
Ir salt	<1%
$Fe(acac)_3$	<1%
$Rh(PPh_3)Cl_2$	<1%

Scheme 4.20. Step 1: Combinatorial approach.

4.3.4.2 Step 2

Since only $Pd(OAc)_2$ gave compound **162**, retaining AgOAc and *o*-xylene, the nine ligands were arbitrarily divided into three subgroups and evaluated in combination with three different sources of palladium. The best result showed 5% yield when combination of $Pd(OAc)_2$ and xantphos, BBBPY and MesCOOH as ligands were used (Scheme 4.21, step 2b). The last step of deconvolution revealed that only $Pd(OAc)_2$ and MesCOOH gave a maximum of 14% conversion but still a sole regioisomer (Scheme 4.21, step 2c).

[154] C. Arroniz, J. G. Denis, A. Ironmonger, G. Rassias, I. Larrosa, *Chem. Sci*. **2014**, *5*, 3509–3514.

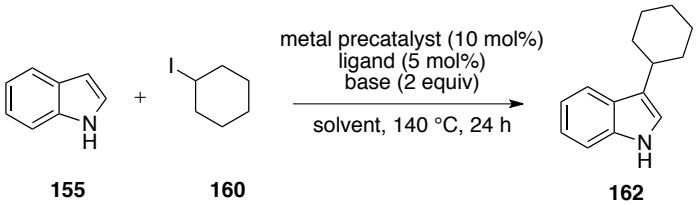

Step 2b-c: All the reactions were run in *o*-xylene with AgOAc, 10 mol% of precatalyst and 5 mol% of ligand.

Step 2b	$[PdCl(C_3H_5)]_2$	$PdCl_2$	$Pd(OAc)_2$
Xantphos, BBBPY, MesCOOH	2%	<1%	5%
PivOH, dppf, PCy_3	2%	<1%	<1%
1,10-Phen, PPh_3, dppp	<1%	<1%	<1%

Step 2c	$Pd(OAc)_2$
Xantphos	<1%
BBBPY	<1%
MesCOOH	14%

Scheme 4.21. Step 2: Deconvolution.

4.3.5 Optimization

Unfortunately, further attempts at optimization did not increase the yield of the desired compound. With 20 mol% $Pd(OAc)_2$ loading and 40 mol% MesCOOH, compound **162** was obtained with 13% yield (Table 4.1, entry 1). Control experiments revealed that $Pd(OAc)_2$ and AgOAc alone gave rise to compound **162** in 8 and 5% yield, respectively (entries 2 and 4). The combination of $Pd(OAc)_2$ and AgOAc also gave 13% yield in the absence of MesCOOH, meaning that no ligand effect was observed in that reaction (entry 5). Upon observing that indole was decomposing at high temperatures, we next ran the reaction at room temperature without observing a noticeable drop in reaction performance (entry 6). Further experimentation showed that, at this temperature, AgOAc gave the best result without the need for a Pd source (entry 8). We therefore decided to screen several silver sources (entries 9-13) in order to increase the reactivity and only Ag_2CO_3 gave similar yield (entry 14). These observations are in agreement with a Friedel-Crafts type mechanism whereby silver is acting as a halide abstractor to facilitate nucleophilic substitution by indole, rather than a mechanism

involving C-H activation.[155] In this light, we elected to abandon further efforts towards optimizing the reaction.

Table 4.1. Optimization of indole alkylation with cyclohexyl iodide.

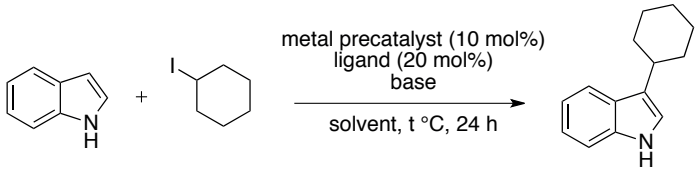

155 **160** **162**

Entry	Pre-catalyst	Ligand	Base (2 equiv)	Solvent	T °C	Yield
1	$Pd(OAc)_2$ (20 mol%)	MesCOOH (40 mol%)	AgOAc	*o*-xylene	140 °C	13%
2	$Pd(OAc)_2$	-	-	*o*-xylene	140 °C	8%
3	-	MesCOOH	-	*o*-xylene	140 °C	<1%
4	-	-	AgOAc	*o*-xylene	140 °C	5%
5	$Pd(OAc)_2$	-	AgOAc	*o*-xylene	140 °C	13%
6	$Pd(OAc)_2$	-	AgOAc	*o*-xylene	23 °C	14%
7	$Pd(OAc)_2$	-	-	*o*-xylene	23 °C	<1%
8	-	-	AgOAc	*o*-xylene	23 °C	17%
9	-	-	$AgBF_4$	*o*-xylene	23 °C	<1%
10	-	-	AgTFA	*o*-xylene	23 °C	13
11	-	-	AgOTf	*o*-xylene	23 °C	<1%
12	-	-	$AgClO_4$	*o*-xylene	23 °C	<1%
13	-	-	AgI	*o*-xylene	23 °C	<1%
14	-	-	Ag_2CO_3	*o*-xylene	23 °C	18

Conditions: [a] indole **155**, iodocyclohexane, 24 h; [b] GC-MS yields based on dodecane (1 equiv) as internal standard.

4.4 Chapter 4 conclusion

In conclusion, we have applied the combinatorial approach to catalyst discovery described in Chapter 3 to more mechanistically complex transition metal catalyzed reactions using a four-dimensional screen of complex mixtures of pre-catalysts and ligands with base and solvent as the variable parameters.

[155] (a) R. P. Houghton, *Metal Complexes in Organic Chemistry*, CUP Archive, **1979; (b)** Y. Wang, C. Kong, Y. Du, H. Song, D. Zhang, Y. Qin, *Org. Biomol. Chem.* **2012**, *10*, 2793–2797.

First, we uncovered new reaction conditions for highly selective Ni-catalyzed directed C-H arylation of benzamide compounds in the absence of blocking groups. As the primary objective of this combinatorial approach was to accelerate the process of catalyst discovery, the purpose was simply to detect the formation of the desired compound. In only nine reactions, we uncovered a combination of base and solvent that could afford 10% of conversion of the desired C-H arylation product. Another sixteen reactions were required to find the best catalytic system in those conditions. In total, twenty-five reactions were needed to identify a highly active and selective catalytic system for arylation of benzamides instead of 324 reactions required in a traditional linear optimization (3x3x4x9). A quick optimization of the continuous parameters led to an efficient catalytic system providing good yields and high selectivity towards multiple substrates. Only electron-poor aryl compounds were not suitable for coupling under those conditions. The catalytic system that has been uncovered in our hands is close to that developed by Chatani using traditional methods, but works at lower temperatures and displays a different ligand effect. This work provides an informative example of how different screening approaches can lead to different final results and highlights the strengths of employing a multidimensional screen for reaction discovery.

The same strategy was applied towards developing a catalytic indole alkylation with secondary aliphatic halides. Once more, the multidimensional screen was rapidly able to identify a potent catalyst system. Thirty-two reactions were run to find a system responsible for selective C3 indole alkylation. Unfortunately, despite significant efforts to optimize these conditions, the efficiency of the system remained low. The potential role of a redox-active metal remains unclear. Further mechanistic and optimization experiments are necessary to render this reaction synthetically useful.

CHAPTER 5

Exploring the Limits of Screening Complex Mixtures in Asymmetric Catalysis

5.1 Introduction

Generating asymmetric molecules is of major importance in chemistry and in the life sciences.[156] Primary metabolites that build the biological macromolecules in living cells are homochiral, meaning that only a single enantiomer has been selected by Nature. For example, nucleic acids are derived from (D)-ribose and only (L)-amino acids are constituents of proteins. The same trend is observed for most secondary metabolites such as alkaloids and terpenes. In pharmacology, a chiral receptor, made of proteins, can therefore discriminate two enantiomers of a molecule affording the appropriate biological activity. As a consequence, numerous scientific fields, from medicinal chemistry to food science to nanomaterials, demand syntheses that provide easy access to a single enantiomer. In the 1960s, racemic thalidomide administration as an antiemetic for pregnant women caused worldwide birth defects due to the teratogenicity of (*S*)-thalidomide.[157] Since this period, the requirements for market approval have evolved by introducing more restrictive rules. In the food industry, (*S*)-aspartame interacts with taste receptors to produce a sweet taste whereas (*R*)-aspartame provides a bitter taste. In response to these demands, efficient methods need to be developed to produce enantiomerically pure compounds. Three major classes of methods are employed to do this:[158]

1) **Chiral resolution**, where a single enantiomer is separated from a racemic mixture with the help of an external enantiopure molecule or material. The interaction with the enantiopure material generates diastereoisomeric pairs that display different physical properties and are thus separable by common purification techniques. One disadvantage of this method is that the undesired enantiomer, typically 50% of the material, is lost as waste.

2) **Chiral pool synthesis**, where the stereochemistry from a naturally occurring enantiopure starting material is directly incorporated into a reaction product and is retained throughout the synthesis. This strategy is only helpful when the desired product has a great similarity to cheap available enantiopure building blocks (e.g sugars or amino acids).

---

[156] A. M. P. Koskinen, *Asymmetric synthesis of natural products* (Second edition. ed.); Wiley, Hoboken, **2013**.
[157] G. W. Mellin, M. N. Katzenstein, *Engl. J. Med.* **1962**, *267*, 1184–1193.
[158] P. Wyatt, S. Warren, *Organic Synthesis : Strategy and Control*; Wiley, Chichester, **2007**.

3) **Asymmetric synthesis**, where stereochemistry is introduced into a reaction product by the action of chiral molecules (either as auxiliaries, stoichiometric reagents or as catalysts) that are not present in the molecule at the end of the synthesis. There are typically three different general approaches to asymmetric synthesis. 1) In the chiral auxiliary approach, a specific motif is temporarily incorporated to the desired molecule and is used to control the stereoselective outcome (e.g Evans oxazolidinone). One of the disadvantages of this approach is that additional steps are needed to install and remove the chiral auxiliary. Though in many cases the auxiliary can be recovered and recycled, in some cases it is lost as waste. 2) In the chiral stoichiometric reagent approach, a reagent involved in the reaction pathway is responsible for the chirality transfer (e.g chiral base). But the requirement of (at least) one equivalent of chiral reagent, increasing the cost of the transformation and generating waste, is not suitable for industrial applications. 3) In asymmetric catalysis, coordinative metal- or organo-complexes generally rendered chiral by the use of chiral ligands induce stereoselective transformations in substoiechiometric amounts. This approach represents a major interest in terms of cost and has shown broad efficiency in many asymmetric reactions. We will use this technique in this chapter.

5.1.1 Asymmetric catalysis

5.1.1.1 Asymmetric induction

Asymmetric induction, the preferential formation of one enantiomer over the other, is a central concept in asymmetric synthesis.[159] Here, we use transition state theory to discuss asymmetric induction in the context of asymmetric catalysis. When a prochiral substrate interacts with an achiral catalyst, there is no differentiation between the free energies of the transitions states leading to enantiomeric products ($\Delta\Delta G^{\ddagger} = 0$) and thus a racemic mixture of products is obtained (Scheme 5.1, figure 1). However, when a prochiral substrate interacts with a chiral catalyst (Scheme 5.1, figure 2), the difference in the free energies of the two diastereomeric transition states ($\Delta\Delta G^{\ddagger} \neq 0$) is related to the product ratio (P_R/P_S) that is given by the following equation:

[159] (a) P. J. Walsh, M. C. Kozlowski, *Fundamentals of Asymmetric Catalysis*; University Science Books: Sausalito, **2009**; (b) R. Noyori. *Asymmetric Catalysis in Organic Synthesis*; Wiley-Interscience: New York, **1994**; (c) E. N. Jacobsen, A. Pfaltz, H. Yamamoto, *Comprehensive Asymmetric Catalysis*; Springer: Berlin, **1999**; Vol. I–III.

$$\frac{P_R}{P_S} = \frac{k_1}{k_2} = e^{-\Delta\Delta G‡/RT}$$

where the rate constants for the formation of P_R and P_S are represented by k_1 and k_2, respectively and $\Delta\Delta G^‡$ is the difference in the transition state energies for each process.

$$\Delta\Delta G‡ = \Delta G‡R - \Delta G‡S$$

where $\Delta G^‡R$ and $\Delta G^‡S$ are the free energies for the formation of P_R and P_S, respectively. The equation demonstrates that small differences in free energies between diastereomeric transition states can lead to large differences in the observed enantiomeric ratio. For example, a difference of 5.4 kJ/mol at 23 °C leads to an enantiomeric ratio of 9:1, whereas a difference of 11.3 kJ/mol leads to an enantiomeric ratio of 99:1. Weak interactions can thus have important consequences for asymmetric induction.

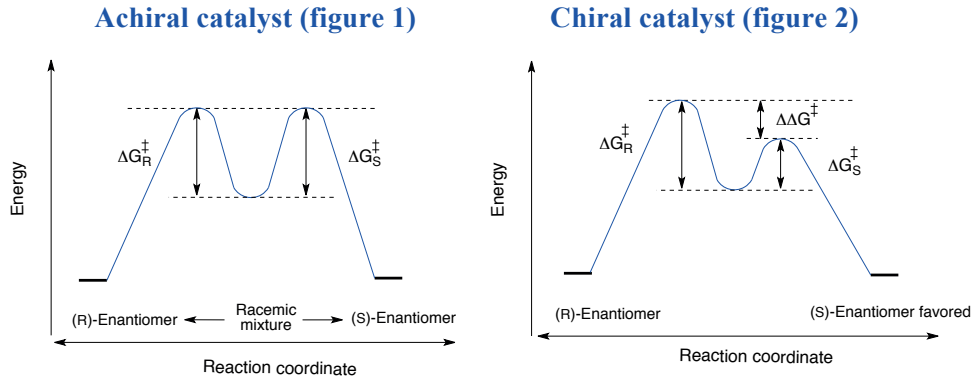

Scheme 5.1. Diagrams showing transition state energies with achiral or chiral catalyst.

It therefore follows that small changes in catalyst structure can drastically affect the enantiomeric excess of a particular reaction. The effect of 3,3'-substitution of chiral phosphoric acid **163** on the enantioselective hydrophosphonylation reaction displayed in scheme 5.2 has been studied experimentally and by density functional theory (DFT) calculations.[160] By measuring the energy differences between the Re-facial attacking transition state (TSr) and the Si-facial attacking transitions state (TSs), small variations in

[160] T. Akiyama, H. Morita, P. Bachu, K. Mori, M. Yamanaka, T. Hirata, *Tetrahedron* **2009**, *65*, 4950–4956.

energy were responsible for large enantiomeric differences (entries 4 and 5). Even in this well-studied system, the large influence of aryl substitution on the enantioselectivity of the reaction can seem surprising to the untrained practitioner. The influence of catalyst structure on asymmetric induction becomes even harder to predict or rationalize in cases where the transition state or mechanism of catalysis are not well understood.

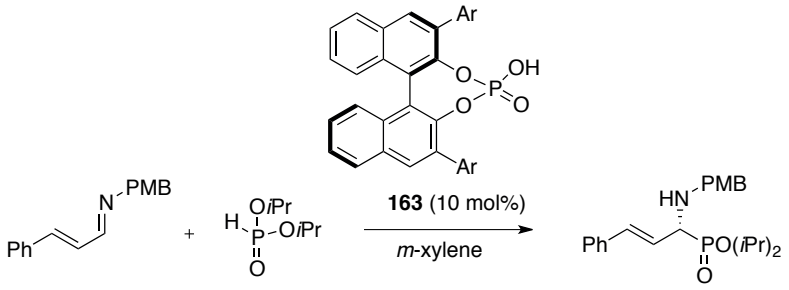

Entry	Ar	ΔΔG	Exp ee[%]
1	H	1.0	11
2	Ph	3.2	30
3	4-$NO_2C_6H_4$	3.4	30
4	4-$CF_3C_6H_4$	3.9	33
5	3,5-$(CF_3)_2C_6H_3$	4.3	84
6	9-Anthryl	0.1	26

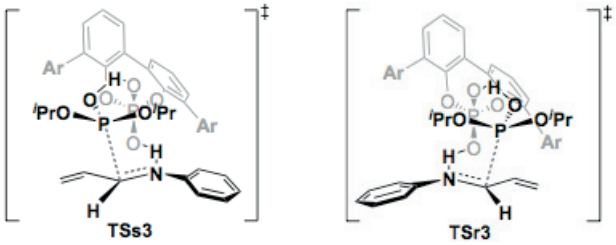

Scheme 5.2. Energy differences between TSs and TSr with various substituents on catalyst **163** with ΔΔG = ΔG‡(TSs3) - ΔG‡(TSr3).

5.1.1.2 Privileged scaffolds in asymmetric catalysis

During the development of the field of asymmetric catalysis, certain catalyst scaffolds have proven to be particularly effective at transmitting their chiral information to furnish enantiopure molecules as products.[161] In most cases, these "privileged chiral catalysts" were carefully designed to induce high selectivity and promote a single reaction pathway. To take some examples only from Lewis acid catalysis,[162] Evans reported the use of chiral bis(oxazoline) copper(II) complexes **164** in cycloadditions, aldol, Michael and Ene reactions

[161] Q.-L. Zhou (ed.) (2011). *Privileged Chiral Ligands and Catalysts.* Weinheim : Wiley–VCH.
[162] H. Yamamoto, (ed.) (2000). *Lewis acids in organic synthesis*. Weinheim: Wiley–VCH.

(Scheme 5.3).[163] Kobayashi described BINOL-lanthanide complexes **165** in diverse cycloadditions.[164] Jacobsen's catalytic alkene epoxidation is accomplished with the well known salen complexes **166**.[165] Corey developed the oxazaborolidine catalyst **167**, described earlier in chapter 3, for enantioselective reduction of ketones to alcohols, though the catalyst has also found widespread application in the Diels-Alder reaction and [3+2] cycloadditions.[166] Despite the undeniable success of privileged scaffolds in asymmetric catalysis, high enantioselectivity with one substrate class is often not transferrable to other closely related classes and results in diminished asymmetric induction to an extent that is not easily predicted.[167] In many cases, these scaffolds have a limited number of synthetic handles for structural variation or have synthetic routes that are not efficient for achieving structural diversity, making them difficult to optimize without extensive efforts in terms of synthesis and screening. The increasing demand for expedient synthetic processes requires the development of new approaches to maximize catalyst diversity and to streamline catalyst screening.

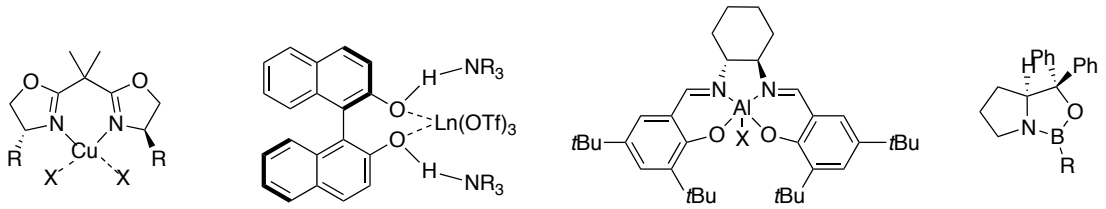

164 **165** **166** **167**

BINOL-Lanthanide complex | Salen complex | CBS catalyst

Scheme 5.3. Examples of privileged scaffolds in asymmetric Lewis acid catalysis.

5.1.1.3 Diversity-Oriented Strategies

One solution to overcome substrate specificities in catalysis is to synthesize a library of diverse ligands that have the same scaffold but that are easily varied at multiple positions, a

[163] For a review on chiral bis(oxazoline) copper(II) complexes, see: J. S. Johnson and D. A. Evans, *Acc. Chem. Res*. **2000**, *33*, 325–335.
[164] S. Kobayashi, *Pure & Appl. Chem*. **1998**, *70*, 1019–1026.
[165] E. N. Jacobsen, W. Zhang, A. R. Muci, J. R. Ecker, L. Deng, *J. Am. Chem. Soc.* **1991**, 113, 7063–7064.
[166] (a) E. J. Corey, R. K. Bakshi, S. Shibata, *J. Am. Chem. Soc.* **1987**, *109*, 5551–5553; (b) E. J. Corey, T. Shibata, T. W. Lee, *J. Am. Chem. Soc.* **2002**, *124*, 3808–3809.
[167] For an example of severe substrate specificity in Brønsted acid catalysis, see : L. Simón, J. M. Goodman, *J. Am. Chem. Soc.* **2008**, *130*, 8741–8747.

strategy referred to as a Diversity-Oriented Synthesis (DOS) approach.[168] In a seminal example of this strategy in catalysis, Hoveyda and coworkers developed a classical asymmetric Michael addition based on catalytic copper and organozinc reagents. Feringa and coworkers had previously achieved very high enantiomeric excess for six-membered Michael acceptors using binaphthol-derived phosphoramidite ligands (98% ee). In contrast, the same catalytic system showed severe limitations with five- or seven-membered Michael acceptors (Scheme 5.4).[169] In response to the limitations, Hoveyda and coworkers used a DOS approach to synthesize and screen a library of bifunctional imino-phosphate ligands that each contained two amino acid moieties.[170] The choice of this particular ligand was made because all the R groups can be readily varied and gave the possibility to quickly create an extensive and diverse library from the chiral pool. By testing each ligand in parallel, candidates could be identified that gave good stereoselectivity for five-, six- and seven-membered substrates (>80% ee).

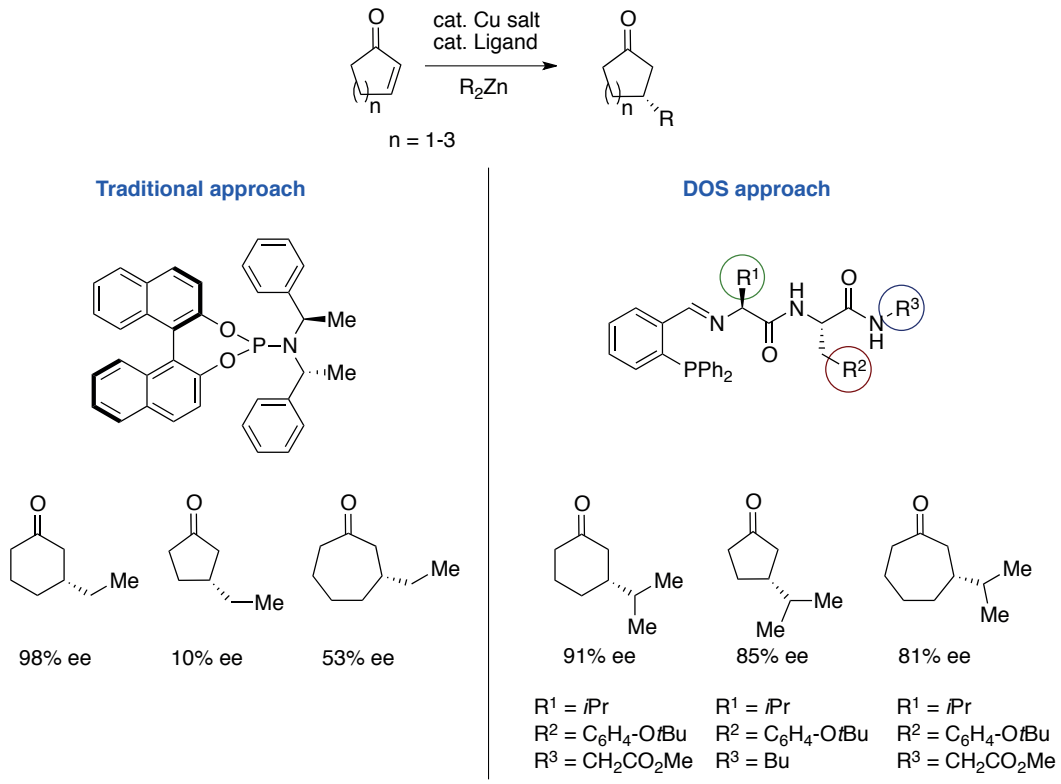

Scheme 5.4. Demonstration of a DOS strategy compared to a traditional approach to overcome substrate scope limitations.

[168] (a) S. L. Schreiber, *Science* **2000**, *287*, 1964–1969; (b) M. D. Burke, S. L. Schreiber, *Angew. Chem. Int. Ed.* **2004**, *43*, 46–58.
[169] B. Feringa, M. Pineschi, L. A. Arnold, R. Imbos, A. H. M. de Vries, *Angew. Chem. Int. Ed.* **1997**, *36*, 2620–2623.
[170] S. J. Degrado, H. Mizutani, A. Hoveyda, *J. Am. Chem. Soc.* **2001**, *123*, 755–756.

5.1.2 Aim of the chapter

Building on the seminal work of Breit[171] and on the catalyst screening strategy described in Chapter 3, the goal of this project was to define the limitations of screening complex mixtures of chiral *in situ* generated catalysts. We hoped that this could be a useful approach for optimizing enantioselective reactions from a pool of diverse pre-catalysts and chiral ligands without having to test every combination individually. Given that the labor-intensive process of enantiomeric excess determination typically requires serial product isolation and chiral chromatographic separation, a solution that drastically reduces the number of experiments would streamline asymmetric catalyst discovery.

As mentioned in the general introduction, a recent report by Breit,[171] describes a combinatorial approach based on screening and deconvoluting mixtures of chiral catalysts where the pre-catalyst was held constant and only the ligands were varied. Furthermore, all the ligands surveyed were structurally very similar. Under these conditions, all the generated catalysts are expected to be present in similar concentrations in the equilibrium and to display very similar rates of reactivity. Although this situation is ideal for the catalyst screening strategy, it is somewhat at odds with the concept of DOS-based catalyst libraries. To test whether such combinatorial approaches are compatible with more diverse catalyst libraries, we chose to synthesize and screen a DOS-based catalyst library inspired by the tartrate-derived organoboron catalysts developed by Yamamoto[172] for Hetero Diels-Alder (HDA) reactions.[173] These catalysts are easily assembled *in situ* from boronic acids and tartrate derivatives. We synthesized our own original library of tartrate derivatives via DOS and then tested them against the HDA reaction using the two-step screen/deconvolute approach.

[171] J. Wieland, B. Breit, *Nature Chem*. **2010**, *2*, 832–837.
[172] K. Furuta, S. Shimizu, Y. Miwa, H. Yamamoto, *J. Org. Chem.* **1989***, 54*, 1483–1484.
[173] Q. Gao, K. Ishihara, T. Maruyama, M. Mouri, H. Yamamoto, *Tetrahedron* **1994**, *50*, 979–988.

5.2 Choice of the reaction and all the components

5.2.1 HDA reaction as a model

The HDA reaction is known to be one of the most powerful reactions in organic chemistry for making six-membered heterocyclic compounds en route to the synthesis of biologically relevant compounds.[174] Since the first report by Gresham in 1949 under thermal conditions[175] and the first HDA reaction with Danishefsky's diene and aldehydes with catalytic $ZnCl_2$,[176] the reaction has been widely investigated using different catalysts and Lewis acids.[177] Selected examples of catalysts used in the HDA reaction are shown in scheme 5.5. In particular, Jacobsen and co-workers reported the use of chiral (Salen)Chromium complexes for the HDA reaction with the Danishefsky diene **10** and a series of aldehydes.[178] In general, complex **169** showed good reactivity and excellent selectivity for the (*R*)-enantiomer **168a** but a loss of selectivity was observed when aldehydes different than the one for which the conditions were optimized were used (**168b**). The same trend was observed when Keck *et al.* reported the (*R*)-BINOL-Ti(O-*i*Pr)$_4$ catalyzed HDA reaction that proceeded in 88% yield and 97% ee for compound **168d**, whereas for compound **168c** the same catalyst led to 83% yield and only 75% ee.[179] Similarly, Yamamoto and Corey described efficient chiral (acyloxy)borane (CAB) catalysts for the HDA reaction based on tartaric acid[180] or amino acids,[181] respectively, to give the products in good enantioselectivity and moderate yields. In general, the catalysts showed excellent selectivity for a few substrates but were less selective under the same conditions for other substrate classes.

[174] V. Eschenbrenner-Lux, K. Kumar, H. Waldmann, *Angew. Chem. Int. Ed.* **2014**, *53*, 11146–11157.
[175] T. L Gresham, T. R. Steadman, *J. Am. Chem. Soc.* **1949**, *71*, 737–738.
[176] S. Danishefsky, J. F. Kerwin, S. J. Kobayashi, *J. Am. Chem. Soc.* **1982**, *104*, 358–360.
[177] For review on HDA reactions, see: (a) K. A. Jorgensen, *Angew. Chem. Int. Ed*. **2000**, *39*, 3558–3588; (b) H. Pellissier, *Tetrahedron* **2009**, *65*, 2839–2877.
[178] S. E. Schaus, J. Brånalt, E. N. Jacobsen, *J. Org. Chem*. **1998**, *63*, 403–405.
[179] G. E. Keck, X.-Y. Li, D. Krishnamurthy, *J. Org. Chem*. **1995**, *60*, 5998–5999.
[180] Q. Gao, T. Maruyama, M. Mouri, H. Yamamoto, *J. Org. Chem*. **1992**, *57*, 1951–1952.
[181] E. J. Corey, C. L. Cywin, T. D. Roper, *Tetrahedron Lett*. **1992**, *33*, 6907–6910.

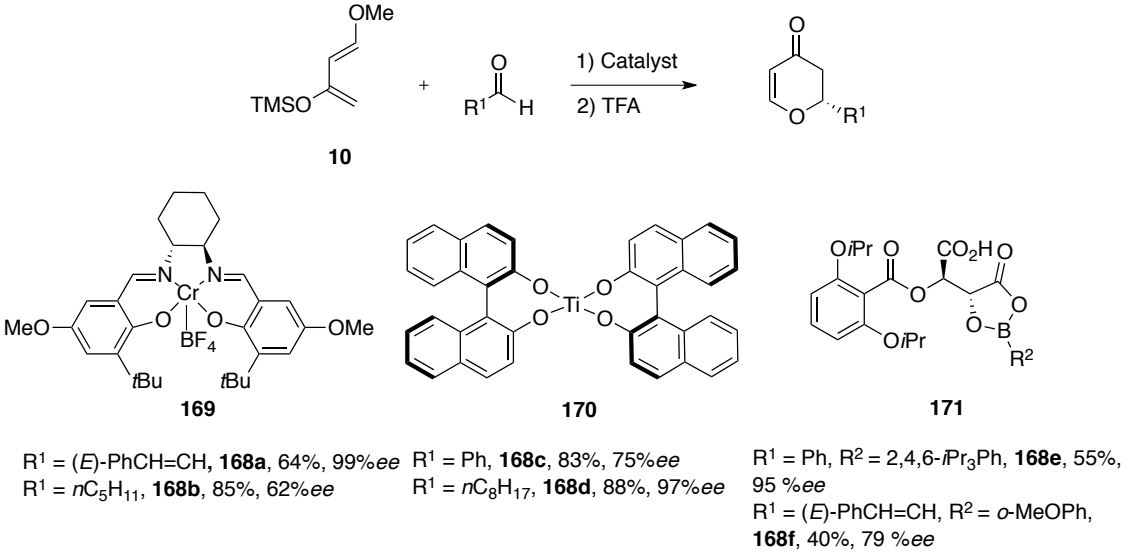

169 170 171

Scheme 5.5. Common catalysts for the HDA reaction of aldehydes and Danishefsky's diene.

The CAB catalyst, made from two components each amenable to several structural modifications, appears well suited for the generation of a DOS-based catalyst library from tartaric acid-based ligands and boronic acids. Furthermore, the substrate-dependent selectivity of the HDA reaction outlined in scheme 5.5 combined with our previous experience in *in situ*-generated boronic acid catalysts led us to consider it as a model reaction for a DOS-based combinatorial approach for catalyst development.

5.2.2 Tartaric acid derivatives

5.2.2.1 Derivatization with apolar amino acids

Applying DOS principles, we developed an original synthesis of ligands starting from tartaric acid. Tartaric acid represents an interesting starting material because it is a cheap commercial chiral compound that is easy to derivatize. Two functions, the carboxy- or the free hydroxy-group, can be varied with a few simple steps. To create our library, we derivatized the hydroxyl position with various *N*-protected amino acids introduced by esterification, thus enhancing structural diversity and including a third stereogenic center (Scheme 5.6). We chose amino acids with apolar side chains such as Glycine, Alanine, Valine, Leucine, Isoleucine and Phenylalanine to observe the effect of bulkiness at that position, as well as introducing an additional stereogenic center in some cases.

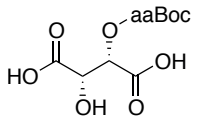

aa= Gly, Ala, Val, Leu, Ile, Phe

Scheme 5.6. Proposed library of amino acid-modified tartaric acid ligands.

5.2.2.2 First synthetic route

The synthetic path of this library begins with benzylic protection of the two carboxylate groups of (D)-(-)-tartaric acid. Bis-esterified compound **172** was obtained with a yield of 92% by mixing (D)-(-)-tartaric acid with benzyl alcohol and catalytic TsOH (Scheme 5.7). The second step involves a Steglich esterification with Boc-protected amino acids that is realized in the presence of DCC and catalytic DMAP.[182] Unfortunately, this method gave a mixture of the bis-esterified and mono-esterified compounds **173a** and **173b** that were difficult to separate by column chromatography due to similar polarities. Moreover, conversions to the selective mono-esterified compounds appeared to be moderate.

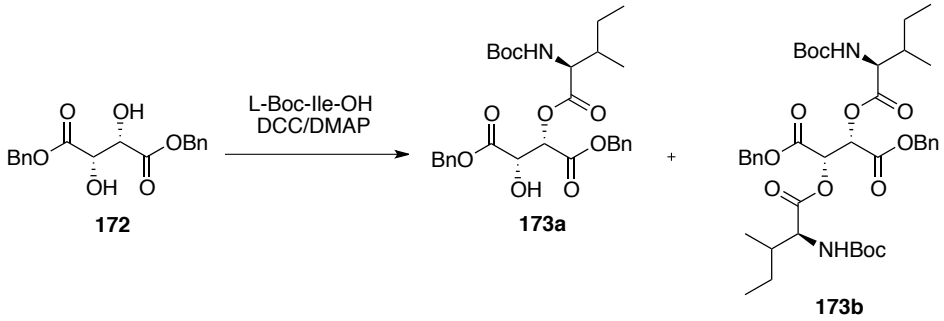

Scheme 5.7. Initial synthetic route to access tartaric acid ligand derivatives.

5.2.2.3 Second synthetic intermediate

To avoid purification problems and increase yields, we sought to modify the synthetic route by selective protection of one of the two free hydroxyl groups of compound **172**. Giordano recently published a report of solvent-free, regioselective benzylic functionalization of vicinal diols with catalytic amounts of Bu_2SnO.[183] By using the same method on compound **172**, we could obtain monoselective benzylic protected compound **174** with a yield of 86% on

[182] B. Neises, W. Steglich, *Angew. Chem. Int. Ed*. **1978**, *17*, 522–524.
[183] M. Giordano, A. Iadonisi, *J. Org. Chem*. **2014**, *79*, 213–222.

multi-gram scale (Scheme 5.8). Moreover, tribenzyl protected compound **174** has the advantage to be fully benzyl-deprotected in a single hydrogenation reaction. Amino acid esterification gave compounds **175a**, **175b**, **175c**, **175d**, **175e** and **175f** with excellent yields with DCC and DMAP. The last stage of the synthesis is a simple hydrogenation with Pd/C affording products **176a**, **176b**, **176c**, **176d**, **176e** and **176f** with quantitative yields. Via this new synthetic route, six structurally diverse chiral ligands could be accessed.

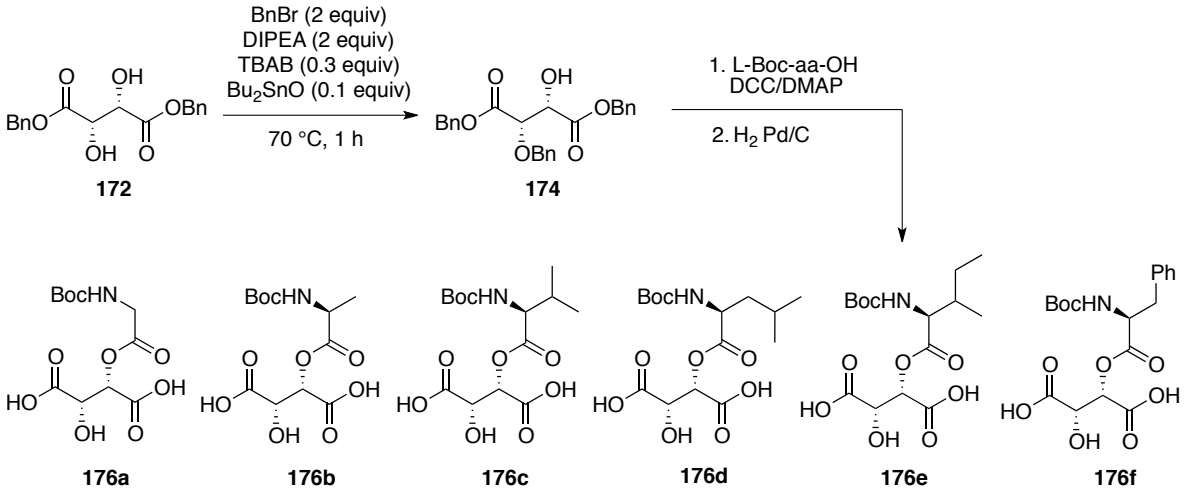

Scheme 5.8. Revised synthetic route to access six tartaric acid ligand derivatives.

5.2.3 Boronic acid choices

In order to maximize the diversity of our catalyst library, we chose six different boronic acid derivatives (including boric acid), some bearing strong electron withdrawing or electron donating groups (Scheme 5.9).

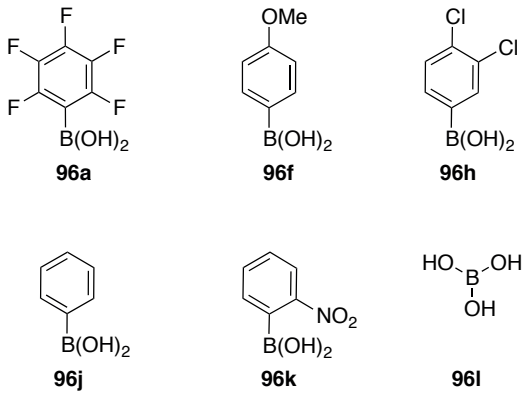

Scheme 5.9. Library of boronic acid derivatives.

5.3 Application of the strategy

Following the same approach as described in Chapter 3, we initially performed a solvent screen to determine the best reaction conditions, followed by iterative deconvolution to identify the combination that led to the best yield and enantiomeric excess.

5.3.1 Step 1

Complex mixtures of the previously synthesized chiral ligands and boronic acid derivatives were screened against different solvent in a model HDA reaction between benzaldehyde and **10** to give dihydropyrone **(*S*)-178 or (*R*)-178**. Four solvents were chosen for screening based on their literature track record at inducing good reactivity and enantioselectivity in [4+2] cycloadditions: DCM, toluene, benzene and propionitrile (Scheme 5.10). The best yield for compound **179** was obtained when DCM was used as the solvent (**(*S*)-178**, 36%, 34% ee) while all the other solvents gave yields below 10%. The best enantiomeric excess for **(*S*)-178** was obtained when benzene was used as the solvent but gave very poor yield (4% yield and 46% ee). At this stage we preferred to select the conditions that gave the best compromise between reactivity and stereoselectivity, therefore pursuing our combinatorial approach with DCM.

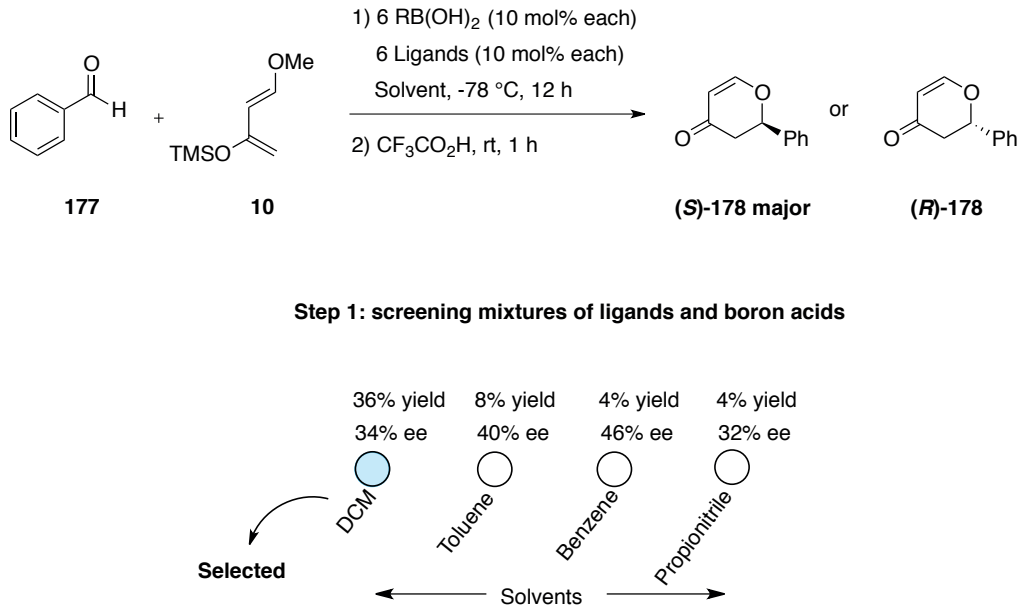

Scheme 5.10. Step 1: Screening mixtures of catalysts against solvents in a model HDA reaction.

5.3.2 Step 2

Iterative deconvolution of the mixtures was attempted in order to identify the best combination of ligand and boronic acid derivative. The six ligands and six boronic acid derivatives were divided into three subgroups and screened as shown in scheme 5.11 (Step 2a). The combination of ligands **176c** and **176d** with boronic acids **96a** and **96f** gave product **(*S*)-178** with 14% yield and 42% ee. A second subgroup of ligands **176b** and **176e** with boronic acid derivatives **96a** and **96f** revealed promising results giving compound **(*S*)-178** with 38% yield and 40% ee. After the first stage of deconvolution, two subgroups of ligands and boronic acid derivatives **96a** and **96f** might be considered as the optimal combination. Due to the uncertainty of which might be optimal, we elected to screen the eight combinations individually (Step 2b and 2b'). In general, reactions with *p*-methoxyphenylboronic acid **96f** led to poor yields (<20%). However, the specific combination of *p*-methoxyphenylboronic acid **96f** and ligand **176d** gave 96% ee, representing the most selective result. A good compromise between reactivity and stereoselectivity was obtained when boronic acid **96a** was combined with ligand **176e** leading to compound **(*S*)-178** with 53% yield and 74% ee. Finally 17 reactions were needed to test 36 combinations without finding a suitable compromise between reactivity and enantioselectivity.

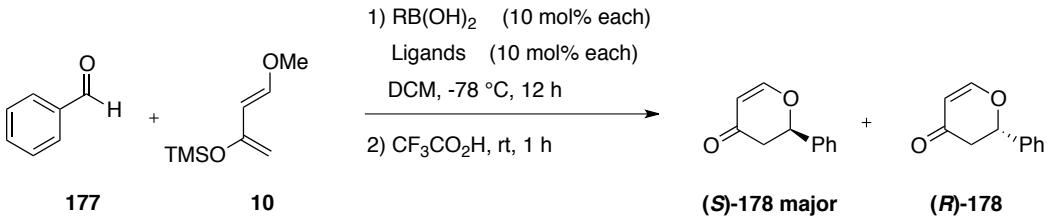

Step 2 (17 reactions)**:** all the reactions are performed in DCM

Step 2a *t* = 12 h	**96j, 96l**	**96k, 96h**	**96a, 96f**
176c **176d**	10% yield 2% ee	12% yield 24% ee	14% yield 42% ee
176b **176e**	10% yield 2% ee	6% yield 32% ee	38% yield 40% ee
176a **176f**	24% yield 2% ee	13% yield 12% ee	26% yield 24% ee

Step 2b *t* = 12 h	**96a**	**96f**
176d	50% yield 54% ee	6% yield 96% ee
176c	33% yield 54% ee	9% yield 38% ee

Step 2b' *t* = 12 h	**96a**	**96f**
176e	53% yield 72% ee	7% yield 42% ee
176b	28% yield 22% ee	18% yield 34% ee

Scheme 5.11. Step 2: Deconvolution of catalyst components.

5.4 Chapter 5 conclusion

Although the first step led to promising initial results, the second step did not point in a clear direction and required the eight remaining combinations to be individually screened. It is therefore not clear whether the combinatorial approach is generally suitable to asymmetric catalysis. A true assessment of the combinatorial approach would require a comparison with all catalyst combinations screened using a traditional approach. Likely difficulties encountered using this approach might be that 1) the binding constants of all catalyst species are probably not the same, meaning that they are not present in equal concentrations and 2) catalysts that are fast but non-selective might mask the presence of catalysts that are slow but highly selective as they all compete for the same substrate. Either of these scenarios would be highly detrimental to the identification of highly selective catalysts using the combinatorial

approach. Compared to previously published reports that identified selective chiral catalysts from homogeneous catalyst mixtures, it is probably not wise to screen mixtures of pre-catalysts (ie. the boronic acid) and ligands at the same time. Screening complex mixtures of *in situ* generated catalysts is only likely to be an effective technique for discovery of asymmetric catalysts if all catalyst combinations have similar kinetics and are present in solution in similar concentration. A corollary of this statement is that high catalyst diversity is likely not compatible with screening mixtures for the purpose of finding highly enantioselective catalysts.

CHAPTER 6

GENERAL CONCUSION AND PERSPECTIVES

Multiple reaction parameters are often crucial to a desired reactivity and most of the time, it is nearly impossible to predict such complex systems. The development of a specific reaction can be considered as a multidimensional problem and very often the fortuitous optimization of several parameters at once is critical to the desired reactivity.

From this perspective, it is important to have an educated guess of which reaction parameters are the most crucial for achieving reactivity in a given reaction. In direct alcohol substitution, solvent, catalyst, substrates and nucleophile are all critical variables in the reaction. The hydrates of $B(C_6F_5)_3$ equaled or surpassed the reactivity of all catalysts described in the literature for direct alcohol activation. The combination of $B(C_6F_5)_3 \bullet nH_2O$ and nitromethane as solvent enabled a wide variety of allylic and benzylic alcohols to undergo dehydrative substitution with a wide variety of nucleophiles under the mildest conditions described to date, showing impressive acid-sensitive group tolerance (Scheme 6.1, equation 1). Moreover, the presence of nitro compounds dramatically accelerated the acid catalyzed azidation of tertiary aliphatic alcohols, enabling catalytic turnover for the first time (Scheme 6.1, equation 2). Mechanistic studies into the role of the nitro compound revealed that it is not just a solvent but a co-catalyst for the reaction, and that it likely forms aggregates that are the competent Brønsted acids.

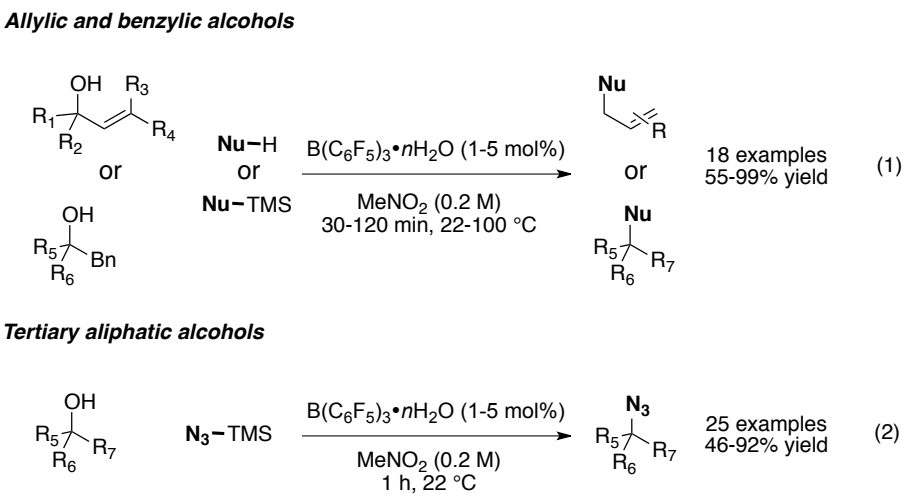

Scheme 6.1. The specific combination of $B(C_6F_5)_3 \bullet nH_2O$ and nitromethane leads to high reactivity towards allylic, benzylic and tertiary aliphatic alcohols.

In response to the fundamental experimental challenges of reaction/catalyst development, namely the large number of experiments that are required, we developed a screening approach intended to reduce the number of reactions to obtain a lead result for a specific transformation by screening and deconvoluting complex mixtures. As a proof of principle of this combinatorial strategy, we explored the *in situ* generation of boron catalysts for a Friedel-Crafts reaction by mixing boronic acid derivatives and *O*-bidentate ligands, whereby solvent was chosen as the additional reaction parameter for study. A very high solvent dependence was observed. Product was observed in only four of the 14 solvents assayed and nitromethane was by far the best solvent. A deconvolution process revealed that pentafluorophenylboronic acid and oxalic acid were the components responsible for the reactivity. NMR and MS studies revealed that covalent assembly occurs very quickly to give a tetrahedral hydrated boron at room temperature in the absence of desiccant. Thirty-one reactions compared to 2016 reactions for traditional screening were required to identify optimal reaction conditions (Scheme 6.2). Further exploration of substrate scope under the identified conditions demonstrated impressive reactivity and chemoselectivity.

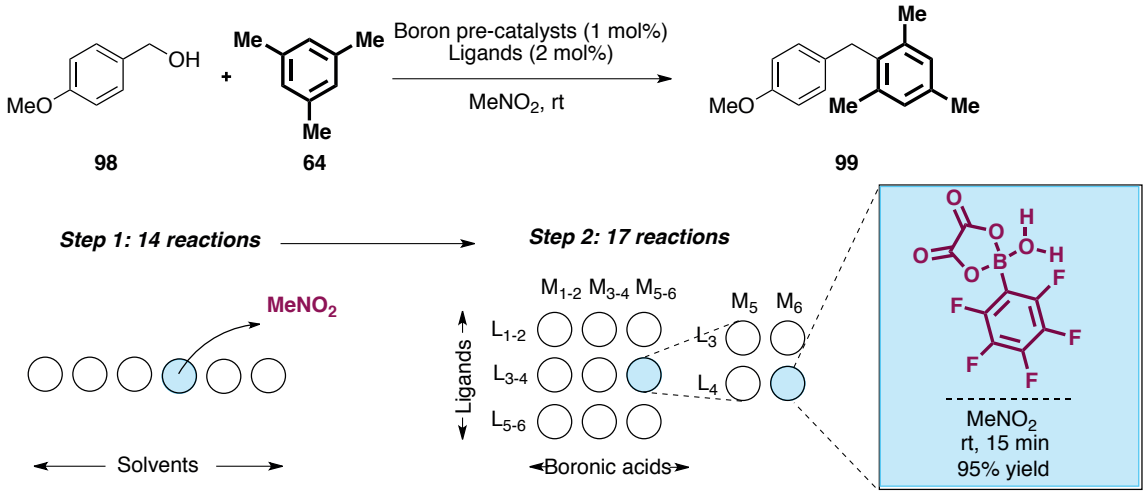

Scheme 6.2. Summary of the two-step catalyst screening strategy for a dehydrative Friedel-Crafts reaction.

The desire to apply the combinatorial screening strategy to a more mechanistically complex reaction led to the investigation of transition metal-catalyzed C-H activation reactions. A four-dimensional screen was carried out by screening complex mixtures of different metal pre-catalysts and ligands against two other reaction parameters. This screen

led to the identification of a novel and mono-selective Ni-catalyzed C-H arylation of unsubstituted benzamide compounds. An initial hit was rapidly uncovered in just nine reactions and sixteen additional deconvolution reactions were required to identify key catalyst components. In total, twenty-five reactions were needed to identify a highly active and selective catalytic system for monoarylation of benzamides instead of 324 reactions in a traditional linear optimization (Scheme 6.3). Exploration of the substrate scope revealed that electron-rich iodoarenes and benzamides are more mono-selective than their electron-poor cousins.

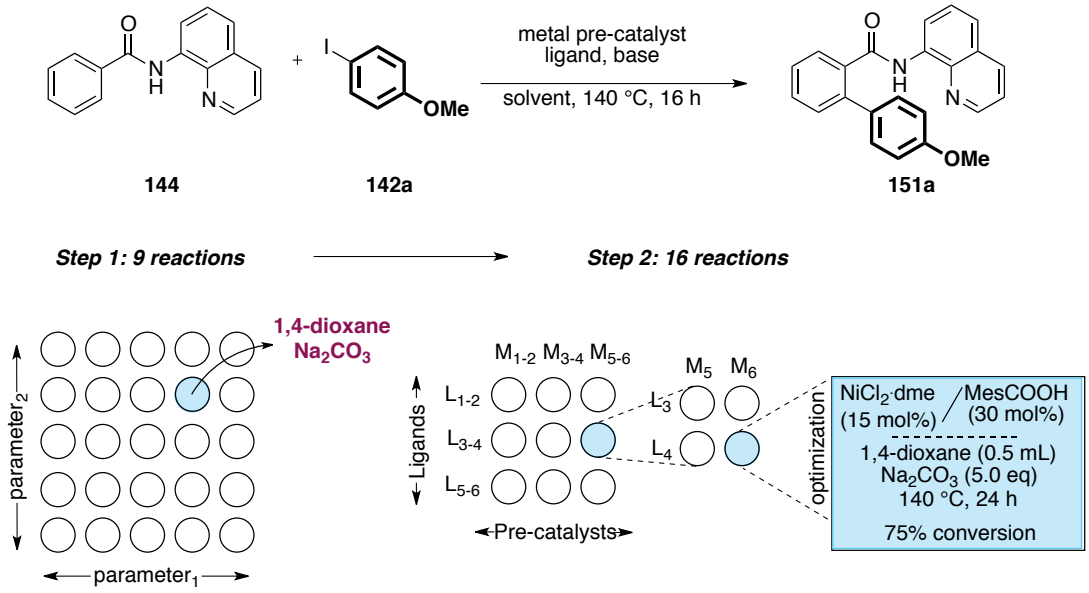

Scheme 6.3. Summary of the two-step catalyst screening strategy for benzamide arylation.

An attempt to address another frontier area in catalytic C-C bond formation led to the design of a combinatorial screen aimed to discover conditions for selective C2 or C3 indole cross coupling with secondary aliphatic iodo compounds. Complex mixtures of various metal pre-catalysts and ligands were screened against different solvents and bases. The combination of $Pd(OAc)_2$ and AgOAc in *o*-xylene in the absence of base was found to give the C3-alkylated indole selectively, albeit in low yield. In total thirty-two reactions were screened to explore more than 600 reaction conditions and led to the identification of $Pd(OAc)_2$ and MesCOOH as the most efficient combination giving 14% conversion to **162**. Further experiments showed that, under these reaction conditions, the mechanism of the reaction does not exclusively require a transition metal-catalyzed pathway but proceeds likely through a silver-mediated Friedel-Crafts type pathway. Extensive efforts to optimize this useful reaction

were unsuccessful. At this stage, we abandoned further efforts towards optimizing the reaction.

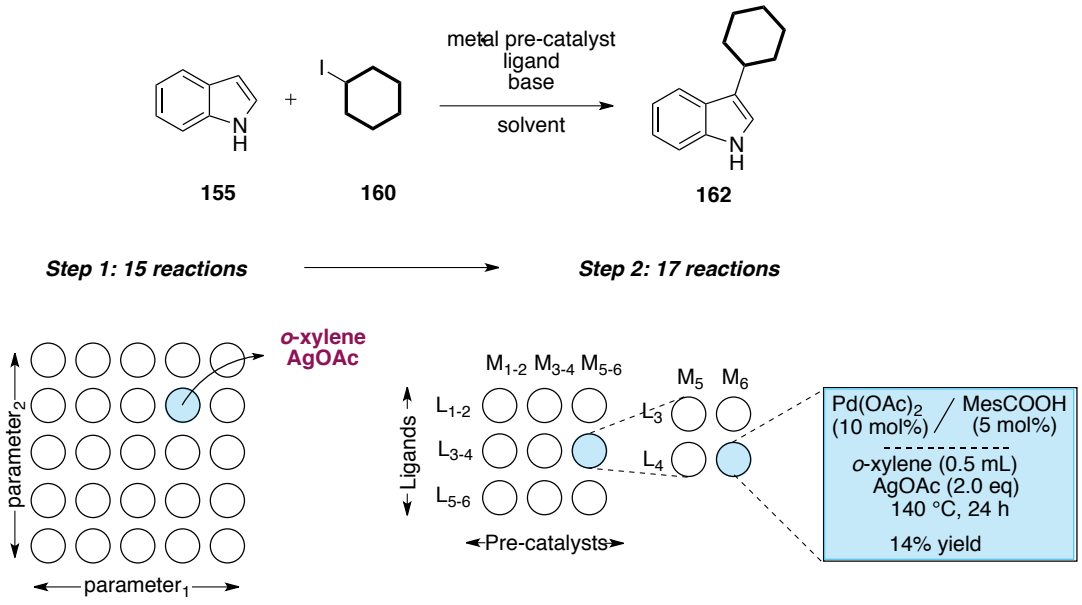

Scheme 6.4. Summary of the two-step catalyst screening strategy for indole alkylation.

To explore the limitations and usefulness of the combinatorial strategy in asymmetric transformations, we synthesized a small library of amino acid-modified tartaric acid derivatives as chiral ligands. Taking a known hetero Diels-Alder reaction as a proof of concept, the chiral ligands and boronic acids were screened as mixtures with solvent as the third reaction parameter (Scheme 6.5). This project pointed out the difficulties associated with screening mixtures when high selectivity is the most desirable outcome, since slow but selective catalysts can be masked by fast but non-selective catalysts. Hence, to avoid missing such catalysts, multiple subgroups had to be deconvoluted, reducing the reaction economy associated with the strategy. However, one combination of components gave excellent enantiomeric excess, albeit in very low yield.

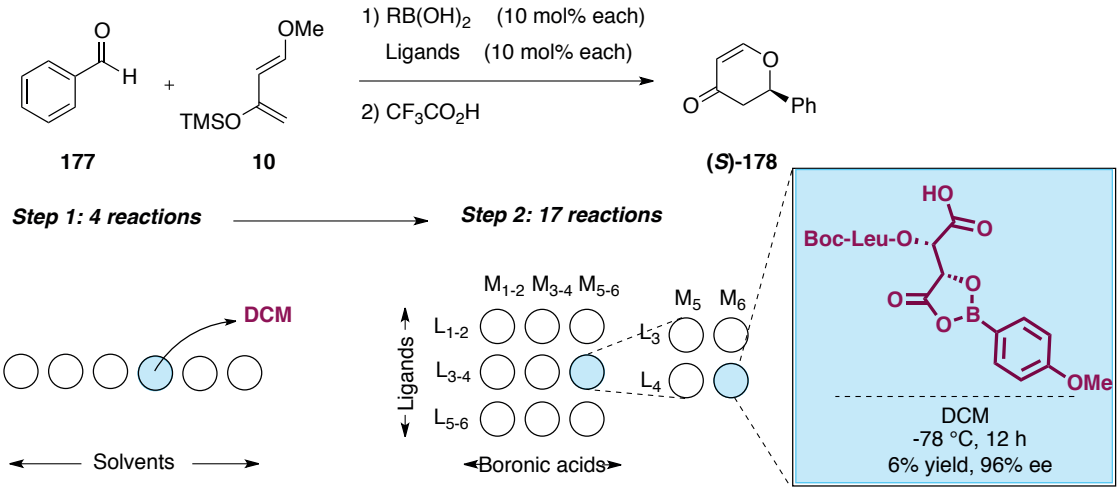

Scheme 6.5. Summary of the two-step catalyst screening strategy for asymmetric hetero Diels-Alder reactions.

Though the combinatorial strategy's generality and ability to handle larger sets of catalyst components remain to be evaluated in many more types of catalytic reactions, we developed a simple method whereby screening mixtures of *in situ* generated catalysts and one or two additional reaction parameters can lead to the discovery of new catalytic systems in a very efficient manner. The method fills an existing gap in catalyst screening strategies by providing a complementary approach that can reduce the number of reactions required to obtain a lead result in a given reaction without the use of high throughput instrumentation. Moreover, the entire process is easy to implement for chemists using commonplace lab equipment and requires no specialized instrumentation or techniques. Each combinatorial application can be tailored to the preference of the user who can choose the number of components and reaction parameters to test. In comparison to the undirected reaction discovery strategies put forward by Taran and Hartwig, it is clear that strategies directed towards a particular reaction are more likely to provide a positive result but also offer less potential to discover truly novel reactivity. In contrast, undirected strategies have greater potential to discover new transformations or new scaffolds. To that end, the screening approach was recently applied by others in the laboratory to substrates that might conceivably undergo multiple transformations. By employing mixtures of pre-catalysts and reductants, with solvent and base taken as the additional parameters to screen, an unexpected Ni-catalyzed alkyne semi-reduction was found to proceed under reductive zinc conditions

(Scheme 6.6).[184] In this combinatorial approach, the potential utility of the screening strategy was increased by the demonstration that not only pre-catalysts and ligands can be screened as mixtures but also mixtures of pre-catalysts and reductants. Furthermore, the presence of specific ligands was found to induce a complete switch in the stereoselectivity of the reduction.

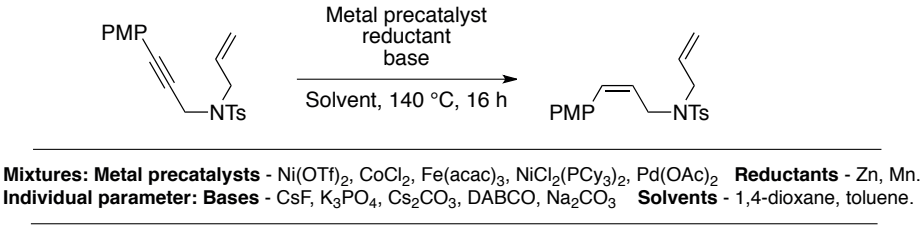

Scheme 6.6. Unexpected alkyne semi-reduction discovered by a combinatorial approach mixing pre-catalysts and reductants.

Looking forward, it is true that the full potential and true strength of screening complex mixtures of pre-catalysts and ligands has not yet been explicitly explored, since this approach has the unique advantage of being able to uncover cooperative effects between different pre-catalysts or between different ligands, which would normally not be screened in the same flask using traditional screening approaches. The discovery of unique catalytic properties associated with bi- or polynuclear complexes holds much promise for the future of transition metal catalysis.[185,186] By simply mixing multiple pre-catalysts in one pot, the chances to discover unexpected polynuclear reactivity are multiplied. Unfortunately, the types of ligands that were screened in this thesis were generally intended to give rise to well-defined mononuclear complexes. To take this idea further, screening ligands that are explicitly designed to promote the formation of bimetallic complexes could lead to interesting novel catalytic properties.[187] We anticipate that this approach will increase the chances of uncovering unique synergy between catalytic components that would not otherwise be screened in the same reaction vessel.

[184] E. Richmond, J. Moran, *J. Org. Chem.* **2015**, *80*, 6922−6929.
[185] For Rh bimetallic complexes, see: M. P. Doyle, *J. Org. Chem.* **2006**, *71*, 9253−9260.
[186] For Pd-Ni bimetallic nanocluster, see: K. Seth, P. Purohit, A. K. Chakraborti, *Org.Lett.* **2014**, *16*, 2334−2337.
[187] S. Pal, C. Uyeda, *J. Am. Chem. Soc.* **2015**, *137*, 8042−8045.

EXPERIMENTAL SECTION

EXPERIMENTAL SECTION – CHAPTER 2

1. Material and methods

General Information. All reactions to synthesize starting materials were performed in air-dried flasks under nitrogen atmosphere, unless otherwise noted. All azidation reactions were performed in 10 mL sealed tubes under an air atmosphere. Purification of reaction products was carried out by flash column chromatography using Merck silica gel (40-63 μm). Analytical thin layer chromatography (TLC) was performed on aluminum sheets pre-coated with silica gel 60 F254 (E. Merck), cut to size. Visualization was accomplished with UV light followed by dipping in a potassium permanganate, *p*-anisaldehyde and/or Seebach's staining solutions and heating. ^{1}H NMR spectra were recorded on a Bruker Avance400 (400 MHz) spectrometer at ambient temperature unless otherwise noted and are reported in ppm using solvent as the internal standard ($CDCl_3$ at 7.26 ppm). Data are reported as: multiplicity (ap = apparent, br = broad, s = singlet, d = doublet, t = triplet, q = quartet, m = multiplet), integration and coupling constant(s) in Hz. ^{13}C NMR spectra were recorded on a Bruker Avance400 (100 MHz) spectrometer. Chemical shifts are reported in ppm from tetramethylsilane, with the residual solvent resonance employed as the internal standard ($CDCl_3$ at 77.0 ppm). Unless otherwise noted, all commercial materials were purchased from *Sigma-Aldrich* and used without further purification.

Materials. Unless otherwise noted, all commercial materials were purchased from *Sigma Aldrich* and used without further purification. The alcohols **77i**,[188] **77l**,[189] **77q**,[190] **77r**,[191] **77s**,[192] **77w,**[193] **77v**[194]**, 77x**[195] and **77z**[196] were prepared following a literature procedure. Tris(pentafluorophenyl)borane $B(C_6F_5)_3$ was purchased from *Alfa Aesar* and used under air, without any precaution to exclude moisture or air.

[188] N. Suzuki, C. J. Rousset, K. Aoyagi, M. Kotora, T. Takahashi, M. Hasegawa, Y. Nitto, M. Saburi, *J. Organomet. Chem.* **1994**, *473*, 117–218.
[189] M. E. Jung, S. Abrecht, *J. Org. Chem.* **1988**, *53*, 423–425.
[190] L. Li, N. Navasero, *Org. Lett*. **2004**, *6*, 3091–3094.
[191] K. Oshima, *Science of Synthesis* **2004**, *7*, 573–596.
[192] S. Nicolai, J. Waser, *Org. Lett.* **2011**, *13*, 6324–6327.
[193] K. Maruoka, T. Itoh, M. Sakurai, K. Nonoshita, H. Yamamoto, *J. Am. Chem. Soc.* **1988**, *110*, 3588–3597.
[194] F. B. Kipping, F. Wild, *J. Chem. Soc.* **1940**, 1239–1242.
[195] B. H. Lipshutz, J. A. Kozlowski, C. M. Breneman, *J. Am. Chem. Soc.* **1985**, *107*, 3197–3204.
[196] S. Panev, V. Dimitrov, *Tetrahedron: Asymm*. **2000**, *11*, 1517–1526.

2. Synthesis of starting materials from section 2.2

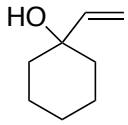

1-vinylcyclohexanol 54.[197]
To a stirred solution of cyclohexanone (1.04 mL, 981mg, 10.0 mmol) dissolved in THF (10 mL) at 0 °C was added vinylmagnesium bromide solution (22.0 mL, 1M in THF, 22.0 mmol). The reaction mixture was allowed to warm up to room temperature and stirred for 10 h. NH_4Cl aqueous solution (20 mL) was added to quench the reaction and the reaction mixture was extracted with EtOAc (2 x 20 mL). The organic layers were dried over Na_2SO_4, filtered and concentrated. The residue was purified by column chromatography on silica gel (5% EtOAc in heptane) affording a colorless oil (1.0 g, 80%). R_f = 0.30 (5% EtOAc in petroleum ether).
^{1}H NMR (400 MHz, $CDCl_3$) δ 5.95 (dd, *J* = 17.0 Hz, *J* = 11.0 Hz, 1H), 5.22 (dd, *J* = 17.0 Hz, *J* = 1.0 Hz, 1H), 5.01 (dd, *J* = 11.0 Hz, *J* = 1.0 Hz, 1H), 1.75–1.40 (m, 9H), 1.30–1.19 (m, 1H); **^{13}C NMR** (100 MHz, $CDCl_3$) δ 145.9, 111.4, 71.6, 37.4, 26.9, 21.9. The analytical data are in accordance with those reported in the literature.

Synthesis of compound 60.

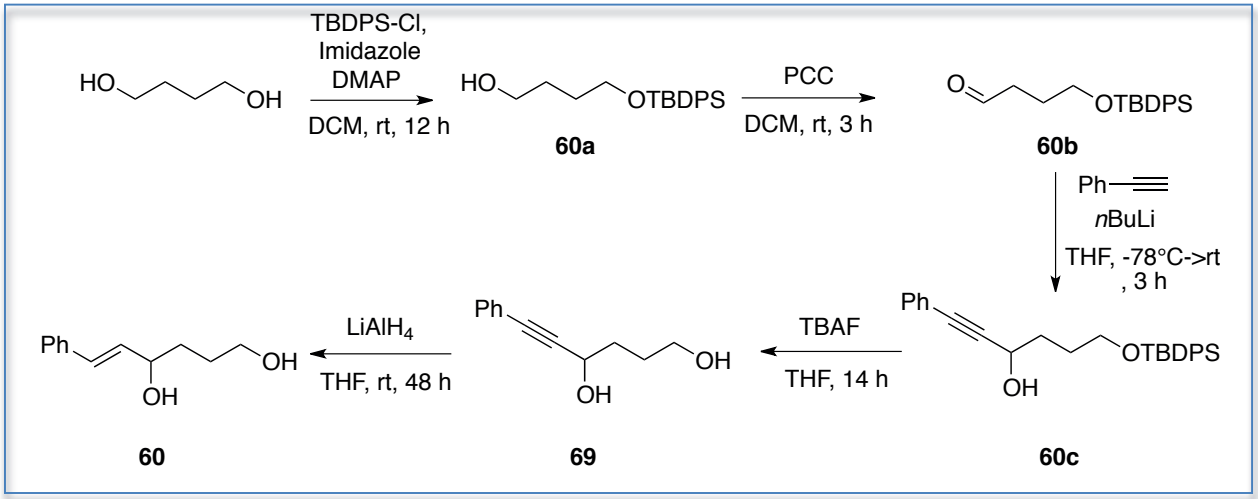

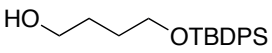

4-((*tert*-butyldiphenylsilyl)oxy)butan-1-ol 60a.[198]
To a stirred solution of 1,4-butanediol (10.3 g, 114 mmol) in anhydrous DCM (20 mL) was added DIPEA (20.6 mL, 15.3 g, 118 mmol) followed by TBDPS-Cl (9.88 mL, 10.4 g, 38.0 mmol) dropwise at 0 °C. The mixture was allowed to warm up to room temperature and was stirred for 15 h. The solvent was removed in vacuo. The residue was purified by column

[197] U. Albrecht, P. Langer, *Tetrahedron* **2007**, *63*, 4648–4654.
[198] M. von Delius, F. Hauke, A. Hirsch, *Eur. J. Org. Chem.* **2008**, *24*, 4109–4119.

chromatography on silica gel (15% EtOAc in heptane) affording a colorless oil (12.4 g, >99%). R_f = 0.23 (20% EtOAc in petroleum ether).
^{1}H NMR (400 MHz, $CDCl_3$) δ 7.73 (dd, *J* = 7.6 Hz, *J* = 1.9 Hz, 4H), 7.47-7.41 (m, 6H), 3.76-3.70 (m, 4H), 2.21 (t, *J* = 5.5 Hz, 1H), 1.73-1.69 (m, 4H), 1.10 (s, 9H); **^{13}C NMR** (100 MHz, $CDCl_3$) δ 135.6, 133.7, 129.7, 127.7, 63.9, 62.8, 29.7, 29.2, 26.8, 19.1. The analytical data are in accordance with those reported in the literature.

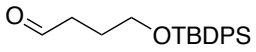

4-((*tert*-butyldiphenylsilyl)oxy)butanal 60b.[199]
To a stirred solution of pyridinum chlorochromate (10.5 g, 48.6 mmol) in anhydrous DCM (60 mL) was added **60a** (7.98 g, 24.2 mmol). The resulting mixture was stirred at room temperature for 5 h and then diluted with petroleum ether (400 mL) and filtered through Celite. The filtrate was concentrated and the resulting residue was purified by column chromatography on silica gel (10% EtOAc in petroleum ether) affording a solid compound (6.87 g, 87%). R_f = 0.40 (10% EtOAc in petroleum ether).
^{1}H NMR (400 MHz, $CDCl_3$) δ 9.77 (s, 1H), 7.73 (dd, *J* = 7.6 Hz, *J* = 1.5 Hz, 4H), 7.47-7.41 (m, 6H), 3.76-3.70 (m, 2H), 2.57 (td, *J* = 6.9 Hz, *J* = 1.5 Hz, 2H), 1.90-1.79 (m, 2H), 1.10 (s, 9H); **^{13}C NMR** (100 MHz, $CDCl_3$) δ 202.2, 135.4, 133.5, 129.6, 127.6, 62.8, 40.6, 26.7, 25.1, 19.1. The analytical data are in accordance with those reported in the literature.

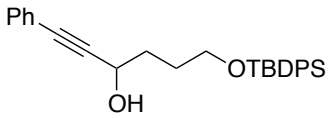

6-((*tert*-butyldiphenylsilyl)oxy)-1-phenylhex-1-yn-3-ol 60c.[200]
To a stirred solution of phenylacetylene (1.53 g, 15.0 mmol) in THF (50 mL) at -78 °C was added *n*BuLi (6.0 mL, 2.5 M in hexanes, 15.0 mmol). The solution was stirred for 1 h at -78 °C followed by 30 minutes at 0 °C. Then the solution was cooled again to -78 °C and aldehyde **60b** (1.63 g, 15.0 mmol) was added. The reaction mixture was allowed to warm up to room temperature and stirred for 3 h. NH_4Cl aqueous solution (50 mL) was added to quench the reaction and the reaction mixture was extracted with EtOAc (3 x 50 mL). The organic layers were combined and washed with water (50 mL), $NaHCO_3$ solution (50 mL) and brine (50 mL), dried over Na_2SO_4, filtered and concentrated. The residue was purified by column chromatography on silica gel (10% EtOAc in heptane) affording a yellow oil (4.95 g, 77%). R_f = 0.30 (10% EtOAc in petroleum ether).
^{1}H NMR (400 MHz, $CDCl_3$) δ 7.73-7.30 (m, 15H), 4.67 (d, *J* = 6.0 Hz, 1H), 3.73 (t, *J* = 6.0 Hz, 2H), 3.10 (d, *J* = 6.0 Hz, 1H), 1.90-1.79 (m, 4H), 1.10 (s, 9H); **^{13}C NMR** (100 MHz, $CDCl_3$) δ 135.4, 133.4, 131.5, 129.5, 128.1, 127.5, 122.7, 90.2, 84.7, 63.8, 62.4, 34.8, 28.1, 26.7, 19.0. The analytical data are in accordance with those reported in the literature.

[199] G. Zhu, E. Negishi, *Org. Lett.* **2007**, *9*, 2771–2774.
[200] F. Freeman, D. S. H. L. Kim, *J. Org. Chem.* **1992**, *57*, 1722–1727.

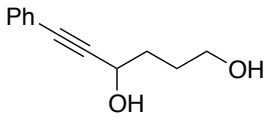

6-phenylhex-5-yne-1,4-diol 69.
A solution of propargylic alcohol **60c** (4.2 g, 9.80 mmol) and TBAF (11.8 mL, 1M in THF, 11.8 mmol) in anhydrous THF was stirred overnight at room temperature. The reaction mixture was extracted with diethylether (40 mL) and washed with H_2O (40 mL). The organic layer was again washed with brine (3 x 20 mL), dried over Na_2SO_4, filtered and concentrated. The residue was purified by silica gel column chromatography (50% EtOAc in heptane) affording a colorless oil (1.70 g, 91%). R_f = 0.20 (Petroleum ether). **^{1}H NMR** (400 MHz, $CDCl_3$) δ 7.48-7.44 (m, 2H), 7.35-7.31 (m, 3H), 4.72 (t, *J* = 5.5 Hz, 1H), 3.83-3.72 (m, 2H), 3.10 (br s, 1H), 2.22 (br s, 1H), 1.99-1.75 (m, 4H); **^{13}C NMR** (100 MHz, $CDCl_3$) δ 136.7, 132.3, 130.1, 122.5, 87.9, 85.8, 63.1, 62.8, 34.3, 28.6.

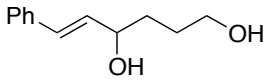

(*E*)-6-phenylhex-5-ene-1,4-diol 60.
To a solution of propargylic alcohol **69** (1.70 g, 8.94 mmol) in anhydrous THF (10 mL) at 0 °C was added dropwise a solution of $LiAlH_4$ (1.01 g, 26.7 mmol) previously dissolved in 10 mL THF. The reaction mixture was allowed to warm up to room temperature and stirred for 48 h. Then the reaction was cooled to 0 °C again. EtOAc (20 mL) and Na_2SO_4•$10H_2O$ were added to the mixture and the reaction mixture was stirred at 0 °C for 20 min. The reaction mixture was filtered through Celite and the filtrate was concentrated. The residue was purified by silica gel column chromatography (50% EtOAc in heptane) affording a colorless oil (1.20 g, 70%). R_f = 0.20 (Petroleum ether). **^{1}H NMR** (400 MHz, $CDCl_3$) δ 7.40-7.24 (m, 5H), 6.60 (d, *J* = 16.0 Hz, 1H), 6.26 (dd, *J* = 16.0, *J* = 6.5 Hz, 1H), 4.40-4.30 (m, 1H), 3.77-3.62 (m, 2H), 3.14 (br s, 1H), 2.87 (br s, 1H), 1.84-1.67 (m, 4H); **^{13}C NMR** (100 MHz, $CDCl_3$) δ 136.7, 132.3, 130.1, 128.6, 127.6, 126.5, 72.7, 62.8, 34.5, 28.8. The analytical data are in accordance with those reported in the literature.

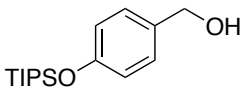

(4-((triisopropylsilyl)oxy)phenyl)methanol 67a.[201]
To a stirred solution of 4-hydroxybenzaldehyde (1.00 g, 7.34 mmol) in anhydrous DCM (50 mL) was added imidazole (1.00 g, 14.7 mmol). Then the reaction was cooled down to 0 °C and TIPS-Cl (1.89 mL, 1.70 g, 8.81 mmol) was added in several portions. After complete addition, the reaction mixture was allowed to warm up to room temperature and stirred for 20 h. The crude reaction was filtered through Celite, rinsed with DCM and the solvent was removed in vacuo obtaining a white solid (3.04 g). The residue was dissolved in EtOH (10 mL) and cooled to 0 °C. To that mixture, $NaBH_4$ was added slowly (416 mg, 11.0 mmol) was added dropwise. The reaction mixture was stirred for 2 h at 0 °C and was quenched with aqueous NH_4Cl solution (1 mL), warmed up to room temperature and extracted with EtOAc

[201] H. Y. Lee, X. Jiang, D. Lee, *Org. Lett.* **2009**, *11*, 2065–2068.

(3 x 50 mL). The organic layer was washed with water and brine, dried over Na_2SO_4, filtered and concentrated. The residue was purified by column chromatography on silica gel (10% EtOAc in petroleum ether) affording a colorless oil (1.64 g, 85%). R_f = 0.35 (10% EtOAc in petroleum ether).
^{1}H NMR (400 MHz, $CDCl_3$) δ 7.24 (d, *J* = 8.4 Hz, 2H), 6.87 (d, *J* = 8.4 Hz, 2H), 4.60 (s, 2H), 1.63 (s, 1H), 1.28 (m, 3H), 1.11 (d, *J* = 7.2 Hz, 18H); **^{13}C NMR** (100 MHz, $CDCl_3$) δ 155.9, 133.7, 128.5, 120.1, 65.0, 18.1, 12.0. The analytical data are in accordance with those reported in the literature.

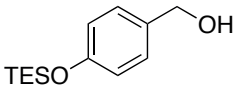

4-(Triethylsilyloxyphenyl)methanol 67b.
To a stirred solution of 4-hydroxybenzaldehyde (1.00 g, 7.34 mmol) in anhydrous DCM (50 mL) was added imidazole (1.00 g, 14.7 mmol). Then the reaction was cooled down to 0 °C and TES-Cl (1.48 mL, 1.33 g, 8.81 mmol) was added in several portions. After complete addition, the reaction mixture was allowed to warm up to room temperature and stirred for 20 h. The crude reaction was filtered through Celite, rinsed with DCM and the solvent was removed in vacuo obtaining a white solid. The residue was dissolved in anhydrous DCM (10 mL) and cooled to -78 °C. A solution of diisobutylaluminum hydride (14.7 mL, 1.0 M in DCM, 14.7 mmol) was added dropwise. The reaction mixture was stirred for 90 min at -78 °C, and was quenched with MeOH (1 mL), warmed up to room temperature and a 1M aqueous solution of potassium tartrate was added. The aqueous layer was extracted with DCM (3 x 50 mL). The organic layer was washed with water and brine, then dried over Na_2SO_4, filtered and the solvent was removed in vacuo. The residue was purified by column chromatography on silica gel (10% EtOAc in petroleum ether) affording a colorless oil (1.25 g, 72%). R_f = 0.33 (10% EtOAc in petroleum ether).
^{1}H NMR (400 MHz, $CDCl_3$) δ 7.20 (d, *J* = 7.8 Hz, 2H), 6.81 (d, *J* = 7.8 Hz, 2H), 4.58 (s, 2H), 0.98 (t, *J* = 7.7 Hz, 9H), 0.72 (q, *J* = 15.4 Hz, 7.7 Hz, 6H); **^{13}C NMR** (100 MHz, $CDCl_3$) δ 155.1, 133.8, 128.5, 119.9, 64.8, 6.59, 5.09; **HRMS** (ESI) for $C_{13}H_{22}OSi$: calcd. 238.1389; found 238.1398.

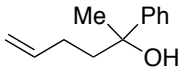

2-Phenylhex-5-en-2-ol 67e.[202]
To a stirred solution of phenylmagnesiumbromide (11 mL, 1M solution in THF, 11 mmol) at 0 °C was added dropwise a solution of 5-hexen-2-one (981 mg, 10.0 mmol) in dry THF (10 mL). The reaction mixture was allowed to warm up to room temperature and stirred for 1 h. NH_4Cl aqueous solution (20 mL) was added to quench the reaction. The organic and the aqueous layers were separated and the latter was extracted twice with EtOAc. The combined organic layers were dried (Na_2SO_4), filtered and the filtrate was concentrated in vacuo. The residue was purified by chromatography on silica gel (5% EtOAc in petroleum ether) affording a colorless oil (1.73 g, 98%). Rf = 0.30 (5% EtOAc in petroleum ether)

[202] M. B. Hay, A. R. Hardin, J. P. Wolfe, *J. Org. Chem.* **2005**, *70*, 3099–3107.

1H NMR (400 MHz, $CDCl_3$) δ 7.50-7.26 (m, 5H), 5.91-5.78 (m, 1H), 5.08-4.93 (m, 2H), 2.16-1.92 (m, 4H), 1.63 (s, 3H). The analytical data are in accordance with those reported in the literature.

3. Azidation reactions on tertiary aliphatic alcohols from section 2.3

General procedure.
To a 10 mL reaction tube containing the alcohol (0.5 mmol) in nitromethane (0.25 mL) was added the nucleophile (3 equiv), followed by $B(C_6F_5)_3 \bullet H_2O$ (5 mol%). The vial was capped and the mixture allowed to stir for 1 to 1h30 at 23 or 0 °C. After cooling to room temperature, the reaction mixture was diluted with water and extracted twice with EtOAc. The organic layers were combined, washed with brine, dried over Na_2SO_4, filtered and volatiles were removed in vacuo. The residue was purified by flash chromatography on SiO_2.

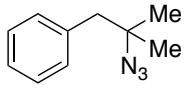

(2-azido-2-methylpropyl)benzene 79a.[203]
Synthesized according to the general procedure after 1 h at 23 °C starting with the alcohol **77a** (75 mg, 0.50 mmol), azidotrimethylsilane (199 µL, 173 mg, 1.50 mmol) and $B(C_6F_5)_3 \bullet H_2O$ (13.3 mg, 0.0250 mmol, 5.00 mol%). Isolated (70 mg, 80%) as a colorless amorphous solid after column chromatography (Petroleum ether). R_f = 0.20 (Petroleum ether).
^{1}H NMR (400 MHz, $CDCl_3$) δ 7.40-7.26 (m, 5H), 2.83 (s, 2H), 1.33 (s, 6H); **^{13}C NMR** (100 MHz, $CDCl_3$) δ 136.6, 130.6, 128.4, 126.8, 61.8, 47.5, 25.9. The analytical data are in accordance with those reported in the literature.

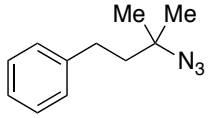

(3-azido-3-methylbutyl)benzene 79b.[204]
Synthesized according to the general procedure after 1 h at 23 °C starting with the alcohol **77b** (82 mg, 0.50 mmol), azidotrimethylsilane (199 µL, 173 mg, 1.50 mmol) and $B(C_6F_5)_3 \bullet H_2O$ (13.3 mg, 0.0250 mmol, 5.00 mol%). Isolated (82 mg, 87%) as a colorless oil after column chromatography (Petroleum ether). R_f = 0.36 (Petroleum ether).
^{1}H NMR (400 MHz, $CDCl_3$) δ 7.40-7.22 (m, 5H), 2.79-2.71 (m, 2H), 1.92-1.83 (m, 2H), 1.41 (s, 6H); **^{13}C NMR** (100 MHz, $CDCl_3$) δ 141.9, 128.5, 128.3, 126.0, 61.4, 43.6, 30.8, 26.1. The analytical data are in accordance with those reported in the literature.

[203] C. L. Hill, J. A. Smegal, T. J. Henly, *J. Org. Chem.* **1983**, *48*, 3277–3281.
[204] J. Waser, B. Gaspar, H. Nambu, E. M. Carreira, *J. Am. Chem. Soc.* **2006**, *128*, 11693–11712.

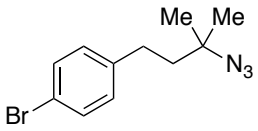

1-(3-Azido-3-methylbutyl)-4-bromobenzene 79c.
Synthesized according to the general procedure after 1 h at 23 °C starting with the alcohol **77c** (122 mg, 0.500 mmol), azidotrimethylsilane (199 μL, 173 mg, 1.50 mmol) and $B(C_6F_5)_3 \bullet H_2O$ (13.3 mg, 0.0250 mmol, 5.00 mol%). Isolated (120 mg, 90%) as a colorless oil after column chromatography (Petroleum ether). $R_f = 0.39$ (Petroleum ether).
^{1}H NMR (400 MHz, $CDCl_3$) δ 7.40 (d, *J* = 8.2 Hz, 2H), 7.07 (d, *J* = 8.2 Hz, 2H), 2.67-2.60 (m, 2H), 1.79-1.72 (m, 2H), 1.33 (s, 6H); **^{13}C NMR** (100 MHz, $CDCl_3$) δ 140.9, 131.6, 130.2, 119.8, 61.4, 43.5, 30.3, 26.2; **HRMS** (ESI) for $C_{11}H_{14}BrN_3$: calcd. 267.03711; found 267.03736.

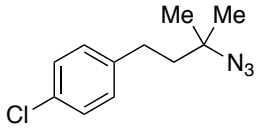

1-(3-Azido-3-methylbutyl)-4-chlorobenzene 79d.
Synthesized according to the general procedure after 1 h at 23 °C starting with the alcohol **77d** (100 mg, 0.50 mmol), azidotrimethylsilane (199 μL, 173 mg, 1.50 mmol) and $B(C_6F_5)_3 \bullet H_2O$ (13.3 mg, 0.0250 mmol, 5.00 mol%). Isolated (95 mg, 85%) as a colorless oil after column chromatography (Petroleum ether). $R_f = 0.42$ (Petroleum ether).
^{1}H NMR (400 MHz, $CDCl_3$) δ 7.28-7.21 (m, 2H), 7.15-7.08 (m, 2H), 2.69-2.60 (m, 2H), 1.80-1.71 (m, 2H), 1.33 (s, 6H); **^{13}C NMR** (100 MHz, $CDCl_3$) δ 140.4, 131.8, 129.8, 128.7, 61.4, 43.5, 30.2, 26.1; **HRMS** (ESI) for $C_{11}H_{14}ClN_3$: calcd. 223.08762; found 223.08631.

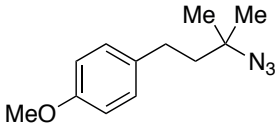

1-(3-Azido-3-methylbutyl)-4-methoxybenzene 79g.
Synthesized according to the general procedure after 1 h at 23 °C starting with the alcohol **77g** (97 mg, 0.50 mmol), azidotrimethylsilane (199 mL, 173 mg, 1.50 mmol) and $B(C_6F_5)_3 \bullet H_2O$ (13.3 mg, 0.0250 mmol, 5.00 mol%). Isolated (94 mg, 86%) as a colorless oil after column chromatography (Petroleum ether). $R_f = 0.25$ (Petroleum ether).
^{1}H NMR (400 MHz, $CDCl_3$) δ 7.16 (d, *J* = 8.6 Hz, 2H), 6.89 (d, *J* = 8.6 Hz, 2H), 3.84 (s, 3H), 2.75-2.61 (m, 2H), 1.87-1.78 (m, 2H), 1.38 (s, 6H); **^{13}C NMR** (100 MHz, $CDCl_3$) δ 157.9, 133.9, 129.2, 113.9, 61.4, 55.2, 43.8, 29.8, 26.0; **HRMS** (ESI) for $C_{12}H_{17}N_3O$: calcd. 219.13716; found 219.13715.

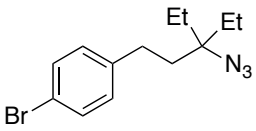

1-(3-Azido-3-ethylpentyl)-4-bromobenzene 79i.
Synthesized according to the general procedure after 1 h at 23 °C starting with the alcohol **77i** (135 mg, 0.500 mmol), azidotrimethylsilane (199 μL, 173 mg, 1.50 mmol) and $B(C_6F_5)_3 \bullet H_2O$ (13.3 mg, 0.0250 mmol, 5.00 mol%). Isolated (95 mg, 64%) as a colorless oil after column chromatography (Petroleum ether). $R_f = 0.37$ (Petroleum ether).
^{1}H NMR (400 MHz, $CDCl_3$) δ 7.41 (d, *J* = 8.2 Hz, 2H), 7.08 (d, *J* = 8.2 Hz, 2H), 2.64-2.54 (m, 2H), 1.78-1.72 (m, 2H), 1.63 (q, *J* = 7.3 Hz, 4H), 0.95 (t, *J* = 7.3 Hz, 6H); **^{13}C NMR** (100 MHz, $CDCl_3$) δ 141.0, 131.6, 130.2, 119.8, 67.0, 38.0, 29.6, 28.5, 8.1; **HRMS** (ESI) for $C_{13}H_{18}BrN_3$: calcd. 295.06841; found 295.07359.

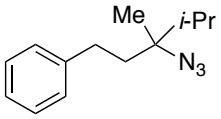

(3-Azido-3,4-dimethylpentyl)benzene 79j.
Synthesized according to the general procedure after 1 h at 23 °C starting with the alcohol **77j** (96 mg, 0.50 mmol), azidotrimethylsilane (199 μL, 173 mg, 1.50 mmol) and $B(C_6F_5)_3 \bullet H_2O$ (13.3 mg, 0.0250 mmol, 5.00 mol%). Isolated (39 mg, 36%) as a colorless oil after column chromatography (Petroleum ether). $R_f = 0.36$ (Petroleum ether).
^{1}H NMR (400 MHz, $CDCl_3$) δ 7.35-7.18 (m, 5H), 2.76-2.65 (m, 2H), 1.95-1.79 (m, 3H), 1.28 (s, 3H), 1.00 (d, *J* = 6.8 Hz, 3H), 0.97 (d, *J* = 6.8 Hz, 3H); **^{13}C NMR** (100 MHz, $CDCl_3$) δ 142.2, 128.6, 128.5, 126.1, 67.1, 39.9, 35.8, 30.4, 19.5, 17.6, 17.5; **HRMS** (ESI) for $C_{13}H_{19}N_3$ – HN_2: calcd. 188.14392; found 188.14494.

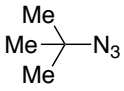

2-azido-2-methylpropane 79n.[205]
Synthesized according to the general procedure after 1 h at 23 °C starting with the alcohol **77n** (37 mg, 0.50 mmol), azidotrimethylsilane (199 μL, 173 mg, 1.50 mmol) and $B(C_6F_5)_3 \bullet H_2O$ (13.3 mg, 0.0250 mmol, 5.00 mol%). Anisole (54 μL, 51 mg, 0.50 mmol, 1.0 equiv) was added as an internal standard and the mixture was taken up in $CDCl_3$. ^{1}H NMR of these solutions were recorded and the % yield calculated based on the ratio of the methyl resonance anisole (δ 3.88 ppm, 3H) to the resonance corresponding to the methylene of compound (δ 1.39, 9H). Yield of **79n** was determined as 95%.
^{1}H NMR (400 MHz, $CDCl_3$) δ 1.39 (s, 9H); **^{13}C NMR** (100 MHz, $CDCl_3$) δ 58.9, 27.2. The analytical data are in accordance with those reported in the literature.

[205] J. C. Bottaro, P. E. Penwell, R. J. Schmitt, *Synth. Comm.* **1997**, *27*, 1465–1467.

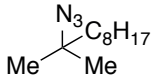

2-Azido-2-methyldecane 79o.
Synthesized according to the general procedure after 1 h at 23 °C starting with the alcohol **77o** (86 mg, 0.50 mmol), azidotrimethylsilane (199 μL, 173 mg, 1.50 mmol) and $B(C_6F_5)_3 \bullet H_2O$ (13.3 mg, 0.0250 mmol, 5.00 mol%). Isolated (84 mg, 85%) as a colorless oil after column chromatography (Petroleum ether). R_f = 0.40 (Petroleum ether).
^{1}H NMR (400 MHz, $CDCl_3$) δ 1.51-1.43 (m, 2H), 1.41-1.25 (m, 12H), 1.24 (s, 6H), 0.88 (t, *J* = 6.9, 3H); **^{13}C NMR** (100 MHz, $CDCl_3$) δ 61.8, 41.6, 32.0, 30.0, 29.7, 29.4, 26.1, 24.4, 22.8, 14.2; **HRMS** (ESI) for $C_{11}H_{23}N_3 - HN_2$: calcd. 168.17522; found 168.17607.

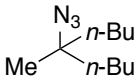

5-Azido-5-methylnonane 79p.[206]
Synthesized according to the general procedure after 1 h at 23 °C starting with the alcohol **77p** (79 mg, 0.50 mmol), azidotrimethylsilane (199 μL, 173 mg, 1.50 mmol) and $B(C_6F_5)_3 \bullet H_2O$ (13.3 mg, 0.0250 mmol, 5.00 mol%). Isolated (69 mg, 75%) as a colorless oil after column chromatography (0 to 2% EtOAc in Petroleum ether). R_f = 0.40 (Petroleum ether 100%).
^{1}H NMR (400 MHz, $CDCl_3$) δ 1.55-1.28 (m, 12H), 1.24 (s, 3H), 0.99-0.91 (m, 6H); **^{13}C NMR** (100 MHz, $CDCl_3$) δ 64.2, 39.0, 26.1, 23.3, 23.0, 14.0. The analytical data are in accordance with those reported in the literature.

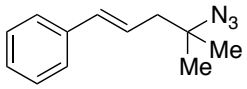

(*E*)-(4-azido-4-methylpent-1-en-1-yl)benzene 79q.
Synthesized according to the general procedure after 1 h at 0 °C starting with the alcohol **77q** (86 mg, 0.50 mmol), azidotrimethylsilane (199 μL, 173 mg, 1.50 mmol) and $B(C_6F_5)_3 \bullet H_2O$ (13.3 mg, 0.0250 mmol, 5.00 mol%). Isolated (46 mg, 46%) as a colorless oil after column chromatography (Petroleum ether). R_f = 0.12 (Petroleum ether).
^{1}H NMR (400 MHz, $CDCl_3$) δ 7.45-7.29 (m, 5H), 6.52 (d, *J* = 15.8 Hz, 1H), 6.31-6.24 (m, 2H), 2.46 (d, *J* = 7.4 Hz, 2H), 1.37 (s, 6H); **^{13}C NMR** (100 MHz, $CDCl_3$) δ 137.2, 133.8, 128.6, 127.4, 126.2, 124.8, 61.8, 45.1, 25.9; **HRMS** (ESI) for $C_{12}H_{15}N_3$: calcd. 201.12660; found 201.12579.

[206] T. Ooi, D. Uraguchi, N. Kagashima, K. Maruoka, *Tetrahedron Lett.* **1997**, *38*, 5679–5682.

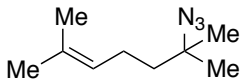

6-azido-2,6-dimethylhept-2-ene 79r.
Synthesized according to the general procedure after 1 h at 23 °C starting with the alcohol **77r** (71 mg, 0.50 mmol), azidotrimethylsilane (199 μL, 173 mg, 1.50 mmol) and $B(C_6F_5)_3 \bullet H_2O$ (13.3 mg, 0.0250 mmol, 5.00 mol%). Anisole (54 μL, 51 mg, 0.50 mmol, 1.0 equiv) was added as an internal standard and the mixture was taken up in $CDCl_3$. ^{1}H NMR of these solutions were recorded and the % yield calculated based on the ratio of the methyl resonance anisole (δ 3.88 ppm, 3H) to the resonance corresponding to the methylene of compound (δ 2.22-2.16, 2H). Yield of **79r** was determined as 70%.
^{1}H NMR (400 MHz, $CDCl_3$) δ 5.17-5.12 (m, 1H), 2.12-2.06 (m, 2H), 1.74 (s, 3H), 1.67 (s, 3H); **^{13}C NMR** (100 MHz, $CDCl_3$) δ 132.0, 123.7, 61.6, 41.5, 26.0, 25.7, 23.0, 17.5; **HRMS** (ESI) for $C_9H_{17}N_3 - HN_2$: calcd. 138.12827; found 138.12835.

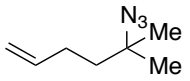

5-azido-5-methylhex-1-ene 79s.[207]
Synthesized according to the general procedure after 1 h at 23 °C starting with the alcohol **77s** (57 mg, 0.50 mmol), azidotrimethylsilane (199 μL, 173 mg, 1.50 mmol) and $B(C_6F_5)_3 \bullet H_2O$ (13.3 mg, 0.0250 mmol, 5.00 mol%). Anisole (54 μL, 51 mg, 0.50 mmol, 1.0 equiv) was added as an internal standard and the mixture was taken up in $CDCl_3$. ^{1}H NMR of these solutions were recorded and the % yield calculated based on the ratio of the methyl resonance anisole (δ 3.88 ppm, 3H) to the resonance corresponding to the methylene of compound (δ 2.20-2.16, 2H). Yield of **79s** was determined as 73%.
^{1}H NMR (400 MHz, $CDCl_3$) δ 5.92-5.82 (m, 1H), 5.11-5.01 (m, 2H), 2.20-2.15 (m, 2H), 1.65-1.61 (m, 2H), 1.33 (s, 6H); **^{13}C NMR** (100 MHz, $CDCl_3$) δ 138.0, 114.8, 61.5, 40.6, 28.6, 26.0. The analytical data are in accordance with those reported in the literature.

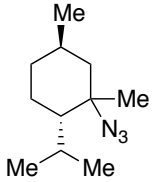

(*2S*,*5R*)-1-azido-2-isopropyl-1,5-dimethylcyclohexane 79t.
Synthesized according to the general procedure after 1 h at 23 °C starting with the alcohol **77t** (85 mg, 0.50 mmol), azidotrimethylsilane (199 μL, 173 mg, 1.50 mmol) and $B(C_6F_5)_3 \bullet H_2O$ (13.3 mg, 0.0250 mmol, 5.00 mol%). Isolated (44 mg, 45%) as a colorless oil after column chromatography (Petroleum ether). $R_f = 0.38$ (Petroleum ether).
^{1}H NMR (400 MHz, $CDCl_3$) δ 2.09-2.01 (m, 1H), 1.81-1.77 (m, 2H), 1.70-1.54 (m, 2H), 1.38-1.25 (m, 4H), 1.24 (s, 3H), 1.02 (s, 1.5H), 1.01 (s, 1.5H), 0.97 (s, 1.5H), 0.95 (s, 1.5H), 0.88 (s, 1.5H), 0.86 (s, 1.5H); **^{13}C NMR** (100 MHz, $CDCl_3$) δ 134.2, 133.8, 132.1, 123.7, 123.6, 120.4, 120.1, 66.6, 66.44, 42.13, 37.8, 30.9, 30.8, 26.7, 26.5, 25.7, 24.1, 23.9, 23.3,

[207] S. Firdous, K. Banert, A. A. Auer, *Chem. Eur. J.* **2011**, *17*, 5539–5543.

23.2, 22.5, 22.3, 20.16, 19.72, 17.6 (mixture of 2 diastereoisomers, ratio 7:3); **HRMS** (ESI) for $C_{11}H_{21}N_3 - HN_2$: calcd. 166.15957; found 166.16263.

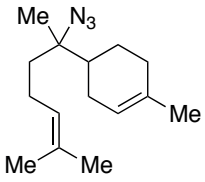

4-(2-azido-6-methylhept-5-en-2-yl)-1-methylcyclohex-1-ene 79u.
Synthesized according to the general procedure after 1 h at 23 °C starting with the alcohol **77u** (111 mg, 0.500 mmol), azidotrimethylsilane (199 µL, 173 mg, 1.50 mmol) and $B(C_6F_5)_3 \bullet H_2O$ (13.3 mg, 0.0250 mmol, 5.00 mol%). Isolated (65 mg, 53%) as a colorless oil after column chromatography (Petroleum ether). $R_f = 0.56$ (Petroleum ether).
^{1}H NMR (400 MHz, $CDCl_3$) δ 5.42 (m, 1H), 5.15 (t, $J = 6.9$ Hz, 1H), 2.11-1.83 (m, 6H), 1.74 (s, 3H), 1.70 (s, 3H), 1.67 (s, 3H), 1.64-1.58 (m, 2H), 1.42-1.33 (m, 1H), 1.29 (s, 1.5H), 1.25 (s, 1.5H); **^{13}C NMR** (100 MHz, $CDCl_3$) δ 134.2, 133.8, 132.1, 123.7, 123.6, 120.4, 120.1, 66.6, 66.4, 42.1, 41.5, 37.8, 37.3, 30.9, 30.8, 26.5, 25.7, 24.0, 23.3, 23.2, 22.5, 20.1, 17.6 (mixture of 2 diastereoisomers, ratio 1:1); **HRMS** (ESI) for $C_{15}H_{25}N_3 - N_2$: calcd. 219.19870; found 219.19812.

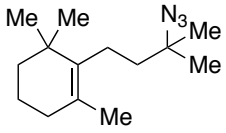

2-(3-azido-3-methylbutyl)-1,3,3-trimethylcyclohex-1-ene 79v.
Synthesized according to the general procedure after 1 h at 23 °C starting with the alcohol **77v** (105 mg, 0.500 mmol), azidotrimethylsilane (199 µL, 173 mg, 1.50 mmol) and $B(C_6F_5)_3 \bullet H_2O$ (13.3 mg, 0.0250 mmol, 5.00 mol%). Isolated (89 mg, 74%) as a colorless oil after column chromatography (Petroleum ether). $R_f = 0.35$ (Petroleum ether).
^{1}H NMR (400 MHz, $CDCl_3$) δ 2.13-2.09 (m, 2H), 1.95 (t, $J = 6.3$ Hz, 2H), 1.65-1.58 (m, 7H), 1.48-1.45 (m, 2H), 1,34 (s, 6H), 1,05 (s, 6H); **^{13}C NMR** (100 MHz, $CDCl_3$) δ 136.2, 127.5, 61.8, 41.5, 39.8, 35.0, 32.8, 28.6, 25.8, 23.0, 19.7, 19.5; **HRMS** (ESI) for $C_{14}H_{25}N_3 - HN_2$: calcd. 206.19087; found 206.18930.

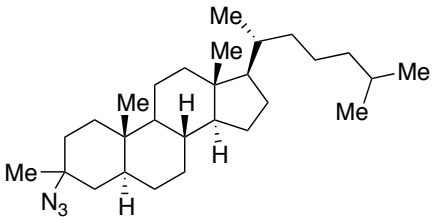

3-azido-3-methyl-5α-cholestane 79w.
Synthesized according to the general procedure after 1 h at 23 °C starting with the alcohol **77w** (80 mg, 0.20 mmol), azidotrimethylsilane (80 µL, 69 mg, 0.60 mmol) and $B(C_6F_5)_3 \bullet H_2O$ (5.3 mg, 0.010 mmol, 5.0 mol%). Isolated (50 mg, 58%) as a colorless oil after column chromatography (Petroleum ether). $R_f = 0.36$ (Petroleum ether).

^{1}H NMR (400 MHz, $CDCl_3$) δ 2.04-1.99 (m, 1H), 1.91-1.82 (m, 1H), 1.75-1.00 (m, 32H), 0.96-0.91 (m, 9H), 0.81 (s, 3H), 0.70 (s, 3H); **^{13}C NMR** (100 MHz, $CDCl_3$) δ 62.2, 56.5, 56.2, 54.04, 41.4, 40.0, 39.5, 36.2, 31.9, 28.2, 28.0, 27.53, 24.2, 23.9, 22.6, 21.0, 18.7, 11.7; **HRMS** (ESI) for $C_{28}H_{49}N_1 - N_2$: calcd. 399.38650; found 399.38101.

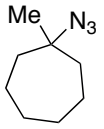

1-Azido-1-Methylcycloheptane 79x.
Synthesized according to the general procedure after 1 h at 23 °C starting with the alcohol **77x** (64 mg, 0.50 mmol), azidotrimethylsilane (199 µL, 173 mg, 1.50 mmol) and $B(C_6F_5)_3 \bullet H_2O$ (13.3 mg, 0.0250 mmol, 5.00 mol%). Isolated (59 mg, 77%) as a colorless oil after column chromatography (Petroleum ether). $R_f = 0.35$ (Petroleum ether).
^{1}H NMR (400 MHz, $CDCl_3$) δ 1.84-1.71 (m, 2H), 1.67-1.35 (m, 10H), 1.29 (s, 3H); **^{13}C NMR** (100 MHz, $CDCl_3$) δ 65.3, 40.2, 29.4, 27.6, 22.7; **HRMS** (ESI) for $C_8H_{15}N_3 - HN_2$: calcd. 124.11262; found 124.11285.

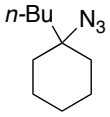

1-azido-1-butylcyclohexane 79y.
Synthesized according to the general procedure after 1 h at 23 °C starting with the alcohol **77y** (78 mg, 0.50 mmol), azidotrimethylsilane (199 µL, 173 mg, 1.50 mmol) and $B(C_6F_5)_3 \bullet H_2O$ (13.3 mg, 0.0250 mmol, 5.00 mol%). Isolated (79 mg, 87%) as a colorless oil after column chromatography (Petroleum ether). $R_f = 0.38$ (Petroleum ether).
^{1}H NMR (400 MHz, $CDCl_3$) δ 1.76-1.16 (m, 16H), 0.92 (t, J = 6.8 Hz, 3H); **^{13}C NMR** (100 MHz, $CDCl_3$) δ 64.2, 40.0, 34.7, 25.6, 25.5, 23.2, 22.3, 14.1; **HRMS** (ESI) for $C_{10}H_{19}N_3 - HN_2$: calcd. 152.14484; found 152.14392.

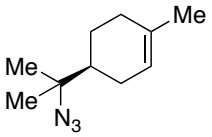

(*S*)-4-(2-azidopropan-2-yl)-1-methylcyclohex-1-ene 79z.
Synthesized according to the general procedure after 1 h at 23 °C starting with the alcohol **77z** (77 mg, 0.50 mmol), azidotrimethylsilane (199 µL, 173 mg, 1.50 mmol) and $B(C_6F_5)_3 \bullet H_2O$ (13.3 mg, 0.0250 mmol, 5.00 mol%). Isolated (49 mg, 58%) as a colorless oil after column chromatography (Petroleum ether). $R_f = 0.60$ (Petroleum ether).
^{1}H NMR (400 MHz, $CDCl_3$) δ 5.42 (br, 1H), 2.18-2.00 (m, 4H), 1.92-1.84 (m, 2H), 1.70 (s, 3H), 1.63-1.56 (m, 1H), 1.31 (s, 3H), 1.28 (s, 3H); **^{13}C NMR** (100 MHz, $CDCl_3$) δ 134.0, 120.1, 64.2, 43.4, 30.9, 26.8, 24.2, 23.9, 23.3, 23.0. The analytical data are in accordance with those reported in the literature.

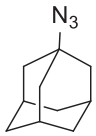

1-Adamantyl azide 79aa.[208]
Synthesized according to the general procedure after 1 h at 23 °C starting with the alcohol **77aa** (76 mg, 0.50 mmol), azidotrimethylsilane (199 μL, 173 mg, 1.50 mmol) and $B(C_6F_5)_3 \bullet H_2O$ (13.3 mg, 0.0250 mmol, 5.00 mol%). Isolated (81 mg, 92%) as a colorless amorphous solid after column chromatography (Petroleum ether). R_f = 0.45 (Petroleum ether).
^{1}H NMR (400 MHz, $CDCl_3$) δ 2.15 (s, 3H), 1.80 (d, *J* = 2.6, 6H), 1.73-1.59 (m, 6H); **^{13}C NMR** (100 MHz, $CDCl_3$) δ 59.1, 41.7, 36.0, 30.0. The analytical data are in accordance with those reported in the literature.

[208] E. Nyfeler, P. Renaud, *Org. Lett.* **2008**, *10*, 985–988.

EXPERIMENTAL SECTION – CHAPTER 3

1. Material and methods

General Information. All reactions were performed in 10 mL sealed tubes under an air atmosphere. Purification of reaction products was carried out by column chromatography using Merck silica gel (40-63 μm). Analytical thin layer chromatography (TLC) was performed on aluminum sheets pre-coated with silica gel 60 F254 (E. Merck), cut to size. Visualization was accomplished with UV light followed by dipping in a potassium permanganate and/or Seebach's staining solutions and heating. ^{1}H NMR spectra were recorded on a Bruker Avance400 (400 MHz) spectrometer at ambient temperature unless otherwise noted and are reported in ppm using solvent as the internal standard ($CDCl_3$ at 7.26 ppm). Data are reported as: multiplicity (ap = apparent, br = broad, s = singlet, d = doublet, t = triplet, q = quartet, m = multiplet), integration and coupling constant(s) in Hz. ^{13}C NMR spectra were recorded on a Bruker Avance400 (100 MHz) spectrometer. Chemical shifts are reported in ppm from tetramethylsilane, with the residual solvent resonance employed as the internal standard ($CDCl_3$ at 77.0 ppm). ^{19}F NMR spectra were recorded on a Bruker Avance400 (376 MHz) spectrometer. ^{11}B NMR spectra were recorded on a Bruker Avance400 (128 MHz) spectrometer. Unless otherwise noted, all commercial materials were purchased from *Sigma-Aldrich* and used without further purification. Alcohol **102**[209] was prepared following a literature procedure. Boronic acids and ligands were used without any special precaution to exclude moisture or air.

[209] M. Rueping, U. Uria, M.-Y. Lin, I. Atodiresei, *J. Am. Chem. Soc*. **2011**, *133*, 3732-3735.

2. Combinatorial approach

General procedure for Step 1 **(12 boronic acids, 12 *O*-ligands, 14 solvents, 2016 possible combinations)**

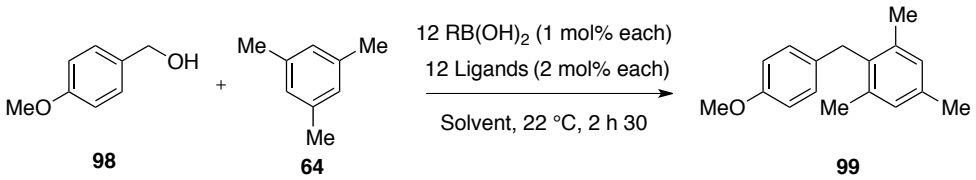

98 **64** **99**

Reactions were carried out in four different solvents simultaneously according to the following procedure using the quantities of boronic acids and ligands described in the table below. Boronic acids **96a-96l** (0.010 mmol, 1.0 mol%) and ligands **97a-97l** (0.020 mmol, 2.0 mol%) were dissolved in solvent (2.5 mL). Mesitylene (418 μL, 360 mg, 3.00 mmol, 3.00 equiv) and *p*-methoxybenzyl alcohol (124 μL, 138 mg, 1.00 mmol, 1.00 equiv) were added, in that order, by syringe. The reactions were stirred at 22 °C and all were monitored by TLC (20% EtOAc in petroleum ether). After completion of the fastest reaction (2.5 h), all reactions were quenched by dilution with DCM, filtered through a short pad of silica and concentrated under reduced pressure. DMSO (71 μL, 78 mg, 1.0 mmol, 1.0 equiv) was added as an internal standard and the mixture was taken up in $CDCl_3$. ^{1}H NMR of these solutions were recorded and the % yield calculated based on the ratio of the DMSO resonance (δ 2.61 ppm, 6H) to the resonance corresponding to the benzylic methylene of compound **99** (δ 4.01, 2H). In the case of the fastest reaction (in $MeNO_2$), compound **99** was isolated as a white solid after flash column chromatography (10% DCM in petroleum ether). R_f = 0.42 (5% EtOAc in petroleum ether). Yields are described below for each case.

1-(4-Methoxybenzyl)-2,4,6-trimethylbenzene 99. [210]
^{1}H NMR (400 MHz, $CDCl_3$) δ 7.01–6.93 (m, 4H), 6.86–6.81 (m, 2H), 4.01 (s, 2H), 3.80 (s, 3H), 2.35 (s, 3H), 2.26 (s, 6H); **^{13}C NMR** (100 MHz, $CDCl_3$) δ 157.8, 137.1, 135.7, 134.3, 132.2, 129.0, 128.9, 113.9, 55.3, 33.9, 21.0, 20.2. The analytical data are in accordance with those reported in the literature.

[210] M. Hofmann, N. Hampel, T. Kanzian, H. Mayr, *Angew. Chem. Int. Ed.* **2004**, *43*, 5402–5405.

*Screening of boronic acids **96a-96l** (1 mol%) – ligands **97a-97l** (2 mol%)*

96a $C_6F_5B(OH)_2$: 2.1 mg
96b 4-F-$C_6H_4B(OH)_2$: 1.4 mg
96c 2,3,4-F_3-$C_6HB(OH)_2$: 1.8 mg
96d 4-CO_2H-$C_6H_4B(OH)_2$: 1.7 mg
96e 3,4-Cl_2-$C_6H_3B(OH)_2$: 1.9 mg
96f 4-OMe-$C_6H_4B(OH)_2$: 1.5 mg
96g 2,3,4,5- F_4-$C_6HB(OH)_2$: 1.9 mg
96h 3,4-F_2-$C_6H_2B(OH)_2$: 1.6 mg
96i 4-Cl-$C_6H_4B(OH)_2$: 1.6 mg
96j $C_6H_5B(OH)_2$: 1.2 mg
96k 2-NO_2-$C_6H_4B(OH)_2$: 1.7 mg
96l $B(OH)_3$: 0.6 mg

97a Oxalic acid dihydrate : 2.5 mg
97b Tartaric acid : 3.0 mg
97c Glycolic acid : 1.5 mg
97d Glyoxylic acid : 1.8 mg
97e Tartaric acid dimethylester : 3.6 mg
97f Pinacol : 2.4 mg
97g Catechol : 2.2 mg
97h 3-Hydroxypropanoic acid : 1.8 mg
97i Succinic acid : 2.4 mg
97j Malonic acid : 2.1 mg
97k Salicylic acid : 2.8 mg
97l Phtalic acid : 3.3 mg

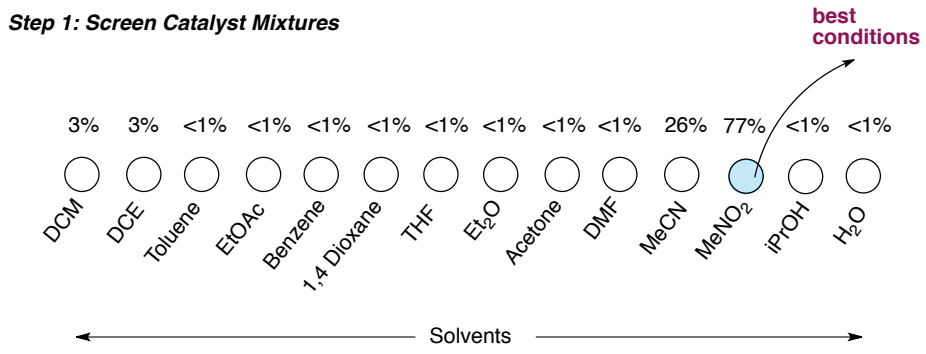

General Procedure for Step 2

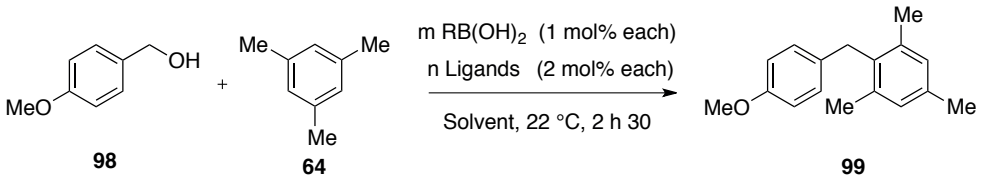

For each deconvolution step, reactions were carried out simultaneously according to the following procedure using the boron acids and ligands described in the tables below. Boronic acids (0.01 mmol, 1.0 mol%) and ligands (0.02 mmol, 2.0 mol%) were dissolved in $MeNO_2$ (2.5 mL). Mesitylene (418 µL, 360 mg, 3.00 mmol, 3.00 equiv), followed by *p*-methoxybenzyl alcohol (124 µL, 138 mg, 1.00 mmol, 1.00 equiv) were added by syringe. The reactions were stirred at 22 °C and all were monitored by TLC (20% EtOAc in petroleum ether). After completion of the fastest reaction for each step, all reactions were quenched by dilution with DCM, filtered through a pad of silica and concentrated under reduced pressure. DMSO (71 µL, 78 mg, 1.0 mmol, 1.0 equiv) was added as an internal standard and the

mixture was taken up in $CDCl_3$. ^1H NMR of these solutions were recorded and the % yield calculated based on the ratio of the DMSO resonance (δ 2.61 ppm, 6H) to the resonance corresponding to the benzylic methylene of compound **99** (δ 4.01, 2H). Yields are described below for each case.

Step 2a - 4 reactions, reaction time: 2.5 h

*Screening of boronic acids **96a-96f** (1 mol%) – ligands **97a-97g** (2 mol%)*

96a $C_6F_5B(OH)_2$: 2.1 mg
96b 4-F-$C_6H_4B(OH)_2$: 1.4 mg
96c 2,3,4-F_3-$C_6HB(OH)_2$: 1.8 mg
96d 4-CO_2H-$C_6H_4B(OH)_2$: 1.7 mg
96e 3,4-Cl_2-$C_6H_3B(OH)_2$: 1.9 mg
96f 4-OMe-$C_6H_4B(OH)_2$: 1.5 mg

97a Oxalic acid dihydrate : 2.5 mg
97b Tartaric acid : 3.0 mg
97c Glycolic acid : 1.5 mg
97d Glyoxylic acid : 1.8 mg
97e Tartaric acid dimethylester : 3.6 mg
97f Pinacol : 2.4 mg
97g Catechol : 2.2 mg

→ 90 % yield

*Screening of boronic acids **96g-96l** (1 mol%) – ligands **97a-97g** (2 mol%)*

96g 2,3,4,5- F_4-$C_6HB(OH)_2$: 1.9 mg
96h 3,4-F_2-$C_6H_2B(OH)_2$: 1.6 mg
96i 4-Cl-$C_6H_4B(OH)_2$: 1.6 mg
96j $C_6H_5B(OH)_2$: 1.2 mg
96k 2-NO_2-$C_6H_4B(OH)_2$: 1.7 mg
96l $B(OH)_3$: 0.6 mg

97a Oxalic acid dihydrate : 2.5 mg
97b Tartaric acid : 3.0 mg
97c Glycolic acid : 1.5 mg
97d Glyoxylic acid : 1.8 mg
97e Tartaric acid dimethylester : 3.6 mg
97f Pinacol : 2.4 mg
97g Catechol : 2.2 mg

→ 63 % yield

*Screening of boronic acids **96a-96f** (1 mol%) – ligands **97h-97l** (2 mol%)*

96a $C_6F_5B(OH)_2$: 2.1 mg
96b 4-F-$C_6H_4B(OH)_2$: 1.4 mg
96c 2,3,4-F_3-$C_6HB(OH)_2$: 1.8 mg
96d 4-CO_2H-$C_6H_4B(OH)_2$: 1.7 mg
96e 3,4-Cl_2-$C_6H_3B(OH)_2$: 1.9 mg
96f 4-OMe-$C_6H_4B(OH)_2$: 1.5 mg

97h 3-Hydroxypropanoic acid : 1.8 mg
97i Succinic acid : 2.4 mg
97j Malonic acid : 2.1 mg
97k Salicylic acid : 2.8 mg
97l Phtalic acid : 3.3 mg

→ 7 % yield

*Screening of boronic acids **96g-96l** (1 mol%) – ligands **97h-97l** (2 mol%)*

96g 2,3,4,5- F_4-$C_6HB(OH)_2$: 1.9 mg
96h 3,4-F_2-$C_6H_2B(OH)_2$: 1.6 mg
96i 4-Cl-$C_6H_4B(OH)_2$: 1.6 mg
96j $C_6H_5B(OH)_2$: 1.2 mg
96k 2-NO_2-$C_6H_4B(OH)_2$: 1.7 mg
96l $B(OH)_3$: 0.6 mg

97h 3-Hydroxypropanoic acid : 1.8 mg
97i Succinic acid : 2.4 mg
97j Malonic acid : 2.1 mg
97k Salicylic acid : 2.8 mg
97l Phtalic acid : 3.3 mg

→ 5 % yield

Step 2a *t* = 2.5 h	$RB(OH)_2$ **96a-96f**	$RB(OH)_2$ **96g-96l**
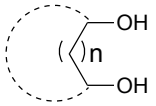 n = 0 **97a-97g**	**90% yield**	63%
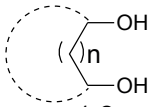 n = 1-2 **97h-97l**	7%	5%

Step 2b - 9 reactions, reaction time: 1 h

*Screening of boronic acids **96a** and **96b** (1 mol%) – ligands **97a** and **97b** (2 mol%)*

96a $C_6F_5B(OH)_2$: 2.1 mg
96b 4-F-$C_6H_4B(OH)_2$: 1.4 mg

97a Oxalic acid dihydrate : 2.5 mg
97b Tartaric acid : 3.0 mg

→ 91 % yield

*Screening of boronic acids **96c** and **96d** (1 mol%) – ligands **97a** and **97b** (2 mol%)*

96c 2,3,4-F_3-$C_6HB(OH)_2$: 1.8 mg
96d 4-CO_2H-$C_6H_4B(OH)_2$: 1.7 mg

97a Oxalic acid dihydrate : 2.5 mg
97b Tartaric acid : 3.0 mg

→ 33 % yield

*Screening of boronic acids **96e** and **96f** (1 mol%) – ligands **97a** and **97b** (2 mol%)*

96e 3,4-Cl_2-$C_6H_3B(OH)_2$: 1.9 mg
96f 4-OMe-$C_6H_4B(OH)_2$: 1.5 mg

97a Oxalic acid dihydrate : 2.5 mg
97b Tartaric acid : 3.0 mg

→ 29 % yield

*Screening of boronic acids **96a** and **96b** (1 mol%) – ligands **97c** and **97d** (2 mol%)*

96a $C_6F_5B(OH)_2$: 2.1 mg
96b 4-F-$C_6H_4B(OH)_2$: 1.4 mg

97c Glycolic acid : 1.5 mg
97d Glyoxylic acid : 1.8 mg

→ 8 % yield

*Screening of boronic acids **96c** and **96d** (1 mol%) – ligands **97c** and **97d** (2 mol%)*

96c 2,3,4-F_3-$C_6HB(OH)_2$: 1.8 mg
96d 4-CO_2H-$C_6H_4B(OH)_2$: 1.7 mg

97c Glycolic acid : 1.5 mg
97d Glyoxylic acid : 1.8 mg

→ 2 % yield

*Screening of boronic acids **96e** and **96f** (1 mol%) – ligands **97c** and **97d** (2 mol%)*

96e 3,4-Cl_2-$C_6H_3B(OH)_2$: 1.9 mg
96f 4-OMe-$C_6H_4B(OH)_2$: 1.5 mg

97c Glycolic acid : 1.5 mg
97d Glyoxylic acid : 1.8 mg

→ 3 % yield

*Screening of boronic acids **96a** and **96b** (1 mol%) – ligands **97e, 97f** and **97g** (2 mol%)*

96a $C_6F_5B(OH)_2$: 2.1 mg
96b 4-F-$C_6H_4B(OH)_2$: 1.4 mg

97e Tartaric acid dimethylester : 3.6 mg
97f Pinacol : 2.4 mg
97g Catechol : 2.2 mg

→ <1 % yield

*Screening of boronic acids **96c** and **96d** (1 mol%) – ligands **97e, 97f** and **97g** (2 mol%)*

96c 2,3,4-F_3-$C_6HB(OH)_2$: 1.8 mg
96d 4-CO_2H-$C_6H_4B(OH)_2$: 1.7 mg

97e Tartaric acid dimethylester : 3.6 mg
97f Pinacol : 2.4 mg
97g Catechol : 2.2 mg

→ <1 % yield

*Screening of boronic acids **96e** and **96f** (1 mol%) – ligands **97e, 97f** and **97g** (2 mol%)*

96e 3,4-Cl_2-$C_6H_3B(OH)_2$: 1.9 mg
96f 4-OMe-$C_6H_4B(OH)_2$: 1.5 mg

97e Tartaric acid dimethylester : 3.6 mg
97f Pinacol : 2.4 mg
97g Catechol : 2.2 mg

→ <1 % yield

Step 2b *t* = 1 h	**96a**, **96b**	**96c**, **96d**	**96e**, **96f**
97a **97b**	**91%**	33%	29%
97c **97d**	8%	2%	3%
97e **97f** **97g**	<1%	<1%	<1%

Step 2c - 4 reactions, reaction time: 15 min

*Screening of boronic acids **96a** and **96b** (1 mol%) – ligands **97a** and **97b** (2 mol%)*

96a $C_6F_5B(OH)_2$: 2.1 mg
→ 95 % yield

97a Oxalic acid dihydrate : 2.5 mg

96a $C_6F_5B(OH)_2$: 2.1 mg
→ 19 % yield

97b Tartaric acid : 3.0 mg

96b 4-F-$C_6H_4B(OH)_2$: 1.4 mg
→ 16 % yield

97a Oxalic acid dihydrate : 2.5 mg

96b 4-F-$C_6H_4B(OH)_2$: 1.4 mg
→ <1 % yield

97b Tartaric acid : 3.0 mg

Step 2c *t* = 15 min	96a	96a
97a	95%	16%
97b	19%	<1%

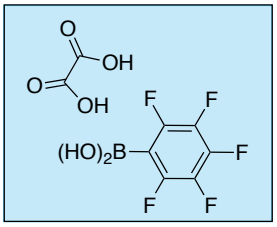

3. Linear optimization

Representative procedure for ligand optimization

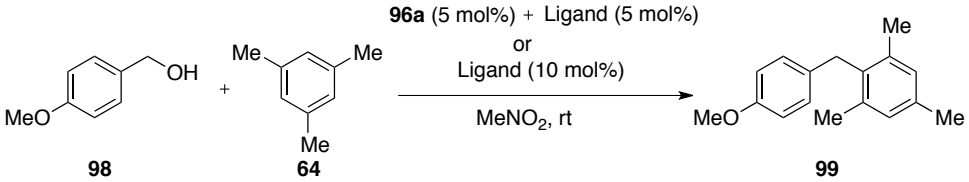

Mesitylene (209 µL, 180 mg, 1.50 mmol, 3.00 equiv) and *p*-methoxybenzyl alcohol (62 µL, 69 mg, 0.50 mmol, 1.0 equiv) were added by syringe into $MeNO_2$ (2.5 mL). Pentafluorophenylboronic acid **96a** (0.025 mmol, 5.0 mol%) and ligand (0.025 mmol, 5.0 mol%) were added to the solution. The reaction mixture was stirred for 4 h at 22 °C except for ligands **97a** and **97b** where the reaction went to completion after 5 and 90 minutes, respectively. Yields are described below for each case (blue).

Control experiment (ligand only): Mesitylene (209 µL, 180 mg, 1.5 mmol, 3.00 equiv) and *p*-methoxybenzyl alcohol (62 µL, 69 mg, 0.50 mmol, 1.0 equiv) were added by syringe into $MeNO_2$ (2.5 mL). Ligand **97a-97l** (0.050 mmol, 10 mol%) was added to the solution. The reaction mixture was stirred for 4 h at 22 °C. Yields are described below for each case (light blue).

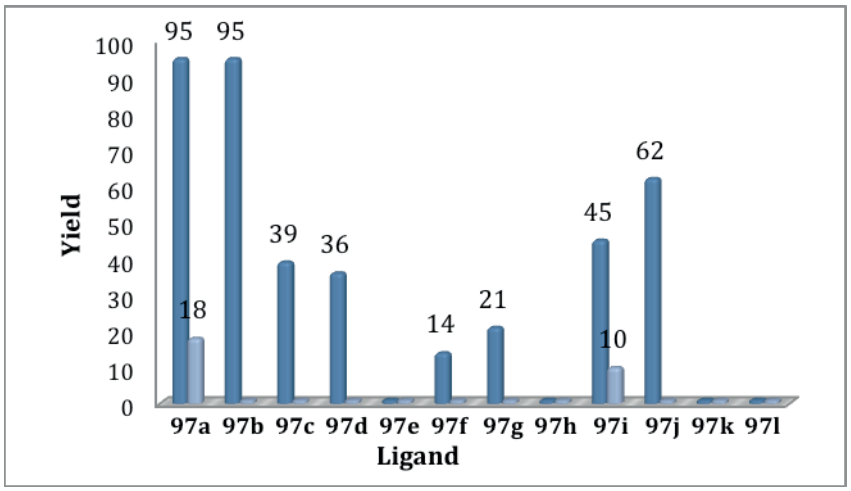

Representative procedure for boronic acid optimization

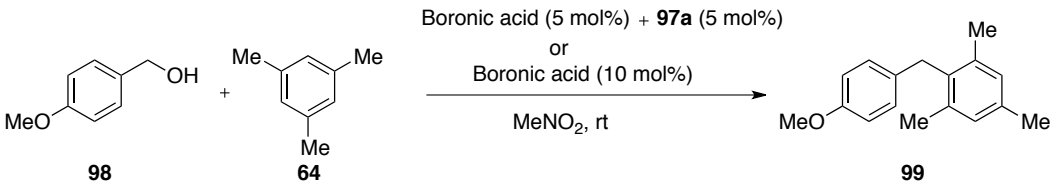

Mesitylene (209 µL, 180 mg, 1.50 mmol, 3.00 equiv) and *p*-methoxybenzyl alcohol (62 µL, 69 mg, 0.50 mmol, 1.0 equiv) were added by syringe into $MeNO_2$ (2.5 mL). Boronic acid **96a-96l** (0.025 mmol, 5.0 mol%) and oxalic acid **97a** (0.025 mmol, 5.0 mol%) were added to the solution. The reaction mixture was stirred for 5 min at 22 °C. Yields are described below for each case (blue).

Control experiment: Mesitylene (209 µL, 180 mg, 1.50 mmol, 3.00 equiv) and *p*-methoxybenzyl alcohol (62 µL, 69 mg, 0.50 mmol, 1.0 equiv) were added by syringe into $MeNO_2$ (2.5 mL). Boronic acid **96a-96l** (0.050 mmol, 10 mol%) was added to the solution. The reaction mixture was stirred for 4 h at 22 °C. Yields are described below for each case (light blue).

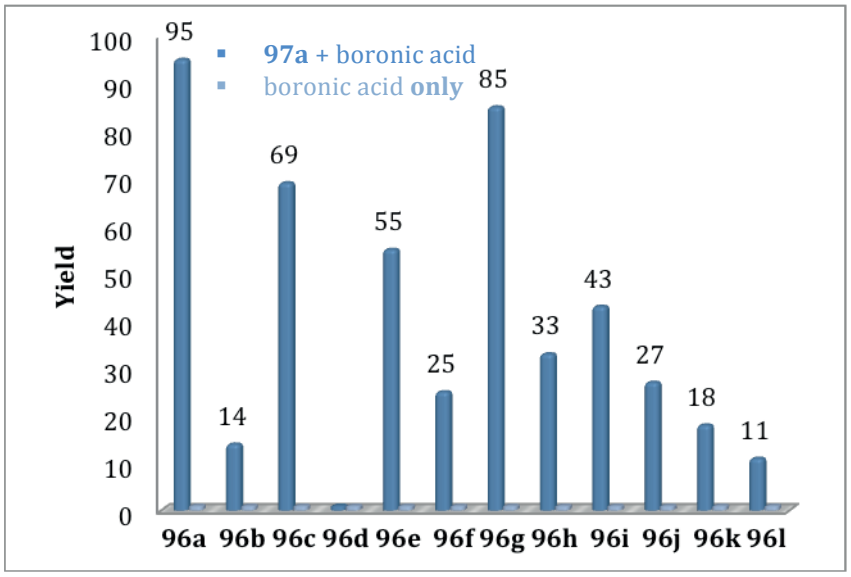

4. Monitoring assembly dynamics by NMR

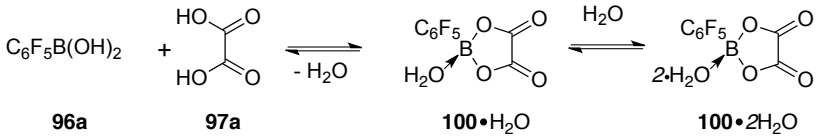

96a **97a** **100•H_2O** **100•$2H_2O$**

A **B** **C**

^{19}F NMR

Effect of different ratios **$C_6F_5B(OH)_2$ – oxalic acid**

$C_6F_5B(OH)_2$ **96a** (10.5 mg, 0.0500 mmol, 1.00 equiv) and oxalic acid **97a** (6.3 -25 mg, 0.050-0.20 mmol, 1.0-4.0 equiv) were dissolved into CD_3NO_2 (500 µL).

Experiment 1: **96a** (10.5 mg, 0.0500 mmol)

Experiment 2: **96a** (10.5 mg, 0.0500 mmol, 1.00 equiv) + **97a** (6.3 mg, 0.050 mmol, 1.0 equiv)

Experiment 3: **96a** (10.5 mg, 0.0500 mmol, 1.00 equiv) + **97a** (12.6 mg, 0.100 mmol, 2.0 equiv)

Experiment 4: **96a** (10.5 mg, 0.0500 mmol, 1.00 equiv) + **97a** (18.6 mg, 0.150 mmol, 3.0 equiv)

Experiment 5: **96a** (10.5 mg, 0.0500 mmol, 1.00 equiv) + **97a** (25 mg, 0.20 mmol, 4.0 equiv)

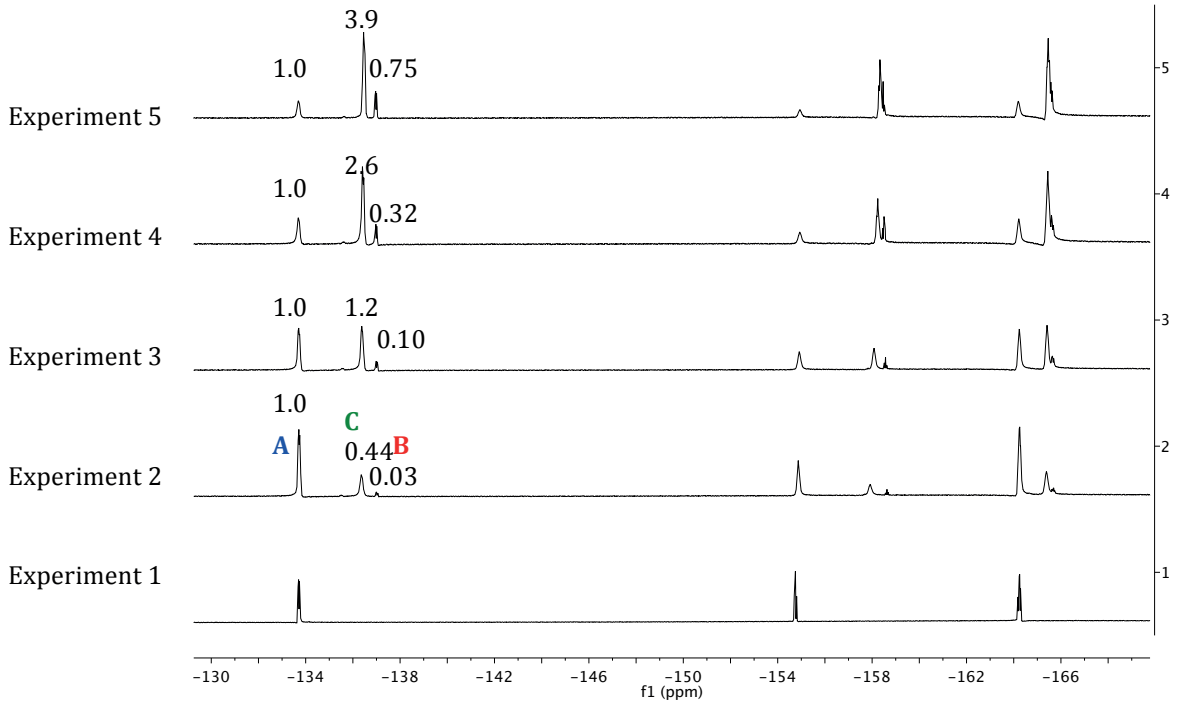

Effect of H_2O on catalyst assembly

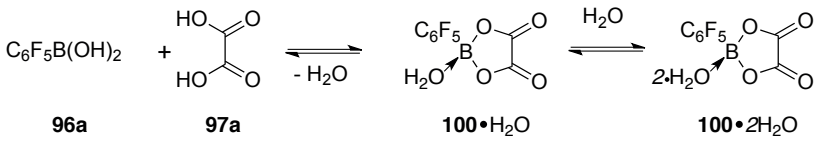

$C_6F_5B(OH)_2$ **96a** (10.5 mg, 0.0500 mmol, 1.00 equiv) and oxalic acid **97a** (6.3 mg, 0.050 mmol, 1.0 equiv) were dissolved into CD_3NO_2 (500 µL). Additional H_2O is added via syringe to the solution (0.2 mmol – 1.2 mmol, 4 equiv – 24 equiv).

Experiment 1: **96a** (10.5 mg, 0.0500 mmol, 1.00 equiv) + **97a** (6.3 mg, 0.050 mmol, 1.0 equiv)

Experiment 2: **96a** (10.5 mg, 0.0500 mmol, 1.00 equiv) + **97a** (6.3 mg, 0.050 mmol, 1.0 equiv) + H_2O (3.6 mg, 0.20 mmol, 4.0 equiv)

Experiment 3: **96a**(10.5 mg, 0.0500 mmol, 1.00 equiv) + **97a** (6.3 mg, 0.050 mmol, 1.0 equiv) + H_2O (7.2 mg, 0.40 mmol, 8.0 equiv)

Experiment 4: **96a** (10.5 mg, 0.0500 mmol, 1.00 equiv) + **97a** (6.3 mg, 0.050 mmol, 1.0 equiv) + H_2O (10.8 mg, 0.600 mmol, 12.0 equiv)

Experiment 5: **96a** (10.5 mg, 0.0500 mmol, 1.00 equiv) + **97a** (6.3 mg, 0.050 mmol, 1.0 equiv) + H_2O (21.6 mg, 1.20 mmol, 24.0 equiv)

Experiment 6: **96a** (10.5 mg, 0.0500 mmol, 1.00 equiv) + **97a** (6.3 mg, 0.050 mmol, 1.0 equiv) + H_2O (32.4 mg, 1.80 mmol, 36.0 equiv)

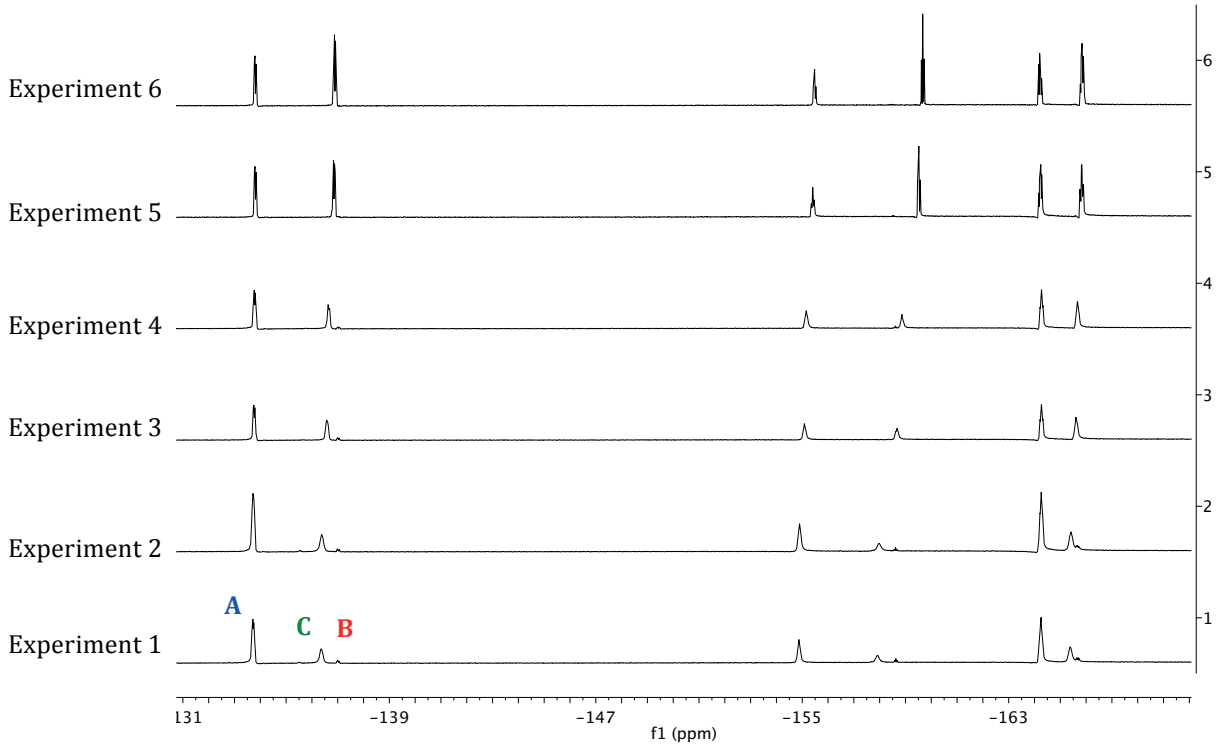

^{11}B NMR

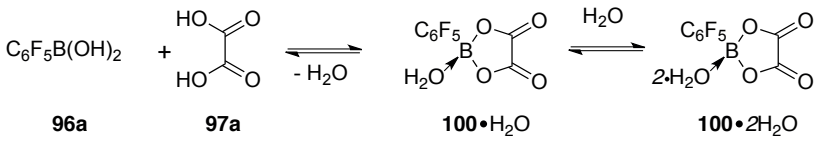

96a **97a** **100•H_2O** **100•2H_2O**

A **B** **C**

$C_6F_5B(OH)_2$ **96a** (10.5 mg, 0.0500 mmol, 1.00 equiv) and oxalic acid **97a** (6.3 mg, 0.050 mmol, 1.0 equiv) were dissolved into CD_3NO_2 (500 μL). Additional H_2O (24 equiv) is added via syringe to the solution in experiment 4.

Experiment 1: **96a** (10.5 mg, 0.0500 mmol)

Experiment 2: **96a** (10.5 mg, 0.0500 mmol, 1.00 equiv) + **97a** (6.3 mg, 0.050 mmol, 1.0 equiv)

Experiment 3: **96a** (10.5 mg, 0.0500 mmol, 1.00 equiv) + **97a** (12.6 mg, 0.100 mmol, 2.00 equiv)

Experiment 4: **96a** (10.5 mg, 0.0500 mmol, 1.00 equiv) + **97a** (12.6 mg, 0.100 mmol, 2.00 equiv) + H_2O (21.6 mg, 1.20 mmol, 24.0 equiv)

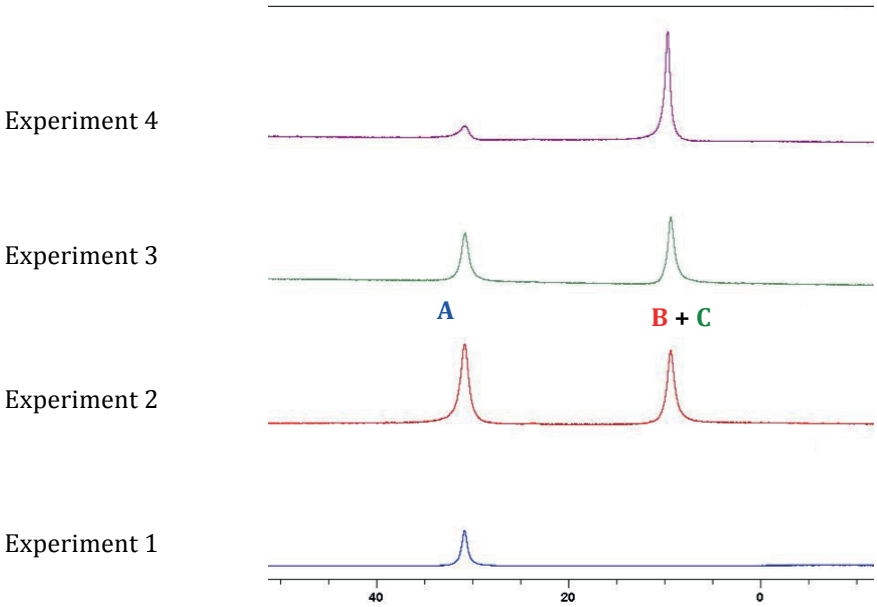

Effect of solvent on catalyst assembly

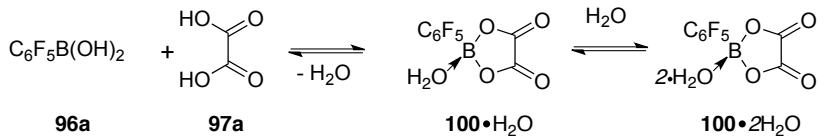

A B C

$C_6F_5B(OH)_2$ **96a** (10.5 mg, 0.0500 mmol, 1.00 equiv) and oxalic acid **97a** (6.3 mg, 0.050 mmol, 1.0 equiv) were dissolved into deuterated solvent (500 µL).

Experiment 1: **96a** (10.5 mg, 0.0500 mmol, 1.00 equiv) in CD_3CN.

Experiment 2: **96a** (10.5 mg, 0.0500 mmol, 1.00 equiv) + **97a** (6.3 mg, 0.050 mmol, 1.0 equiv) in CD_3CN.

Experiment 3: **96a** (10.5 mg, 0.0500 mmol, 1.00 equiv) in CD_2Cl_2.

Experiment 4: **96a** (10.5 mg, 0.0500 mmol, 1.00 equiv) + **97a** (6.3 mg, 0.050 mmol, 1.0 equiv) in CD_2Cl_2.

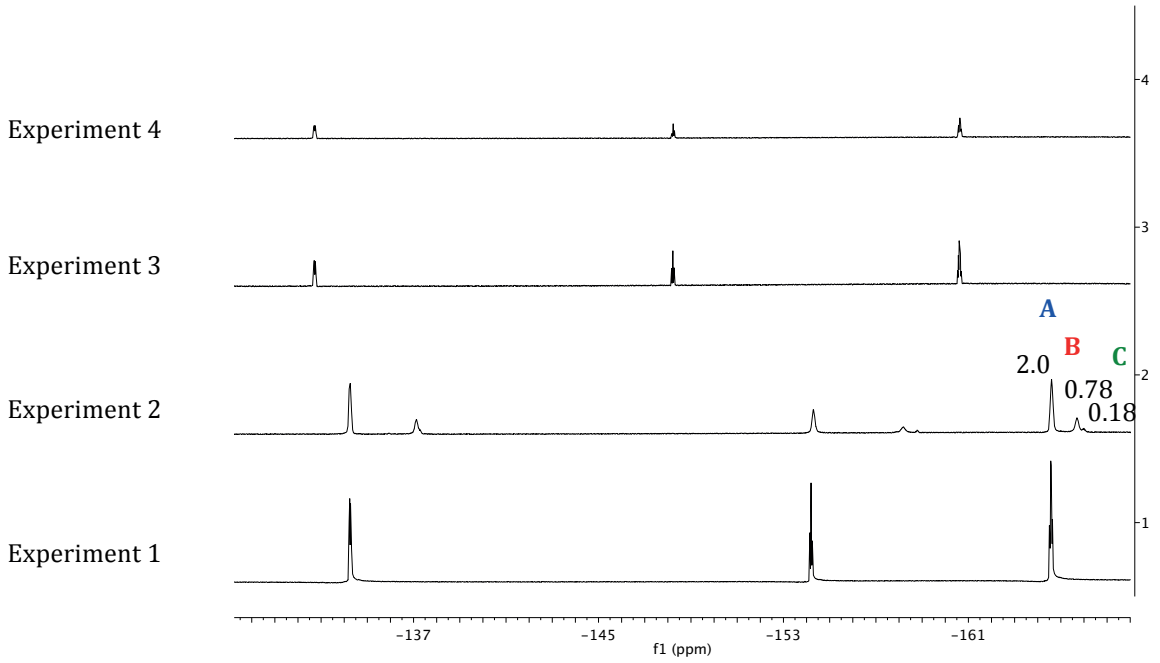

5. Kinetics of the Friedel-Crafts reaction

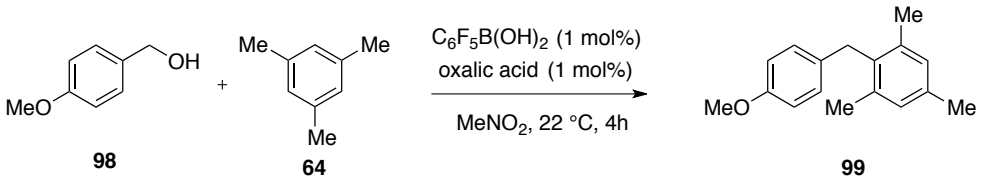

Mesitylene (209 µL, 180 mg, 1.50 mmol, 3.00 equiv) and *p*-methoxybenzyl alcohol (62 µL, 69 mg, 0.50 mmol, 1.0 equiv) were added by syringe into $MeNO_2$ (2.5 mL). $C_6F_5B(OH)_2$ (0.005 mmol, 1.0 mol%) and oxalic acid (0.005 mmol, 1.0 mol%) were added to the solution. The reaction mixture was stirred at room temperature. Samples were taken every two minutes over 30 minutes and dissolved in DCM. Dodecane (1 equiv) was added as the GC-MS internal standard. The increasing conversion of compound **99** was calculated from the crude GC-MS sample compared to internal standard.

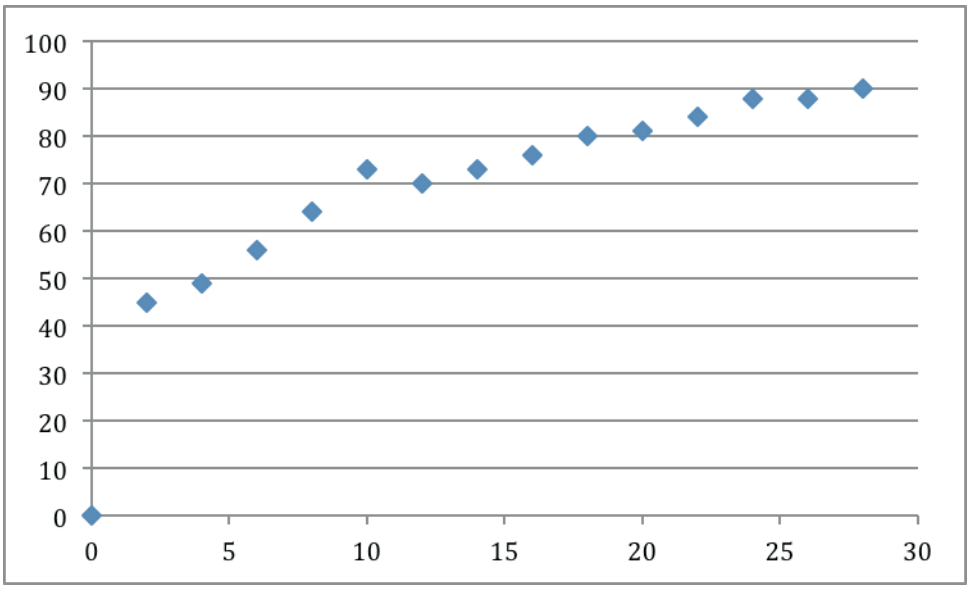

6. Measurement of effective acidity by the Gutmann-Beckett method

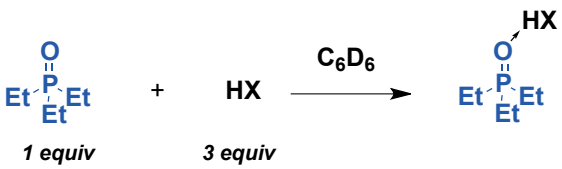

Triethylphosphine oxide (4 mg, 0.03 mmol, 1 equiv) and acid (0.09 mmol, 3 equiv) were dissolved into C_6D_6 (500 µL).

Experiment 1: Triethylphosphine oxide

Experiment 2: Triethylphosphine oxide + **oxalic acid** (11 mg, 0.090 mmol, 3.0 equiv)

Experiment 3: Triethylphosphine oxide + **$C_6F_5B(OH)_2$** (19 mg, 0.090 mmol, 3.0 equiv)

Experiment 4: Triethylphosphine oxide + **$C_6F_5B(OH)_2$** (19 mg, 0.090 mmol, 3.0 equiv) + **oxalic** (11 mg, 0.090 mmol, 3.0 equiv)

Experiment 5: Triethylphosphine oxide + **boric acid** (5.6 mg, 0.090 mmol, 3.0 equiv)

Experiment 6: Triethylphosphine oxide + **boric acid** (5.6 mg, 0.090 mmol, 3.0 equiv) + **oxalic** (11 mg, 0.090 mmol, 3.0 equiv)

Experiment 7: Triethylphosphine oxide + **$B(C_6F_5)_3nH_2O$** (47 mg, 0.090 mmol, 3.0 equiv)

Experiment 8: Triethylphosphine oxide + **TsOH** (15 mg, 0.090 mmol, 3.0 equiv)

Experiment 9: Triethylphosphine oxide + **37% aq. HCl** (3.3 mg, 0.090 mmol, 3.0 equiv)

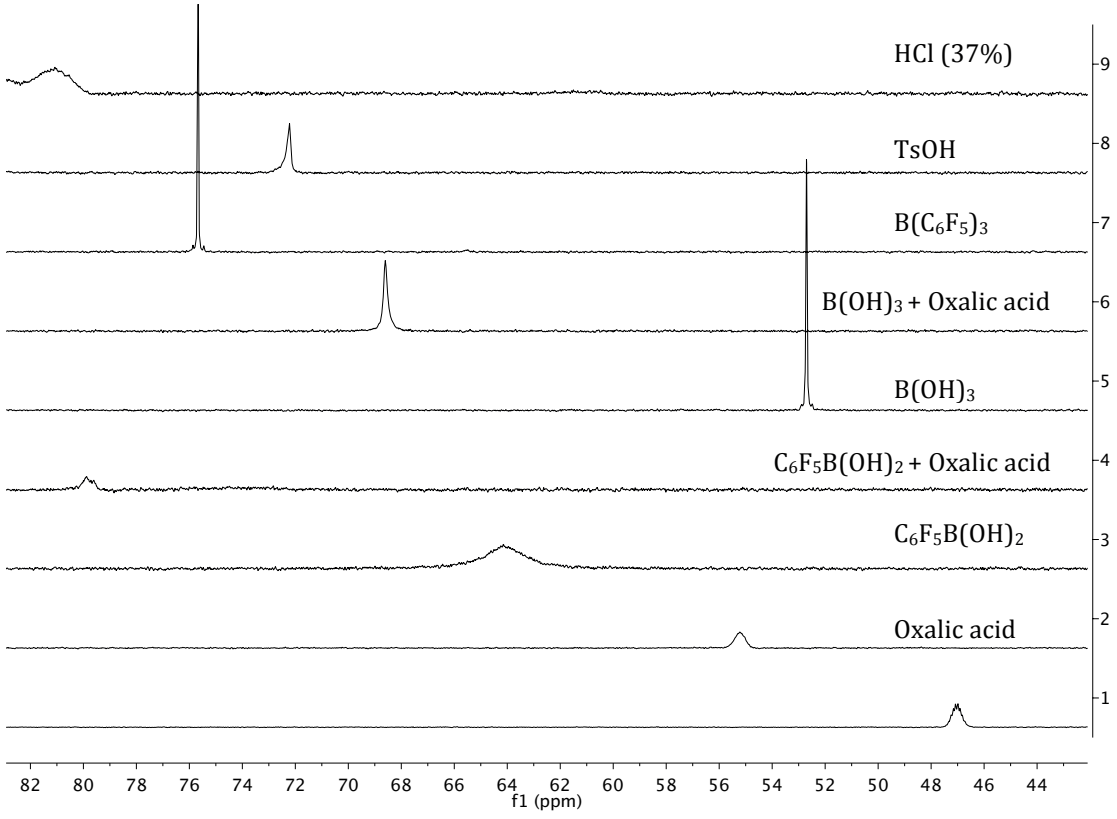

7. Substrate/nucleophile scope

General procedure A.

Pentafluorophenyl boronic acid (1.0 mol%) and oxalic acid (1.0-2.0 mol%) were dissolved in $MeNO_2$ (1 or 2M) in a 10 mL reaction tube. Nucleophile (1.02-5.0 equiv) and alcohol (1.0 equiv) were added, in that order, by syringe. The vial was capped and the mixture allowed to stir for 5 min to 1 h at 23 °C. The volatiles were removed in vacuo. The residue was purified by flash chromatography on SiO_2.

General procedure B.

Pentafluorophenyl boronic acid (1.0-5.0 mol%) and oxalic acid (2.0-5.0 mol%) were dissolved in HFIP/$MeNO_2$ (4:1, 1M) in a 10 mL reaction tube. Nucleophile (1.02-5.0 equiv) and alcohol (1.0 equiv) were added, in that order, by syringe. The vial was capped and the mixture allowed to stir for 15 min to 10 h at 23-50 °C. The volatiles were removed in vacuo. The residue was purified by flash chromatography on SiO_2.

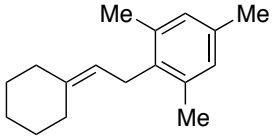

1-(2-Cyclohexylidenethyl)-2,4,6-trimethylbenzene 66a.[35a]
Synthesized according to the general procedure A after 1 h at 23 ^{o}C starting with pentafluorophenylboronic acid (2.1 mg, 0.010 mmol, 1.0 mol%) and oxalic acid (1.3 mg, 0.010 mmol, 1.0 mol%) in $MeNO_2$ (1.0 mL), mesitylene (418 μl, 360 mg, 3.00 mmol) and alcohol **54** (126 mg, 1.00 mmol). Isolated (215 mg, 60%) as a colorless liquid after column chromatography (100% Petroleum ether). R_f = 0.64 (Petroleum ether).
^{1}H NMR (400 MHz, $CDCl_3$) δ 6.92 (s, 2H), 5.03 (t, *J* = 6.8 Hz, 1H), 3.39 (d, *J* = 6.8 Hz, 2H), 2.41-2.37 (m, 2H), 2.36 (s, 6H), 2.33 (s, 3H), 2.16-2.10 (m, 2H), 1.70-1.34 (m, 6H); **^{13}C NMR** (100 MHz, $CDCl_3$) δ 139.2, 136.2, 135.5, 135.1, 128.9, 118.9, 37.2, 29.0, 28.6, 27.8, 27.6, 27.0, 20.9, 20.0. The analytical data are in accordance with those reported in the literature.

Synthesis of allylic and benzylic compounds

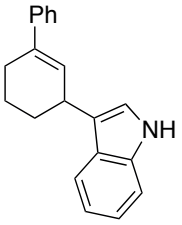

3-phenyl-2-cyclohexen-1-(*1H*)-indole 103.
Synthesized according to the general procedure A after 30 min at 23 °C starting with pentafluorophenyl boronic acid (1.1 mg, 0.0050 mmol, 1.0 mol%) and oxalic acid (1.3 mg, 0.010 mmol, 2.0 mol%) in $MeNO_2$ (0.5 mL), indole (61 mg, 0.52 mmol) and alcohol **101** (87 mg, 0.50 mmol). Isolated (135 mg, 99%) as a colorless liquid after column chromatography (10% Et_2O in petroleum ether). R_f = 0.30 (10% Et_2O in petroleum ether).
^{1}H NMR (400 MHz, $CDCl_3$) δ 7.93 (br, 1H), 7.80 (d, *J* = 7.6 Hz, 1H), 7.80 (d, *J* = 8.0 Hz, 2H), 7.54-7.48 (m, 6H), 7.04 (s, 1H), 6.43 (s, 1H), 4.04 (s, 1H), 2.64 (s, 2H), 2.31-2.14 (m, 1H), 2.09-1.85 (m, 3H); **^{13}C NMR** (100 MHz, $CDCl_3$) δ 142.5, 136.9, 136.7, 128.3, 128.0, 126.9, 126.7, 125.3, 122.0, 121.6, 120.9, 119.3, 119.2, 111.3, 95.6, 95.3, 92.2, 80.0, 79.0, 33.5, 29.9, 27.6, 21.5; **HRMS** (ESI) for $C_{20}H_{19}N$: calcd. 273.15173; found 273.15175.

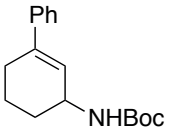

***tert*-butyl *N*-[(3-phenyl-2-cyclohexenyl]-carbamate 104.**
Synthesized according to the general procedure A after 30 min at 23 °C starting with pentafluorophenyl boronic acid (1.1 mg, 0.0050 mmol, 1.0 mol%) and oxalic acid (1.3 mg, 0.010 mmol, 2.0 mol%) in $MeNO_2$ (0.5 mL), *tert*-butylcarbamate (117 mg, 1.00 mmol) and alcohol **101** (87 mg, 0.50 mmol). Isolated (134 mg, 98%) as a colorless liquid after column chromatography (10% Et_2O in petroleum ether). R_f = 0.20 (10% Et_2O in petroleum ether).
^{1}H NMR (400 MHz, $CDCl_3$) δ 7.49-726 (m, 5H), 6.05 (s, 1H), 4.66 (d, *J* = 7.6 Hz, 1H), 4.42 (d, *J* = 5.2 Hz, 1H), 2.55-2.34 (m, 2H), 2.08-1.94 (m, 1H), 1.91-1.79 (m, 2H), 1.68-1.58 (m, 1H), 1.52 (s, 9H); **^{13}C NMR** (100 MHz, $CDCl_3$) δ 155.3, 141.5, 139.9, 128.3, 127.4, 125.3, 125.1, 46.4, 29.6, 28.5, 27.3, 20.3.

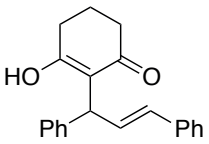

2-[(2*E*)-1,3-diphenyl-2-propen-1-yl]-3-hydroxy-2-cyclohexen-1-one 105.[211]
Synthesized according to the general procedure A after 30 min at 23 °C starting with pentafluorophenyl boronic acid (2.1 mg, 0.010 mmol, 1.0 mol%) and oxalic acid (1.3 mg, 0.010 mmol, 1.0 mol%) in $MeNO_2$ (1.0 mL), 1,3-cyclohexanedione (168 mg, 1.50 mmol) and alcohol **39** (105 mg, 0.500 mmol, 1.00 equiv). Isolated (146 mg, 96%) as a white solid after column chromatography (20 to 50% EtOAc in petroleum ether). R_f = 0.20 (50% EtOAc in petroleum ether). mp: 146-147 ºC.
^{1}H NMR (400 MHz, $CDCl_3$) δ 10.13 (br s, 1H), 7.51-7.24 (m, 10H), 7.00 (dd, *J* = 15.9, *J* = 8.3 Hz, 1H), 6.57 (d, *J* = 15.9 Hz, 1H), 5.28 (d, *J* = 8.3 Hz, 1H), 2.53-2.39 (m, 4H), 2.01-1.90 (m, 2H); **^{13}C NMR** (100 MHz, $CDCl_3$) δ 143.3, 137.7, 131.2, 131.1, 128.6, 128.2, 127.7, 127.2, 126.4, 125.9, 117.8, 42.4, 33.2, 20.7. The analytical data are in accordance with those reported in the literature.

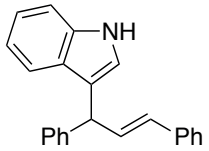

3-[(2*E*)-1,3-diphenyl-2-propen-1-yl]-(*1H*)-indole 106.[212]
Synthesized according to the general procedure A after 15 min at 23 °C starting with pentafluorophenylboronic acid (2.1 mg, 0.010 mmol, 1.0 mol%) and oxalic acid (1.3 mg, 0.010 mmol, 1.0 mol%) in $MeNO_2$ (1.0 mL), indole (258 mg, 1.10 mmol) and alcohol **39** (420 mg, 1.00 mmol). Isolated (635 mg, 99%) as a yellow oil after column chromatography (0 to 10% EtOAc in petroleum ether). R_f = 0.26 (10% EtOAc in petroleum ether).
^{1}H NMR (400 MHz, $CDCl_3$) δ 7.82 (br s, 1H), 7.66 (d, *J* = 7.8 Hz, 1H), 7.57-7.21 (m, 13H), 6.95 (d, *J* = 7.3 Hz, 1H), 6.93-6.88 (m, 1H), 6.65 (d, *J* = 15.8 Hz, 1H), 5.31 (d, *J* = 7.3 Hz, 1H); **^{13}C NMR** (100 MHz, $CDCl_3$) δ 143.6, 137.7, 136.8, 132.8, 130.7, 128.7, 128.7, 128.6, 127.4, 127.0, 126.6, 126.5, 122.9, 122.3, 120.1, 119.6, 118.7, 111.4, 46.4. The analytical data are in accordance with those reported in the literature.

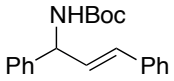

***tert*-butyl *N*-[(2E)-1,3-diphenyl-2-propen-1-yl]-carbamate 107.**[213]
Synthesized according to the general procedure A after 5 min at 23 °C starting with pentafluorophenylboronic acid (2.1 mg, 0.010 mmol, 1.0 mol%) and oxalic acid (1.3 mg, 0.010 mmol, 1.0 mol%) in $MeNO_2$ (1.0 mL), *tert*-butyl carbamate (129 mg, 1.10 mmol) and alcohol **39** (210 mg, 1.00 mmol). Isolated (295 mg, 95%) as a white solid after column

[211] R. Sanz, A. Martínez, D. Miguel, J. M. Álvarez-Gutiérrez, F. Rodríguez, *Adv. Synth. Catal.* **2006**, *348*, 1841–1845.
[212] M. Yasuda, T. Somyo, A. Baba, *Angew. Chem. Int. Ed.* **2006**, *45*, 7393–7396.
[213] Paz Trillo, Alejandro Baeza, Carmen Najera, *J. Org. Chem.* **2012**, *77*, 7344−7354.

chromatography (10% EtOAc in petroleum ether). R_f = 0.39 (10% EtOAc in petroleum ether). mp: 116-117 ºC.
^{1}H NMR (400 MHz, $CDCl_3$) δ 7.43-7.24 (m, 10H), 6.58 (dd, *J* = 15.9, *J* = 1.0 Hz, 1H), 6.36 (dd, *J* = 15.9, *J* = 6.0 Hz, 1H), 5.50 (br s, 1H), 5.03 (br s, 1H), 1.50 (s, 9H); **^{13}C NMR** (100 MHz, $CDCl_3$) δ 155.0, 141.4, 136.6, 131.0, 129.6, 128.7, 128.6, 127.7, 127.5, 127.0, 126.5, 79.8, 56.3, 28.4. The analytical data are in accordance with those reported in the literature.

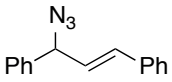

(*E*)-(3-Azidoprop-1-ene-1,3-diyl)dibenzene 108.[214]
Synthesized according to the general procedure A after 15 min at 23 °C starting with pentafluorophenylboronic acid (2.1 mg, 0.010 mmol, 1.0 mol%) and oxalic acid (1.3 mg, 0.010 mmol, 1.0 mol%) in $MeNO_2$ (1.0 mL), azidotrimethylsilane (265 μl, 230 mg, 2.00 mmol) and alcohol **39** (210 mg, 1.00 mmol). Isolated (225 mg, 96%) as a yellow liquid after column chromatography (0 to 3% EtOAc in petroleum ether). R_f = 0.25 (2% EtOAc in petroleum ether).
^{1}H NMR (400 MHz, $CDCl_3$) δ 7.51-7.31 (m, 10H), 6.79 (d, *J* = 15.7 Hz, 1H), 6.37 (dd, *J* = 15.7, *J* = 7.2 Hz, 1H), 5.27 (d, *J* = 7.2 Hz, 1H); **^{13}C NMR** (100 MHz, $CDCl_3$) δ 138.7, 136.0, 133.0, 128.9, 128.7, 128.4, 128.3, 127.2, 127.0, 126.9, 67.3. The analytical data are in accordance with those reported in the literature.

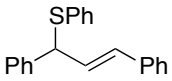

1-[(2*E*)-1,3-Diphenyl-2-propen-1-yl]phenyl sulfide 109.[215]
Synthesized according to the general procedure A after 15 min at 23 °C starting with pentafluorophenylboronic acid (2.1 mg, 0.010 mmol, 1.0 mol%) and oxalic acid (1.3 mg, 0.010 mmol, 1.0 mol%) in $MeNO_2$ (1.0 mL), thiophenol (114 μl, 122 mg, 1.10 mmol) and alcohol **39** (210 mg, 1.00 mmol). Isolated (287 mg, 95%) as a yellow liquid after column chromatography (0 to 5% EtOAc in Petroleum ether). R_f = 0.31 (3% EtOAc in petroleum ether).
^{1}H NMR (400 MHz, $CDCl_3$) δ 7.62-7.30 (m, 15H), 6.65 (dd, *J* = 15.7, *J* = 8.3 Hz, 1H), 6.47 (d, *J* = 15.7 Hz, 1H), 5.11 (d, *J* = 8.3 Hz, 1H); **^{13}C NMR** (100 MHz, $CDCl_3$) δ 140.4, 136.8, 135.0, 133.2, 131.7, 129.3, 128.9, 128.8, 128.6, 128.1, 127.8, 127.7, 127.6, 126.6, 56.8. The analytical data are in accordance with those reported in the literature.

[214] M. Rueping, C. Vila, U. Uria, *Org Lett.* **2012**, *14*, 768–771.
[215] A. B. Zaitsev, H. F. Caldwell, P. S. Pregosin, L. F. Veiros, *Chem. Eur. J.* **2009**, *15*, 6468–6477.

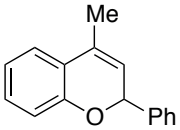

4-methyl-2-phenyl-2*H*-chromene 110.[214]
Synthesized according to the general procedure A after 45 min at 23 °C starting with pentafluorophenylboronic acid (2.1 mg, 0.010 mmol, 1.0 mol%) and oxalic acid (1.3 mg, 0.010 mmol, 1.0 mol%) in $MeNO_2$ (1.0 mL) and alcohol **102** (240 mg, 1.00 mmol). Isolated (200 mg, 90%) as a white solid after column chromatography (10 to 20% EtOAc in petroleum ether). R_f = 0.25 (10% EtOAc in petroleum ether).
^{1}H NMR (400 MHz, $CDCl_3$) δ 7.69 (d, *J* = 8.1 Hz, 2H), 7.30 (d, *J* = 8.1 Hz, 2H), 3.26-3.14 (m, 4H), 2.41 (s, 3H), 1.78-1.68 (m, 4H); **^{13}C NMR** (100 MHz, $CDCl_3$) δ 143.3, 134.0, 129.6, 127.5, 47.9, 25.2, 21.5. The analytical data are in accordance with those reported in the literature.

Synthesis of allylic compounds

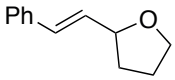

(*E*)-2-styryltetrahydrofuran 61.[216]
Synthesized according to the general procedure A after 1 h at 23 °C starting with pentafluorophenyl boronic acid (1.1 mg, 0.0050 mmol, 1.0 mol%) and oxalic acid (1.3 mg, 0.010 mmol, 1.0 mol%) in $MeNO_2$ (0.5 mL) and alcohol **60** (96 mg, 0.50 mmol). Isolated (65 mg, 75%) as a colorless oil after column chromatography (1% EtOAc in petroleum ether). R_f = 0.35 (5% EtOAc in petroleum ether).
^{1}H NMR (400 MHz, $CDCl_3$) δ 7.46-7.24 (m, 5H), 6.64 (d, *J* = 15.9 Hz, 1H), 6.25 (dd, *J* = 15.9 and 6.6 Hz, 1H), 4.56-4.48 (m, 1H), 4.05-3.98 (m, 1H), 3.93-3.85 (m, 1H), 2.22-1.92 (m, 4H); **^{13}C NMR** (100 MHz, $CDCl_3$) δ 136.9, 130.6, 130.4, 128.5, 127.5, 126.5, 79.7, 68.2, 32.4, 25.9. The analytical data are in accordance with those reported in the literature.

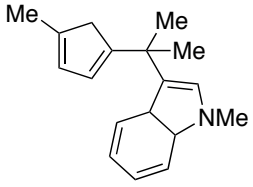

1-methyl-3-(2-(4-methylcyclopenta-1,3-dien-1-yl)propan-2-yl)-*N*-methylindole 114.
Synthesized according to the general procedure A after 30 min at 23 °C starting with pentafluorophenyl boronic acid (1.1 mg, 0.0050 mmol, 1.0 mol%) and oxalic acid (1.3 mg, 0.010 mmol, 2.0 mol%) in $MeNO_2$ (0.5 mL), *N*-methylindole (79 mg, 0.60 mmol) and alcohol **112** (87 mg, 0.50 mmol). Isolated (117 mg, 92%) as a colorless liquid after column chromatography (100% Petroleum ether). R_f = 0.64 (Petroleum ether).

[216] M.B. Hay, A.R. Hardin, J. P. Wolfe, *J. Org. Chem.* **2005**, *70*, 3099-3107.

^{1}H NMR (400 MHz, $CDCl_3$) δ 7.66 (d, *J* = 8.0 Hz, 1H), 7.41 (d, *J* = 8.0 Hz, 1H), 7.34 (t, *J* = 7.2 Hz, 1H), 7.18 (t, *J* = 7.2 Hz, 1H), 6.98 (s, 1H), 6.12 (d, *J* = 3.2 Hz, 1H), 6.04 (s, 1H), 3.84 (s, 3H), 2.39 (s, 3H), 1.94 (s, 6H); **^{13}C NMR** (100 MHz, $CDCl_3$) δ 160.9, 150.4, 137.7, 125.4, 122.2, 121.3, 118.5, 109.3, 105.7, 104.6, 36.1, 32.7, 28.7, 13.8.

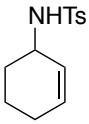

***N*-(cyclohex-2-en-1-yl)-4-methylbenzenesulfonamide 115.**
Synthesized according to the general procedure B after 30 min at 23 °C starting with pentafluorophenyl boronic acid (1.1 mg, 0.0050 mmol, 1.0 mol%) and oxalic acid (1.3 mg, 0.010 mmol, 2.0 mol%) in HFIP/$MeNO_2$ (4:1, 0.5 mL), *p*-toluenesulfonamide (89 mg, 0.52 mmol) and alcohol **111** (87 mg, 0.50 mmol). Isolated (123 mg, 98%) as a colorless liquid after column chromatography (100% petroleum ether). R_f = 0.64 (100% petroleum ether).
^{1}H NMR (400 MHz, $CDCl_3$) δ 7.82 (d, *J* = 8.4 Hz, 1H), 7.33 (d, *J* = 8.0 Hz, 1H), 5.78 (d, *J* = 10.0 Hz, 1H), 5.38 (d, *J* = 12.4 Hz, 1H), 4.96 (d, *J* = 8.4 Hz, 1H), 3.84 (br, 1H), 2.46 (s, 3H), 2.06-1.89 (m, 2H), 1.85-1.73 (m, 1H), 1.68-1.51; **^{13}C NMR** (100 MHz, $CDCl_3$) δ 143.2, 138.4, 131.4, 129.7, 127.1, 127.0, 49.0, 30.2, 24.5, 21.5, 19.3; **HRMS** (ESI) for $C_{18}H_{19}NO_2S$: calcd. 313.1137; found 313.1157.

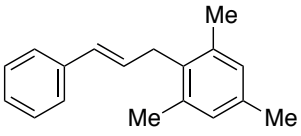

2-cinnamyl-1,3,5-trimethylbenzene 65.[217]
Synthesized according to the general procedure B after 30 min at 23 °C starting with pentafluorophenyl boronic acid (1.1 mg, 0.0050 mmol, 1.0 mol%) and oxalic acid (1.3 mg, 0.010 mmol, 2.0 mol%) in HFIP/$MeNO_2$ (4:1, 0.5 mL), mesitylene (348 μl, 300 mg, 2.50 mmol) and alcohol **63** (64 μl, 67 mg, 0.50 mmol). Isolated (109 mg, 92%) as a colorless liquid after column chromatography (100% petroleum ether). R_f = 0.64 (100% petroleum ether).
^{1}H NMR (400 MHz, $CDCl_3$) δ 7.32-7.14 (m, 5H), 6.88 (s, 2H), 6.31-6.21 (m, 2H), 2.78 (d, *J* = 4.0 Hz, 1H), 2.31 (s, 6H), 2.28 (s, 3H); **^{13}C NMR** (100 MHz, $CDCl_3$) δ 137.8, 136.7, 135.6, 133.2, 130.0, 129.0, 128.5, 127.8, 127.0, 126.1, 32.7, 21.0, 20.0. The analytical data are in accordance with those reported in the literature.

[217] M. Hofmann, N. Hampel, T. Kanzian, H. Mayr, *Angew. Chem. Int. Ed.* **2004**, *43*, 5402–5405.

Synthesis of benzylic compounds

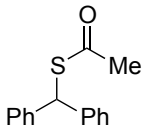

_S_-Benzhydryl-ethanethioate 68d.[218]
Synthesized according to the general procedure B after 1 h at 23 °C starting with pentafluorophenyl boronic acid (1.1 mg, 0.0050 mmol, 1.0 mol%) and oxalic acid (1.3 mg, 0.010 mmol, 2.0 mol%) in HFIP/$MeNO_2$ (4:1, 0.5 mL), thioacetic acid (107 μL, 114 mg, 1.50 mmol) and alcohol **51** (92 mg, 0.50 mmol). Isolated (88 mg, 73%) as a white solid after column chromatography (10-20% DCM in petroleum ether). R_f = 0.28 (20% DCM in petroleum ether). mp: 55-56 °C.
^{1}H NMR (400 MHZ, $CDCl_3$) δ 7.38–7.21 (m, 10H), 5.97 (s, 1H), 2.35 (s, 3H); **^{13}C NMR** (100 MHz, $CDCl_3$) δ 193.9, 141.1, 128.7, 128.5, 127.4, 52.0, 30.4. The analytical data are in accordance with those reported in the literature.

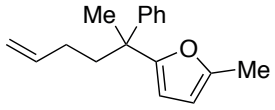

2-methyl-5-(2-phenylhex-5-en-2-yl)furan 116.
Synthesized according to the general procedure B after 1 h at 23 °C starting with pentafluorophenyl boronic acid (1.1 mg, 0.0050 mmol, 1.0 mol%) and oxalic acid (1.3 mg, 0.010 mmol, 2.0 mol%) in HFIP/$MeNO_2$ (4:1, 0.5 mL), 2-methylfuran (135 μL, 123 mg, 1.50 mmol) and alcohol **67e** (88 mg, 0.50 mmol). Isolated (110 mg, 92%) as a colorless oil after column chromatography (5% DCM in petroleum ether). R_f = 0.38 (5% DCM in petroleum ether).
^{1}H NMR (400 MHZ, $CDCl_3$) δ 7.44–7.28 (m, 5H), 6.12 (d, *J* = 2.9 Hz, 1H), 6.00 (s, 1H), 5.98-5.87 (m, 1H), 5.13-5.03 (m, 2H), 2.34 (s, 3H), 2.31-2.16 (m, 2H), 2.08-2.01 (m, 2H), 1.74 (s, 3H); **^{13}C NMR** (100 MHz, $CDCl_3$) δ 159.3, 150.8, 147.3, 139.01, 128.2, 126.5, 126.1, 114.2, 106.3, 105.6, 43.7, 39.9, 29.2, 25.3, 13.7.

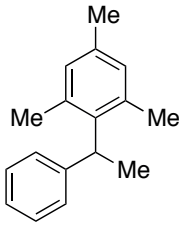

1,3,5-trimethyl-2-(1-phenylethyl)benzene 117.[219]
Synthesized according to the general procedure B after 1 h at 23 °C starting with pentafluorophenyl boronic acid (1.1 mg, 0.0050 mmol, 1.0 mol%) and oxalic acid (1.3 mg, 0.010 mmol, 2.0 mol%) in HFIP/$MeNO_2$ (4:1, 0.5 mL), mesitylene (208 μL, 180 mg, 1.50

[218] C. Liu, M.-B. Li, C.-F. Yang, S.-K. Tian, *Chem. Eur. J.* **2009**, *15*, 793–797.
[219] Y. Sawama, Y. Shishido, T. Kawajiri, R. Goto, Y. Monguchi, H. Sajiki, *Chem. Eur. J.* **2014**, *20*, 510–516.

mmol) and alcohol **48** (60 μL, 61 mg, 0.50 mmol). Isolated (89 mg, 79%) as a colorless oil after column chromatography (100% petroleum ether). R_f = 0.37 (100% petroleum ether).
^{1}H NMR (400 MHZ, $CDCl_3$) δ 7.47–7.30 (m, 5H), 7.00 (s, 2H), 4.82 (q, *J* = 14.4 Hz, *J* = 7.2 Hz, 3H), 2.43 (s, 3H), 2.29 (s, 6H), 1.83 (d, *J* = 7.2 Hz, 3H); **^{13}C NMR** (100 MHz, $CDCl_3$) δ 145.6, 140.2, 136.6, 135.5, 130.1, 128.2, 126.9, 125.4, 37.9, 21.2, 20.9, 17.0. The analytical data are in accordance with those reported in the literature.

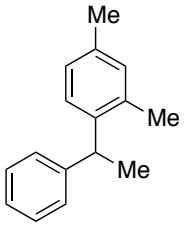

2,4-dimethyl-1-(1-phenylethyl)benzene 118.[220]
Synthesized according to the general procedure B after 1 h at 23 °C starting with pentafluorophenyl boronic acid (1.1 mg, 0.0050 mmol, 1.0 mol%) and oxalic acid (1.3 mg, 0.010 mmol, 2.0 mol%) in HFIP/$MeNO_2$ (4:1, 0.5 mL), *m*-xylene (305 μL, 265 mg, 2.50 mmol) and alcohol **48** (60 μL, 61 mg, 0.50 mmol). Isolated (82 mg, 79%) as a colorless oil after column chromatography (10% EtOAc in petroleum ether). R_f = 0.24 (10% EtOAc in petroleum ether).
^{1}H NMR (400 MHZ, $CDCl_3$) δ 7.40–7.37 (m, 2H), 7.30-7.27 (m, 4H), 7.16-7.10 (m, 2H), 4.42 (q, *J* = 16.0 Hz, *J* = 8.0 Hz, 1H), 2.44 (s, 3H), 2.34 (s, 3H), 1.75 (d, *J* = 7.2 Hz, 3H); **^{13}C NMR** (100 MHz, $CDCl_3$) δ 146.5, 141.1, 136.0, 135.5, 131.3, 128.4, 127.7, 127.2, 126.7, 125.8, 40.7, 22.2, 21.0, 19.7. The analytical data are in accordance with those reported in the literature.

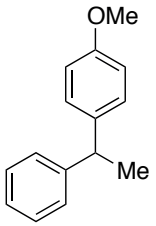

1-methoxy-4-(1-phenylethyl)benzene 119.[221]
Synthesized according to the general procedure B after 1 h at 23 °C starting with pentafluorophenyl boronic acid (1.1 mg, 0.0050 mmol, 1.0 mol%), oxalic acid (1.3 mg, 0.010 mmol, 2.0 mol%) in HFIP/$MeNO_2$ (4:1, 0.5 mL), anisole (273 μL, 270 mg, 2.50 mmol) and alcohol **48** (60 μL, 61 mg, 0.50 mmol). Isolated (85 mg, 80%) as a colorless oil after column chromatography (5% DCM in petroleum ether). R_f = 0.15 (100% petroleum ether).
^{1}H NMR (400 MHZ, $CDCl_3$) δ 7.41–7.20 (m, 7H), 6.97-6.88 (m, 2H), 4.21 (q, *J* = 14.4 Hz, *J* = 7.2 Hz, 1H), 3.86 (s, 3H), 1.71 (d, *J* = 7.2 Hz, 3H); **^{13}C NMR** (100 MHz, $CDCl_3$) δ 157.9, 146.8, 138.6, 128.6, 128.4, 127.6, 126.0, 113.8, 55.3, 44.0, 22.1. The analytical data are in accordance with those reported in the literature.

[220] C. L. Ricardo, X. Mo, J. A. McCubbin, D. G. Hall, *Chem. Eur. J.* **2015**, *21*, 4218–4223.
[221] R. Savela, M. Majewski and R. Leino, *Eur. J. Org. Chem.* **2014**, 4137–4147.

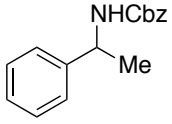

Benzyl (1-phenylethyl)carbamate 120.[222]
Synthesized according to the general procedure B after 1 h at 23 °C starting with Pentafluorophenyl boronic acid (1.1 mg, 0.0050 mmol, 1.0 mol%) and oxalic acid (1.3 mg, 0.010 mmol, 2.0 mol%) in HFIP/$MeNO_2$ (4:1, 0.5 mL), benzylcarbamate (151 mg, 1.00 mmol) and alcohol **48** (60 μL, 61 mg, 0.50 mmol). Isolated (115 mg, 90%) as a colorless oil after column chromatography (10% EtOAc in petroleum ether). R_f = 0.14 (20% Et_2O in petroleum ether).
^{1}H NMR (400 MHZ, $CDCl_3$) δ 7.51–7.22 (m, 10H), 5.21-5.11 (m, 3H), 4.96-4.93 (m, 1H), 1.54 (d, *J* = 6.4 Hz, 3H); **^{13}C NMR** (100 MHz, $CDCl_3$) δ 155.6, 143.6, 136.5, 128.7, 128.6, 128.2, 127.4, 126.0, 66.8, 50.8, 22.5. The analytical data are in accordance with those reported in the literature.

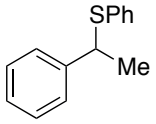

Phenyl(1-phenylethyl)sulfane 121.[223]
Synthesized according to the general procedure B after 1 h at 23 °C starting with pentafluorophenyl boronic acid (1.1 mg, 0.0050 mmol, 1.0 mol%) and oxalic acid (1.3 mg, 0.010 mmol, 2.0 mol%) in HFIP/$MeNO_2$ (4:1, 0.5 mL), thiophenol (102 μL, 110 mg, 1.0 mmol) and alcohol **48** (60 μL, 61 mg, 0.50 mmol). Isolated (99 mg, 92%) as a colorless oil after column chromatography (10% DCM in petroleum ether). R_f = 0.28 (100% petroleum ether).
^{1}H NMR (400 MHZ, $CDCl_3$) δ 7.47–7.28 (m, 10H), 4.46 (q, *J* = 14.0 Hz, *J* = 7.2 Hz, 1H), 1.75 (d, *J* = 7.0 Hz, 3H); **^{13}C NMR** (100 MHz, $CDCl_3$) δ 143.3, 135.2, 132.5, 128.8, 128.5, 127.4, 127.2, 127.2, 48.1, 22.4. The analytical data are in accordance with those reported in the literature.

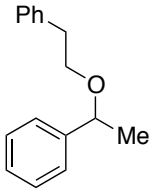

(1-phenethoxyethyl)benzene 68e.[224]
Synthesized according to the general procedure B after 1 h at 23 °C starting with pentafluorophenyl boronic acid (1.1 mg, 0.0050 mmol, 1.0 mol%) and oxalic acid (1.3 mg, 0.010 mmol, 2.0 mol%) in HFIP/$MeNO_2$ (4:1, 0.5 mL), 2-phenylethanol (180 μL, 183 mg, 1.5

[222] K. D. Collins, A. Roehling, F. Lied, F. Glorius, *Chem. Eur. J.* **2014**, *20*, 3800–3805.
[223] S. S. Badsara , Y.-C. Liu , P.-A. Hsieh, J.-W. Zeng , S.-Y. Lu , Y.-W. Liu, C.-F. Lee, *Chem. Commun.* **2014**, *50***,** 11374–11377.
[224] D. C. Rosenfeld, S. Shekhar, A. Takemiya, M. Utsunomiya, J. F. Hartwig, *Org. Lett.* **2006**, *8*, 4179–4182.

mmol) and alcohol **48** (60 μL, 61 mg, 0.50 mmol). Isolated (97 mg, 86%) as a colorless oil after column chromatography (5% DCM in petroleum ether). R_f = 0.28 (100% petroleum ether).
^{1}H NMR (400 MHZ, $CDCl_3$) δ 7.40–7.23 (m, 10H), 4.47 (q, *J* = 12.8 Hz, *J* = 6.4 Hz, 1H), 3.58 (d, *J* = 7.2 Hz, 2H), 3.01-2.88 (m, 2H), 1.50 (d, *J* = 6.5 Hz, 3H); **^{13}C NMR** (100 MHz, $CDCl_3$) δ 144.0, 139.1, 132.5, 129.0, 128.4, 128.3, 127.4, 126.1, 126.1, 78.1, 69.6, 36.6, 24.1. The analytical data are in accordance with those reported in the literature.

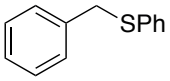

Benzyl(phenyl)sulfane 122.[225]
Synthesized according to the general procedure B after 10 h at 50 °C starting with pentafluorophenyl boronic acid (1.1 mg, 0.0050 mmol, 1.0 mol%) and oxalic acid (1.3 mg, 0.010 mmol, 2.0 mol%) in HFIP/$MeNO_2$ (4:1, 0.5 mL), thiophenol (102 μL, 110 mg, 1.0 mmol) and alcohol **115** (52 μL, 54 mg, 0.50 mmol). Isolated (74 mg, 74%) as a colorless oil after column chromatography (5% DCM in petroleum ether). R_f = 0.29 (100% petroleum ether).
^{1}H NMR (400 MHZ, $CDCl_3$) δ 7.41–7.25 (m, 10H), 4.21 (s, 2H); **^{13}C NMR** (100 MHz, $CDCl_3$) δ 137.5, 136.4, 129.9, 128.9, 128.6, 127.2, 126.4, 39.1. The analytical data are in accordance with those reported in the literature.

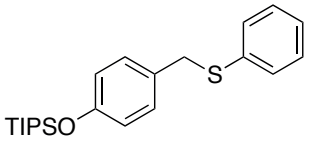

Triisopropyl(4-((phenylthio)methyl)phenoxy)silane 68a.
Synthesized according to the general procedure A after 1 h at 23 °C starting with pentafluorophenylboronic acid (1.1 mg, 0.0050 mmol, 1.0 mol%) and oxalic acid (1.3 mg, 0.010 mmol, 2.0 mol%) in $MeNO_2$ (0.5 mL), thiophenol (56 μl, 61 mg, 0.55 mmol) and TIPS protected benzylic alcohol **67a** (140 mg, 0.500 mmol). Isolated (169 mg, 91%) as a colorless oil after column chromatography (100% petroleum ether). R_f = 0.24 (100% petroleum ether).
^{1}H NMR (400 MHz, $CDCl_3$) δ 7.37-7.23 (m, 5H), 7.19 (d, *J* = 8.3 Hz, 2H), 6.87 (d, *J* = 8.3 Hz, 2H), 4.12 (s, 2H), 1.33 (m, 3H), 1.17 (d, *J* = 7.3 Hz, 18H); **^{13}C NMR** (100 MHz, $CDCl_3$) δ 155.3, 136.4, 130.2, 129.9, 129.8, 128.8, 126.4, 119.9, 38.8, 17.9, 12.7; **HRMS** (ESI) for $C_{22}H_{32}OSSi$: calcd. 372.1943; found 372.1960.

[225] J. Mao, T. Jia, G. Frensch, P. J. Walsh, *Org. Lett.* **2014**, *16*, 5304−5307.

Synthesis of tertiary aliphatic compounds

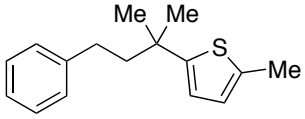

2-methyl-5-(2-methyl-4-phenylbutan-2-yl)thiophene 123.
Synthesized according to the general procedure B after 1 h at 23 °C starting with pentafluorophenyl boronic acid (5.3 mg, 0.025 mmol, 5.0 mol%) and oxalic acid (3.2 mg, 0.025 mmol, 5.0 mol%) in HFIP/$MeNO_2$ (4:1, 0.5 mL), 2-methylthiophene (145 μL, 147 mg, 1.50 mmol) and alcohol **77b** (85 μL, 82 mg, 0.50 mmol). Isolated (109 mg, 89%) as a colorless oil after column chromatography (100% petroleum ether). R_f = 0.33 (100% petroleum ether).
^{1}H NMR (400 MHZ, $CDCl_3$) δ 7.43–7.31 (m, 2H), 7.29–7.23 (m, 3H) 6.74 (d, *J* = 3.6 Hz, 1H), 6.69-6.68 (m, 1H), 2.70-2.54 (m+s, 5H), 2.04-2.00 (m, 2H), 1.52 (s, 6H); **^{13}C NMR** (100 MHz, $CDCl_3$) δ 153.2, 143.0, 137.1, 128.4, 128.4, 125.7, 124.4, 122.1, 47.8, 37.8, 31.5, 30.2, 15.4; **HRMS** (ESI) for $C_{16}H_{20}S$ + Na: calcd. 267.11780; found 267.11671.

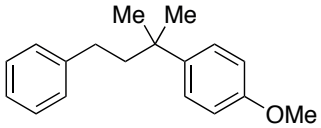

1-methoxy-4-(2-methyl-4-phenylbutan-2-yl)benzene 124.
Synthesized according to the general procedure B after 1 h at 23 °C starting with pentafluorophenyl boronic acid (5.3 mg, 0.025 mmol, 5.0 mol%) and oxalic acid (3.2 mg, 0.025 mmol, 5.0 mol%) in HFIP/$MeNO_2$ (4:1, 0.5 mL), anisole (271 μL, 270 mg, 2.50 mmol) and alcohol **77b** (85 μL, 82 mg, 0.50 mmol). Isolated (75 mg, 60%) as a colorless oil after column chromatography (100% petroleum ether). R_f = 0.26 (100% petroleum ether).
^{1}H NMR (400 MHZ, $CDCl_3$) δ 7.40–7.16 (m, 7H), 6.98-6.95 (m, 2H), 3.89 (s, 3H), 2.46-2.41 (m, 2H), 2.00-1.96 (m, 2H), 1.43 (s, 6H); **^{13}C NMR** (100 MHz, $CDCl_3$) δ 158.5, 143.8, 136.1, 128.3, 128.2, 128.2, 127.9, 127.3, 125.4, 120.4, 111.4, 55.0, 43.1, 38.4, 32.1, 28.5; **HRMS** (ESI) for $C_{18}H_{22}O$: calcd. 254.16665; found 254.16707.

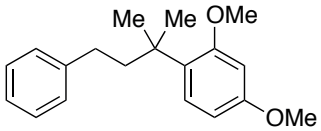

2,4-dimethoxy-1-(2-methyl-4-phenylbutan-2-yl)benzene 125.
Synthesized according to the general procedure B after 1 h at 23 °C starting with pentafluorophenyl boronic acid (5.3 mg, 0.025 mmol, 5.0 mol%) and oxalic acid (3.2 mg, 0.025 mmol, 5.0 mol%) in HFIP/$MeNO_2$ (4:1, 0.5 mL), 1,3-dimethoxybenzene (327 μL, 345 mg, 2.50 mmol) and alcohol **77b** (85 μL, 82 mg, 0.50 mmol). Isolated (68 mg, 48%) as a colorless oil after column chromatography (100% petroleum ether). R_f = 0.26 (100% petroleum ether).
^{1}H NMR (400 MHZ, $CDCl_3$) δ 7.34–7.17 (m, 6H), 6.58-6.53 (m, 2H), 3.58 (d, *J* = 7.2 Hz, 2H), 3.91 (s, 6H), 2.38-2.34 (m, 2H), 2.23-2.19 (m, 2H), 1.48 (s, 6H); **^{13}C NMR** (100 MHz, $CDCl_3$) δ 159.4, 159.2, 143.9, 128.7, 128.3, 128.2, 128.2, 125.3, 103.3, 99.5, 55.3, 55.0, 43.2, 37.9, 32.1, 28.7; **HRMS** (ESI) for $C_{19}H_{24}O_2$ + Na: calcd. 284.17815; found 284.17763.

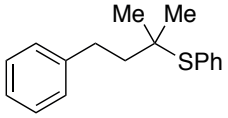

(2-methyl-4-phenylbutan-2-yl)(phenyl)sulfane 126.[226]
Synthesized according to the general procedure B after 10 min at 23 °C starting with pentafluorophenyl boronic acid (5.3 mg, 0.025 mmol, 5.0 mol%) and oxalic acid (3.2 mg, 0.025 mmol, 5.0 mol%) in HFIP/$MeNO_2$ (4:1, 0.5 mL), thiophenol (56 μL, 61 mg, 0.55 mmol) and alcohol **77b** (85 μL, 82 mg, 0.50 mmol). Isolated (127 mg, 99%) as a colorless oil after column chromatography (100% petroleum ether). R_f = 0.25 (100 % petroleum ether).
^{1}H NMR (400 MHZ, $CDCl_3$) δ 7.62 (d, *J* = 6.8 Hz, 2H), 7.44-7.31 (m, 5H), 7.28-7.23 (m, 3H), 2.91-2.87 (m, 2H), 1.88-1.81 (m, 2H), 1.37 (s, 6H); **^{13}C NMR** (100 MHz, $CDCl_3$) δ 142.3, 137.4, 132.2, 128.6, 128.4, 128.4, 128.3, 125.7, 49.1, 44.0, 31.3, 28.9. The analytical data are in accordance with those reported in the literature.

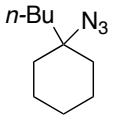

1-azido-1-butylcyclohexane 79y.
Synthesized according to the general procedure A after 1 h at 23 °C starting with pentafluorophenyl boronic acid (5.3 mg, 0.025 mmol, 5.0 mol%) and oxalic acid (3.2 mg, 0.025 mmol, 5.0 mol%) in $MeNO_2$ (0.25 mL), azidotrimethylsilane (199 μL, 173 mg, 1.50 mmol) and alcohol **77y** (78 mg, 0.50 mmol). Isolated (79 mg, 87%) as a colorless oil after column chromatography (100 % petroleum ether). R_f = 0.38 (100% petroleum ether).
^{1}H NMR (400 MHz, $CDCl_3$) δ 1.76-1.16 (m, 16H), 0.92 (t, *J* = 6.8 Hz, 3H); **^{13}C NMR** (100 MHz, $CDCl_3$) δ 64.2, 40.0, 34.7, 25.6, 25.5, 23.2, 22.3, 14.1. The analytical data are in accordance with those reported earlier in this experimental section-chapter 2.

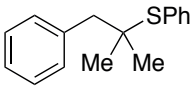

(2-methyl-1-phenylpropan-2-yl)(phenyl)sulfane 127.[227]
Synthesized according to the general procedure B after 1 h at 23 °C starting with pentafluorophenyl boronic acid (5.3 mg, 0.025 mmol, 5.0 mol%) and oxalic acid (3.2 mg, 0.025 mmol, 5.0 mol%) in HFIP/$MeNO_2$ (4:1, 0.5 mL), thiophenol (103 μL, 110 mg, 1.00 mmol) and alcohol **77a** (77 μL, 75 mg, 0.50 mmol). Isolated (108 mg, 89%) as a white solid after column chromatography (100% petroleum ether). R_f = 0.11 (100 % petroleum ether). mp: 60 °C.
^{1}H NMR (400 MHZ, $CDCl_3$) δ 7.69–7.67 (m, 2H), 7.50-7.26 (m, 8H), 3.00 (s, 2H), 1.31 (m, 6H); **^{13}C NMR** (100 MHz, $CDCl_3$) δ 137.8, 137.7, 132.1, 130.8, 128.7, 128.6, 127.9, 126.5, 49.3, 49.0, 28.1. The analytical data are in accordance with those reported in the literature.

[226] Y. Nishimoto, A. Okita, M. Yasuda, A. Baba, *Org. Lett.* **2012**, *14*, 1846–1849.
[227] D. Babin, J. D. Fourneron, L. M. Harwood, M. Julia, *Tetrahedron* **1981**, *37*, 325–332.

EXPERIMENTAL SECTION – CHAPTER 4

---

1. Material and methods

All reactions reactions were performed in 10 mL sealed tubes under an air atmosphere, unless otherwise noted. Purification of reaction products was carried out by flash column chromatography using Merck silica gel (40-63 μm). Analytical thin layer chromatography (TLC) was performed on aluminum sheets pre-coated with silica gel 60 F254 (E. Merck), cut to size. Visualization was accomplished with UV light followed by dipping in a potassium permanganate, *p*-anisaldehyde and/or Seebach's staining solutions and heating.
^{1}H NMR spectra were recorded on a Bruker Avance400 (400 MHz) spectrometer at ambient temperature unless otherwise noted and are reported in ppm using solvent as the internal standard ($CDCl_3$ at 7.26 ppm). Data are reported as: multiplicity (ap = apparent, br = broad, s = singlet, d = doublet, t = triplet, q = quartet, m = multiplet), integration and coupling constant(s) in Hz. ^{13}C NMR spectra were recorded on a Bruker Avance400 (100 MHz) spectrometer. Chemical shifts are reported in ppm from tetramethylsilane, with the residual solvent resonance employed as the internal standard ($CDCl_3$ at 77.0 ppm).
Unless otherwise noted, all commercial materials were purchased from *Sigma-Aldrich* and used without further purification. 8-Aminoquinoline was purchased from *Combi-Blocks*. 1,4-Dioxane refers to >99.5 (GC grade) stored over molecular sieves (product number 42510-250mL) also purchased from *Sigma-Aldrich.*

2. Directed Benzamide C-H Arylation

General procedure for Step 1 (4 metals, 9 ligands, 3 solvents, 3 bases, 324 possible combinations)

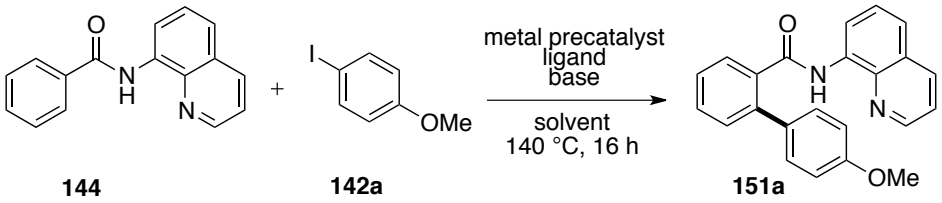

144 **142a** **151a**

To an oven dried 10 mL screw-top vial equipped with a magnetic stirrer bar was added benzamide **144** (25 mg, 0.1 mmol), 4-iodoanisole **142a** (47 mg, 0.2 mmol), base (0.5 mmol), $Ni(acac)_2$ (2.6 mg, 10 mol%), $Fe(acac)_3$ (3.5 mg, 10 mol%), $CoCl_2$ (1.3 mg, 10 mol%),

$Cu(OAc)_2$ (1.8 mg, 10 mol%), benzoic acid (0.6 mg, 5 mol%), PivOH (0.5 mg, 5 mol%), 2,6-dimethoxybenzoic acid (0.9 mg, 5 mol%), 2,4,6-trimethylbenzoic acid (0.8 mg, 5 mol%), PPh_3 (1.3 mg, 5 mol%), PCy_3 (1.4 mg, 5 mol%), xantphos (2.9 mg, 5 mol%), dppf (2.7 mg, 5 mol%), and dppp (2.2 mg, 5 mol%). Solvent (2.5 mL) was then introduced by syringe, the vial sealed and stirred for 10 min at room temperature to allow for complete dissolution. The vial was then transferred to a heating block at 140 °C and stirred rapidly (1200 rpm) at this temperature for 16 h. The reaction was monitored by TLC analysis (20% EtOAc in petroleum ether). After allowing to cool, the crude reaction mixture was filtered through a celite plug, the filter cake washed with DCM and the crude reaction mixture concentrated *in vacuo*. The conversion of the best reaction was calculated as approximately 10% from the crude ^{1}H NMR spectrum.

Step 1	1,4-dioxane	toluene	DMF
NaO^tBu	<5%	<1%	<1%
Na_2CO_3	10%	<5%	<1%
CsF	<1%	<1%	<1%

General Procedure for Step 2a

To an oven dried 10 mL screw-top vial equipped with a magnetic stirrer bar was added benzamide **144** (25 mg, 0.1 mmol), 4-iodoanisole **142a** (47 mg, 0.2 mmol), Na_2CO_3 (53 mg, 0.5 mmol), metal salt (10 mol%), benzoic acid (0.6 mg, 5 mol%), PivOH (0.5 mg, 5 mol%), 2,6-dimethoxybenzoic acid (0.9 mg, 5 mol%), 2,4,6-trimethylbenzoic acid (0.8 mg, 5 mol%), PPh_3 (1.3 mg, 5 mol%), PCy_3 (1.4 mg, 5 mol%), xantphos (2.9 mg, 5 mol%), dppf (2.7 mg, 5 mol%), and dppp (2.2 mg, 5 mol%). 1,4-dioxane (1.0 mL) was then introduced by syringe, the vial sealed and stirred for 10 min at room temperature to allow for complete dissolution. The vial was then transferred to a heating block at 140 °C and stirred rapidly (1200 rpm) at this temperature for 16 h. The reaction was monitored by TLC analysis (20% EtOAc in petroleum ether). After allowing to cool, the crude reaction mixture was filtered through a celite plug, the filter cake washed with DCM and the crude reaction mixture concentrated *in vacuo*. The conversion of the best reaction was calculated as approximately 11% from the crude ^{1}H NMR spectrum.

Step 2a	**Conversion**
$Ni(acac)_2$	11%
$CoCl_2$	<1%
$Cu(OAc)_2$	<1%
$Fe(acac)_3$	<1%

General Procedure for Step 2b

To an oven dried 10 mL screw-top vial equipped with a magnetic stirrer bar was added benzamide **144** (25 mg, 0.1 mmol), 4-iodoanisole **142a** (47 mg, 0.2 mmol), Na_2CO_3 (53 mg, 0.5 mmol), $NiCl_2$•dme (10 mol%) or $Ni(acac)_2$ (10 mol%), PCy_3 (1.4 mg, 5 mol%), dppf (2.7 mg, 5 mol%), MesCOOH (0.8 mg, 5 mol%), or PivOH (0.5 mg, 5 mol%), dppp (2.2 mg, 5 mol%), 2,6-dimethoxybenzoic acid (0.9 mg, 5 mol%), or benzoic acid (0.6 mg, 5 mol%), PPh_3 (1.3 mg, 5 mol%) and xantphos (2.9 mg, 5 mol%). 1,4-dioxane (2.5 mL) was then introduced by syringe, the vial sealed and stirred for 10 min at room temperature to allow for complete dissolution. The vial was then transferred to a heating block at 140 °C and stirred rapidly (1200 rpm) at this temperature for 16 h. The reaction was monitored by TLC analysis (20% EtOAc in petroleum ether). After allowing to cool, the crude reaction mixture was filtered through a celite plug, the filter cake washed with DCM and the crude reaction mixture concentrated *in vacuo*. The conversion of the best reaction was calculated as approximately 64% from the crude ^{1}H NMR spectrum.

Step 2b	$Ni(acac)_2$	$NiCl_2$·dme
PCy_3, dppf, MesCOOH	32%	64%
PivOH, dppp, 2,6-DMBA	18%	47%
BzOH, PPh_3, xantphos	21%	48%

General Procedure for Step 2c

To an oven dried 10 mL screw-top vial equipped with a magnetic stirrer bar was added benzamide **144** (25 mg, 0.1 mmol), 4-iodoanisole **142a** (47 mg, 0.2 mmol), Na_2CO_3 (53 mg, 0.5 mmol), $NiCl_2$•dme (2.2 mg, 10 mol%) and PCy_3 (10 or 20 mol%) or dppf (10 or 20 mol%) or MesCOOH (10 or 20 mol%). 1,4-dioxane (2.5 mL) was then introduced by syringe, the vial sealed and stirred for 10 min at room temperature to allow for complete dissolution. The vial was then transferred to a heating block at 140 °C and stirred rapidly (1200 rpm) at this temperature for 16 h. The reaction progress was monitored by TLC analysis (20% EtOAc in petrol). After allowing to cool, the crude reaction mixture was filtered through a celite plug, the filter cake washed with DCM and the crude reaction mixture concentrated *in vacuo*. The conversion of the best reaction was calculated as approximately 67% from the crude ^{1}H NMR spectrum.

Step 2c	M (10 mol%)/ L (10 mol%)	M (10 mol%)/ L (20 mol%)
$NiCl_2$·dme/PCy_3	33%	40%
$NiCl_2$·dme/dppf	13%	29%
$NiCl_2$·dme/MesCOOH	53%	67%

Optimized Reaction Conditions – General Procedure A

To an oven dried 10 mL screw-top vial equipped with a magnetic stirrer bar was added benzamide **144** (50 mg, 0.20 mmol), 4-iodoanisole **142a** (94 mg, 0.2 mmol), Na_2CO_3 (106 mg, 1.00 mmol), $NiCl_2$•dme (6.6 mg, 0.030 mmol) and MesCOOH (9.9 mg, 0.060 mmol). 1,4-dioxane (1.0 mL) was then introduced by syringe, the vial sealed and stirred for 10 min at room temperature to allow for complete dissolution. The vial was then transferred to a heating block at 140 °C and stirred rapidly (1200 rpm) at this temperature for 24 h. The reaction was monitored by TLC analysis (20% EtOAc in petroleum ether). After allowing to cool, the crude reaction mixture was filtered through a celite plug, the filter cake washed with DCM and the crude reaction mixture concentrated *in vacuo* directly onto silica gel. The arylated benzamides (**151a-151d**) were then purified by flash column chromatography over silica with the eluent systems stated and the conversions of arylated benzamides (**151e-151g**) were approximately calculated from the crude ^{1}H NMR spectrum.

Products

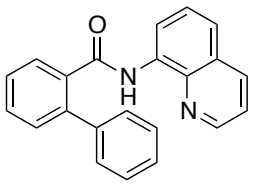

_N_-(Quinolin-8-yl)benzamide 144.[139]

To a stirred solution of 8-aminoquinoline (3.00 g, 21.0 mmol, 1.05 equiv) in DCM (20 mL) was added DMAP (80.0 mg, 0.65 mmol, 0.03 equiv) followed by Et_3N (3.30 mL, 24.0 mmol, 1.2 equiv). The reaction mixture was cooled to 0 °C and benzoyl chloride (2.30 mL, 20 mmol, 1 equiv) was added dropwise. The reaction mixture was stirred for 16 h allowing to warm to rt. After such time, the reaction was quenched with saturated aqueous $NaHCO_3$ (10 mL) and stirred rapidly for 10 min. The organic layer was separated, diluted with DCM (20 mL) and washed with 1M HCl (20 mL) followed by brine (20 mL). The organic layers were dried over Na_2SO_4, filtered and concentrated *in vacuo* prior to purification by flash column chromatography over silica (20% EtOAc in petroleum ether) to yield benzamide **144** as a white solid (3.25 g, 65%).

^{1}H NMR (400 MHz, $CDCl_3$) δ 10.76 (br s, 1H), 8.95 (dd, J = 7.5 Hz, J = 1.5 Hz, 1H), 8.86 (dd, J = 4.2 Hz, J = 1.7 Hz, 1H), 8.20 (dd, J = 8.3 Hz, J = 1.7 Hz, 1H), 8.11-8.08 (m, 2H), 7.63-7.54 (m, 5H), 7.49 (dd, J = 8.3 Hz, J = 4.2 Hz, 1H). The analytical data are in accordance with those reported in the literature.

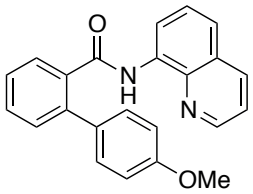

4'-Methoxy-*N*-(quinolin-8-yl)-[1,1'-biphenyl]-2-carboxamide 151a.

Synthesized according to the general procedure A after 24 h at 140 ^{o}C starting with benzamide **144** and 4-iodoanisole **142a**. Isolated (46 mg, 65%) as a white solid after column chromatography (0-20% EtOAc in petroleum ether). mp 113-114 °C; ν_{max} cm^{-1} (ATR) 3337, 1668; **^{1}H NMR** (400 MHz, $CDCl_3$) δ 9.81 (br s, 1H), 8.82 (dd, *J* = 7.5 Hz, *J* = 1.0 Hz, 1H), 8.54 (dd, *J* = 4.2 Hz, *J* = 1.6 Hz, 1H), 8.09 (dd, *J* = 8.3 Hz, *J* = 1.4 Hz, 1H), 7.90 (dd, *J* = 7.9 Hz, *J* = 1.2 Hz, 1H), 7.57-7.51 (m, 2H), 7.48-7.43 (m, 5H), 7.36 (dd, *J* = 8.3 Hz, *J* = 4.2 Hz, 1H), 6.82 (d, *J* = 8.7 Hz, 2H), 3.66 (s, 3H); **^{13}C NMR** (100 MHz, $CDCl_3$) δ 168.0, 159.4, 147.7, 139.9, 138.5, 136.0, 136.0, 134.7, 132.4, 130.6, 130.5, 130.2, 129.3, 127.8, 127.3, 127.2, 121.5, 121.4, 116.3, 114.0, 55.2; **HRMS** (ESI) for $C_{23}H_{18}O_2N_2$: calcd. 354.1368; found 354.1372.

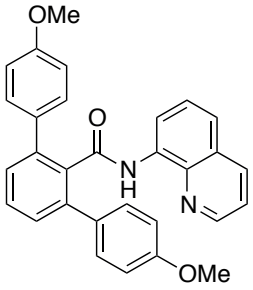

4,4''-Dimethoxy-*N*-(quinolin-8-yl)-[1,1':3',1''-terphenyl]-2'-carboxamide 151b.

Synthesized according to the general procedure A after 24 h at 140 ^{o}C starting with benzamide **144** and 4-iodoanisole **142a**. Isolated as a byproduct (trace, <5%) as a white solid after column chromatography (0-20% EtOAc in petroleum ether). mp 189-190 °C; ν_{max} cm^{-1} (ATR) 3321,1672; **^{1}H NMR** (400 MHz, $CDCl_3$) δ 9.62 (br s, 1H), 8.59-8.55 (m, 2H), 8.06 (dd, *J* = 8.3 Hz, *J* = 1.4 Hz, 1H), 7.54-7.40 (m, 9H), 7.35 (dd, *J* = 8.2 Hz, *J* = 4.2 Hz, 1H), 6.78 (d, *J* = 8.7 Hz, 4H), 3.67 (s, 6H); **^{13}C NMR** (100 MHz, $CDCl_3$) δ 167.9, 159.0, 147.8, 140.2, 138.4, 136.1, 136.0, 134.4, 132.9, 129.8, 129.2, 129.1, 127.7, 127.2, 121.4, 121.3, 116.5, 113.7, 55.1; **HRMS** (ESI) for $C_{30}H_{24}O_3N_2$: calcd. 460.1787; found 460.1799.

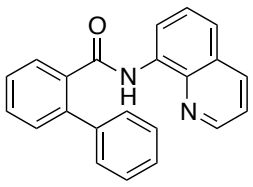

***N*-(Quinolin-8-yl)-[1,1'-biphenyl]-2-carboxamide 151c.**

Synthesized according to the general procedure A after 24 h at 140 ^{o}C starting with benzamide **144** and iodobenzene **142c**. Isolated (49 mg, 75%) as a white solid after column

chromatography (0-10% EtOAc in petroleum ether). mp 117-118 °C; ν_{max} cm^{-1} (ATR) 3321, 1661; **^{1}H NMR** (400 MHz, $CDCl_3$) δ 9.78 (br s, 1H), 8.81 (d, *J* = 7.5 Hz, 1H), 8.53 (dd, *J* = 4.1 Hz, *J* = 1.4 Hz, 1H), 8.08 (dd, *J* = 8.3 Hz, *J* = 1.4 Hz, 1H), 7.91 (d, *J* = 7.8 Hz, 1H), 7.59-7.45 (m, 8H), 7.35 (dd, *J* = 8.3 Hz, *J* = 4.2 Hz, 1H), 7.30-7.26 (m, 1H), 7.16 (t, *J* = 7.4 Hz, 1H); **^{13}C NMR** (100 MHz, $CDCl_3$) δ 167.8, 147.8, 140.3, 140.1, 138.4, 136.2, 136.0, 134.6, 130.7, 130.5, 129.2, 129.0, 128.4, 127.7, 127.6, 127.6, 127.3, 121.5, 121.4, 116.3; **HRMS** (ESI) for $C_{22}H_{16}ON_2$: calcd. 248.0950; found 248.0951.

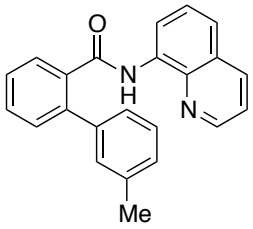

3'-Methyl-*N*-(quinolin-8-yl)-[1,1'-biphenyl]-2-carboxamide 151d.
Synthesized according to the general procedure A after 24 h at 140 °C starting with benzamide **144** and 3-iodotoluene **142d**. Isolated (44 mg, 65%) as a white solid after column chromatography (0-10% EtOAc in petroleum ether). mp 92-93 °C; ν_{max} cm^{-1} (ATR) 3331, 1661; **^{1}H NMR** (400 MHz, $CDCl_3$) δ 9.77 (br s, 1H), 8.81 (d, *J* = 7.5 Hz, 1H), 8.54 (dd, *J* = 4.1 Hz, *J* = 1.3 Hz, 1H), 8.08 (dd, *J* = 8.2 Hz, *J* = 1.1 Hz, 1H), 7.90 (d, *J* = 7.5 Hz, 1H), 7.58-7.45 (m, 5H), 7.37-7.34 (m, 2H), 7.29 (d, *J* = 7.6 Hz, 1H), 7.13 (t, *J* = 7.6 Hz, 1H), 6.96 (d, *J* = 7.3 Hz, 1H), 2.25 (s, 3H); **^{13}C NMR** (100 MHz, $CDCl_3$) δ 167.9, 147.7, 140.5, 140.0, 138.5, 138.0, 136.2, 136.0, 134.7, 130.6, 130.5, 129.7, 129.2, 128.3, 128.2, 127.7, 127.5, 127.3, 126.1, 121.5, 121.4, 116.3, 21.4; **HRMS** (ESI) for $C_{23}H_{18}O_2N_2$: calcd. 248.0950; found 248.0950.

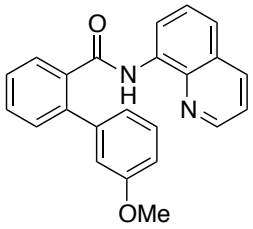

3'-Methoxy-*N*-(quinolin-8-yl)-[1,1'-biphenyl]-2-carboxamide 151e.
Synthesized according to the general procedure A after 24 h at 140 °C starting with benzamide **144** and 3-iodoanisole **151e**. Isolated (42 mg, 59%) as a white solid after column chromatography (0-20% EtOAc in petroleum ether). mp 111-112 °C; ν_{max} cm^{-1} (ATR) 3323, 1661; **^{1}H NMR** (400 MHz, $CDCl_3$) δ 9.79 (br s, 1H), 8.82 (d, *J* = 7.4 Hz, 1H), 8.54 (dd, *J* = 4.0 Hz, *J* = 0.9 Hz, 1H), 8.08 (d, *J* = 8.2 Hz, 1H), 7.91 (d, *J* = 7.3 Hz, 1H), 7.58-7.34 (m, 5H), 7.36 (dd, *J* = 8.2 Hz, *J* = 4.2 Hz, 1H), 7.16 (t, *J* = 8.0 Hz, 1H), 7.09 (br s, 2H), 6.70 (d, *J* = 7.3 Hz, 1H), 3.70 (s, 3H); **^{13}C NMR** (100 MHz, CD_3CN) δ 167.5, 159.8, 148.5, 141.5, 139.8, 138.1, 136.3, 136.2, 134.6, 130.6, 130.5, 129.5, 128.7, 127.8, 127.0, 122.0, 121.8, 121.2, 115.5, 114.3, 113.3, 54.9 (*only 22 ^{13}C signals are observed*); **HRMS** (ESI) for $C_{23}H_{18}O_2N_2$: calcd. 354.1368; found 354.1374.

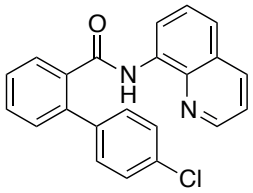

4'-chloro-*N*-(quinolin-8-yl)-[1,1'-biphenyl]-2-carboxamide 151f.
Synthesized according to the general procedure A after 24 h at 140 °C starting with benzamide **144** and 4-chloroanisole **142f**. The conversion and the ratio of mono:bis arylation were calculated as approximately 70% and 10:1 from the crude ^{1}H NMR spectrum.

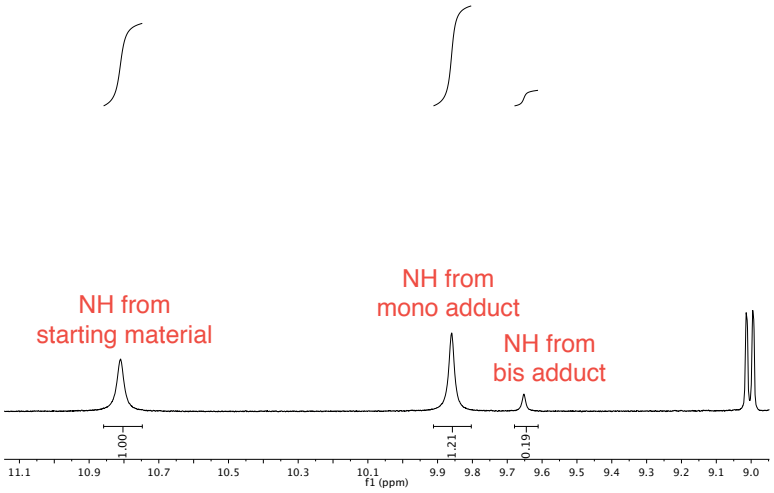

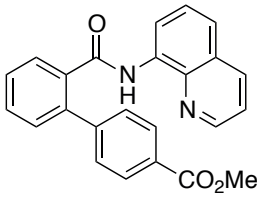

Methyl 2'-(quinolin-8-ylcarbamoyl)-[1,1'-biphenyl]-4-carboxylate 151g.
Synthesized according to the general procedure A after 24 h at 140 °C starting with benzamide **144** and methyl 4-iodobenzoate **142g**. The conversion and the ratio of mono:bis arylation were calculated as approximately 54% and >10:1 from the crude ^{1}H NMR spectrum.

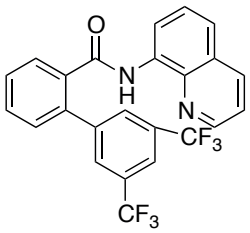

***N*-(quinolin-8-yl)-3',5'-bis(trifluoromethyl)-[1,1'-biphenyl]-2-carboxamide 151h.**
Synthesized according to the general procedure A after 24 h at 140 ^{o}C starting with benzamide **144** and 1-iodo-3,5-bis(trifluoromethyl)benzene **151h**. The conversion and the ratio of mono:bis arylation were calculated as approximately 60% and 2:1 from the crude ^{1}H NMR spectrum.

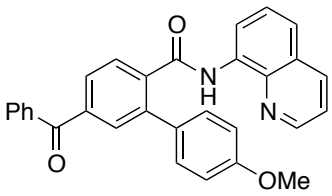

5-benzoyl-4'-methoxy-*N*-(quinolin-8-yl)-[1,1'-biphenyl]-2-carboxamide 154.
Synthesized according to the general procedure A after 24 h at 140 ^{o}C starting with benzamide **153** and 4-iodoanisole **142a**. The conversion and the ratio of mono:bis arylation were calculated as approximately 78% and 10:1 from the crude ^{1}H NMR spectrum.

3. Indole C3-alkylation

General procedure for Step 1 **(5 metals, 9 ligands, 3 solvents, 5 bases, 675 possible combinations)**

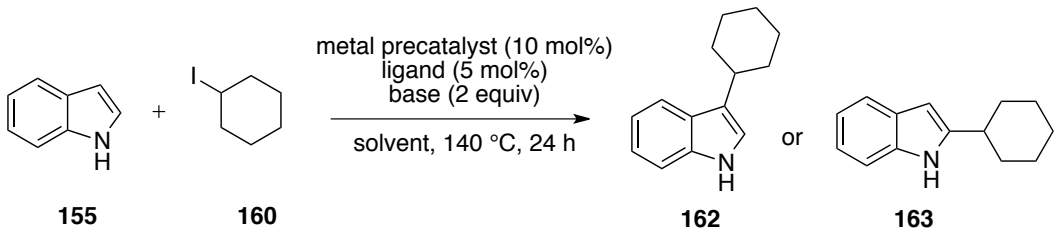

155 **160** **162** **163**

To an oven dried 10 mL screw-top vial equipped with a magnetic stirrer bar was added indole **155** (12 mg, 0.1 mmol), iodoclyclohexane **160** (26 μL, 42 mg, 0.2 mmol), base (0.5 mmol), $NiCl_2$•dme (2.6 mg, 10 mol%), $Pd(OAc)_2$ (2.2 mg, 10 mol%), $[Ir(OMe)(cod)]_2$ (6.6 mg, 10 mol%),, $Fe(acac)_3$ (3.5 mg, 10 mol%), $Rh(PPh_3)Cl_2$ (9.3 mg, 10 mol%), PCy_3 (1.4 mg, 5 mol%), dppf (2.7 mg, 5 mol%), PPh_3 (1.3 mg, 5 mol%), xantphos (2.9 mg, 5 mol%), MesCOOH (0.8 mg, 5 mol%), PivOH (0.5 mg, 5 mol%), 1,10-Phenanthroline (1.8 mg, 5 mol%), dppp (2.2 mg, 5 mol%) and BBBPY (2.7 mg, 5 mol%). Solvent (1.0 mL) was then introduced by syringe, the vial sealed and stirred for 24 h at 140 °C. The reaction was monitored by TLC analysis (20% EtOAc in petroleum ether). After allowing to cool, the crude reaction mixture was filtered through a celite plug, the filter cake washed with DCM

and the crude reaction mixture concentrated *in vacuo*. Dodecane (1 equiv) was added as the internal standard. The yield of compound **162** was calculated from the crude GC-MS sample compared to internal standard.

Step 1	1,4-dioxane	toluene	*o*-xylene
AgOAc	3%	3%	5%
KOAc	<1%	<1%	<1%
LiO^{t}Bu	<1%	<1%	<1%
K_2CO_3	<1%	<1%	<1%
CsF	<1%	<1%	<1%

General Procedure for Step 2a

To an oven dried 10 mL screw-top vial equipped with a magnetic stirrer bar was added indole **155** (12 mg, 0.1 mmol), iodoclyclohexane **160** (26 μL, 42 mg, 0.2 mmol), AgOAc (33 mg, 0.2 mmol), metal (10 mol%), PCy_3 (1.4 mg, 5 mol%), dppf (2.7 mg, 5 mol%), PPh_3 (1.3 mg, 5 mol%), xantphos (2.9 mg, 5 mol%), MesCOOH (0.8 mg, 5 mol%), PivOH (0.5 mg, 5 mol%), 1,10-Phenanthroline (1.8 mg, 5 mol%), dppp (2.2 mg, 5 mol%) and BBBPY (2.7 mg, 5 mol%). *O*-xylene (1.0 mL) was then introduced by syringe, the vial sealed and stirred for 24 h at 140 °C. The reaction was monitored by TLC analysis (20% EtOAc in petroleum ether). After allowing to cool, the crude reaction mixture was filtered through a celite plug, the filter cake washed with DCM and the crude reaction mixture concentrated *in vacuo*. Dodecane (1 equiv) was added as the internal standard. The yield of compound **162** was calculated from the crude GC-MS sample compared to internal standard.

Step 2a	**Conversion**
$NiCl_2 \cdot dme$	<1%
$Pd(OAc)_2$	5%
Ir salt	<1%
$Fe(acac)_3$	<1%
Rh salt	<1%

General Procedure for Step 2b

To an oven dried 10 mL screw-top vial equipped with a magnetic stirrer bar was added indole **155** (12 mg, 0.1 mmol), iodoclyclohexane **160** (26 μL, 42 mg, 0.2 mmol), AgOAc (33 mg, 0.2 mmol), $[PdCl(C_3H_5)]_2$ (3.7 mg, 10 mol%), $PdCl_2$ (1.8 mg, 10 mol%) or $Pd(OAc)_2$ (2.2 mg, 10 mol%) and xantphos (2.9 mg, 5 mol%), BBBPY (2.7 mg, 5 mol%) and MesCOOH (0.8 mg, 5 mol%), or PivOH (0.5 mg, 5 mol%), dppf (2.7 mg, 5 mol%) and PCy_3 (1.4 mg, 5 mol%) or 1,10-Phenanthroline (1.8 mg, 5 mol%), PPh_3 (1.3 mg, 5 mol%) and dppp (2.2 mg, 5 mol%).

O-xylene (1.0 mL) was then introduced by syringe, the vial sealed and stirred for 24 h at 140 °C. The reaction was monitored by TLC analysis (20% EtOAc in petroleum ether). After allowing to cool, the crude reaction mixture was filtered through a celite plug, the filter cake washed with DCM and the crude reaction mixture concentrated *in vacuo*. Dodecane (1 equiv) was added as the internal standard. The yield of compound **162** was calculated from the crude GC-MS sample compared to internal standard.

Step 2b	$[PdCl(C_3H_5)]_2$	$PdCl_2$	$Pd(OAc)_2$
Xantphos, BBBPY, MesCOOH	2%	<1%	5%
PivOH, dppf, PCy_3	2%	<1%	<1%
1,10-Phen, PPh_3, dppp	<1%	<1%	<1%

General Procedure for Step 2c

To an oven dried 10 mL screw-top vial equipped with a magnetic stirrer bar was added indole **155** (12 mg, 0.1 mmol), iodoclyclohexane **160** (26 μL, 42 mg, 0.2 mmol), AgOAc (33 mg, 0.2 mmol), $Pd(OAc)_2$ (2.2 mg, 10 mol%) and xantphos (5.8 mg, 10 mol%) or BBBPY (5.4 mg, 10 mol%) or MesCOOH (1.6 mg, 10 mol%). *O*-xylene (1.0 mL) was then introduced by syringe, the vial sealed and stirred for 24 h at 140 °C. The reaction was monitored by TLC analysis (20% EtOAc in petroleum ether). After allowing to cool, the crude reaction mixture was filtered through a celite plug, the filter cake washed with DCM and the crude reaction mixture concentrated *in vacuo*. Dodecane (1 equiv) was added as the internal standard. The yield of compound **162** was calculated from the crude GC-MS sample compared to internal standard.

Step 2c	$Pd(OAc)_2$
Xantphos	<1%
BBBPY	<1%
MesCOOH	14%

Optimization process

To an oven dried 10 mL screw-top vial equipped with a magnetic stirrer bar was added indole **155** (12 mg, 0.1 mmol), iodoclyclohexane **160** (26 μL, 42 mg, 0.2 mmol), base (0.2 mmol), pre-catalyst (10 mol%) and ligand (10 mol%). *O*-xylene (1.0 mL) was then introduced by syringe, the vial sealed and stirred for 24 h at room temperature or 140 °C. The reaction was monitored by TLC analysis (20% EtOAc in petroleum ether). After allowing to cool, the crude reaction mixture was filtered through a celite plug, the filter cake washed with DCM and the crude reaction mixture concentrated *in vacuo*. Dodecane (1 equiv) was added as the internal standard. The yield of compound **162** was calculated from the crude GC-MS sample compared to internal standard.

Entry	Pre-catalyst	Ligand	Base (2 equiv)	Solvent	T °C	Yield
1	$Pd(OAc)_2$ (20 mol%)	MesCOOH (40 mol%)	AgOAc	*o*-xylene	140 °C	13%
2	$Pd(OAc)_2$	-	-	*o*-xylene	140 °C	8%
3	-	MesCOOH	-	*o*-xylene	140 °C	<1%
4	-	-	AgOAc	*o*-xylene	140 °C	5%
5	$Pd(OAc)_2$	-	AgOAc	*o*-xylene	140 °C	13%
6	$Pd(OAc)_2$	-	AgOAc	*o*-xylene	23 °C	14%
7	$Pd(OAc)_2$	-	-	*o*-xylene	23 °C	<1%
8	-	-	AgOAc	*o*-xylene	23 °C	17%
9	-	-	$AgBF_4$	*o*-xylene	23 °C	<1%
10	-	-	AgTFA	*o*-xylene	23 °C	13
11	-	-	AgOTf	*o*-xylene	23 °C	<1%
12	-	-	$AgClO_4$	*o*-xylene	23 °C	<1%
13	-	-	AgI	*o*-xylene	23 °C	<1%
14	-	-	Ag_2CO_3	*o*-xylene	23 °C	18

Product

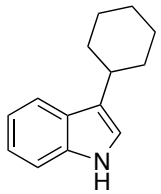

3-cyclohexyl-1*H*-indole 162.[228]
Synthesized according to the general procedure after 24 h at 140 °C starting with indole **155** and iodocyclohexane **160**. Isolated (1 mg, 5%) as a slight brown solid after column chromatography (5% EtOAc in petroleum ether). R_f = 0.32 (0.1% EtOAc in petroleum ether). mp: 74 °C.
^{1}H NMR (400 MHz, $CDCl_3$) δ 7.88 (br s, 1H), 7.67 (d, *J* = 8.0 Hz, 1H), 7.35 (d, *J* = 8.0 Hz, 1H), 7.17 (t, *J* = 7.4 Hz, 1H), 7.10 (t, *J* = 7.4 Hz, 1H), 6.95 (m, 1H), 2.85 (m, 1H), 2.12-2.10 (m, 2H), 1.84-1.76 (m, 3H), 1.52-1.41 (m, 4H), 1.33-1.26 (m, 1H); **^{13}C NMR** (100 MHz, $CDCl_3$) δ 136.3, 126.8, 123.2, 121.8, 119.3, 119.3, 118.9, 111.1, 35.4, 34.1, 26.9, 26.5. The analytical data are in accordance with those reported in the literature.

[228] N. P. Grimster, C. Gauntlett, C. R. A. Godfrey, M. J. Gaunt, *Angew. Chem. Int. Ed.* **2005**, *44*, 3125–3129

EXPERIMENTAL SECTION – CHAPTER 5

1. Material and methods

All reactions were performed under a nitrogen atmosphere. Purification of reaction products was carried out by column chromatography using Merck silica gel (40-63 μm). Analytical thin layer chromatography (TLC) was performed on aluminum sheets pre-coated with silica gel 60 F254 (E. Merck), cut to size. Visualization was accomplished with UV light followed by dipping in a potassium permanganate and/or Seebach's staining solutions and heating. Elevated temperatures were achieved by way of a stirrer-hotplate, heating block and thermocouple. Melting points were obtained on a Büchi Melting Point B-450 apparatus and High Resolution Mass Spectra were obtained on an Agilent Technologies LCMS (ESI) system. ^{1}H NMR spectra were recorded on a Bruker Avance400 (400 MHz) spectrometer at ambient temperature unless otherwise noted and are reported in ppm using solvent as the internal standard ($CDCl_3$ at 7.26 ppm). Data are reported as: multiplicity (ap = apparent, br = broad, s = singlet, d = doublet, t = triplet, q = quartet, m = multiplet), integration and coupling constant(s) in Hz. ^{13}C NMR spectra were recorded on a Bruker Avance400 (100 MHz) spectrometer. Chemical shifts are reported in ppm from tetramethylsilane, with the residual solvent resonance employed as the internal standard ($CDCl_3$ at 77.0 ppm).

Unless otherwise noted, all commercial materials were purchased from *Sigma-Aldrich* and used without further purification. Boronic acids and ligands were used without any special precaution to exclude moisture.

2. Synthesis of chiral ligands

The chemical strategy used to obtain the chiral tartaric acid derivatives ligands is recalled below. Starting from compound **172**, seven ligands have been successfully synthezised.

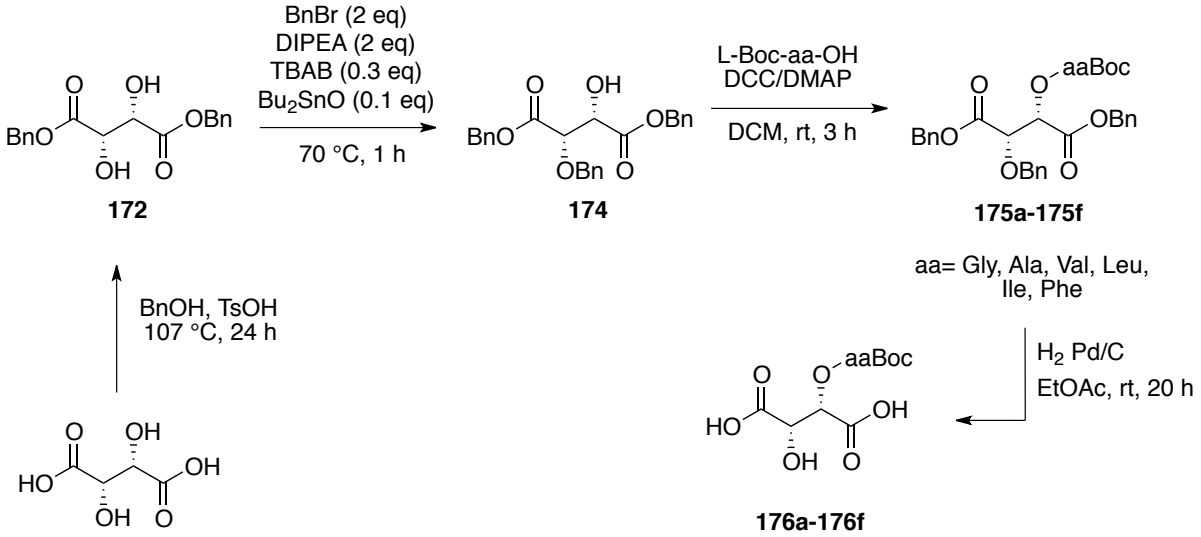

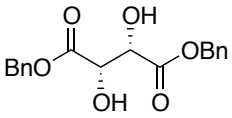

Dibenzyl-(2*S*,3*S*)-2,3-dihydroxysuccinate 172. [229]
(*D*)-(-)-tartaric acid (7.5 g, 50 mmol) and TsOH (430 mg, 2.5 mmol) were dissolved in benzene (25 mL) and benzyl alcohol (10.9 mL, 20.0 mmol) was added to the mixture. The suspension was heated to 107 °C and the evolving water was collected in a Dean Stark apparatus. After 24 h, the mixture is allowed to cool down to room temperature and diethylether (20 mL) was added. The solution was washed with brine (3x20 mL) and saturated aqueous $NaHCO_3$ (3x15 mL). The organic layer was dried over Na_2SO_4 and concentrated in vacuo affording **172** as a white solid (92%). R_f = 0.37 (30% EtOAc in petroleum ether); mp: 50 °C. $[\alpha]^{20}_D$ = -16.6° (c = 1.3, DCM).
^{1}H NMR (400 MHz, $CDCl_3$) δ 7.38-7.34 (m, 10H), 5.28 (dd, *J* = 20.3 Hz, *J* = 12.5 Hz, 2H), 4.61 (d, *J* = 6.9 Hz, 2H), 3.34-3.30 (m, 2H); **^{13}C NMR** (100 MHz, $CDCl_3$) δ 171.4, 134.8, 128.8, 128.5, 72.2, 68.2. The analytical data are in accordance with those reported in the literature.

[229] B. Buschhaus, W. Bauer, A. Hirsch, *Tetrahedron* **2003**, *59*, 3899–3915

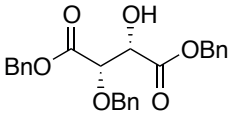

(2*S*,3*S*)-dibenzyl 2-(benzyloxy)-3-hydroxysuccinate 174.[230,231]
To **172** (3.30 g, 10 mmol) were sequentially added under air, Bu_2SnO (249 mg, 1.00 mmol), TBAB (966 mg, 3.00 mmol), DIPEA (3.48 mL, 2.58 g, 20.0 mmol) and benzylbromide (2.37 mL, 3.42 g, 20.0 mmol). The reaction mixture was then heated at 70 °C for 1 h. The reaction was allowed to cool down at room temperature, dissolved in DCM and adsorbed by evaporation of the solvent to a pad of silica gel. The residue was purified by column using 100% petroleum ether to 20% EtOAc in petroleum ether. After the evaporation of the solvents, the white solid was tritured in petroleum ether and filtered through a glass funnel affording a white solid (3.60 g, 86%). R_f = 0.12 (30% EtOAc in petroleum ether). mp: 55 °C. $[\alpha]^{20}_D$ = -64.0° (c = 1.7, EtOAc).
^{1}H NMR (400 MHz, $CDCl_3$) δ 7.43-7.29 (m, 10H), 7.26-7.20 (m, 2H), 5.31 (d, *J* = 3.6 Hz, 2H), 5.24 (d, *J* = 12.0 Hz, 1H), 5.07 (d, *J* = 12.0 Hz, 1H), 4.85 (d, *J* = 11.6 Hz, 1H), 4.72 (dd, *J* = 9.2 Hz, *J* = 2.4 Hz 1H), 4.44 (d, *J* = 2.4 Hz, 1H), 4.39 (d, *J* = 11.6 Hz, 1H), 3.23 (d, *J* = 9.2 Hz, 1H); **^{13}C NMR** (100 MHz, $CDCl_3$) δ 170.9, 169.1, 136.7, 135.3, 134.8, 128.7, 128.6, 128.5, 128.4, 128.3, 128.2, 128.1, 78.4, 73.0, 72.5, 67.7, 67.2. The analytical data are in accordance with those reported in the literature.

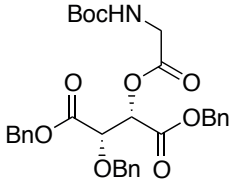

(2*S*,3*S*)-dibenzyl 2-(benzyloxy)-3-(2-((*tert*-butoxycarbonyl)-L-glycyl)oxy)succinate 175a.
To a stirred solution of **174** (800 mg, 1.90 mmol, 1.00 eq) in anhydrous DCM (10 mL) were added DCC (470 mg, 2.28 mmol, 1.20 eq), DMAP (35 mg, 0.29 mmol, 0.20 eq) and (L)-Boc-Gly-OH (399 mg, 2.28 mmol, 1.20 eq) in that order. The reaction mixture was stirred at room temperature for 3 h. DCU was then filtered off and the filtrate was concentrated. Isolated (1.05 g, 96%) as a colorless oil after column chromatography (0 to 10% EtOAc in petroleum ether). R_f = 0.32 (30% EtOAc in petroleum ether).
^{1}H NMR (400 MHz, $CDCl_3$) δ 7.41-7.23 (m, 15H), 5.71 (d, *J* = 2.8 Hz, 1H), 5.34-5.04 (m, 4H), 4.86 (d, *J* = 11.6 Hz, 1H), 4.64 (d, *J* = 3.2 Hz, 1H), 4.47 (d, *J* = 11.6 Hz, 1H), 4.00-3.83 (m, 2H), 1.49 (s, 9H); **^{13}C NMR** (100 MHz, $CDCl_3$) δ 169.6, 167.9, 165.9, 155.4, 136.3, 135.0, 134.8, 128.9, 128.7, 128.7, 128.6, 128.4, 128.2, 80.0, 76.3, 73.6, 73.2, 67.7, 67.5, 42.0, 28.3.

[230] M. Giordano, A. Iadonisi, *J. Org. Chem*. **2014**, *79*, 213–222.
[231] N. Nagashima, M. Ohno, *Chem. Pharm. Bull*. **1991**, *39*, 1972–1982.

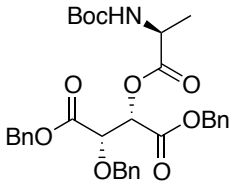

(2*S*,3*S*)-dibenzyl 2-(benzyloxy)-3-((*tert*-butoxycarbonyl)-L-alanyl)oxy)succinate 175b.
To a stirred solution of **174** (800 mg, 1.90 mmol, 1.00 eq) in anhydrous DCM (10 mL) were added DCC (470 mg, 2.28 mmol, 1.20 eq), DMAP (35 mg, 0.29 mmol, 0.20 eq) and (L)-Boc-Ala-OH (431 mg, 2.28 mmol, 1.20 eq) in that order. The reaction mixture was stirred at room temperature for 3 h. DCU was then filtered off and the filtrate was concentrated. Isolated (1.06 g, 94%) as a colorless oil after column chromatography (0 to 20% EtOAc in petroleum ether). R_f = 0.31 (30% EtOAc in petroleum ether).
^{1}H NMR (400 MHz, $CDCl_3$) δ 7.43-7.27 (m, 15H), 5.74 (d, *J* = 2.8 Hz, 1H), 5.25-5.22 (m, 4H), 4.87 (d, *J* = 11.6 Hz, 1H), 4.68 (d, *J* = 2.8 Hz, 1H), 4.49 (d, *J* = 12.0 Hz, 1H), 4.40-4.35 (m, 1H), 1.49 (s, 9H), 1.31 (d, *J* = 6.0 Hz, 3H); **^{13}C NMR** (100 MHz, $CDCl_3$) δ 171.3, 170.8, 169.1, 155.9, 136.7, 135.4, 134.8, 127.9, 127.8, 127.6, 127.4, 127.1, 79.8, 77.4, 73.4, 67.7, 66.7, 66.4, 54.0, 28.3, 17.3.

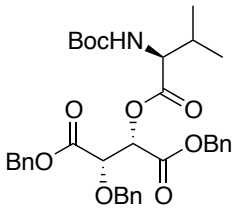

(2*S*,3*S*)-dibenzyl 2-(benzyloxy)-3-(((*tert*-butoxycarbonyl)-L-valyl)oxy)succinate 175c.
To a stirred solution of **174** (800 mg, 1.90 mmol, 1.00 eq) in anhydrous DCM (10 mL) were added DCC (470 mg, 2.28 mmol, 1.20 eq), DMAP (35 mg, 0.29 mmol, 0.20 eq) and (L)-Boc-Val-OH (495 mg, 2.28 mmol, 1.20 eq) in that order. The reaction mixture was stirred at room temperature for 3 h. DCU was then filtered off and the filtrate was concentrated. Isolated (1.14 g, 97%) as a colorless oil after column chromatography (0 to 10% EtOAc in petroleum ether). R_f = 0.55 (20% EtOAc in petroleum ether).
^{1}H NMR (400 MHz, $CDCl_3$) δ 7.41-7.24 (m, 15H), 5.72 (d, *J* = 3.2 Hz, 1H), 5.27-5.12 (m, 4H), 4.87 (d, *J* = 11.6 Hz, 1H), 4.64 (d, *J* = 2.8 Hz, 1H), 4.47 (d, *J* = 11.6 Hz, 1H), 4.37-4.30 (m, 1H), 2.34 (br s, 1H, NH), 1.48 (s, 9H), 1.01-0.88 (m, 6H); **^{13}C NMR** (100 MHz, $CDCl_3$) δ 171.3, 168.2, 166.0, 156.9, 134.9, 134.8, 128.8, 128.5, 128.4, 128.3, 79.8, 77.4, 77.3, 73.5, 67.7, 67.5, 58.5, 31.4, 28.4, 19.0.

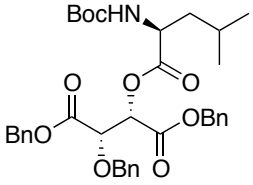

(2*S*,3*S*)-dibenzyl 2-(benzyloxy)-3-(((*tert*-butoxycarbonyl)-L-leucyl)oxy)succinate 175d.
To a stirred solution of **174** (800 mg, 1.90 mmol, 1.00 eq) in anhydrous DCM (10 mL) were added DCC (470 mg, 2.28 mmol, 1.20 eq), DMAP (35 mg, 0.29 mmol, 0.20 eq) and (L)-Boc-

Leu-OH (527 mg, 2.28 mmol, 1.20 eq) in that order. The reaction mixture was stirred at room temperature for 3 h. DCU was then filtered off and the filtrate was concentrated. Isolated (1.08 g, 90%) as a colorless oil after column chromatography (0 to 10% EtOAc in petroleum ether). R_f = 0.46 (20% EtOAc in petroleum ether).
^{1}H NMR (400 MHz, $CDCl_3$) δ 7.40-7.27 (m, 15H), 5.74 (d, *J* = 2.8 Hz, 1H), 5.30-5.06 (m, 4H), 4.89 (d, *J* = 12.0 Hz, 1H), 4.66 (d, *J* = 2.8 Hz, 1H), 4.50 (d, *J* = 11.6 Hz, 1H), 4.41-4.36 (m, 1H), 1.83-1.68 (m, 3H), 1.48 (s, 9H), 0.93 (t, *J* = 6.0 Hz, 6H); **^{13}C NMR** (100 MHz, $CDCl_3$) δ 172.6, 168.0, 166.2, 155.2, 136.7, 134.7, 128.6, 128.6, 128.4, 128.4, 128.2, 128.0, 79.7, 77.4, 77.3, 73.4, 67.6, 66.6, 51.9, 41.2, 28.3, 24.7, 22.9, 21.7.

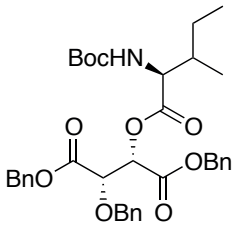

(2*S*,3*S*)-dibenzyl-2-(benzyloxy)-3-(((*tert*-butoxycarbonyl)-L-isoleucyl)oxy)succinate 175e.
To a stirred solution of **174** (800 mg, 1.90 mmol, 1.00 eq) in anhydrous DCM (10 mL) were added DCC (470 mg, 2.28 mmol, 1.20 eq), DMAP (35 mg, 0.29 mmol, 0.20 eq) and (L)-Boc-Ile-OH (527 mg, 2.28 mmol, 1.20 eq) in that order. The reaction mixture was stirred at room temperature for 3 h. DCU was then filtered off and the filtrate was concentrated. Isolated (1.16 g, 96%) as a colorless oil after column chromatography (0 to 10% EtOAc in petroleum ether). R_f = 0.47 (20% EtOAc in petroleum ether).
^{1}H NMR (400 MHz, $CDCl_3$) δ 7.41-7.27 (m, 15H), 5.77 (d, *J* = 2.8 Hz, 1H), 5.32-5.08 (m, 4H), 4.89 (d, *J* = 12.0 Hz, 1H), 4.67 (d, *J* = 2.8 Hz, 1H), 4.51 (d, *J* = 12.0 Hz, 1H), 4.40-4.36 (m, 1H), 1.90-1.85 (m, 1H), 1.72-1.58 (m, 2H), 1.50 (s, 9H), 0.95 (t, *J* = 7.2 Hz, 3H); **^{13}C NMR** (100 MHz, $CDCl_3$) δ 172.5, 168.0, 166.2, 155.2, 136.7, 134.7, 128.6, 128.6, 128.4, 128.3, 128.2, 128.0, 79.7, 77.4, 77.3, 73.4, 67.6, 66.7, 51.8, 38.5, 28.4, 24.8, 15.0, 11.2.

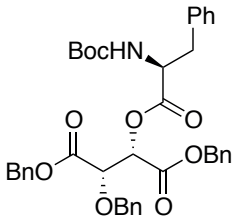

(2*S*,3*S*)-dibenzyl-2-(benzyloxy)-3-(((*tert*-butoxycarbonyl)-L-phenylalanyl)oxy)succinate 175f.
To a stirred solution of **174** (800 mg, 1.90 mmol, 1.00 eq) in anhydrous DCM (10 mL) were added DCC (470 mg, 2.28 mmol, 1.20 eq), DMAP (35 mg, 0.29 mmol, 0.20 eq) and (L)-Boc-Phe-OH (605 mg, 2.28 mmol, 1.20 eq) in that order. The reaction mixture was stirred at room temperature for 3 h. DCU was then filtered off and the filtrate was concentrated. Isolated (1.26 g, 99%) as a colorless oil after column chromatography (0 to 10% EtOAc/Petroleum ether). R_f = 0.64 (20% EtOAc in petroleum ether).
^{1}H NMR (400 MHz, $CDCl_3$) δ 7.34-7.16 (m, 20H), 5.75 (d, *J* = 2.8 Hz, 1H), 5.22-5.01 (m, 4H), 4.88 (d, *J* = 12.0 Hz, 1H), 4.65 (d, *J* = 2.8 Hz, 1H), 4.44 (d, *J* = 11.6 Hz, 1H), 4.48-4.40 (m, 1H), 3.23 (d, *J* = 11.8 Hz, 1H), 3.00 (d, *J* = 12.0 Hz, 1H), 1.48 (s, 9H); **^{13}C NMR** (100 MHz, $CDCl_3$) δ 171.4, 168.0, 166.2, 155.0, 136.6, 135.9, 135.1, 134.8, 129.7, 128.8, 128.7, 128.5, 128.4, 128.2, 126.9, 79.9, 76.8, 76.5, 73.6, 67.8, 53.8, 37.6, 28.4.

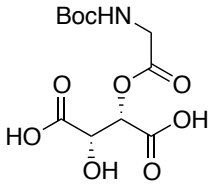

(2*S*,3*S*)-2-(2-((*tert*-butoxycarbonyl)-L-glycyl)oxy)3-hydroxysuccinic acid 176a.
Compound **175a** (646 mg, 1.12 mmol) was dissolved in EtOAc (5 mL) and Pd/C (65 mg, 10molw%) was added to the reaction mixture under a nitrogen atmosphere. The nitrogen is then replaced by H_2 and the reaction mixture was stirred at atmospheric pressure at room temperature overnight. The mixture was then filtered throught a Celite pad, concentrated in vacuo affording compound **176a** (1.12 mmol, quantitative yield) as a white solid. mp: 56 °C ; $[\alpha]_{D20}$: -8.2 (c = 7.1 mM, $CHCl_3$).
^{1}H NMR (400 MHz, DMSO-d_6) δ 5.26 (d, *J* = 2.4 Hz, 1H), 4.54 (d, *J* = 2.4 Hz, 1H), 3.74 (d, *J* = 6.0 Hz, 2H), 1.39 (s, 9H); **^{13}C NMR** (400 MHz, DMSO-d_6) δ 171.7, 169.8, 168.1, 156.2, 78.2, 73.6, 69.7, 41.3, 28.1; **HRMS** (ESI) for $C_{11}H_{17}NO_9$ + Na: calcd. 330.080; found 330.080.

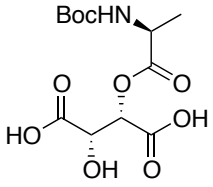

(2*S*,3*S*)-2-(2-((*tert*-butoxycarbonyl)-L-alanyl)oxy)-3-hydroxysuccinic acid 176b.
Compound **175b** (800 mg, 1.35 mmol) was dissolved in EtOAc (5 mL) and Pd/C (80 mg, 10molw%) was added to the reaction mixture under a nitrogen atmosphere. The nitrogen was then replaced by H_2 and the reaction mixture was stirred at atmospheric pressure at room temperature overnight. The mixture was then filtered throught a Celite pad, concentrated in vacuo affording **176b** (434 mg, quantitative yield) as a white solid. mp: 74 °C ; $[\alpha]_{D20}$: -16.8 (c = 7.1 mM, $CHCl_3$).
^{1}H NMR (400 MHz, $CDCl_3$) δ 7.25 (br, 1H), 5.24 (d, *J* = 2.5 Hz, 1H), 4.58 (d, *J* = 2.5 Hz, 1H), 4.01-3.97 (m, 1H), 1.39 (s, 9H), 1.24-1.15 (m, 3H); **^{13}C NMR** (400 MHz, $CDCl_3$) δ 169.9, 169.5, 166.0, 154.9, 78.6, 73.4, 73.2, 51.5, 28.1, 15.0; **HRMS** (ESI) for $C_{12}H_{19}NO_9$ + Na: calcd. 344.0952; found 344.0979.

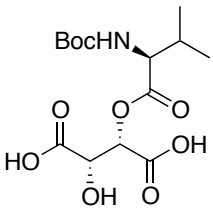

(2*S*,3*S*)-2-(2-((*tert*-butoxycarbonyl)-L-valyl)oxy)-3-hydroxysuccinic acid 176c.
Compound **175c** (900 mg, 1.45 mmol) was dissolved in EtOAc (5 mL) and Pd/C (90 mg, 10molw%) was added to the reaction mixture under a nitrogen atmosphere. The nitrogen was then replaced by H_2 and the reaction mixture was stirred at atmospheric pressure at room temperature overnight. The mixture was then filtered throught a Celite pad, concentrated in

vacuo affording **176c** (505 mg, quantitative yield) as a white solid. mp: 80 °C ; $[\alpha]_{D20}$: -18.9 (c = 7.1 mM, $CHCl_3$).
^{1}H NMR (400 MHz, DMSO-d_6) δ 7.06 (br, 1H), 5.24 (d, *J* = 2.4 Hz, 1H), 4.15-4.11 (m, 1H), 2.17-2.08 (m, 1H), 1.40 (s, 9H), 0.88-0.79 (m, 6H); **^{13}C NMR** (400 MHz, DMSO-d_6) δ 172.1, 171.0, 168.1, 155.0, 78.1, 73.6, 73.2, 69.9, 28.1, 18.8, 17.2; **HRMS** (ESI) for $C_{15}H_{25}NO_9$ + Na: calcd. 386.142; found 386.143.

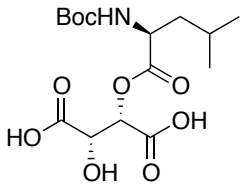

(2*S*,3*S*)-2-(2-((*tert*-butoxycarbonyl)-L-leucyl)oxy)-3-hydroxysuccinic acid 176d.
Compound **175d** (900 mg, 1.42 mmol) was dissolved in EtOAc (5 mL) and Pd/C (90 mg, 10molw%) was added to the reaction mixture under a nitrogen atmosphere. The nitrogen was then replaced by H_2 and the reaction mixture was stirred at atmospheric pressure at room temperature overnight. The mixture was then filtered throught a Celite pad, concentrated in vacuo affording **176d** (516 mg, quantitative yield) as a white solid. mp: 70 °C ; $[\alpha]_{D20}$: -15.3 (c = 7.1 mM, $CHCl_3$).
^{1}H NMR (400 MHz, $CDCl_3$) δ 7.06 (br, 1H), 5.56 (d, *J* = 2.4 Hz, 1H), 4.99 (d, *J* = 2.4 Hz, 1H), 4.44-4.35 (m, 1H), 1.83-1.58 (m, 3H), 1.45 (s, 9H), 0.96 (t, *J* = 7.2 Hz, 6H); **^{13}C NMR** (400 MHz, $CDCl_3$) δ 172.9, 170.1, 167.2, 155.0, 79.8, 73.3, 73.1, 67.7, 53.1, 41.5, 28.5, 24.8, 22.9, 16.1; **HRMS** (ESI) for $C_{15}H_{25}NO_9$ + Na: calcd. 386.1420; found 386.1422.

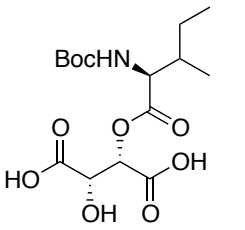

(2*S*,3*S*)-2-(2-((*tert*-butoxycarbonyl)-L-isoleucyl)oxy)-3-hydroxysuccinic acid 176e.
Compound **175e** (900 mg, 1.42 mmol) was dissolved in EtOAc (5 mL) and Pd/C (90 mg, 10molw%) was added to the reaction mixture under a nitrogen atmosphere. The nitrogen was then replaced by H_2 and the reaction mixture was stirred at atmospheric pressure at room temperature overnight. The mixture was then filtered throught a Celite pad, concentrated in vacuo affording **176e** (516 mg, quantitative yield) as a white solid. mp: 77 °C ; $[\alpha]_{D20}$: -36.4 (c = 7.1 mM, $CHCl_3$).
^{1}H NMR (400 MHz, $CDCl_3$) δ 7.61 (br, 1H, NH), 5.65 (d, *J* = 2.8 Hz, 1H), 4.94 (d, *J* = 2.8 Hz, 1H), 4.28-4.24 (m, 1H), 1.95-1.87 (m, 1H), 1.70-1.58 (m, 2H), 1.50 (s, 9H), 1.04 (d, *J* = 6.8 Hz, 3H), 0.96 (t, *J* = 6.8 Hz, 3H); **^{13}C NMR** (400 MHz, $CDCl_3$) δ 172.2, 172.1, 169.0, 155.2, 84.5, 74.3, 71.1, 67.9, 58.6, 38.5, 28.4, 24.8, 15.7, 11.5; **HRMS** (ESI) for $C_{15}H_{25}NO_9$ + Na: calcd. 386.142; found 386.140.

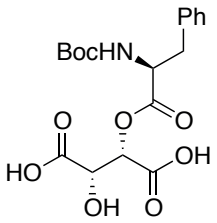

(2*S*,3*S*)-2-(2-((*tert*-butoxycarbonyl)-L-phenylalanyl)oxy)-3-hydroxysuccinic acid 176f.
Compound **175f** (900 mg, 1.35 mmol) was dissolved in EtOAc (5 mL) and Pd/C (90 mg, 10molw%) was added to the reaction mixture under a nitrogen atmosphere. The nitrogen was then replaced by H_2 and the reaction mixture was stirred at atmospheric pressure at room temperature overnight. The mixture was then filtered throught a Celite pad, concentrated in vacuo affording **176f** (536 mg, quantitative yield) as a white solid. mp: 80 °C ; $[\alpha]_{D20}$: -46.2 (c = 7.1 mM, $CHCl_3$).
^{1}H NMR (400 MHz, $CDCl_3$) δ 7.75 (br, 1H, NH), 7.36-7.23 (m, 5H), 5.73 (d, *J* = 2.4 Hz, 1H), 5.02 (d, *J* = 2.4 Hz, 1H), 4.57-4.52 (m, 1H), 3.25 (dd, *J* = 13.6 Hz, *J* = 4.8 Hz, 1H), 3.00 (dd, *J* = 13.6 Hz, *J* = 10.4 Hz, 1H), 1.42 (s, 9H); **^{13}C NMR** (400 MHz, $CDCl_3$) δ 172.9, 170.1, 167.2, 155.0, 135.0, 128.6, 127.6, 125.9, 79.8, 73.1, 67.7, 53.1, 41.5, 28.5; **HRMS** (ESI) for $C_{15}H_{25}NO_9$ + Na: calcd. 386.1432; found 386.1433.

3. Racemic HDA reaction

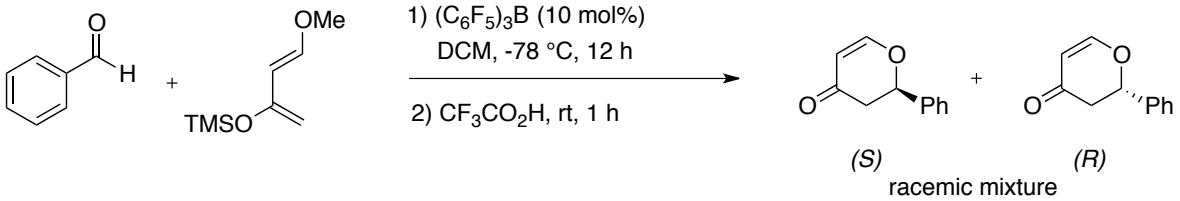

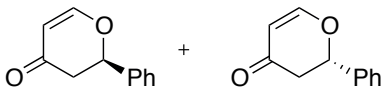

2-phenyl-2*H*-pyran-4(3*H*)-one 178.[232]
To a solution of DCM (1 mL) was added $B(C_6F_5)_3$ (21 mg, 0.04 mmol, 10 mol%). The system was cooled down to -78 °C and benzaldehyde (41 µL, 42 mg, 0.4 mmol, 1.0 equiv) followed by the Danishefsky's diene (93 µL, 83 mg, 0.48 mmol, 1.2 equiv) were added by syringe. The reaction was stirred at the same low temperature for 12 h before being poured in 4N HCl. The crude product was extracted with Et_2O (3x5 mL). The organic layers were combined, dried over Na_2SO_4 and concentrated. The residue was then dissolved in DCM (5 mL), treated with TFA (1 equiv) and stirred for an additional hour at 0 °C. This mixture was poured into water and extracted with DCM (3x5 mL). The organic layers were combined, dried over Na_2SO_4 and concentrated. Isolated (42 mg, 60%) as a yellow oil after column chromatography (40% EtOAc in petroleum ether) and was subjected to chiral HPLC analysis. R_f = 0.27 (40% EtOAc in petroleum ether).

[232] J. D. White, S. Shaw, *Org. Lett*. **2011**, *13*, 2488–2491.

Chiralcel OD, hexane:*i*PrOH 92:8, 1.0 mL/min, t_R (*R*) 22.9 min, t_R (*S*) 24.4 min. **^{1}H NMR** (400 MHz, $CDCl_3$) δ 7.51 (d, *J* = 6.1 Hz, 1H), 7.44 (m, 5H), 5.56 (dd, *J* = 6.0 Hz, *J* = 1.1 Hz, 1H), 5.46 (dd, *J* = 14.5 Hz, *J* = 3.9 Hz, 1H), 2.92-2.70 (m, 1H); **^{13}C NMR** (400 MHz, $CDCl_3$) δ 192.2, 163.2, 137.8, 128.9, 128.1, 126.1, 107.4, 81.1, 43.4. The analytical data are in accordance with those reported in the literature.

4. Combinatorial approach

General procedure for Step 1 **(6 boronic acids, 6 chiral ligands, 4 solvents, 144 possible combinations)**

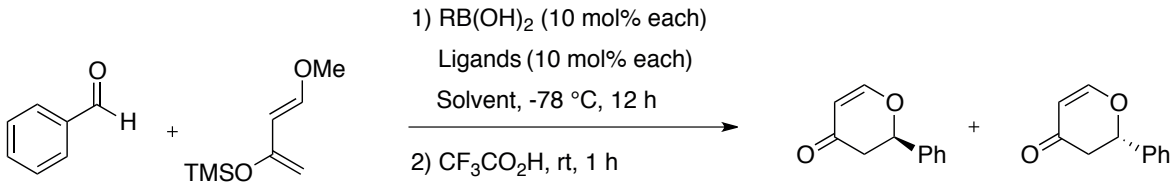

177 **10** ***(S)*-178** ***(R)*-178**

Reactions were carried out in four different solvents simultaneously according to the following procedure using the quantities of boronic acids and ligands described in the table below. Boronic acids **96a, 96f, 96h, 96j, 96k, 96l** (0.04 mmol, 10 mol%) and ligands **176a-176f** (0.04 mmol, 10 mol%) were dissolved in solvent (1 mL) under a nitrogen atmosphere. The system was cooled down to -78 °C and benzaldehyde (41 µL, 42 mg, 0.40 mmol, 1.0 equiv) followed by the Danishefsky's diene (93 µL, 83 mg, 0.48 mmol, 1.2 equiv) were added by syringe. The reactions were stirred at the same low temperature for 12 h before being poured in 4N HCl. The crude product was extracted with Et_2O (3x5 mL). The organic layers were combined, dried over Na_2SO_4 and concentrated. The residue was then dissolved in DCM (5 mL), treated with TFA (1 equiv) and stirred for an additional hour at 0 °C. This mixture was poured into water and extracted with DCM (3x5 mL). The organic layers were combined, dried over Na_2SO_4 and concentrated. Compound **178** was isolated as a yellow oil after flash column chromatography (40% EtOAc in petroleum ether) and was subjected to chiral HPLC analysis. Yields and enanti excess are described below for each case. Compound **(*S*)-178** was found to be the major enantiomer.

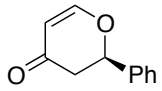

(S)

(*S*)-2-phenyl-2*H*-pyran-4(3*H*)-one 178.
Chiralcel OD, hexane:*i*PrOH 92:8, 1.0 mL/min, t_R (*S*) 24.4 min. **^{1}H NMR** (400 MHz, $CDCl_3$) δ 7.51 (d, *J* = 6.1 Hz, 1H), 7.44 (m, 5H), 5.56 (dd, *J* = 6.0 Hz, *J* = 1.1 Hz, 1H), 5.46 (dd, *J* = 14.5 Hz, *J* = 3.9 Hz, 1H), 2.92-2.70 (m, 1H); **^{13}C NMR** (400 MHz, $CDCl_3$) δ 192.2, 163.2, 137.8, 128.9, 128.1, 126.1, 107.4, 81.1, 43.4. The analytical data are in accordance with those reported in the literature.

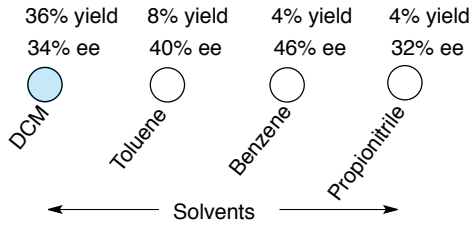

General Procedure for Step 2a

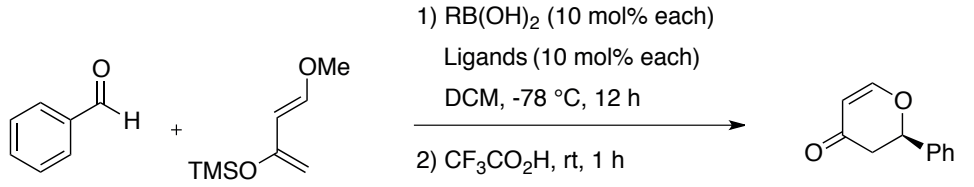

177 **10** ***(S)*-178 major**

For each deconvolution step, reactions were carried out simultaneously according to the following procedure using the boronic acids and ligands described in the tables below. Boronic acids **96j**, **96l** or **96k**, **96h** or **96a**, **96f** (0.04 mmol, 10 mol%) and ligands **176c**, **176d** or **176b**, **176e** or **176a**, **176f** (0.04 mmol, 10 mol%) were dissolved in DCM (1 mL) under a nitrogen atmosphere. The system was cooled down to -78 °C and benzaldehyde (41 µL, 42 mg, 0.40 mmol, 1.0 equiv) followed by the Danishefsky's diene (93 µL, 83 mg, 0.48 mmol, 1.2 equiv) were added by syringe. The reactions were stirred at the same low temperature for 12 h before being poured in 4N HCl. The crude product was extracted with Et_2O (3 x 5 mL). The organic layers were combined, dried over Na_2SO_4 and concentrated. The residue was then dissolved in DCM (5 mL), treated with TFA (1 equiv) and stirred for an additional hour at 0 °C. This mixture was poured into water and extracted with DCM (3 x 5 mL). The organic layers were combined, dried over Na_2SO_4 and concentrated. Compound **178** was isolated as a yellow oil after flash column chromatography (40% EtOAc in petroleum ether) and was subjected to chiral HPLC analysis. Yields and enantiomeric excess are described below for each case. Compound **(*S*)-178** was found to be the major enantiomer.

Step 2a *t* = 12 h	**96j, 96l**	**96k, 96h**	**96a, 96f**
176c **176d**	10% yield 2% ee	12% yield 24% ee	14% yield 42% ee
176b **176e**	10% yield 2% ee	6% yield 32% ee	38% yield 40% ee
176a **176f**	24% yield 2% ee	13% yield 12% ee	26% yield 24% ee

General Procedure for Step 2b and 2b'

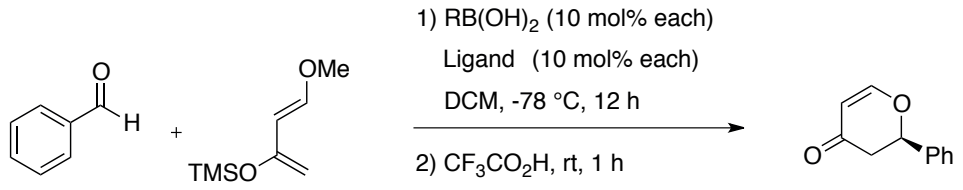

177 **10** ***(S)*-178 major**

For each individual step, reactions were carried out simultaneously according to the following procedure using the boronic acids and ligands described in the tables below. Boronic acids **96a** or **96f** (0.04 mmol, 10 mol%) and ligands **176c** or **176d** or **176b** or **176e** (0.04 mmol, 10 mol%) were dissolved in DCM (1 mL) under a nitrogen atmosphere. The system was cooled down to -78 °C and benzaldehyde (41 µL, 42 mg, 0.40 mmol, 1.0 equiv) followed by the Danishefsky's diene (93 µL, 83 mg, 0.48 mmol, 1.2 equiv) were added by syringe. The reactions were stirred at the same low temperature for 12 h before being poured in 4N HCl. The crude product was extracted with Et_2O (3 x 5 mL). The organic layers were combined, dried over Na_2SO_4 and concentrated. The residue was then dissolved in DCM (5 mL), treated with TFA (1 equiv) and stirred for an additional hour at 0 °C. This mixture was poured into water and extracted with DCM (3 x 5 mL). The organic layers were combined, dried over Na_2SO_4 and concentrated. Compound **178** was isolated as a yellow oil after flash column chromatography (40% EtOAc in petroleum ether) and was subjected to chiral HPLC analysis. Yields and enantiomeric excess are described below for each case. Compound **(*S*)-178** was found to be the major enantiomer.

Step 2b *t* = 12 h	**96a**	**96f**
176d	50% yield 54% ee	6% yield 96% ee
176c	33% yield 54% ee	9% yield 38% ee

Step 2b' *t* = 12 h	**96a**	**96f**
176e	53% yield 72% ee	7% yield 42% ee
176b	28% yield 22% ee	18% yield 34% ee

Eléna WOLF

Screening and Deconvoluting Complex Mixtures of Catalyst Components in Reaction Development

Résumé

Le développement réactionnel est problème multidimensionnel complexe qui, dans un scénario représentatif, implique l'unique convergence de plusieurs paramètres à une réactivité désirée. Le choix incorrect d'un seul paramètre réactionnel tel que le pré-catalyseur, le ligand mais aussi le solvant ou encore l'acide/base peut complètement supprimer la réactivité du système. De ce fait, ce processus requiert souvent de nombreuses expérimentations pour obtenir un premier résultat probant. Pour éviter de tester toutes les combinaisons en parallèle, des approches créatives de criblage ont été développées ces dernières années mais le nombre important de reactions nécessaires à l'exploration de juste trois ou quatre paramètres est toujours un challenge pour les chimistes qui n'ont pas accès au criblage à haut debit. Afin de répondre à cette problèmatique, une stratégie combinatoire réaction-économique pour l'identification d'un lead hit dans une reaction spécifique est proposée. Des mélanges complexes de pré-catalyseurs et de ligands, choisis au préalable, sont testés avec un ou deux autres paramètres de reaction supplémentaires pour identifier de bonnes conditions de réaction dans un nombre minimum de manipulations. La déconvolution iterative permet ensuite d'identifier le catalyseur, généré *in situ,* le plus actif dans les conditions réactionnelles. L'application de cette approche est décrite sur une réaction de Friedel-Crafts, une arylation *ortho*-C–H sélective de composés benzamides, une alkylation C3 d'indole et en catalyse asymétrique sur une réaction d'hétéro Diels-Alder.

Mots clés : catalyse, criblage combinatoire, composé du bore, métaux de transition.

Abstract

Reaction development is a complex multidimensional problem that, in a representative scenario, requires often the unique convergence of multiple parameters for a desired reactivity. The incorrect choice of a single parameter, such as the pre-catalyst, the ligand, the solvent or the acid/base, can completely eliminate the reactivity of the system. Thus, the process often requires extensive manipulations to obtain a lead hit. To avoid this time consuming process, many creative screening approaches have been developed but the large number of reactions necessary to explore the intersection of just three or four parameters is still a challenge for chemists who do not have access to high throughput experimentation. A reaction-economic combinatorial strategy is described for lead hit identification in catalyst discovery directed towards a specific transformation. Complex mixtures of rationally chosen pre-catalysts and ligands are screened against various reaction parameters to identify lead conditions in a small number of reactions. Iterative deconvolution of the resulting hits identifies which components contribute to the lead *in situ* generated catalyst. The application of this screening approach is described in the dehydrative Friedel-Crafts reaction, in the *ortho*-C–H arylation of benzamides, in the C3-indole alkylation and in the asymmetric hetero Diels-Alder cycloaddition.

Key words : catalysis, combinatorial screen, boron components, transition metals.